OCRWM	MODEL COVER SHEET	1. QA: QA Page 1 of 147

2. Type of Mathematical Model

☒ Process Model ☐ Abstraction Model ☐ System Model

Describe Intended Use of Model

Colloids process models for the waste form and engineered barrier system components of the Total System Performance Assessment for License Application. The process models describe: (1) the types and concentrations of colloids that could potentially be generated in the waste package from degradation of the waste forms, (2) concentrations of colloids produced from the corrosion of steel materials in the engineered barrier system and (3) types and concentrations of colloids present in natural waters in the vicinity of Yucca Mountain that could potentially come in contact with waste forms. In addition, attachment/detachment mechanisms and stability and potential transport characteristics of colloids anticipated in the repository are addressed.

3. Title

Waste Form and Indrift Colloids-Associated Radionuclide Concentrations: Abstraction and Summary

4. DI (including Rev. No. and Change No., if applicable):

MDL-EBS-PA-000004 REV 00

5. Total Attachments	6. Attachment Numbers - No. of Pages in Each
1	I – 6 pages

	Printed Name	Signature	Date
7. Originator	Richard Aguilar	SIGNATURE ON FILE	6/24/03
8. CSO	David Stahl	SIGNATURE ON FILE	6-24-03
9. Checker	Joe Pearson	SIGNATURE ON FILE	6/24/03
10. QER	Darrell Svalstad	SIGNATURE ON FILE	6/24/03
11. Responsible Manager/Lead	Howard Adkins, Lead	SIGNATURE ON FILE	06-24-03
12. Responsible Manager	Thomas Doering	SIGNATURE ON FILE	6-24-03

13. Remarks

Contributions:

Stephen Alcorn: Co-authored entire document. Lead contributor to Section 6.5.

Carol Mertz: Technical input for Section 6.3.1.1. Technical input and co-author of Section 6.3.1.2.

Margaret Goldberg: Technical input for Section 6.3.1.2. Co-author of Section 6.3.1.2

Kaveh Zarrabi: Technical input for Section 6.3.1.3.

Additional checkers:

Emma Thomas, Susan LeStrange, Dash Sayala, Kathy Economy, Carol Mertz (all sections except Sections 6.3.1.1 and 6.3.1.2), Kaveh Zarrabi (all sections except Section 6.3.1.3).

OFFICE OF CIVILIAN RADIOACTIVE WASTE MANAGEMENT
MODEL REVISION RECORD

2. Model Title:

Waste Form and Indrift Colloids–Associated Radionuclide Concentrations: Abstraction and Summary

3. DI (including Rev. No. and Change., if applicable):

MDL-EBS-PA-000004 REV 00

4. Revision/Change No.	5. Description of Revision/Change
00	Initial Issue

EXECUTIVE SUMMARY

This Model Report describes the analysis and abstraction of the colloids process model for the waste form and engineered barrier system components of the total system performance assessment calculations to be performed with the Total System Performance Assessment–License Application model. Included in this report is a description of (1) the types and concentrations of colloids that could be generated in the waste package from degradation of the waste forms and the corrosion of the waste package materials, (2) types and concentrations of colloids produced from the steel components of the repository and their potential role in radionuclide transport, and (3) types and concentrations of colloids present in natural waters in the vicinity of Yucca Mountain. Additionally, attachment/detachment characteristics and mechanisms of colloids anticipated in the repository are addressed and discussed. The abstraction of the process model is intended to capture the most important characteristics of radionuclide-colloid behavior for use in predicting the potential impact of colloid-facilitated radionuclide transport on repository performance.

Data used to develop model parameters and model process elements are based on both field and laboratory data developed by the project and, to some degree, information found in the open literature. Experimental data developed from ongoing research at Argonne National Laboratory, Los Alamos National Laboratory, and at the University of Nevada at Las Vegas are relied upon to establish parameters associated with colloid formation from waste forms and steel corrosion products, concentrations of colloids in groundwaters in the vicinity of Yucca Mountain, and sorption/desorption characteristics of radionuclides associated with colloids. The abstraction on colloid behavior also relies on fundamental properties of colloids taken from the literature. In some cases, assumptions are used in the colloid abstraction to aid in the establishment of model parameter value ranges. The rationale for these assumptions and their confirmation status are described.

Four waste package types, each containing a different waste type or combination of waste types, are defined in *Yucca Mountain Science and Engineering Report*: (1) commercial spent nuclear fuel, (2) a combination of defense high-level waste glass and U.S. Department of Energy spent nuclear fuel (codisposal package), (3) defense high-level waste glass, and (4) naval fuel. Colloids will likely be produced as a result of alteration of defense high-level radioactive waste. The abundance of colloids within the breached waste package will depend on the extent of waste form alteration and the alteration products formed. Colloid abundance and stability also depend on environmental factors including the ionic strength, pH, and cation and colloid concentrations of waters entering the waste package from the surrounding drift. The model considers the potential effects of these factors and processes on colloid formation and subsequent stability. Transport processes are not discussed in this model report. These processes and their effects on the migration of radionuclides generated from waste degradation are reported in an analysis of potential radionuclide transport within engineered barrier system—the results of this analysis are reported in ANL-WIS-PA-000001 REV 01, *EBS Radionuclide Transport Abstraction.*

The colloids formed from the degradation products of defense high-level waste glass have been shown to be predominantly smectite clay with discrete radionuclide-bearing phases, which are incorporated in the clay. These “embedded” radionuclides are stipulated to be permanently fixed in the clay particles and are modeled as permanently attached radionuclides that would

subsequently be transported with the colloids. There are no direct colloid source term contributions from commercial and U.S. Department of Energy spent nuclear fuel wastes in the Total System Performance Assessment–License Application model. Argonne National Laboratory investigations indicate the formation of some quantities of stable colloids for these waste forms, especially for U.S Department of Energy spent nuclear fuel. However, these research findings are too preliminary at this time to incorporate into the Total System Performance Assessment–License Application model. Specifically, U colloids that have been observed to form are meta-schoepite or other oxyhydroxides that are soluble in the dilute oxic waters anticipated in the unsaturated and saturated zone environments. Consequently, these colloids will eventually dissolve, in part because of their very small size and large reactive surface area, and in part because of increasingly dilute groundwater conditions away from the near-field. Therefore, U is modeled within the engineered barrier system as U aqueous complexes not associated with colloids. Colloid concentrations in natural groundwater samples in the vicinity of Yucca Mountain are used to establish ranges of colloid mass concentrations in seepage waters that might come into contact with waste packages and waste forms. In general, bounding relationships are employed in the abstraction to incorporate uncertainties in the data used to formulate parameters used in the abstraction.

Analysis related to colloids formation and behavior within the repository drift outside the waste package include the formation of steel corrosion product colloids (iron oxyhydroxides) and potential concentrations of seepage water colloids that might be available to transport radionuclides within the drift. As in the waste package analyses, colloids identified in groundwaters underlying the repository are used as surrogates for natural colloids in the seepage waters. Additional analyses within the drift outside the waste package include assessment of the stability of all three general classes of colloids considered in this model report (i.e., waste form colloids, steel corrosion product colloids, and natural seepage water colloids). Bounding relationships are again employed in the abstraction to incorporate uncertainties in the data used to formulate parameters used in the abstraction.

Model outputs include data developed for direct use in the Total System Performance Assessment–License Application model calculations. Additional outputs include parameters for use in other submodel components in the Total System Performance Assessment–License Application model calculations (e.g., unsaturated and saturated zone components of the natural barriers system underlying the repository). Specifically, the developed model output can be categorized as: (1) waste form colloid masses from defense high-level waste glass; (2) radionuclide concentrations embedded in waste form colloids; (3) colloid masses from corrosion of steel repository components, including the waste package; (4) colloid masses in seepage water entering the waste package; and (5) concentrations of radionuclides sorbed to all colloid types. These five categories comprise the final product assemblage that exits a failed waste package in the model, interacts with the invert fluid, and enters the unsaturated zone. Specific parameters developed in this model analysis for use elsewhere in the Total System Performance Assessment–License Application model include waste form colloid mass concentrations (derived from defense high-level waste glass), corrosion product colloid mass concentrations, sorption partition coefficients (K_d values) for selected radionuclides onto smectite and iron oxyhydroxide colloids, and specific surface area of iron oxyhydroxide colloids.

CONTENTS

Page

CONTENTS (Continued)

Page

CONTENTS (Continued)

Page

FIGURES

Page

FIGURES (Continued)

Page

TABLES

Page

ACRONYMS

ATM	approved testing material
BWR	boiling water reactor
DLVO	Darjaguin, Landau, Verwey and Overbeek
DOE	U.S. Department of Energy
DTN	data tracking number
EPA	U.S. Environmental Protection Agency
FEPs	features, events, and processes
NRC	U.S. Nuclear Regulatory Commission
PWR	pressurized water reactor
S_A	surface area
SNF	spent nuclear fuel
TSPA-LA	Total System Performance Assessment–License Application
TSPA-SR	Total System Performance Assessment–Site Recommendation
V	volume
YMP	Yucca Mountain Project

1. PURPOSE

The purpose of this model report is to present and describe the abstraction of the colloids process model for the waste form and engineered barrier system components of the total system performance assessment calculations to be performed with the Total System Performance Assessment (TSPA)-License Application (LA) model. The model describes (1) the types and concentrations of colloids that could be generated in the waste package from degradation of the waste forms and the corrosion of the waste package materials, (2) types and concentrations of colloids produced from the steel components of the repository and their potential role in radionuclide transport, and (3) types and concentrations of colloids present in natural waters in the vicinity of Yucca Mountain. In addition, attachment/detachment characteristics and mechanisms of colloids anticipated in the repository are addressed and discussed. The abstraction of the process model is intended to capture the most important characteristics of radionuclide-colloid behavior for use in predicting the potential impact of colloid-facilitated radionuclide transport on repository performance.

Experimental data developed from ongoing research (BSC 2002 [DIRS 161534]; BSC 2002 [DIRS 161535]; BSC 2002 [DIRS 158197]), primarily by Argonne National Laboratory, Los Alamos National Laboratory, and at the University of Nevada at Las Vegas and information from other pertinent studies reported in the open literature are used as the basis for the selection of input parameters used in the process models. The application of new testing data to the development of the model parameters and model abstractions for TSPA-LA are discussed in Section 4, Inputs, and Section 6.0, Model Discussion.

1.1 APPLICABILITY OF MODEL TO REPOSITORY

It is anticipated that unsaturated conditions will prevail within the engineered barrier system during the 10,000-year regulatory compliance period. The TSPA-LA model examines two cases: (1) condensation of water vapor (pure water) onto engineered barrier system components with development of thin films and (2) seepage influx to the engineered barrier system with no accumulation of seepage water within the WP and water films up to about 0.25 cm thick, for three seepage water compositions: J-13 and two pore water compositions (BSC 2003 [DIRS 163919].

The colloid model abstraction is used in TSPA-LA to estimate the stability and concentration of colloids, as well as concentrations of radionuclides associated with the colloids, based on in-package and in-drift fluid chemistry and in-package dissolved radionuclide concentrations. As such, the colloid parameters are estimated based on fluid chemistry only, i.e., regardless of fluid quantity and spatial distribution. Feeds for in-package ionic strength and pH are received from *In-Package Chemistry Abstraction* (BSC 2003 [DIRS 163919]) and feeds for in-drift ionic strength and pH are received from the engineered barrier system physical and chemical environment (BSC 2002 [DIRS 160315], analysis described in Section 1.2.2). Feeds for dissolved radionuclide concentrations are developed in *Dissolved Concentrations of Radioactive Elements* (BSC 2003 [DIRS 163152]).

The colloid model abstraction relies on laboratory tests of waste form degradation (performed at Argonne National Laboratory, mentioned above) that are specific to Yucca Mountain conditions

and objectives. These tests can be broadly described as immersion tests in which the sample is completely submerged in water, drip tests in which measured quantities of water are injected into the vessel onto the waste form sample, and humid-condition tests in which samples are degraded under humid conditions with no liquid water contacting the sample. The test data used directly or indirectly in the abstraction come from all test types but primarily the first two (immersion and drip). Generally, at the end of the tests, colloids were removed from the fluid and both colloids and fluid analyzed. Measured stabilities and concentrations of colloids were related to fluid compositions. The abstraction also relies on fundamental properties of colloids taken from the literature. Colloid properties are determined by testing (in water) and by calculation and modeling. Because in-package chemistry calculations, including fluid chemistry, are performed for scenarios in which water layers or films are modeled, and since colloid behavior is determined by fluid properties, regardless of fluid quantity or shape, the methodology employed in the colloid model abstraction is deemed appropriate for its purpose.

Although colloid transport under saturated conditions is not postulated for the regulatory period of concern, limited movement of colloids within thin water films could occur. The extent and longevity of these thin films depend upon the specific hydrologic conditions within the waste package and various locations in the surrounding engineered barrier system environment at a particular time, as does the degree of continuity of the films. Consequently, transport of colloids and associated radionuclides from the waste package to the invert may be impeded to some degree. Transport in the engineered barrier system is described in *EBS Radionuclide Transport Abstraction* (BSC 2003 [DIRS 163935]).

1.2 MODEL LIMITATIONS AND RANGE OF APPLICATION

For the purposes of this report, colloidal systems are defined as those in which the component phases are dispersed in an aqueous medium ranging in size from approximately 1 to 10 nm to 1 μm. The environmental behavior of colloids has been studied extensively over the past few decades but, due largely to their small size and unique surface-dominated chemical and physical characteristics, colloids have proven difficult to study. Additionally, testing on the degradation of high-level radioactive waste and the formation of colloids from these materials has generally been limited to government-sponsored research. The approach taken in this analysis and modeling effort was to bound the probable behavior of colloid-associated radionuclides, using accessible data from these government-sponsored projects to the fullest extent possible. The absence of certain data can be mitigated as well by comparing these bounds with other relevant laboratory and field studies and with other sites in which environmental conditions are analogous in critical respects to those anticipated in the repository. These approaches have been used to the fullest extent possible to reduce the uncertainties associated with predictions of colloid-associated radionuclide concentrations, stability, and subsequent transport characteristics.

Colloid facilitated transport may play a significant role in radionuclide transport, and recent studies of plutonium (Pu) migration in natural (non-karst) hydrologic systems suggest relatively rapid transport times for Pu in association with colloids (Kersting et al. 1999 [DIRS 103282]; Penrose et al. 1990 [DIRS 100811]). However, in some cases, other researchers have concluded that other mechanisms may have been responsible for the transport of this radionuclide. For example, Marty et al. (1997 [DIRS 161670]) concluded that transport through rapid flow transport paths (i.e., uncapped sampling wells) might have led to the accelerated movement of Pu

at Mortandad Canyon at Los Alamos National Laboratory (Penrose et al. 1990 [DIRS 100811]. Consequently, it is apparent that a complex assemblage of processes would play a role in the potential transport of radionuclides from waste package containers emplaced within the repository through the engineered barrier system and the underlying natural barrier system (unsaturated and saturated zones). The models described in this report focus first on the processes and physical/hydrological factors that might lead to the formation of colloid-size waste products from the degradation of the high-level nuclear wastes materials and secondly on their subsequent stability within the waste package and surrounding engineered barrier system environment. Other analysis and models developed for the TSPA-LA address the processes and mechanisms responsible for the stability and transport/retardation of radionuclides associated with colloids released from the engineered barrier system to the underlying unsaturated zone (BSC 2002 [DIRS 160819]) and saturated zone environments (BSC 2001 [DIRS 156308]).

Colloid source term is defined here as the total of those radionuclides associated in some manner with colloids that (1) are mobilized at the surface of the waste form, (2) are transported within the waste package to the waste package wall, (3) leave the waste package at a breach or breaches in the waste package wall, and (4) enter the drift.

The model describing colloid formation through waste form degradation and their subsequent stability within the drift is valid only over the range of chemical and hydrological conditions anticipated within the waste package and drift during the postclosure regulatory compliance period. Discussion on the valid range of application for the various process models is included in Section 7, Validation.

1.3 SCOPE OF MODEL DOCUMENTATION

This model report was developed, in part, by building upon previously developed concepts on colloid formation and stability within the waste form (CRWMS M&O 2001 [DIRS 153933]) and in-drift (CRWMS M&O 2000 [DIRS 129280]) environments.

The modeling and abstraction activities reported in this document are specified in and are carried out in accordance with the work scope described in the technical work plan for the Waste Form Department (BSC 2002 [DIRS 160779]). Additionally, implementation of this model will rely on inputs from models developed from activities within the engineered barrier system model component (BSC 2002 [DIRS 160315], analysis described in Section 1.2.2), as well as other activities within the Waste Form Department (BSC 2003 [DIRS 163919], 2003 [DIRS 163152]). There were no deviations from the work/activities outlined in *Technical Work Plan for Waste Form Degradation Modeling, Testing, and Analyses in Support of SR and LA* (BSC 2002 [DIRS 160779]).

1.4 MODEL REPORT OVERVIEW

Section 2.0 lists the procedures, technical work plan, and requirements under which this report was prepared. Section 3.0 discusses the software used in report preparation.

A summary of parameters used in the process models developed and used in this abstraction is listed in Section 4.1, Data and Parameters, Table 1. Section 4.0 describes the development of inputs for the colloid model abstraction and lists the information used in Table 1 (direct input—

Q data) and Table 2 (other input, including corroborative non-Q data). The Yucca Mountain Review Plan (NRC 2002 [DIRS 158449]) acceptance criteria and the codes and standards that apply to this report are listed as well.

Section 5.0 presents the assumptions used in the colloid abstraction with their rationale, confirmation status, and the report sections in which the assumptions are used. The assumptions are used primarily in two situations. In those cases where data are inadequate to support a particular concept or model technique (e.g., sorptive properties of protactinium), a bounding assumption is generally used. Similarly, where a process would add complexity to the model without adding a significant and defensible component to the output (e.g., gravitational settling), it was left out of the model and a bounding assumption was established. An assumption regarding colloid-microbe interactions (Section 5, Assumption 5.9) is based on a review of literature and on professional judgment; a review of the issue and description of pertinent data is presented in Section 6.3.4.

Conceptual models and background information on colloid formation and behavior (including potential stability and their potential role in radionuclide transport) are presented in Section 6. A description of the model and its objectives are presented in Section 6.1. Pertinent features, events, and processes (FEPs) evaluated for their pertinence to this analysis are addressed in Section 6.2.

Section 6.3 presents the base-case colloid model elements in several subsections. The background information and rationale are provided for the approaches used as well as for elements considered but not incorporated into the model (e.g., colloids from commercial spent nuclear fuel [SNF] and U.S. Department of Energy [DOE] SNF). Colloid formation, stability, and concentration; radionuclide attachment to colloids; and microbial interactions are discussed within each of these subsections. Section 6.4 describes alternative models that were considered during the development of the colloid model and the rationale for not using them.

Section 6.5 presents the abstraction of the colloid model elements and the methodology and logic for implementing the abstraction in the TSPA-LA model calculations. The section begins with a summary description of the abstraction and a schematic overview figure (Figure 17). Section 6.5.1 presents the in-package abstraction in some detail, with figures; Section 6.5.2 similarly provides the in-drift abstraction. Section 6.5.3 presents an overview of the disposition of colloids and associated radionuclides “downstream” from the engineered barrier system in the unsaturated zone and saturated zone.

Sections 6.6, 6.7, and 6.8 present the model results, description and analyses of the barrier capability, and an evaluation of the alternative models.

Section 7.0 validates the colloids process model. It also describes the waste form, corrosion products, and groundwater colloid parameters (used as surrogates for seepage water colloids in this analysis); radionuclide attachment characteristics; model uncertainty; and processes not incorporated into the model abstraction.

Section 8.0 provides a summary of analysis, describes the developed output parameters and uncertainties, and presents conclusions drawn from the model results. Section 9.0 lists references cited, codes, standards, regulations, procedures, and source data.

2. QUALITY ASSURANCE

Development of this analysis and model report and the supporting analyses have been determined to be subject to the Yucca Mountain Project's quality assurance program (BSC 2002 [DIRS 160779], Section 2.1.4.4, Work Package AWFM01). *Quality Assurance Requirements and Description* (DOE 2003) applies to the development of this Model Report. Approved quality assurance procedures identified in the technical work plan (BSC 2002 [DIRS 160779], Section 4, Implementing Procedures) have been used to conduct and document the activities described in this model report. The technical work plan also identifies the methods used to control the electronic management of data (BSC 2002 [DIRS 160779], Section 8)—there were no deviations from these methods.

The report contributes to the analysis and modeling data used to support performance assessment by developing and providing source terms for waste form colloids, corrosion product colloids, and natural groundwater colloids for the TSPA-LA model; the conclusions do not directly impact engineered features or engineered and natural barriers important to waste isolation, as defined in AP-2.22Q, *Classification Criteria and Maintenance of the Monitored Geologic Repository Q-List.*

3. USE OF SOFTWARE

No computer software was used for calculations and/or modeling in support of this analysis. No codes or routines were developed.

Reference to parameters used in calculations by the TSPA-LA model is made in this model report. The parameters are provided for use by the TSPA-LA model, but no total system performance assessment model calculations were performed for this model report. The logic presented in this report is intended for implementation in the TSPA-LA model, but no computer runs with GoldSim (BSC 2003 [DIRS 161572]) were executed for this report.

Graphs and figures were prepared with Microsoft Excel 2000, Microsoft PowerPoint 2000, and Adobe Illustrator 8.0.1. Excel was used for tabular presentation of data only and to execute simple mathematical operations (addition, subtraction, and multiplication) in the evaluation of these data; no built-in functions or mathematical operations were employed. PowerPoint was used for presentation (i.e., figures) of data extracted from Excel spreadsheets. These "off-the-shelf" software programs are exempt per AP-SI.1Q, *Software Management*, Sections 2.1.1 and 2.1.2.

4. INPUTS

Technical product inputs and sources are direct inputs (Table 1). Corroborating/supporting data and information are used to develop the model (Table 2) as stipulated by AP-SIII.10Q, *Models.*

4.1 DATA AND PARAMETERS

Direct technical inputs have been taken from data inputs provided by Argonne National Laboratory and Los Alamos National Laboratory (Table 1, direct Q-data inputs) that address the types of colloids formed from waste form degradation, steel corrosion degradation products, and natural seepage water colloids that might potentially come in contact with waste forms and the surrounding engineered barrier system. Also included in the input tables are sources of data used for the development of sorption partition coefficients (K_d values) that are used to model radionuclide attachment to colloids. During the colloids source term model implementation by the TSPA-LA model, pertinent output parameters from the in-package (BSC 2003 [DIRS 163919]) and in-drift chemistry calculations (BSC 2002 [DIRS 160315] analysis described in Section 1.2.2) are used as direct input during each model iteration (i.e., these inputs are sampled stochastically during each modeled time step). For purposes of description, the parameters developed in this analysis have been broadly grouped as follows:

- Waste form colloid parameters (modeled colloid: smectite; experimental work at Argonne National Laboratory has shown that the colloids formed from defense high-level waste glass are smectite).
- Corrosion product colloid parameters (modeled colloid: iron oxyhydroxide/goethite)
- Seepage water (groundwater) colloid parameters (modeled colloid: smectite)
- Radionuclide sorption partition coefficients (K_d values)

These parameter groups are described in the next section, and the parameters are listed and described in Table 1. The parameters listed in Table 1 are based technically on findings from applicable analytical, laboratory, and field research, including investigations specific to the Yucca Mountain region and the Yucca Mountain Project (YMP). More detailed discussion on the technical bases for the development of these parameters may be found in Section 5, Assumptions, and Section 6, Model Discussion.

Uncertainty associated with the model analysis, including development of parameter values and their implementation in the TSPA-LA model, is discussed in Section 6.6.2, Uncertainty Associated with the Model Analysis. Parameter uncertainties are addressed by providing ranges, probability distributions, and bounding assumptions as appropriate for each given parameter. Many of the parameters are derived from data directly relevant to colloid formation, stability, and capacity to associate with radionuclides. However, many of these data were not collected from the YMP site and may not fully represent the physical and chemical conditions of the repository. Departure from anticipated repository conditions is addressed by acknowledging uncertainties in the parameters and providing a means to incorporate these uncertainties into the total system performance assessment calculations. These uncertainties are addressed by providing ranges, probability distributions, and bounding assumptions as appropriate for each given parameter or process.

Table 1. Summary of Direct Input Data Used in Model Parameter Development

Data Tracking Number (DTN) or Report	Data/Parameter Description	Units[a]	Locations in Model Report
Waste Form Colloids			
LL000905312241.018 [DIRS 152621] LL991109751021.094 [DIRS 142910]	Plutonium concentration associated with DHLWG colloids from ANL tests—see Figures 3 and 8	mol/L	Section 6.3.1
LA0003NL831352.002 [DIRS 148526], LA0005NL831352.001 [DIRS 149623] EPA 1999 [DIRS 147475]; Honeyman and Rainville 2002 [DIRS 161657]; Stenhouse 1995 [DIRS 147477]; Lu et al. 1998 [DIRS 100946]; Lu et al. 2000 [DIRS 154422]	K_d values for radionuclides on rocks, minerals, and colloids; modeling results for partitioning of radionuclides between colloids and stationary phases	mL/g	Section 6.3.3.1, Table 6, 7, 8. 9
Corrosion-Generated [iron oxyhydroxide] Colloids			
MO0212UCC034JC.002 [DIRS 161457]	Concentration of iron oxyhydroxide colloids resulting from the corrosion of steel corrosion products in waste packages	mg/L	Section 6.3.1.3
LA0003NL831352.002 [DIRS 148526], LA0005NL831352.001 [DIRS 149623] EPA 1999 [DIRS 147475]; Honeyman & Ranville 2002 [DIRS 161657]; Stenhouse 1995 [DIRS 147477]	K_d values for radionuclides on rocks, minerals, and colloids; modeling results for partitioning of radionuclides between colloids and stationary phases	mL/g	Section 6.3.3.1, Table 6, 7, 8. 9
Groundwater Colloids			
LA0002SK831352.001 [DIRS 149232]; LA0002SK831352.002 [DIRS 149194], LA9910SK831341.005 [DIRS 144991] LA0211SK831352.002 [DIRS 161581], LA0211SK831352.004 [DIRS 161458], LA0211SK831352.001 [DIRS 161580] LA0211SK831352.003 [DIRS 161582]	Colloid particle size distributions and concentration values for groundwater samples in the Yucca Mountain vicinity	nm (size); pt/ml (conc.)	Section 6.3.2.5 and Attachment I
Lide 1995 [DIRS 101876]	Particle density values for silicate minerals—used to estimate general particle density value for groundwater colloids.	g/cm^3	Attachment I
LA0003NL831352.002 [DIRS 148526], LA0005NL831352.001 [DIRS 149623]	K_d values for radionuclides on rocks, minerals, and colloids	mL/g	Section 6.3.3.1, Table 6

NOTES: [a] mol/L Pu = moles per liter of dispersion, not molarity in the strict sense.
ANL = Argonne National Laboratory; N/A = not applicable.

Parameters Developed in this Model Analysis/Abstraction:

Waste Form Colloid Parameters—The parameters listed under the category "Waste Form Colloids" in Table 1 relate primarily to the expected colloid composition resulting from the degradation of defense high-level waste glass, commercial SNF, and DOE SNF, determination of colloid stability and estimated colloid mass concentrations, and estimated

concentrations of radionuclides embedded within these colloids. Parameters used to describe reversible radionuclide attachment ("sorption") include sorption partition coefficients (K_d values), colloid specific surface areas, and "effective" K_d values derived from surface complexation calculations. Ionic strength and pH are parameters taken directly from *In-Package Chemistry Abstraction* (BSC 2003 [DIRS 163919]), *Dissolved Concentrations of Radioactive Elements* (BSC 2003 [DIRS 163152]), and near-field chemical environment analyses (BSC 2002 [DIRS 160315], analysis described in Section 1.2.2). In addition there are functions and intermediate parameters listed in Table 16 resulting from the model abstraction as implemented in the total system performance assessment calculations.

Waste form parameter ranges and distributions were established using the available knowledge of processes and principles, utilizing necessary conceptual simplifications, and consideration of measurement error. Parameter ranges and/or distributions are listed in Table 16.

Corrosion-Generated (Iron Oxyhydroxide) Colloid Parameters—The colloid parameters listed under "Corrosion-generated (iron oxyhydroxide) Colloids" in Table 1 are related to estimates of corrosion product colloid mass concentrations in the waste package and the invert and determination of their stability. Parameters used to describe reversible radionuclide attachment ("sorption") include sorption partition coefficients (K_d values), colloid specific surface areas, and "effective" K_d values derived from surface complexation calculations. Ionic strength, pH, and dissolved radionuclide concentrations are input parameters taken directly from data resulting from *In-Package Chemistry Abstraction* (BSC 2003 [DIRS 163919]) and *Dissolved Concentrations of Radioactive Elements* (BSC 2003 [DIRS 163152]). In addition, listed in Table 16 are functions and intermediate parameters resulting from model abstraction for total system performance assessment calculations.

Parameter ranges and distributions were formulated using the available knowledge of processes and principles associated with iron oxyhydroxide colloids, utilizing necessary conceptual simplifications, and consideration of measurement error. Parameter ranges and/or distributions are listed in Table 16.

Seepage Water Colloid Parameters—The colloid parameters listed under "Groundwater Colloids" in Table 1 define seepage water colloid mass concentrations entering the waste package and other components of the engineered barrier system. Groundwater parameter ranges and distributions (as appropriate) were formulated using all known available data on groundwater colloid concentration in wells evaluated in the vicinity of Yucca Mountain. Data sources are listed in Table 1 (direct input).

Radionuclide Attachment Parameters—Sorption partition coefficients (K_d values) are used, with one exception, in the abstraction to estimate concentrations on colloids of the reversibly sorbed radionuclides considered in the abstraction. The ranges and distributions of these K_d values are given in Table 16. In the exception (reversible sorption of Pu on corrosion-generated colloids), surface complexation calculations were performed and/or reliance was placed on laboratory, field, and modeling investigations in the peer-reviewed

literature to derive "effective" K_d values, which were derived from the "effective," or specific, surface areas (S_A) of the colloids.

Other Parameters Critical to the Implementation of this Abstraction in the TSPA-LA Model:

Chemical and Environmental Parameters— When this colloids process model is implemented in the TSPA-LA model, it is fed certain chemical and environmental parameters from other submodels implemented in the TSPA-LA. Ionic strength and pH are developed in the in-package chemistry model (BSC 2003 [DIRS 163919]) and engineered barrier system physical and chemical environment model (BSC 2002 [DIRS 160315]) abstractions, and dissolved radionuclide concentrations are developed in *Dissolved Concentrations of Radioactive Elements* (BSC 2003 [DIRS 163152]). In-drift chemical environmental parameters (e.g., seepage water pH and ionic strength) are provided in the engineered barrier system's physical and chemical environment model (BSC 2002 [DIRS 160315], analysis described in Section 1.2.2). This abstraction does not use these parameters directly, rather the parameters are used to implement the colloid subprocess models within the TSPA-LA model calculations.

4.2 CRITERIA

The following *Yucca Mountain Review Plan, Information Only* (NRC 2002 [DIRS 158449]) acceptance criteria as outlined in Table 5 of *Technical Work Plan for Waste Form Degradation Modeling, Testing, and Analyses in Support of SR and LA* (BSC 2002 [DIRS 160779]) apply to this model report:

Degradation of Engineered Barriers:

- AC1: System Description and Integration Are Adequate—that is, total system performance assessment adequately incorporates important physical phenomena, and couplings, and uses consistent and appropriate assumptions throughout the engineered barrier system abstraction process.

- AC2: Data Are Sufficient for Model Justification—that is, parameters used to evaluate the degradation of engineered barriers in the safety case are adequately justified (e.g., colloid concentrations formed from waste degradation and steel corrosion). Additionally, sufficient data have been collected to establish initial boundary conditions for abstraction of degradation of engineered barriers.

- AC3: Data Uncertainty Is Characterized and Propagated through the Model Abstraction—that is, subprocess models use parameter values, assumed ranges, probability distributions, and bounding assumptions that are technically defensible, reasonably account for uncertainties and variabilities, and do not result in an under representation of the risk estimate.

- AC4: Model Uncertainty Is Characterized and Propagated through the Model Abstraction—that is, alternative modeling approaches of FEPs are considered and

are consistent with available data and current scientific understanding, and the results and limitations are appropriately considered in the abstraction. Conceptual model uncertainties are defined and documented and conclusions are properly assessed.

Quantity and Chemistry of Water Contacting Waste Packages and Waste Forms:

- AC1: System Description and Integration Are Adequate—that is, the total system performance assessment adequately incorporates important design features, physical phenomena, and couplings and uses consistent and appropriate assumptions throughout the modeling of the quantity and chemistry of water contacting waste packages and waste forms. Additionally, sufficient technical bases and justification are provided for modeling coupled processes, including the waste package chemical environment, and the chemical environment for radionuclide release.

4.3 CODES AND STANDARDS

This Model Report was prepared to comply with the *Yucca Mountain Review Plan, Draft for Comment* (NRC 2002 [DIRS 158449]) and the specified subparts/sections of the U.S. Nuclear Regulatory Commission (NRC) high-level waste rule, 10 CFR Part 63 [DIRS 158535]. Subparts of this rule that are particularly applicable to data include Subpart B, Section 15 (Site Characterization) and Subpart E, Section 114 (Requirements for Performance Assessment). Subparts applicable to models are outlined in Subpart E, Sections 114 (Requirements for Performance Assessment) and 115 (Requirements for Multiple Barriers). The work conforms to the guidance provided in American Society of Testing and Materials (ASTM) Standard C 1174-97 [DIRS 105725] as stated in Section 3 of *Technical Work Plan for Waste Form Degradation Modeling, Testing, and Analyses in Support of SR and LA* (BSC 2002 [DIRS 160779]). Another regulatory requirement adhered to in this analysis is the U.S. Environmental Protection Agency's (EPA) rule 40 CFR Part 197 [DIRS 155238] with reference to screening of FEPs.

4.4 INDIRECT INPUTS TO MODEL ANALYSIS

Corroborating/supporting data and information sources used in the model analysis are listed in Table 2.

Table 2. Summary of Corroborating/Supporting Information Used in Model Parameter Development

Reference	Data/Parameter Description	Units	Locations in Model Report
Corrosion-Generated (iron oxyhydroxide) Colloids			
Laaksoharju et al. (1995 [DIRS 106449]); Vilks et al. (1993) [DIRS 108261]	Concentration of iron oxyhydroxide colloids observed in natural groundwaters.	mg/L	Section 6.3.1.3
Langmuir 1997 [DIRS 100051]; Dzombak and Morel 1990 [DIRS 105483]; Davis and Kent 1990 [DIRS 143280]	Specific surface area and site density estimates for iron phases.	m^2/g and # sites/ nm^2	Section 6.3.3.2
Langmuir 1997 [DIRS 100051]; Dzombak and Morel 1990 [DIRS 105483]; Davis and Kent [DIRS 143280]; Jenne 1998 [DIRS 162328]	Specific surface area (S_A) for iron oxyhydroxide colloids	m^2/g	Sections 5.12, 6.3.3.2
Groundwater Colloids			
LA0002SK831352.003 [DIRS 161771], LA0002SK831352.004 [DIRS 161579]	Colloid particle size distributions and concentration values for groundwater samples in the Yucca Mountain vicinity	nm (size); pt/ml (conc.)	Section 6.3.2.5 and Attachment I

5. ASSUMPTIONS

The assumptions used in the colloid abstraction are presented here along with their rationale, confirmation status, and the report sections in which the assumptions are implemented. The assumptions were established under one of two distinct circumstances. First, a bounding assumption was established when data were deemed to be inadequate to fully support a particular concept or model technique (see Assumptions 5.1, 5.2, 5.3, 5.5, 5.12). Additionally, an assumption that it is appropriate to exclude a particular process from the modeling effort was established if it was determined that consideration of the process (or in some cases the subprocesses needed to define the process) in the TSPA-LA analyses would add complexity to the model without significantly impacting the output (see Assumptions 5.4, 5.6, 5.7, 5.8, 5.9, 5.10, 5.11).

5.1 AMERICIUM BEHAVES SIMILARLY TO PLUTONIUM WITH RESPECT TO ATTACHMENT TO COLLOIDS

Assumption—It is assumed that Am behaves in a similar manner to Pu in terms of mobilization from waste degradation and irreversible association with (i.e., embedment within) smectite colloids formed from defense high-level waste glass.

Rationale—Reasonable assumption based on chemical characteristics of Pu and Am. The binding of Am to soil components has been shown to be similar to Pu and the sorption partition coefficient (K_d value) of Am to freshwater sediments is similar to that of Pu (Coughtrey et al. 1985 [DIRS 154494], see pp. 11 and 119).

Confirmation Status—No confirmation required; this is a bounding assumption.

Section(s) Used In—Section 6.3.1, Colloid Formation and Occurrence, and Section 6.3.3, Radionuclide Sorption to Colloids

5.2 DISTRIBUTION COEFFICIENTS OF THORIUM AND PROTACTINIUM ARE THE SAME AS THAT OF AMERICIUM

Assumption—The K_d values ranges and distributions for Th and Pa are assumed to be those of Am primarily because of limited data on Th and Pa.

Rationale—Because K_d values ranges and distributions for Am are the highest reported in the input data formulating the ranges and distributions (see Table 10, Section 6.3.3.1), this is a conservative bounding assumption with respect to radionuclide attachment to colloids.

Confirmation Status—No confirmation required; this is a bounding assumption.

Section(s) Used In—Section 6.3.3.1, Table 10.

5.3 SORPTIVE CHARACTERISTICS OF CESIUM

Assumption—The K_d value ranges and distributions for Cs are assumed to be those lower than those of Pu, Am, Th, and Pa. Additionally, it is assumed that the adsorption and retention of Cs to smectite is greater than to iron oxyhydroxides.

Rationale—In contrast to the other radionuclides modeled in this analysis (see Table 10, Section 6.3.3.1), dissolved Cs in groundwater tends to be present in the monovalent form (Cs^+). Additionally, unlike the other radionuclides considered in this reversible sorption analysis in this report (see Table 10, Section 6.3.3.1), there is strong evidence that the K_d value ranges and distributions for Cs adsorption and retention should be different for smectite and iron oxyhydroxides. This is based largely on the fact that Cs has been shown to attach very strongly to certain sheet silicate minerals (Brady et al. 2002 [DIRS 161649]).

Confirmation Status—No confirmation required; this is a bounding assumption. The establishment of the K_d value ranges and distributions intentionally encompass a broad range of K_d values, and this approach is deemed to be conservative to the TSPA-LA model analysis.

Section(s) Used In—Section 6.3.3.1, Table 10

5.4 EFFECT OF TEMPERATURE ON WASTE FORM COLLOIDS

Assumption—It is assumed that waste form colloids produced at 90°C are stable at 25°C.

Rationale—The colloid stability ratio predicts increased stability as temperature drops (Section 6.3.2.1, Equation 2); therefore if colloids are stable at 90°C, they should be stable at 25°C.

Confirmation Status—No confirmation required; this is a bounding assumption.

Section(s) Used In—Section 6.3.2, Colloid Stability and Concentration

5.5 PU AND AM EMBEDDED WITHIN DEFENSE HIGH-LEVEL WASTE GLASS COLLOIDS

Assumption—It is assumed that Pu and Am associated with defense high-level waste glass colloids are embedded within the colloids.

Rationale—It was observed that Pu was associated with abundant colloids generated from the corrosion of defense high-level waste glass, but the mechanism of attachment was not determined. The irreversibility of attachment estimates or over-estimates the concentration of radionuclides associated with colloids. Inclusion of Am is based on assumption in Section 5.1.

Confirmation Status—No confirmation required; this is a bounding assumption.

Section(s) Used In—Section 6.3.1, Colloid Formation and Occurrence, and Section 6.3.3, Radionuclide Sorption to Colloids

5.6 PHYSICAL FILTRATION OF COLLOIDS

Assumption—It is assumed that physical filtration of colloids will not occur within the waste package and the drift.

Rationale—Colloid filtration as discussed here refers to the physical removal of colloids from a flow system by pore clogging, sieving, and straining. Filtration of colloids generally means the retention of colloids moving with the suspending fluid in pores, channels, and fracture apertures that are too small or dry to allow passage of the colloids. Two types of physical filtration are recognized (e.g., Wan and Tokunaga 1997 [DIRS 108285]), conventional straining and film straining. Conventional straining filters colloids if they are larger than a pore throat diameter or fracture aperture. Where water saturation is low, colloids may be filtered by film straining if their size is greater than the thickness of the adsorbed water film coating the grains of the rock. The rate of colloid transport through thin water films depends upon the colloid size relative to the film thickness.

Within the waste package, colloids may form within the defense high-level waste glass (e.g., corroded waste fuel pellets) and at its outer surfaces (e.g., corroded defense high-level waste glass). They could be filtered within fractures in fuel pellets or trapped at the boundaries of disaggregating grains. Colloids forming within fuel rods whose cladding has been breached could be filtered at perforations in the cladding. Colloids formed and spalled from the defense high-level waste glass could be filtered at perforations in the stainless steel high-level radioactive waste container. Colloids reaching the interior of the waste package (after escaping from fuel-rod cladding and high-level radioactive waste containers) could be filtered at perforations in the skin of the waste package.

Existing colloid filtration models are empirically derived and so are specific to the system experimentally characterized. There have been no comprehensive studies of colloid filtration within the spent fuel and defense high-level waste glass waste package environments. Meaningful analysis of colloid filtration within the waste package is currently not feasible. Therefore, a conservative assumption is made: all colloids formed within the waste package (the calculated colloid source term) are assumed to exit the waste package and enter the drift without filtration. Inclusion of colloid transport processes resulting in retardation in the waste form or

waste package in the TSPA–Site Recommendation (SR) calculation would reduce interpreted doses.

As an example of a model applied to nuclear waste disposal, Aguilar et al. (1999 [DIRS 161648]) modeled the filtration potential of degraded concrete material in plugged boreholes in an analysis for the performance assessment of the Waste Isolation Pilot Plant in Carlsbad, New Mexico. Their model predicted complete filtration of colloids suspended in Waste Isolation Pilot Plant brines, often in borehole vertical distances of a few meters or less. In this abstraction, all stable colloids are considered to leave a failed waste package through the failure opening and are subsequently not filtered in the surrounding engineered barrier system material—this assumption overestimates the potential consequences of colloid-facilitated transport of radionuclides and is considered bounding.

Confirmation Status—No confirmation required; this is a bounding assumption.

Section(s) Used In—This assumption is used throughout. This process is not modeled and therefore a discussion on its application is not included in this report.

5.7 COLLOID SORPTION AT THE AIR-WATER INTERFACE

Assumption—It is assumed that colloid sorption at the air-water interface will not occur within the waste package.

Rationale—Colloid sorption at the air-water interface may occur within the waste package but is not considered in the abstraction. As colloid sorption to stationary air-water interfaces would retard colloid transport, the assumption that such colloid sorption does not occur over-estimates the potential consequences of colloid-facilitated transport and is considered bounding.

Both hydrophilic and hydrophobic colloids may be sorbed irreversibly at the gas-water interface under partially saturated conditions (Wan and Wilson 1994 [DIRS 114430]). Models of colloid transport in partially saturated media have been developed in recent years, but there have been no experimental studies of transient flow in partially saturated porous media for model comparison and calibration.

As summarized, the concentration of colloids sorbed at the gas-water interface is a function of the following conditions:

- The interface surface area available for colloid uptake, which is a function of the total gas saturation
- The affinity of colloids for the gas-water interface (hydrophobic colloids have higher affinities than hydrophilic colloids)
- The electrostatic charge on the colloid—colloids with lower negative charge exhibit a stronger affinity
- The salinity of the aqueous phase with higher salinity promoting sorption.

Empirical evidence suggests that the sorption of colloids at the gas-water interface is irreversible and the affinity may be stronger than to the rock matrix (Wan and Wilson 1994 [DIRS 114430]).

Partially saturated conditions may be described or classified by considering degrees of saturation. At low water saturations the surface area of the gas-water interface approximates that of the rock matrix. Overall, colloid migration is retarded, although colloids may still move through the adsorbed water films. At intermediate water saturations there is still an interconnected gas phase, although gas flux may be lower. The interface may act as a static sorbing surface, but the estimating geometry and surface area is complicated, more so under changing saturation state. At high water saturations the majority of the gas is present at small gas bubbles that may migrate, transporting sorbed colloids. However, a proportion of the bubbles may become trapped in the rock and will effectively immobilize sorbed colloids.

Colloid migration rates depend more strongly on colloid size as lower saturation states are considered (CRWMS M&O 2000 [DIRS 152773]; McGraw 1996 [DIRS 108218]). To examine the influence of colloid size on transport, McGraw (1996 [DIRS 108218]) investigated transport of monodisperse colloids (five different sizes, between 20 nm and 1900 nm) under both saturated and unsaturated conditions in a quartz sand. The results indicated that under saturated conditions the time required for breakthrough of each colloid at C/C_o = 50 percent was the same as that of the breakthrough of a non-reactive tracer, indicating no relationship of colloid size to migration under saturated conditions. However, the times required for breakthroughs of the colloids under highly unsaturated conditions exhibited a strong relationship between the colloid breakthrough and the colloid size with fairly complete breakthrough of the 20-nm colloid and little or no breakthrough of the 1900-nm colloid.

In another set of experiments, McGraw (1996 [DIRS 108218]) compared four sets of hydrophobic and hydrophilic colloids (functionalized latex microspheres). Her results indicated that transport of hydrophobic colloids depends on colloid size, water film thickness, and colloid charge density. In contrast, hydrophilic colloids were not affected by these variables and were rapidly transported through the system even under very low moisture contents. McGraw (1996 [DIRS 108218]) concluded that for hydrophobic colloids, the cumulative mass of colloids recovered relative to that input into the column was logarithmically dependent upon the ratio of the water film thickness to colloid diameter. In contrast, for hydrophilic colloids, the cumulative mass of colloids recovered relative to that input into the column was linearly dependent upon the ratio of the water film thickness to colloid diameter, similar but more pronounced than the effect with the non-reactive tracer. McGraw's findings suggest that unsaturated porous media may not greatly impede colloid migration, even for relatively large colloids, although larger colloids will tend to be retarded more than smaller ones.

Although the potential effects of degree of saturation on colloid transport are varied and complex, on balance it appears that colloids would be somewhat retarded under low-saturation conditions. Therefore, neglect of colloid sorption onto the air-water interface in the total system performance assessment calculations is conservative.

Confirmation Status—No confirmation required; this is a bounding assumption.

Section(s) Used In—This assumption is used throughout. This process is not modeled and therefore a discussion on its application is not included in this report.

5.8 GRAVITATIONAL SETTLING OF COLLOIDS

Assumption—It is assumed that gravitational settling of colloids will not occur within the waste package.

Rationale—Gravitational settling of colloids may occur within the waste package, but this process is not considered in the abstraction. The use of this assumption, that gravitational settling will not occur within the waste package, results in an overestimation of the consequences of potential colloid-facilitated transport of radionuclides and is considered bounding because all stable colloids are assumed not to settle but to leave a failed waste package through the failure opening.

Confirmation Status—No confirmation required; this is a bounding assumption.

Section(s) Used In— This assumption is used throughout. This process is not modeled and therefore a discussion on its application is not included in this report.

5.9 MICROBES AND COLLOIDAL ORGANIC COMPONENTS

Assumption—It is assumed that processes involving interactions between contaminants and microbes and organic components (such as humic, fulvic acids, and microbial debris) do not affect the stability of inorganic colloids.

Rationale—The assumption that it would be appropriate to ignore colloid-microbe interactions within the engineered barrier system is based on the review of pertinent literature and on professional judgment. This is considered to overestimate the consequences and is considered bounding because biological influences are, for the most part, known to encourage colloid agglomeration (flocculation and settling out). The basis for this argument is presented in Section 6.3.4.

Confirmation Status—No confirmation required; this is a bounding assumption.

Section(s) Used In—Section 6.3.4, Potential Effects of Microbes and Organic Components.

5.10 PARTICLE DENSITY AND SHAPE OF GROUNDWATER COLLOIDS

Assumption—A colloid mineral density of 2.5 g/cm^3 (2.5E-18 mg/nm^3) was assumed in the calculation of colloid mass concentrations from colloid particle data. Furthermore, all colloid particles were assumed to be spherical.

Rationale—These assumptions were founded on documented measurements of particle density on a large range of minerals, including silicate layer-lattice clays (Lide 1995 [DIRS 101876]). Silicate minerals have shown to have a particle density of ranging from 2.27 to 2.33 g/cm^3 at the low range, cristobalite and tridymite, respectively, and 2.67 g/cm^3 at the high range (pure quartz) (Lide 1995 [DIRS 101876], pp. 4-132 through 4-138). Due to the variability in the particle density of silicate layer-lattice clays it is therefore assumed that a value of 2.5 g/cm^3 should be used for groundwater colloids that are primarily silicate layer-lattice clay minerals. The assumption that all colloid particles are spherical is reasonable and is ultimately conservative in that it results in larger masses than the use of other configurations such as sheet or rod shaped

particles of a given diameter size. Note that in Section 6.3.1.3 it is stated that natural groundwater colloids in the vicinity of Yucca Mountain include hematite and goethite. However, for the purposes of modeling the potential effects of groundwater colloids on radionuclide transport, it is stipulated that all natural groundwater/seepage water colloids are smectite.

Confirmation Status—This assumption is used throughout; no confirmation required—assumed density is based on recorded data from standard *Handbook of Chemistry and Physics*. Confirmation of assumed particle shape (spherical) is not necessary since this is established as a bounding assumption.

Section(s) Used In—Attachment I.

5.11 COLLOIDS ARE UNSTABLE IN GROUNDWATER SAMPLES WITH IONIC STRENGTH EXCEEDING 0.05 M

Assumption—For ionic strengths greater than or equal to 0.05 M, the concentration of colloids is assumed to be 1×10^{-6} mg/L. This small deterministic value represents that colloids are unstable (i.e., will agglomerate and settle out of suspension).

Rationale—This assumption is based upon experimental work that has shown the virtual complete flocculation of colloids at high ionic strengths (Liang and Morgan 1990 [DIRS 109524]; Tombacz et al. 1990 [DIRS 112690]; CRWMS M&O 2001 [DIRS 154071]).

Confirmation Status—No confirmation required; this is a bounding assumption. Assumption is deemed sound based on credible published scientific literature.

Section(s) Used In—Attachment I.

5.12 SPECIFIC SURFACE AREA OF IRON OXYHYDROXIDE COLLOIDS

Assumption—It is assumed that the specific surface area (S_A) for iron oxyhydroxide colloids, including α-FeOOH (goethite), α-Fe_2O_3 (hematite), and $Fe(OH)_3 \cdot nH_2O$ (ferrihydrite or hydrous ferric oxide) can range from values as low as 1 to 2 m^2/g to as high as greater than 700 m^2/g.

Rationale—The assumptions are based upon published values in the literature (Langmuir 1997 [DIRS 100051]; Dzombak and Morel 1990 [DIRS 105483]; Davis and Kent 1990 [DIRS 143280]). Davis and Kent and Jenne (1998 [DIRS 162328]) acknowledged that there is large uncertainty in the measurements of specific surface area on iron oxyhydroxide minerals. Therefore, a wide range in S_A values is recommended for use in the TSPA-LA model.

Confirmation Status—No confirmation required; this is a bounding assumption. Assumption is deemed sound based on credible published scientific literature.

Section(s) Used In—Section 6.3.3.2.

6. MODEL DISCUSSION

This section describes the (1) model objectives, (2) features, events, and processes considered in the analysis, (3) base-case model, (4) consideration of alternative models, (5) model formulation for base-case assessment, (6) base-case model results, (7) description and analysis of the barrier capability, and (8) evaluation of alternative models. The supporting information (indirect/corroborative data) used in the analysis is described in Section 4.4.

6.1 MODEL OBJECTIVES

The purpose of this colloid model abstraction is to provide colloid source terms to the total system performance assessment system model. Four waste package types, each containing a different waste type or combination of waste types, are defined in *Yucca Mountain Science and Engineering Report* (DOE 2002 [DIRS 155943]): (1) commercial spent nuclear fuel, (2) a combination of defense high-level waste glass and DOE spent nuclear fuel (codisposal package), (3) defense high-level waste glass, and (4) naval fuel. Colloids will likely be produced as a result of the alteration of defense high-level waste glass (commercial and defense SNF waste forms have not been shown to produce significant quantities of colloids and those that do form are unstable in highly oxidizing environments; see Section 6.3.1.2). The abundance of colloids within the breached waste package will depend on the degree of waste form alteration, on the quantity of steel corrosion product colloids formed, and on quantities of natural colloids present in seepage water. Colloid abundance and stability also depend on many environmental factors including the ionic strength, pH, cation concentrations, colloid content of waters entering the waste package from the drift, presence or absence of fulvic and humic acids, and microbe fragments. Suspended colloids may subsequently flocculate (i.e., particles may coalesce and coagulate) and settle by gravity, be chemically or mechanically filtered, or dissolve. If the environmental factors change through time colloids may be peptized (i.e., dispersed), colloid-sized particles may precipitate, or other natural processes may occur. Furthermore, colloids may sorb readily at the interfaces between air and water in rocks and engineered barriers. Also, depending upon the degree of saturation of the porous medium as well as its configuration, colloids may be retarded (or perhaps even be immobilized) or may be transported. These issues are relevant to colloid transport, which is of primary concern within the engineered barrier system within the drift and in the far field.

Colloids may affect repository performance if they are generated in significant quantities and are stable within the waste package, engineered barrier system, and unsaturated and saturated zones, respectively, and are transported. Colloids could potentially carry a significant radionuclide load and readily transport these contaminants from the engineered barrier system to the unsaturated zone and saturated zone and beyond (see Section 1.1) (Kersting et al. 1999 [DIRS 103282]; Penrose et al. 1990 [DIRS 100811]). Processes relevant to the waste package and surrounding engineered barrier system environment are discussed in this section in the context of the approach to abstraction used in this effort.

In this section the types and concentrations of colloids that could potentially be generated in the waste package from the degradation of the waste (waste form colloids) and corrosion of the waste package (corrosion-generated iron oxyhydroxide colloids) are described. Additionally, the types of colloids that might be produced from the degradation of steel materials introduced

during repository construction and operations are discussed. Additional materials that might be present in the repository include ferrous alloys such as those used in rockbolts and waste package support structures; inorganic liquids such as water for drilling and dust control; organic liquids such as antifreeze, hydraulic fluids, and lubricants. There is currently no concrete or cement grout in the repository design. The treatment here on man-made materials is focused only on steel corrosion products. Potential interactions between inorganic colloids and microbes and organic compounds are discussed in Sections 5.9 and 6.3.4. Also the observed types and concentrations of colloids naturally present in groundwater (groundwater colloids) that would potentially seep or flow into the engineered barrier system during the postclosure regulatory period are described. In addition, sorption and desorption of dissolved radionuclides to and from colloid surfaces are discussed as well as transport characteristics and mechanisms of colloids anticipated in the repository environment. The abstraction is intended to capture the most important characteristics of radionuclide-colloid behavior for use in predicting the potential impact of colloid-facilitated radionuclide transport on repository performance. Colloid transport in the waste package and drift is discussed in *EBS Radionuclide Transport Abstraction* (BSC 2003 [DIRS 163935]).

Output quantities from the waste form and engineered barrier system colloid abstraction to the unsaturated zone include defense high-level waste glass colloid concentrations, corrosion product (iron oxyhydroxide) colloids, and natural groundwater colloids, discussed in Sections 6.3.1 and 6.3.2. Colloids potentially produced from degradation of commercial and DOE SNF are not modeled, for reasons discussed in Section 6.3.1. Three types of radionuclide association with colloids are modeled and described in Section 6.3.3: (1) embedded Pu and Am as a consequence of the formation of colloids from defense high-level waste glass; (2) irreversibly sorbed Pu and Am on iron oxyhydroxide corrosion products colloids; and (3) reversible sorption of Pu, Am, Th, Pa, and Cs onto all colloid types including oxyhydroxide corrosion products.

Model inputs from upstream data sources include ionic strength and pH of the in-package fluid resulting from reaction of water with the waste, ionic strength and pH of the seepage water entering the drift, estimates of colloid masses formed from waste form degradation (Argonne National Laboratory testing), the concentrations of radionuclides generated from degradation of the waste, and K_d values for radionuclides on rocks, minerals, and colloids.

Model outputs feed the unsaturated zone transport models and include (as described above) defense high-level waste glass colloids with embedded radionuclides, irreversibly- and reversibly-sorbed radionuclides, and colloid masses.

The uncertainty associated with the development of parameters representing major processes or features modeled in this analysis is described in general terms in Section 6.6.2, Uncertainty Associated with the Model Analysis. Additionally, specific details on the types of uncertainties associated with the various components of the model elements and the cause(s) for these uncertainties are provided within each of the pertinent subsections of Section 6, Model Discussion and Section 6.3, Base-Case Model.

6.2 FEATURES, EVENTS, AND PROCESSES CONSIDERED IN MODEL

As stipulated in *Technical Work Plan for Waste Form Degradation Modeling, Testing, and Analyses in Support of SR and LA* (BSC 2002 [DIRS 160779], Section 2.1.4), this model report addresses the key colloid-oriented FEPs for the waste form and engineered barrier system components of the repository that are screened in (i.e., Included FEPs) for TSPA-LA (Table 3). FEPs that were screened out (i.e., Excluded FEPs) for TSPA-LA are listed in Table 4.

Each FEP was screened for inclusion or exclusion in the total system performance assessment against three criteria, which are stated as regulatory requirements at NRC's rule 10 CFR 63.114(d)(e)(f)) [DIRS 158535]. The development of a comprehensive list of FEPs potentially relevant to postclosure performance of the potential Yucca Mountain repository is an ongoing, iterative process based on site-specific information, design, and regulations. The approach for developing an initial list of FEPs, in support of TSPA-SR (CRWMS M&O 2000 [DIRS 153246]), was documented in Freeze et al. (2001 [DIRS 154365]). The initial FEP list contained 328 FEPs, of which 176 were included in TSPA-SR models (CRWMS M&O 2000 [DIRS 153246], Tables B-9 through B-17). To support TSPA-LA, the FEP list was re-evaluated in accordance with the Enhanced FEP Plan (BSC 2002 [DIRS 158966]).

Tables 3 and 4 provide lists of FEPs that are evaluated in this model analysis, summarize the details of their implementation in the TSPA-LA model, and provide specific references to the various sections within this document where the issues associated with the FEPs are addressed.

The TSPA-SR FEP identification numbers and names have been changed for the TSPA-LA; however, the changes to the FEPs related to this analyses and document are generally a switch in numbers ending in ".00" to ".0A" (or in one case ".0B"). *Technical Work Plan for Waste Form Degradation Modeling, Testing, and Analyses in Support of SR and LA* (BSC 2002 [DIRS 160779]) lists the FEPs related to waste form that should be included in the total system performance assessment model and refers to this report as the source for the disposition of eight FEPs (see BSC 2002 [DIRS 160779], Table 3A). Deviations from the list of FEPs assigned to this Model Report include:

- Removal of FEP No. 2.1.09.14.00 (see BSC 2002 [DIRS 160779], Table 3A). This FEP was deemed to be too general (i.e., redundant, and should be split to other FEPs), and the effects of the FEP are addressed more succinctly in other FEPs of more detailed scope.

- Addition of FEP No. 2.1.09.02.0A "Chemical Interaction with Corrosion Products" (see Table 3, this document). This FEP was reviewed and determined to be appropriately included in discussion in this document.

- Title of FEP No. 2.1.09.23.00 (BSC 2002 [DIRS 160779], Table 3A) has been changed to "Stability of Colloids in EBS" (see FEP No. 2.1.09.23.0A, Table 3, this document).

- FEP No. 2.1.09.01.00 (BSC 2002 [DIRS 160779], Table 3A) has been split and changed to FEP No. 2.1.09.01.0A and FEP No. 2.1.09.01.0B, which are addressed in

engineered barrier system models (see BSC 2002 [DIRS 160315], Section 1.2.2.3, Table 7) and in the in-package chemistry model report (BSC 2003 [DIRS 163919]).

- Addition of FEP No. 2.1.09.18.0A "Formation of Microbial Colloids in EBS" (see Table 4, this document).

- Removal of FEP Nos. 2.1.09.24.00, 2.1.09.19.00, 2.1.09.05.00, 2.1.09.19.0B, 2.1.09.20.0A, 2.1.09.21.0A, 2.1.09.22.0A, 2.1.09.26.0A, and 2.1.13.03.0A. Of these, the FEPs related to in-package and in-drift transport processes are included in BSC (2003 [DIRS 163935]).

Table 3. Features, Events, and Processes Included (Screened In) in TSPA-LA and Addressed in this Model Report

FEP YMP No.	FEP Title	FEP Description	Location Addressed in Report	TSPA-LA Disposition
2.1.09.02.0A	Chemical Interaction with Corrosion Products	Corrosion products produced during degradation of the waste form and the metallic portions of the waste package may affect the mobilization and transport of radionuclides. Corrosion products may facilitate sorption/desorption and coprecipitation/dissolution processes. Corrosion products may form a "rind" around the fuel that could (1) restrict the availability of water for dissolution of radionuclides or (2) inhibit advective or diffusive transport of water and radionuclides from the waste form to the EBS. Corrosion products also have the potential to retard the transport of radionuclides to the EBS. Finally, corrosion products may alter the local chemistry, possibly enhancing dissolution rates for specific waste forms, or altering radionuclide solubility.	Sections 6.3.1.1, 6.3.1.3, 6.3.2.2, 6.3.2.3, 6.3.2.4, 6.3.3.1, 6.3.3.2	With respect to colloids, the development of altered fuel and glass waste surfaces has been implicitly included by incorporating laboratory data derived from fuel and glass waste corrosion experiments. Corrosion of steel within the waste package is modeled such that iron oxyhydroxide colloids form to which radionuclides may sorb and be transported. The following phenomena related to colloids and waste form degradation are modeled in this Model Report: • Formation of smectite colloids containing embedded (permanently attached) Pu and Am from corrosion of Defense High-Level Waste Glass (DHLWG) (Section 6.3.1.1). • Estimation of stability and mass concentration of smectite waste form colloids, and concentrations of associated Pu and Am, from experimental data and calculated ionic strength and pH of in-package and in-drift fluids (Section 6.3.2.2 and 6.3.2.4). • Reversible sorption of dissolved Pu, Am, Pa, Th, and Cs onto the smectite colloids using developed K_d values and the estimated colloid mass concentrations (Section 6.3.3.1). The following phenomena related to colloids and steel corrosion are modeled in this Model Report: • Formation of iron oxyhydroxide colloids and fixed corrosion products in the waste package (Section 6.3.1.3). • Estimation of stability and mass concentration of iron oxyhydroxide colloids from experimental results and calculated ionic strength and pH of in-package and in-drift fluids (Section 6.3.2.3). • Irreversible sorption of Pu and Am onto iron oxyhydroxide colloids and fixed corrosion products (Section 6.3.3.2). • Reversible sorption of dissolved Pu, Am, Pa, Th, and Cs onto iron oxyhydroxide colloids using developed Kd values and the estimated colloid mass concentrations (Section 6.3.3.1).

Table 3. Features, Events, and Processes Included (Screened In) in TSPA-LA and Addressed in this Model Report (Continued)

FEP YMP No.	FEP Title	FEP Description	Location Addressed in Report	TSPA-LA Disposition
2.1.09.16.0A	Formation of Pseudocolloids (Natural) in EBS	Pseudo-colloids are colloidal-sized assemblages (between approximately 1 nanometer and 1 micrometer in diameter) of nonradioactive material that has radionuclides bound or sorbed to it. Natural pseudo-colloids include microbial colloids, mineral fragments (clay, silica, iron oxyhydroxides), and humic and fulvic acids. This FEP addresses radionuclide-bearing colloids formed from host-rock materials and all interactions of the waste and EBS with the host rock environment except Pseudo-colloids formed from corrosion of the waste form and EBS are discussed in FEP 2.1.09.17.0A. Microbial colloids are discussed in FEP 2.1.09.18.0A. Humic and fulvic acids are discussed in FEP 2.1.09.13.0A.	Sections 6.3.1, 6.3.1.4, 6.3.2.2, 6.3.2.5, 6.3.3.1	Natural colloids are modeled as smectite clay colloids in this Model Report (Section 6.3.1.4). Pseudocolloids generally form as a result of dissolved (aqueous) radionuclides sorbing to existing colloids (Section 6.3.1). K_d values are developed to model reversible sorption of Pu, Am, Th, Pa, and Cs onto smectite groundwater colloids to form pseudocolloids (Section 6.3.3.1). Stability of the colloids is determined based on ionic strength and pH; concentration is modeled as a sampled parameter based on field observations in the Yucca Mountain vicinity (Section 6.3.2.2 and 6.3.2.5).
2.1.09.17.0A	Formation of Pseudo-colloids (Corrosion Product) in EBS	Pseudo-colloids are colloidal-sized assemblages (between approximately 1 nanometer and 1 micrometer in diameter) of nonradioactive material that has radionuclides bound or sorbed to it. Corrosion product pseudo-colloids include iron oxyhydroxides from corrosion and degradation of the metals in the EBS and silica from degradation of cementitious materials. Pseudo-colloids formed from host-rock materials and all interactions of the waste and EBS with the host rock environment except corrosion are discussed in FEP 2.1.09.16.0A. Microbial colloids are discussed in FEP 2.1.09.18.0A. Waste form glass colloids are discussed in FEP 2.1.09.25.0A.	Sections 6.3.1, 6.3.1.3, 6.3.2.3, 6.3.3.1, 6.3.3.2	Colloids formed from the corrosion of steel in the EBS are modeled as iron oxyhydroxide colloids in this Model Report (Section 6.3.1.3). Pseudocolloids generally form as a result of dissolved (aqueous) radionuclides sorbing to existing colloids (Section 6.3.1). K_d values are developed to model reversible sorption of Pu, Am, Th, Pa, and Cs onto iron oxyhydroxide corrosion colloids to form pseudocolloids (Section 6.3.3.1). In addition, Pu and Am are modeled as sorbing irreversibly to iron oxyhydroxide corrosion colloids (Section 6.3.3.2). Stability of iron oxyhydroxide corrosion colloids is determined from the ionic strength and pH of in-package and in-drift fluids (Section 6.3.2.3); mass concentrations are modeled as a sampled parameter based on laboratory studies of the corrosion of miniature waste packages under YMP-relevant conditions and on published studies of iron oxyhydroxide colloid concentrations in groundwaters associated with high-iron bearing geologic strata (Section 6.3.2.3). Both fixed and colloidal corrosion products are modeled in the waste package (Section 6.3.3.2).

Table 3. Features, Events, and Processes Included (Screened In) in this Model Report (Continued)

FEP YMP No.	FEP Title	FEP Description	Location Addressed in Report	TSPA Disposition
2.1.09.23.0A	Stability of Colloids in EBS	For radionuclide-bearing colloids to affect repository performance, the colloids in the dispersion must remain suspended, that is, be stable, for time scales that are long relative to time required for groundwater travel. Further, they must carry significant concentrations of radionuclides. The stability of smectite colloids, which is applicable for YMP groundwater colloids and waste form colloids, is determined primarily by ionic strength but also to an extent by pH. The stability of iron oxyhydroxide colloids, which is applicable to corrosion-product colloids, is determined by both ionic strength and pH.	Sections 6.3.2, 6.3.3, 6.5	Colloids in the EBS modeled in this Model Report are smectite (waste form and groundwater colloids) and iron oxyhydroxide (steel corrosion colloids). Their stabilities are determined from ionic strength and pH of the in-package and in-drift fluids, as calculated in the TSPA-LA model calculations. The stabilities of both smectite and iron hydroxide colloids are determined at each time step executed in the TSPA-LA calculations (Section 6.3.2). These determination are then used to calculate concentrations of radionuclides associated with the colloids (Section 6.3.3). Ionic strength, pH values, and dissolved radionuclide concentrations are taken from intermediate TSPA-LA calculation values from submodels described in the in-package chemistry waste package (ionic strength and pH), solubility limits (dissolved radionuclides), and near-field chemical environment (drift ionic strength and pH) model reports (Section 6.5).
2.1.09.25.0A	Formation of Colloids (Waste Form) by Coprecipitation in the EBS	Dissolved radionuclides and other ions may co-precipitate to form colloids. Co-precipitates may consist of radionuclides bound in the crystal lattice of a dominating mineral phase or may consist of radionuclides engulfed by a dominating mineral phase.	Sections 6.3.1.1, 6.3.2.2, 6.3.2.4	Colloids apparently formed from coprecipitation of smectite and embedded radionuclide-bearing phases were observed in the DHLWG degradation tests (Section 6.3.1.1). Colloids produced from degradation of DHLWG are modeled as smectite colloids with “embedded” (assumed permanently attached) radionuclides (Pu and Am). These may, in a broad sense, be considered coprecipitates. The concentrations of radionuclides associated with those colloids are based on empirical results from YMP-relevant DHLWG corrosion experiments (Section 6.3.1.1 and 6.3.2.4). Mass concentrations of the colloids are based on those experiments together with consideration of colloid mineralogy and the effects of ionic strength and pH on the stability of the colloids (Section 6.3.1.1, 6.3.2.2, and 6.3.2.4).

NOTE: EBS = engineered barrier system; TSPA = total system performance assessment; DHLWG = defense high-level waste glass.

Table 4. Features, Events, and Processes Excluded (Screened Out) in this Model Report

FEP YMP No.	FEP Title	FEP Description	Location Addressed in Report	Technical Basis for Exclusion
2.1.09.18.0A	Formation of Microbial Colloids in EBS	Biological activity is important to consider because of the potential impact on aqueous chemical conditions within the waste and EBS. In deep subsurface environments, biological activity is limited to microbiological activity and may include effects of natural and anthropogenic bacteria (e.g., anaerobic, methanogenic, sulfate reducers, etc.), protozoans, yeast, viruses, and algae. This FEP includes a broad range of effects of biological impacts, including the effects of microbes on corrosion of waste containers, cladding, and the waste form; bioreduction of multivalent contaminants, metals, and sulfate; generation of organic complexants and gases as metabolic by-products; and the formation of biofilms and impact on transport.	Sections 5.9, 6.3.4	The effects of colloid-facilitated radionuclide transport stemming from biological activity have generally been excluded from the TSPA-LA on the basis of low probability and consequence. Because inorganic aqueous conditions dominate DHLWG degradation rates, and microbial degradation is secondary, this is excluded on the basis of low consequence. The potential influence of organic complexants from microbial metabolism on radionuclide transport is assumed not to affect the stability of inorganic (mineral) colloids (Sections 5.9 and 6.3.4), i.e., inorganic colloid stability is determined by fluid chemistry (ionic strength and pH); therefore this process is also excluded on the basis of low consequence. Microbe-induced reduction of radionuclide, metal, and sulfate contaminants would decrease their mobility (see Section 6.3.4), which is beneficial, and therefore excluded on the basis of low consequence. Since biofilms would tend to retard radionuclides, which is beneficial, this process is also excluded on the basis of low consequence. Consequently, it is concluded that there will not be a significant change in either time or magnitude of the expected annual dose due to microbial activity in the EBS.
2.1.09.15.0A	Formation of true (intrinsic) colloids in EBS	True colloids are colloidal-sized assemblages (between approximately 1 nanometer and 1 micrometer in diameter) consisting of hydrolyzed and polymerized radionuclides. They may form in the waste package and EBS during waste-form degradation and radionuclide transport. True colloids are also called primary colloids, real colloids, Type I colloids, Eigenkolloide, and intrinsic colloids (or actinide intrinsic colloids, for those including actinide elements).	Section 6.3.1	True colloids may form from saturated solutions in close proximity to degrading waste (Section 6.3.1). However, true colloids may not be routinely detectable, as they would be determined as dissolved radionuclides. Further, they would be likely to dissociate in dilute fluids as well as sorb to substrates. Therefore, the formation of true colloids in the EBS has been excluded from the TSPA-SR on the basis of low consequence.

NOTE: EBS = engineered barrier system; DHLWG = defense high-level waste glass.

6.3 BASE-CASE MODEL

A discussion of the colloid model is presented here, organized by major concepts considered and the specific ideas and values developed and incorporated into the model. Accordingly, the following subjects are discussed: colloid formation from defense high-level waste glass, commercial SNF, and DOE SNF; formation of corrosion products, including colloids, from degradation of steel within the waste package and drift; natural occurrence of groundwater colloids; stability and concentration of all modeled colloid types; radionuclide attachment to colloids; and microbial interactions.

For reasons explained in the following respective sections, colloids potentially generated from the degradation of commercial and DOE SNF are not included in the colloid model abstraction. However, to present the background information that was necessary to reach this decision, relevant research is described in Section 6.3.1, including laboratory testing and natural analog field observations.

Colloids formed from corrosion of introduced materials are modeled only as iron oxyhydroxide colloids. As described in Section 6.1, materials introduced during repository construction may include various steel alloys, organic liquids, and cementitious materials. Concrete and cement grout are currently not a part of the repository design, and colloids derived from them are not considered. The assumption is made that microbes and organic compounds do not affect the stability of inorganic colloids (colloids comprised of mineral fragments); therefore, organic colloids are not modeled (see Section 5, Assumption 5.9). Potential interactions between inorganic colloids and microbes and organic compounds are discussed in Sections 5.9 and 6.3.4.

6.3.1 Colloid Formation and Occurrence

Following is a discussion of colloid types, definitions, and pertinence to the repository. A summary of the colloid types modeled in this abstraction is provided at the end of this section. Figure 1 is a schematic illustrating colloid types.

Colloids by definition have at least one dimension between 1 nm and 1 μm. Often, particularly in reporting of experimental results, the upper end of the colloid size range is 450 nm, due to conventional dimensions of laboratory equipment (primarily filters).

True Colloids—True colloids are colloidal-sized assemblages (between approximately 1 nanometer and 1 micrometer in one dimension) formed from the hydrolysis and polymerization of actinide ions dissolved in solution. They may form in the waste package and engineered barrier system during waste form degradation and radionuclide transport. True colloids are also called primary colloids, real colloids, Type I colloids, Eigenkolloide, and intrinsic colloids (or actinide intrinsic colloids, for those including actinide elements). The formation of real colloids will be solubility limited, based on the solution chemistry. This prevents significant introduction of real colloids to the environment (CRWMS M&O 2001 [DIRS 154071], Section 6.1). There has been no evidence of their formation in Argonne National Laboratory defense high-level waste glass degradation tests (Ebert 1995, Sections 6.2.1 and 6.2.2 [DIRS 113219]), and even if present they would be difficult to detect. Degradation of commercial SNF may form real colloids (e.g., schoepite-like U hydroxides) close to the fuel surface where the fluid may be

saturated with respect to U, but they are likely to dissolve in unsaturated fluid. In addition, "the generation and migration of real colloids is of no consequence in natural aquifer systems because real colloids…undergo formation of pseudocolloids in the near- or far-field aquifer system" (Kim 1994 [DIRS 109521], p 50). For these reasons, true colloids are not modeled in the abstraction.

Waste Form Colloids—Waste form colloids may provide one of the most significant contributions to colloid-facilitated radionuclide transport. These colloids form from the nucleation of colloids from waste form dissolution and from spallation (flaking off) of colloid-sized waste form alteration products. Waste form colloids contain radionuclides and have the potential for increasing mobile radionuclide concentrations to levels higher than achievable with real colloids or pseudocolloids (CRWMS M&O 2001 [DIRS 154071], Section 6.1). Dissolved radionuclides and other ions may co-precipitate to form colloids. Co-precipitates may consist of radionuclides bound in the crystal lattice of a dominating mineral phase or may consist of radionuclides engulfed by a dominating mineral phase.

Four broad categories of waste form are to be placed in the repository (DOE 2002 [DIRS 155943]). The most abundant waste type is commercial SNF from commercially owned and operated electric power reactors. DOE SNF is a diverse collection of waste from reactors at DOE nuclear complex sites. Defense high-level waste glass is a borosilicate glass-based waste form containing radionuclides. In the following descriptions, commercial and DOE SNF are treated together.

Investigations of the degradation of defense high-level waste glass (CRWMS M&O 2001 [DIRS 154071]) show that waste form colloids have formed by co-precipitation of radionuclide-bearing phases with colloid-sized clay phases formed homogeneously in the solution contacting the waste. Under conditions in which water drops onto the waste, spallation of colloid-sized fragments of co-precipitated clay (primarily) and radionuclide-bearing phases from the alteration layers formed on the waste form surfaces. Through these mechanisms, radionuclide-bearing phases can become embedded in alteration phases, primarily clays.

Pseudocolloids—Pseudocolloids are colloidal-sized particles (between approximately 1 nanometer and 1 micrometer in diameter) that consist of usually (but not necessarily) nonradioactive particles with radionuclides sorbed to them. Natural pseudocolloids include mineral fragments formed from the host rock, microbes and microbe fragments, and humic and fulvic acids. Pseudocolloids form as a result of dissolved (aqueous) radionuclides sorbing to existing colloids (e.g., clay, iron oxyhydroxides, silica). At YMP, pseudocolloids may develop as a result of radionuclide association with waste form colloids formed during degradation of defense high-level waste glass; radionuclide association with corrosion-product colloids formed during corrosion of waste package materials and other metallic materials; and radionuclide association with naturally occurring groundwater colloids present in YMP groundwater.

Seepage/Groundwater Colloids—Naturally occurring colloids (referred to in this report as "groundwater colloids") may be inorganic (mineral fragments) or organic (microbes and humic substances). At YMP, inorganic groundwater colloids, primarily consisting of clay, silica, and iron oxyhydroxides, may be transported in seepage water into the repository from the vadose zone above it or may be formed due to changes in chemical conditions near the repository.

Pseudocolloids may form due to the sorption onto these natural colloids of radionuclides mobilized from degradation of the waste form. Pseudocolloids thus formed in the waste and engineered barrier system may influence radionuclide transport. At YMP, organic colloids are not important. Humic substances are not sufficiently abundant in YMP groundwaters to impact transport (Section 6.3.1.4). Microbes, as large colloids, are susceptible to filtration during transport.

Colloids are modeled in the abstraction as follows:

- Waste form colloids. Colloids from the corrosion of defense high-level waste glass (Section 6.3.1.1) are modeled as smectite colloids with "embedded" Pu and Am. Colloids from the corrosion of commercial and DOE SNF are not modeled (Section 6.3.1.2).

- Corrosion product colloids. Colloids from the corrosion of steel components in the engineered barrier system are modeled as iron oxyhydroxide colloids, as they will likely be a mixture or combination of hydrous ferric oxide, goethite (FeOOH), and hematite (Fe_2O_3) (Section 6.3.1.3).

- Seepage/groundwater colloids. Naturally occurring colloids are modeled as smectite colloids (Section 6.3.1.4). Such components of groundwater colloids as humic and fulvic acids, microbes and their detritus and metabolic products are not modeled.

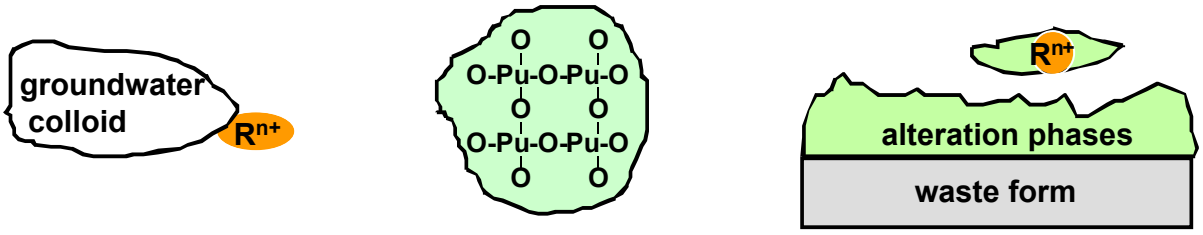

(a) (b) (c)

NOTE: Several types of radionuclide-bearing colloids are depicted: (a) pseudocolloids, (b) true colloids, and (c) waste form colloids. The radionuclide (R^{n+}) associated with the pseudo and waste form colloids can be an ionic species, a real colloid, or a discrete radionuclide-bearing phase. The size range for the colloids is approximately 1 to 1000 nm.

Source: Adapted from CRWMS M&O 2001 [DIRS 154071], Figure 1.

Figure 1. Several Types of Radionuclide-Bearing Colloids

6.3.1.1 Colloids from the Corrosion of Defense High-Level Waste Glass

A description of colloids formed from the corrosion of defense high-level waste glass under unsaturated (drip) test conditions and under static-saturated (product consistency test) test conditions is presented in this section. The unsaturated tests are thought to be representative of conditions likely to occur in a geologic repository with simulated aged canister components

present and periodic injection of groundwater and air. The unsaturated tests allow the spallation mechanism to be examined (Section 6.4.2). The static tests appear to be a suitable method for simulating colloid formation from glass reaction (Buck and Bates 1999 [DIRS 109494]) where similar colloids (smectite clay and rhabdophane colloids) are formed in both unsaturated and saturated tests. Metal-bearing oxide colloids (birnessite, asbolane, and iron oxides) have been detected only in the unsaturated tests, most likely due to the presence of the aged canister components. Uranyl silicates and U-Ti phases have only been found in the saturated tests under conditions that promote saturated silica solutions from the reacted glass corrosion.

Colloids formed from the corrosion of defense high-level waste glass are included in the colloid model and abstraction (Sections 6.3.2.4 and 6.5.1). They are modeled as smectite with associated Pu and Am embedded within (or otherwise permanently attached to) the colloids. This is based on observations of colloids with associated Pu that formed during corrosion testing of defense high-level waste glass at Argonne National Laboratory. A description of the testing follows.

Testing on corrosion of defense high-level waste glass has gone on for over four years in the case of static-saturated tests wherein glass samples are immersed in fluid and for over sixteen years in the case of drip tests where fluid is dripped at specified rates onto the glass sample (CRWMS M&O 2001 [DIRS 154071]). In the static tests, surface area (SA) of the sample was varied relative to the volume (V) of fluid used; this proportion is referred to as SA/V. SA was determined using geometric estimates of crushed materials, not by a gas adsorption method. Glass waste forms tested include Savannah River Laboratory and West Valley Demonstration Project glasses. Fluids used were tuff-equilibrated J-13 water (EJ-13) and deionized water. Methods used to characterize colloids produced during the tests include transmission electron microscopy and filtration (analysis of filtrates with inductively coupled plasma-mass spectrometry or alpha spectroscopy; CRWMS M&O 2001 [DIRS 154071], Section 6.2). Descriptions of the tests may be found in *Colloid-Associated Radionuclide Concentration Limits: ANL* (CRWMS M&O 2001 [DIRS 154071], Section 6.2.1) and Ebert (1995 [DIRS 113219]).

Colloids produced from the degradation of both types of glass waste were primarily smectite clay containing discrete radionuclide-bearing phases, which are incorporated (embedded) in the clay (CRWMS M&O 2001 [DIRS 154071], Section 6.2.1). Iron silicate colloids were also observed. The embedded phases were identified as primarily brockite (thorium calcium orthophosphate) and an amorphous thorium-titanium-iron silicate, similar to thorutite. The phases also contained other actinides and rare earth elements. Uranium was detected within the clays and iron silicates in some samples.

Currently, limited data are available on the chemical and physical properties of the embedded phases, so that their solubility and disassociation/association properties with the clay cannot be derived and used in the model. The colloidal properties of the embedded radionuclide-bearing phases, therefore, appear to be governed by the properties of the smectite, and the stability (and therefore mobility) of smectite colloids will control the mobility of the embedded phases. Accordingly, the radionuclides are stipulated to be embedded within the smectite colloids.

As stated above, other colloidal phases (besides smectite) have been identified from the saturated and unsaturated defense high-level waste glass corrosion tests. These include manganese-based clays (asbolane and birnessite), phosphate phases (calcium silica phosphate and rare-earth phosphates), carbonate-bearing phases (calcite and dolomite), and uranyl silicates (weeksite) or uranium Si-Ti bearing phases (Buck and Bates 1999 [DIRS 109494]).

Figure 2 depicts the process of defense high-level waste glass degradation with the subsequent formation of waste form colloids. As the glass corrodes, the clay alteration product forms, grows, and evolves as a layer on the surface of the glass. The clay layer grows as the glass beneath the clay is altered and clay-forming elements saturate in the solution and subsequently precipitate on the clay surface. Through these mechanisms colloid-sized clay that does not attach to the clay layer may also precipitate from the solution in proximity to the clay layer (CRWMS M&O 2001 [DIRS 154071], Section 6.2.1).

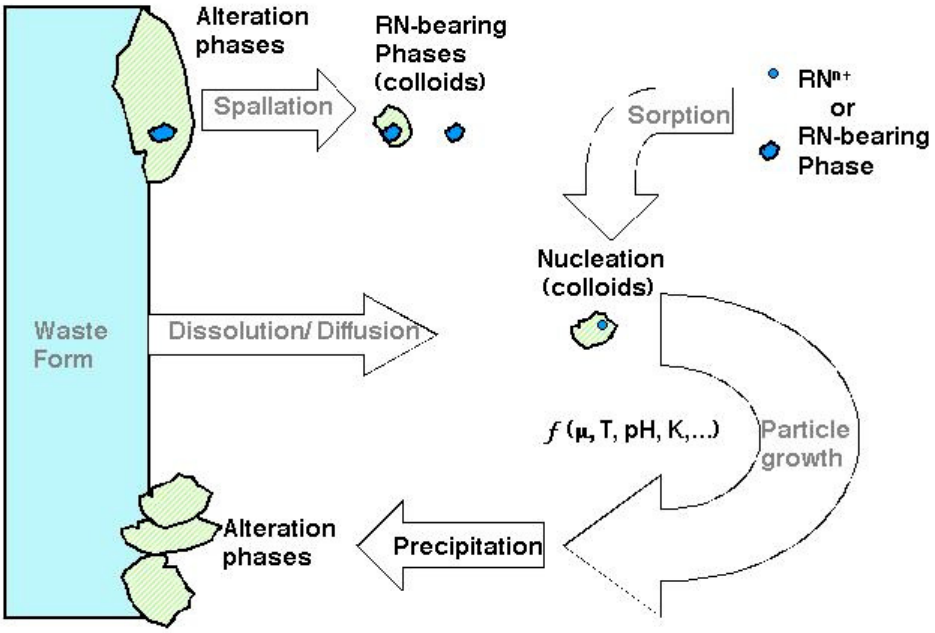

NOTE: Schematic of colloid formation from waste form corrosion whereby several processes are represented: (1) spallation of radionuclide bearing alteration phases from the waste form that are within the colloidal size range, and (2) nucleation of colloids from ions dissolved from the waste form and sorption of ionic radionuclide species or radionuclide -bearing phases. Particle growth occurs by precipitation on nuclei and is controlled by factors such as ionic strength, temperature, pH, and solubility. When particle diameters exceed 1 micron or solution chemistry destabilizes the colloids, deposition, or coagulation and gravitational settling of radionuclide-bearing alteration phases occur.

Source: Modified from Figure 2, CRWMS M&O 2001 [DIRS 154071].

Figure 2. Schematic of Colloid Formation from Waste Form Corrosion

It was observed in the static-saturated tests that colloids developed and increased in concentration (population) with time, up to a point where the colloid concentration reached a

maximum and produced an unstable dispersion. This was attributed by the investigators primarily to the concomitant increase in ionic strength to a threshold above which the colloids flocculated and settled by gravity (CRWMS M&O 2001 [DIRS 154071], Section 6.2.1).

Based on these Argonne National Laboratory's experimental results (DTNs: LL991109751021.094 [DIRS 142910], LL000905312241.018 [DIRS 152621], the following approximate relationship was developed from inspection of the data presented in Figures 3 and 8 and may be used to relate the Pu concentration to colloid concentration:

$$1 \text{ ppm colloids} \equiv 2 \times 10^{-8} \text{M } Pu_{coll} \quad \text{(Eq. 1)}$$

Pu_{coll} is the concentration of Pu associated with colloids. To enable the use of bounding values for applying the relationship, the approximate maximum (and bounding) value for Pu_{coll} of 1×10^{-7} from Figure 8 was adopted to correspond with the approximate maximum (and bounding) colloid mass concentration of 5.0 ppm from Figure 3. Division of maximum Pu_{coll} by the maximum colloid mass concentration yields the relationship in Equation 1.

Since Pu and Am are assumed to behave similarly (Section 5.1), the colloid-associated Am concentration was calculated by multiplying the ratio of Am to Pu in the radionuclide inventory by the Pu concentration at each time step of the TSPA-LA model calculations.

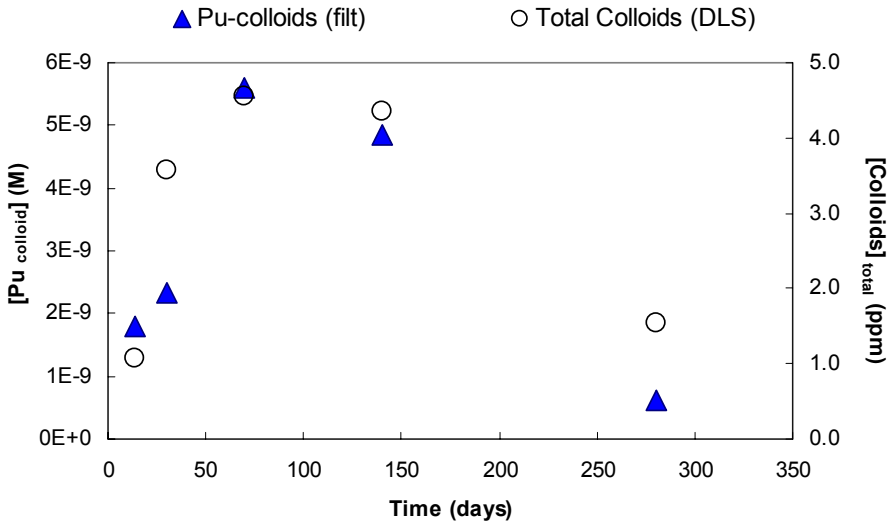

NOTE: Plutonium concentration associated with colloids fraction (6 to 450 nm size fraction from filtration data) and total colloid concentration (from dynamic light scattering measurements) as a function of test duration for the SRL 131A glass at 2,000/m (T = 90°C). The triangles, representing concentration of plutonium in filtered colloids, correspond to the left axis. The circles, representing the total colloid mass, correspond to the right axis. Note that, with the scales used in the graph, the triangles and circles coincide.

Source: Adapted from CRWMS M&O 2001 [DIRS 154071], Figure 24; DTN: LL000905312241.018 [DIRS 152621], data: p. 70, 131A/2K, time 14–980 days, Pu_s(M); right-hand x-axis values from DTN: LL991109751021.094 [DIRS 142910], p. 32.

Figure 3. Concentrations of Pu and Colloids as a Function of Defense High-Level Waste Glass Corrosion Test Duration

6.3.1.2 Colloids from the Corrosion of Commercial and DOE Spent Nuclear Fuel

Long-term corrosion testing of commercial SNF and DOE SNF under hydrologically unsaturated, oxidizing conditions have been performed to examine the release of radionuclides and, specifically for the context of this report, the release in the form of colloids. Testing was designed to simulate a variety of Yucca Mountain repository relevant water-exposure conditions for several spent nuclear fuels with a range of fuel burnups and compositions. Results from the unsaturated testing of commercial SNF and DOE SNF indicated spallation of alteration products containing low concentrations of uranium-based colloids (and low concentrations of actinides), dissolution of the uranium-based colloids over a short time duration (less than several months), and sorption dominating the behavior of the actinides (onto clay colloids or onto metal surfaces). Thus, colloids from commercial SNF and DOE SNF were neglected in the colloid modeling and abstraction based upon the unsaturated testing results from the commercial SNF and DOE SNF, characterization of uranium phase colloid suspensions, and natural analog studies. A summary of results affecting colloid release from the fuels during unsaturated testing is presented in Sections 6.3.1.2.1 and 6.3.1.2.2.

6.3.1.2.1 Commercial Spent Nuclear Fuel

Assessment of the importance of potential colloid formation from commercial SNF is based on four major observations: (1) very low colloid concentrations were observed in the commercial SNF degradation tests, at least an order of magnitude less than concentrations observed in the defense high-level waste glass degradation tests (based on dynamic light scattering measurements) (Mertz et al. 2003 [DIRS 162032]); (2) the fraction of uranium in the colloid mass was uniformly low in the commercial SNF tests, the only deviation from this occurring immediately following one of two changes in vessel configuration in which the uranium fraction increased but rapidly decreased to the approximate level of earlier values (Mertz et al. 2003 [DIRS 162032]); (3) suspensions of meta-schoepite and UO_{2+x} colloids in J-13 groundwater appear to dissolve in short-term hydrologically saturated tests; their stability in unsaturated solutions has not been tested (Mertz et al. 2003 [DIRS 162032]); and (4) field studies at uranium-bearing deposits indicate generally that under oxidizing conditions at near-neutral pH, colloid particles contain little uranium and there is little sorption of uranium complexes to colloids.

In contrast to the defense high-level waste glass unsaturated tests, few colloids have been detected in the test solutions from unsaturated corrosion tests of commercial SNF under likely water contact scenarios at Yucca Mountain (Mertz et al. 2003 [DIRS 162032]). A detailed discussion of the tests and uncertainties is found elsewhere (Mertz et al. 2003 [DIRS 162032]); only a summary of the test results and uncertainties associated with the testing follows here. One of the reasons surmised for the low colloid release in the commercial SNF tests was the test configuration in which the Zircaloy-4 support for the fuel fragments had 7-micron holes. However, the results from the unirradiated UO_2 tests also show few colloids after the formation of alteration products (Wronkiewicz et al. 1997 [DIRS 102048]). The unsaturated tests on unirradiated UO_2 had a test configuration with large 2–3 mm holes at the holder base allowing for the spallation of UO_{2+x} particulate during initial corrosion; however, the formation of a dense mat of alteration products during the UO_2 corrosion apparently reduced particulate release by trapping particulate in the altered products (Wronkiewicz et al. 1997 [DIRS 102048]). A similar

mechanism whereby the alteration products minimize particulate release may be applicable to the commercial SNF unsaturated tests.

The concentration of released particulates or colloids from the commercial SNF tests is very low except during test conditions corresponding to disruptive events, such as movement of the fuel from one retainer to another (Mertz et al. 2003 [DIRS 162032]). In that case, colloid and particulate concentrations increased temporarily but returned to very low concentrations after the disruption (Mertz et al. 2003 [DIRS 162032]). While this indicates that disruptive events may contribute to the release of particulates and colloids from commercial SNF, it also indicates that the longevity of the colloids in the leachate is short. It is possible that the dense mat of alteration products acts as a filter for reducing particulate concentrations under unsaturated test conditions as was observed in the unirradiated UO_2 tests (Wronkiewicz et al. 1997 [DIRS 102048]). The stability of these alteration phases is unknown at this time. Likewise, it is possible that the uranium-bearing colloidal material dissolved in the chemically under-saturated leachate.

During the oxidative dissolution of commercial SNF in the Argonne National Laboratory unsaturated tests, a suite of alteration products were formed on the fuel surface. In the vapor tests (corrosion of UO_2 with water vapor), uranyl oxyhydroxides were observed, such as dehydrated schoepite and meta-schoepite. However, the introduction of sodium and silicon-rich groundwater in the drip tests allow the incorporation of sodium and silicon in the alteration products. In the high drip rate tests, Na-, Ca-, and Si-bearing uranyl compounds were identified (such as Na-boltwoodite, $(Na,K)(UO_2)(SiO_3OH)(H_2O)$). Of those colloids identified in the commercial SNF tests (CRWMS M&O 2001 [DIRS 154071], Section 6.2.2), one sample contained primarily a hydrous uranium oxide (schoepite) and a partially crystalline uranium silicate (soddyite). The colloids contained the rare earth elements: La, Ce, Pr, Nd, Sm, and Eu. Plutonium was not detected in these colloids; however, alteration on the corroded surface of the spent fuel contained significant concentrations of Pu, along with Zr, Ru, and rare earth elements in a layer approximately 100 nm thick (CRWMS M&O 2001 [DIRS 154071], Section 6.2.2). In another sample, smectite clay colloids were formed that were similar structurally and compositionally to the smectites produced in the glass tests.

The primary sources of uncertainty include measurement errors and limitations associated with the test design and apparatus. Measurement uncertainties arise from determination of mass, calculation of volume, determination of particle sizes by filtration, and measurement of concentrations by inductively coupled plasma mass spectroscopy. Experimental uncertainties include localized inhomogeneity of nuclides in irradiated fuel and loss of leachate or fuel during sampling operations. Discussion of these uncertainties is found in the commercial SNF colloid data report (Mertz et al. 2003 [DIRS 162032]).

6.3.1.2.2 DOE Spent Nuclear Fuel

Of the approximately 250 different types of fuel in the DOE SNF inventory, metallic uranium fuel comprises approximately 85 percent (by weight) of that inventory and thus was selected for corrosion testing. An irradiated uranium metal fuel from the N-Reactor at Hanford was tested in an experimental setup similar to that used at Argonne National Laboratory for testing commercial SNF. Additional details on the testing can be found elsewhere (DTN: MO0306ANLSF001.459 [DIRS 163910]). Corrosion testing of metallic uranium samples

resulted in rapid oxidization (within a few months) of the uranium primarily to an oxide sludge consisting of UO_2 and higher oxides of uranium (DTN: MO0306ANLSF001.459 [DIRS 163910]). Although the uranium fuel disintegrated rapidly, corrosion testing was continued to determine the effect of groundwater leaching on the fuel sludge. Results from the corrosion tests showed that the composition of the DOE SNF colloids evolve over time from an initially UO_2-rich population, to a mixed colloid population containing UO_2 and higher oxides of U as well as smectite clays, to a population that appears to be dominated by U-containing smectite clays.

After approximately one year of testing the DOE SNF, the total quantity of uranium in the sludge represented approximately 99 weight percent of the original uranium fuel sample, while that in the colloid size group corresponded to 0.002 to 0.006 weight percent of the original uranium fuel sample. The quantity of uranium in the sorbed fraction was 0.1 to 0.3 weight percent of the original fuel sample (DTN: MO0306ANLSF001.459 [DIRS 163910]). Sorbed material is operationally defined as material that adhered to the stainless steel vessel wall and was subsequently solubilized in HNO_3; it includes sorbed solutes, sorbed colloids, and precipitates (DTN: MO0306ANLSF001.453 [DIRS 163910]). The disposition of Pu during DOE SNF corrosion showed that Pu is associated predominantly with the colloidal, particulate, and sorbed size fractions. The $^{239}Pu/ ^{238}U$ ratios in the colloid fraction are significantly larger than those in the other fractions (sorbed, particulate, and dissolved) and is the only fraction that showed enrichment of Pu in comparison to that in the fuel prior to corrosion (DTN: MO0306ANLSF001.459 [DIRS 163910]). Results from the testing support a model of metallic uranium corrosion in which Pu is both incorporated in spalled particulates and colloids and is significantly adsorbed to the surface of colloids (such as groundwater clays) upon dissolution of spalled particulates or colloids (DTN: MO0306ANLSF001.459 [DIRS 163910]).

Uncertainties associated with these data and experiments include measurement uncertainties and uncontrolled experimental factors. Measurement uncertainties arise from determination of mass, calculation of volume, determination of particle sizes by filtration, and measurement of concentrations by inductively-coupled plasma mass spectroscopy. Experimental uncertainties include localized inhomogeneity of nuclides in irradiated metallic uranium fuel, loss of sludge particles from the sample holder during sampling operations, and most significantly the extrapolation of results from only two samples of irradiated fuel. Additional discussion of the uncertainties associated with the DOE SNF unsaturated testing is found elsewhere (DTN: MO0306ANLSF001.459 [DIRS 163910]).

6.3.1.2.3 Uranium Phase Colloid Suspensions

As uranium-based spent nuclear fuels will be prevalent at the high-level waste repository at Yucca Mountain, the colloidal properties of a mixture of two uranium minerals under saturated conditions that promote stable colloids have been examined (Mertz et al. 2003 [DIRS 162032]). The results suggest that meta-schoepite, $(UO_2)_4(OH)_6 \cdot 5H_2O$, and UO_{2+x} colloids are stable under short-duration tests with respect to dissolution and interparticle interactions at near neutral and higher pH values in solutions saturated with respect to these phases (Mertz et al. 2003 [DIRS 162032]). However, under repository relevant conditions, these colloids appear to dissolve after introduction to J-13 groundwater in short duration tests (reduction in colloid size and 84 percent of the uranium was in the dissolved fraction) (Mertz et al. 2003 [DIRS 162032]).

6.3.1.2.4 Field Evidence from Natural Analogs

There are several published studies of uranium mobility and transport at uranium mines and deposits and at locations where other metals are mined. Examples are the Koongarra and Nabarlek uranium deposits in Australia (Short et al. 1988 [DIRS 113937]; Payne et al. 1992 [DIRS 124812]) and the Freiberg zinc-lead-silver mine in Germany (Zänker et al. 2000 [DIRS 162746]). All of the references studied suggest that colloidal uranium will not be a significant contributor to colloid-associated radionuclides under the oxic and essentially pH-neutral conditions prevailing at Yucca Mountain.

Zänker et al. (2000 [DIRS 162746]) investigated a unique situation at the Freiberg mine in which anoxic, relatively acidic mine water issued into oxic drainage gallery water and formed, in the authors' words, "a large geochemical colloid generator." The colloids sampled in the drainage gallery were primarily iron and aluminum hydroxides, ranging in size from 100 to 300 nm and in concentrations of about one mg/L. In the mine water (pH approximately 5) uranium occurred mainly as UO_2CO_3,aq, and approximately 50 percent of total uranium was associated with the relatively few colloids measured. In the oxidized, more neutral drainage gallery water (pH approximately 7.2), uranium occurred mainly as $Ca_2UO_2(CO_3)_3$,aq and $UO_2(CO_3)_2^{-2}$, and the fraction of uranium associated with colloids was essentially zero.

Zänker et al. (2000 [DIRS 162746]) stated that, "[u]ranium showed strictly 'non-colloidal' behavior," and conducted experiments (acidification of samples with nitric acid) to investigate the phenomena observed. They noted that the colloid fraction decreased with decreasing pH, and that the maximum uranium sorption onto colloids occurred at about pH 5. They concluded that acidification destroys uranyl carbonato complexes of ligand numbers greater than one, and as a result uranyl prevails and sorbs to colloids in the mine water. In the neutral drainage gallery water the prevailing uranyl carbonato complexes prevent the uranyl from being adsorbed to the colloids while not sorbing themselves.

The uranium deposit at Koongarra and Narbalek, Northern Territory, Australia, has groundwater that is of low salinity, pH from approximately 6.5 to 7.5, Eh above about +50, and with Mg^{2+} and HCO_3^- as the primary dissolved ions (Short et al. 1988 [DIRS 113937]). Colloids are primarily iron oxyhydroxides and clays, with variable amounts of silica and discrete silica colloids. The colloid sizes ranged from about 18 nm to 1 μm. Fe-colloid concentrations ranged from 1.6 to 4.9 μg/L (one value was 7.9 μg/L); Si-colloids from less than 1 to 37 μg/L (Short et al. 1988 [DIRS 113937]). Particles containing primarily uranium were noted, with sizes of 0.04 to 0.3 μm and concentrations of about 10^8 pt/L (particles per liter; mass concentrations were not reported; Payne et al. 1992 [DIRS 124812]).

Short et al. (1988 [DIRS 113937]) noted that uranium occurs mostly as soluble species; the fraction of total uranium associated with colloids is reported as 2 percent at Nabarlek and up to 11 percent at Koongarra. Payne et al. (1992 [DIRS 124812]) report that in the ore zone the uranium particles comprised less than 1 percent of the total uranium; generally the colloidal uranium makes up from 0.1 to 0.5 percent of the total uranium (one sample was measured at 6.5 percent, but it was distant from the ore body where the total uranium was several orders of magnitude lower).

Dissolved uranium concentrations at Nabarlek and Koongarra decline logarithmically to background with distance down gradient (three orders of magnitude over distances of 125m, Nabarlek, and 200m, Koongarra) (Short et al. 1988 [DIRS 113937]). Colloids down gradient were found to be more depleted in ^{234}U than the solute; this was interpreted by Short et al. (1988 [DIRS 113937]) as systematic leaching of uranium from the colloids. Payne et al. (1992 [DIRS 124812]) estimated that the down-gradient uranium dispersion fan has developed over about two million years.

The Cigar Lake uranium deposit in northern Saskatchewan was studied to evaluate analog features with respect to nuclear fuel disposal. Colloids (1–450 nm) and suspended particles (greater than 450 nm) were measured from 501 groundwater samples. The groundwater has low ionic strength and pH values from 5.6 to 7.7 (Vilks et al. 1993 [DIRS 108261]). Particles ranged in size from 10 nm to about 20 μm; concentrations of colloid-size particles were mostly 1 mg/L or less, although several samples up to 4 mg/L, and two samples up to 13 mg/L, were noted. Low-integrity rock and overburden yielded groundwater with the highest colloid concentrations.

Colloid compositions were primarily clay minerals, X-ray-amorphous Fe-Si oxyhydroxides, quartz, and organic particles. The larger colloid-size fractions contain more iron than the smaller fractions. U concentrations associated with all particles analyzed (including particles larger than colloids) ranged from about 60 to 600 μg/g.

Vilks et al. (1993 [DIRS 108261]) conclude that colloid concentrations at Cigar Lake are sufficiently low that they would have little impact on radionuclide migration, as long as radionuclide attachment is reversible. In that regard, Vilks et al. report that while ^{230}Th and ^{234}U are in secular equilibrium in the host rock, dissolved $^{230}Th/^{234}U$ is very low, as is the ratio for ^{230}Th and ^{234}U sorbed onto particles. This is interpreted as ^{230}Th not having had time to reach secular equilibrium with its parent. Vilks et al. state further that *if* ^{230}Th on particles has ingrown from ^{234}U, *and* has not been sorbed from water, then the particles could be as much as 8,000 years in age.

6.3.1.3 Colloids from the Corrosion of Waste Package and Metallic Invert Materials

The occurrence of iron oxyhydroxide colloids from the corrosion of waste package and metallic invert materials is included in the colloid model. Conceptually (and for purposes of estimating specific surface area and site density for irreversible sorption calculations; see Section 6.3.3.2) the iron oxyhydroxide colloids are likely to be comprised of three species, under the anticipated repository conditions: α-FeOOH (goethite), α-Fe_2O_3 (hematite), and $Fe(OH)_3 \cdot nH_2O$ (ferrihydrite, or hydrous ferric oxide) (Langmuir 1997 [DIRS 100051], p. 436-437). Goethite forms from hydrous ferric oxide by dissolution-reprecipitation, while hematite will form by direct solid-solid transformation ("aging" of hydrous ferric oxide) (Langmuir 1997 [DIRS 100051], p. 437). The iron oxyhydroxides will occur in three forms: immobile scale, large particles that will settle out, and colloid-sized particles.

Maximum concentration values for colloids have been estimated based on experiments performed at the University of Nevada at Las Vegas (see below, this section) and on professional judgment. TSPA-LA model calculations of total quantities of corrosion products are based on known masses of metallic components. The iron oxyhydroxide phases may be expected to

provide abundant sorption sites for dissolved (aqueous) radionuclides in amounts determined by the appropriate K_d value (Section 6.3.3.1). Stable iron oxyhydroxide colloid suspensions may serve to increase the mobility of sorbed radionuclides (see Sections 6.3.2 and 6.3.3). Their stability is controlled by fluid conditions including ionic strength and pH.

An ongoing DOE-funded research project at the University of Nevada at Las Vegas is currently evaluating the corrosion of scaled-down miniature waste packages exposed to groundwater similar to that found at Yucca Mountain. The miniature waste packages are composed of carbon steel and are scaled-down to approximately 1/70 the size of actual waste packages slated for disposal in the Yucca Mountain repository. Corrosion products released from the miniature waste packages were characterized by X-ray diffraction (DTN: MO0302UCC034JC.003 [DIRS 162871]) and the quantity of corrosion products transported out of the waste packages was measured by micro-filtration (DTN: MO0212UCC034JC.002 [DIRS 161457]).

Two configurations were used to introduce water into the miniature waste packages and induce corrosion: (1) a "bath tub" configuration in which water was introduced from the top of the miniature waste package and exits from an opening on the side of the miniature waste package after it has accumulated along the bottom, and (2) a "flow through" configuration in which water was introduced from the top of the miniature waste package and directly exits from the bottom. Water with chemical composition similar to Well J-13 (near Yucca Mountain) water was used in the experiments and the rate of water introduction was similar to projected rates of water movement within the drifts at Yucca Mountain. To establish the total amount of corrosion material transported out of the miniature waste packages, the effluent was passed through a micro-filtration system capable of separating particles of 0.1 micron and upward. Identification of the oxidation corrosion products is ongoing, although to date the data suggest a preponderance of cryptocrystalline corrosion products, including magnetite (Fe_3O_4), lepidocrocite (FeOOH), and goethite (FeOOH) (DTN: MO0302UCC034JC.003 [DIRS 162871]).

The colloidal size fraction of these materials represent viable analogs for the nature and quantity of corrosion-generated iron oxide colloids that could potentially be produced and transported from the engineered barrier system early during the corrosion of the waste packages after breaching. The cumulative results of the miniature waste package corrosion tests to date have yielded average concentrations of colloidal size material in the range of 20 mg/L within the initial four weeks of the experiments (DTN: MO0212UCC034JC.002 [DIRS 161457]). The University of Nevada at Las Vegas researchers have observed that all the miniature waste packages have clogged after several weeks of water influx, probably due to the formation and accumulation of corrosion products (e.g., iron oxyhydroxide) of larger molar volume than the original materials prior to corrosion.

Few data for iron oxyhydroxide colloid concentrations have been found in the scientific literature. Three studies reported groundwater colloid concentrations dominated by iron oxyhydroxide colloids, and the colloid concentrations reported varied greatly. Values ranging from 0.6 mg/L to 261 mg/L were measured in the vicinity of a mined uranium ore formation at Cigar Lake in Northern Saskatchewan (Vilks et al. 1993 [DIRS 108261]). Two Swedish groundwater colloid concentrations measurements were 0.02 mg/L and 0.043 mg/L for saline and none-saline groundwater samples, respectively (Laaksoharju et al. 1995 [DIRS 106449]).

Uncertainty in the data generated by the miniature waste package experiments and the consideration of iron oxyhydroxide colloid concentrations reported in the literature for groundwaters in iron-rich geologic environments is discussed in Section 6.6.2, Uncertainty Associated with the Model Analysis.

6.3.1.4 Natural Colloids Originating from Unsaturated Zone Seepage Water/Groundwater

Natural colloids occurring in seepage water/groundwater in the repository vicinity are modeled as smectite. Seepage water and colloids enter the drift and breached waste package.

Three types of seepage water/groundwater colloids may be present at Yucca Mountain:

1. Mineral fragments are generally hydrophobic, hard particles (i.e., particles that tend not to interact with water molecules) that are kinetically stabilized or destabilized by electrostatic forces and may consist of crystalline or amorphous solids (Kim 1994 [DIRS 109521]). Steric coatings (i.e., coatings whose molecular topology may result in "protuberances") may enhance the stability of mineral fragments by preventing close contact. Mineral fragments may act as substrates for sorption of radionuclides.

2. Humic substances are generally hydrophilic particles (i.e., particles that tend to interact with water molecules) that are stabilized by solvation forces (i.e., the forces involved in particle—water molecule interactions, generally involving electrostatic and van der Waals forces). They can be powerful substrates for uptake of metal cations and are relatively small (less than 100,000 atomic mass units).

3. Microbes are relatively large colloidal particles that are stabilized by hydrophilic coatings on their surfaces, which behave as steric stabilizing compounds. They may act as substrates for extracellular actinide sorption, or they may actively bioaccumulate radionuclides intracellularly.

Clays, silica, hematite, and goethite colloids occur in groundwater in the vicinity of Yucca Mountain (*cf.* Kingston and Whitbeck 1991 [DIRS 113930]), and the colloid model calls for these colloids to enter a failed waste package and be available to interact with released radionuclides. The presence and potential influence of natural seepage water colloids on the formation of radionuclide-bearing colloids in the engineered barrier system are considered by modeling all seepage water colloids as smectite; these are referred to as "groundwater colloids" throughout this document.

An assessment of the concentration of humic substances in groundwaters collected near the Yucca Mountain was conducted by Minai et al. (1992 [DIRS 100801]). In that study, humic substances were extracted from several thousand gallons of J-13 well water through a series of steps including acidification, purifying with ion exchange columns, and freeze drying. The humic substances that were collected were characterized with nuclear magnetic resonance and other spectroscopic techniques. Experiments were conducted to characterize site binding densities and complexation with Am. Results and supporting calculations indicated that the presence of humic substances in J-13 well water could affect oxidation speciation by reducing some radionuclide species. Considering the presence of calcium in J-13 well water, however, the authors estimated that the effective complexation capacity of humic substances is about

2.3×10^{-10} eq/L (equivalents per liter) at pH 6.9 and 2.7×10^{-11} eq/L at pH 8.2 (Minai et al. 1992 [DIRS 100801], p. 199). Considering the very low complexation capacity of humic substances in this system, they are not included among the groundwater colloids considered in this abstraction.

Because of the relatively large sizes of microbes (up to tens of microns), they are very susceptible to filtration in geologic media and, partly because of this microbe-radionuclide complexes, are not modeled in this abstraction. Discussion on the probable influences of microbes on the colloids that are considered in this analysis (inorganic waste form colloids, steel corrosion product colloids, and natural seepage water/groundwater colloids) is presented in Section 6.3.4.

6.3.2 Colloid Stability and Concentration

In order for radionuclide-bearing colloids to affect repository performance, the colloidal dispersion must be stable for the time frame of transport and must carry significant amounts of radionuclides. Transport times can range from days/months/years for transport out of a failed waste package under a large seep, to hundreds of thousands of years for retarded transport to the accessible environment. Thus, some relatively unstable colloids generated at the waste form may persist long enough to be transported out of the waste package, increasing the radionuclide release from the waste package, but likely would not travel a significant distance away from the repository. The more stable colloids, however, may remain suspended for years and travel a much greater distance. The clay colloids observed in the defense high-level waste glass and to a limited extent in the SNF corrosion tests are reasonably considered to have similar stability characteristics as natural clay colloids because the waste form-derived clays exhibit similar crystallographic and chemical properties as natural clays (CRWMS M&O 2001 [DIRS 154071]). The iron oxyhydroxide colloids stipulated to form from internal corrosion of the waste package are similarly considered as analogous to natural iron oxyhydroxide colloids. Uranium-phase colloids generated in the commercial SNF and DOE SNF tests are probably not as stable or persistent, as suggested by test results and field observations near uranium deposits (see Section 6.3.1.2.4).

6.3.2.1 DLVO Theory and Surface Complexation

Basic principles—The surfaces of dispersed, stable colloids have an electric charge sufficient to maintain the particles' separation by mutual repulsion. The surface charge of a particle can have two general causes: (1) specific characteristics of the crystal structure (see below) and (2) preferential adsorption of specific ions onto the surface (van Olphen 1977 [DIRS 114428], p. 18). The surface charges are compensated by the attraction of counter-ions, which have the opposite charge to the surface charges and to the vicinity of the particle surface. The charges at the particle surface and the oppositely charged, closely associated counter-ions make up the electric double layer (van Olphen 1977 [DIRS 114428], p. 18). The counter-ions are electrostatically attracted to the oppositely charged surface. However, they tend in water to diffuse away from the surface along a decreasing concentration gradient. As a result, counter-ions develop an "atmosphere" around the colloid that decreases in concentration away from the particle (van Olphen 1977 [DIRS 114428], p. 30).

There are three causes of surface charge related to sheet-silicate crystal structure (Langmuir 1997 [DIRS 100051], pp. 346 to 347): (1) isomorphous substitution in the crystal lattice (e.g., Al^{3+} for Si^{4+} in the tetrahedral layer and Mg^{2+} for Al^{3+} in the octahedral layer resulting in an excess of O^{2-} bonds, the chief cause of negative surface charge in smectites); (2) lattice imperfections or defects (e.g., deficits in octahedral Al^{3+} or interlayer K^{+} causing a net negative surface charge, also important for smectites); and (3) broken or unsatisfied bonds (e.g., at crystal plate corners and edges usually resulting in a net negative surface charge due to exposed O^{2-} and OH^{-}, important for smectites). As clay particles decrease in size, the importance of broken bonds increases (Langmuir 1997, p. 346 [DIRS 100051]).

The surface charge of oxides, hydroxides, phosphates, and carbonates originates chiefly from ionization of surface groups or surface chemical reactions (Langmuir 1997 [DIRS 100051], p. 349). Surface charge among this group is strongly dependent upon pH, being positive at lower pH and negative at higher pH. For example, in oxides and hydroxides, this is due largely to the adsorption of H^{+} at lower pH and OH^{-} at higher pH. The pH at which the net surface charge is neutral is called the zero point of charge; if the change in charge is solely due to adsorption of H^{+} or OH^{-} ions, the pH at neutrality is called the point of zero net proton charge (Langmuir 1997 [DIRS 100051], p. 350).

Far from the zero point of charge or point of zero net proton charge, the surface-charge density is relatively high; the particles are mutually repelled, and the suspension is stable. At or near the zero point of charge or point of zero net proton charge the repulsion force decreases to near zero, and the particles are more likely to agglomerate (“stick”) when particle collisions occur.

The stability and the coagulation, or agglomeration, of colloids is controlled by electrostatic and chemical processes at the colloid surfaces. In the 1940s and 1950s, research on particle coagulation centered around the electrostatic properties of the particles wherein the Derjaguin and Landau, and Verwey and Overbeek theory (DLVO) of the particle electrical double layer was used to explain particle stability in terms of surface charge and potential, the ionic strength of solutions, and the van der Waals forces between particles (Liang and Morgan 1990 [DIRS 109524], p. 33). It was subsequently realized that the double-layer theory by itself was not complete, and that the origin of surface charges and the role of specific chemical interactions in the stabilization and destabilization of colloidal particles should be considered. At low surface potential and low surface charge density of particles, experiments to verify DLVO theory agreed with theoretical prediction. However, at high surface potential and charge density, due to the large repulsive forces of the particles, the theory predicted orders of magnitude higher stability ratios than were observed (Liang and Morgan 1990 [DIRS 109524], p. 34). Beginning in the 1970s, surface complexation adsorption models were developed (Langmuir 1997 [DIRS 125369], p. 771]; these models were used to analyze changes in particles’ surface potential and charge brought about by complexation reactions (described by mass law equations) at the particle surface involving specific adsorbed chemical species (Dzombak and Morel 1987 [DIRS 109505], p. 430; Liang and Morgan 1990, p. 34 [DIRS 109524]).

Temperature—Temperature effects have also been shown to influence the stability of colloids (Langmuir 1997 [DIRS 100051], p. 439). The rate of particle coagulation is described by the "stability ratio," *W*, defined as:

$$W = \exp \frac{V_{\max}}{kT} \quad \text{(Eq. 2)}$$

where

V_{max} = height of free-energy barrier preventing particle coagulation
κ = Boltzmann constant
T = temperature in K

When log $W \approx 0$, coagulation is rapid and colloids settle out of the liquid media. Inspection of *W* shows that when *T* increases, *W* decreases. Therefore, increased temperature causes a colloid suspension to become less stable. Conversely, decreasing temperature will result in an increase in the stability of a suspension formed at a higher temperature. For the purposes of this abstraction, temperature effects are ignored, and it is assumed that waste form colloids produced at 90°C are stable at 25°C (Section 5, Assumption 5.4). The net effect of this assumption on TSPA-LA is that colloids formed at the higher temperatures remain stable as the repository cools.

Ionic strength—In nearly pure water, dissolved ions are likely to contact only other water molecules. As the concentrations of the ions increase, the ions are likely to come in contact with one another. The interactions between and among the ions is proportional to their charge, as reflected in the definition of ionic strength:

$$I = \tfrac{1}{2} \Sigma (m_i z_i^2) \quad \text{(Eq. 3)}$$

where I (and m) is in molal units and z_i is the charge of ion i (e.g., Langmuir 1997 [DIRS 100051]).

According to DLVO theory, colloids become unstable as ionic strength in a solution increases due to compression of the diffuse counter-ion atmosphere and decreases in surface potential, i.e., decreases in repulsive forces. Further, the degree of compression of the electric double layer is dependent on the concentration and valence of ions of opposite sign from that of the surface charge (van Olphen 1977 [DIRS 114428], p. 34). The effect of valence is captured by the Schulze-Hardy rule, which incorporates the principle that for a given counter-ion concentration, the higher the valence of the counter-ions, the more unstable the colloids and the greater the tendency to flocculate (van Olphen 1977, p. 24) [DIRS 114428].

Critical Coagulation Concentration—Critical coagulation concentration is defined as the minimum concentration of an electrolyte that results in the flocculation (coagulation) of a colloidal suspension. In his treatise on clay colloidal dispersions, van Olphen (1977 p. 24) [DIRS 114428] summarized empirically determined critical coagulation concentration values as follows:

Counterion Valence	Critical Coagulation Concentration (μM)
±1	25,000 to 150,000
±2	500 to 2000
±3	10 to 100

At pH values below the pH_{ZPC} for a mineral, the negatively charged counterions are important; above the pH_{ZPC}, positively charged counterions are important (see *Basic Principles*, this section).

For comparison, concentrations of counterions in J-13 well water were reported in a previous report (CRWMS M&O 2000 [DIRS 111880], Table 2, p. 16) as follows:

Ion	Valence	Concentration (μM)
Na	+1	1990
K	+1	129
Ca	+2	324
Mg	+2	82.7
Al	+3	0.0255
Cl	-1	201
S (sulfate)	-2	192

Note that none of the concentrations of individual ions in J-13 well water exceeds van Olphen's empirical critical coagulation concentration values (although Ca^{2+} is close) nor does the sum of the concentrations. The conclusion then is that colloid dispersions will probably be stable in J-13 water, as well as water compositions whose cation and anion concentrations remain below the valence-determined critical coagulation concentrations.

6.3.2.2 Stability of Smectite Colloids as a Function of pH and Ionic Strength

The zero point of charge of smectite is approximately pH 2 (see Figure 4). Since a pH this low is not anticipated in the repository, it is reasonable to expect that smectite colloids will remain in a stable pH range much of the time under anticipated repository conditions (unless ionic strength exceeds a certain threshold). However, it should be recognized that with decreasing pH, the charge density of smectite particle surfaces will decrease as more and more H^+ sorb to the surface and offset negative charges, generally decreasing stability (Buck and Bates 1999 [DIRS 109494]; Tombacz et al. 1990 [DIRS 112690]).

The defense high-level waste glass tests conducted at Argonne National Laboratory resulted in measured pH ranging between approximately 9 and 11.5 (Buck and Bates 1999 [DIRS 109494])

which is part of the range at which smectite colloids exhibit the highest surface charge and, hence, are most stable. Tombacz et al. (1990) [DIRS 112690] investigated the stability of smectite (referred to as montmorillonite by Tombacz et al.) suspensions as a function of pH and ionic strength in an NaCl solution. It was found that suspensions became unstable and flocculated at pH 2, 4, and 8 in 0.01 M, 0.025 M, and 0.04 M NaCl solutions, respectively (Figure 4). Figure 5 illustrates the abstraction and extension of this data to pH 10 and ionic strength of 0.05M for use in the TSPA-LA calculations. Schematic representation was abstracted from data presented in Figure 4. The established relationship between ionic strength and smectite colloid stability ($ST_{coll,\ wf,\ pH}$) as a function of pH for use in the TSPA-LA model is shown in Figure 5.

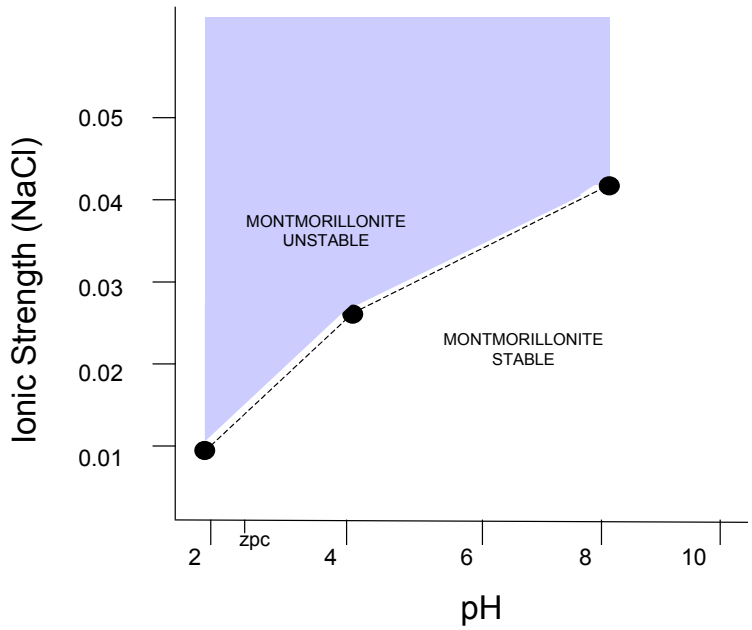

NOTE: Data points represent combinations of ionic strength and pH at which montmorillonite stability is significantly decreased.

Source: Adapted from Tombacz et al. 1990 [DIRS 112690].

Figure 4. Experimental Determination of Montmorillonite (i.e., Smectite) Stability as a Function of pH and Ionic Strength

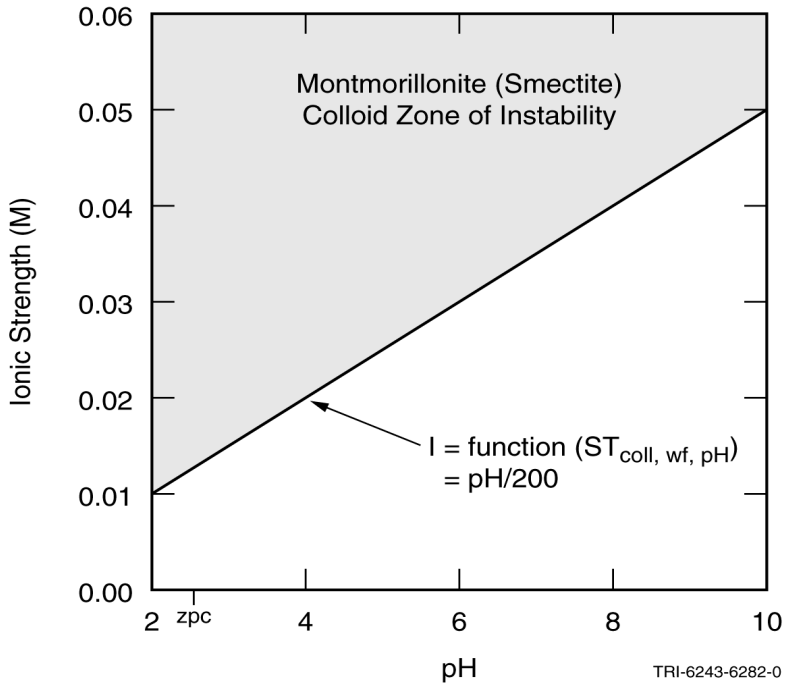

Figure 5. Schematic Representation of Smectite Stability as a Function of pH and Ionic Strength

6.3.2.3 Stability and Concentration of Iron Oxyhydroxide Colloids as a Function of pH and Ionic Strength

The point of zero net proton charge of iron oxyhydroxide colloids ranges between approximately pH 5 and 8.5 (*cf.,* Langmuir 1997 [DIRS 100051], p. 351, Table 10.3), depending on colloid and water composition, and in this range they will tend to be unstable and tend to agglomerate. At higher or lower pH, however, iron oxyhydroxide colloids are stable, depending upon ionic strength. Liang and Morgan (1990 [DIRS 109524]) demonstrated that for a given ionic strength iron oxyhydroxide stability increases as pH both increases and decreases away from the zero point of charge (Figure 6). In general the higher the ionic strength, the wider the pH range about the zero point of charge that iron oxyhydroxide is unstable. For example, at an ionic strength of 0.05 M, iron oxyhydroxide is unstable between approximately pH 6 and 11. The pH of zero proton condition for hematite is indicated in Figure 6 (i.e., pH 8.5). Dashed lines are drawn through the specific experimental points as a guide. The solid line represents a DLVO model calculation for ionic strength 0.05 M. Note that W_{exp} represents the stability of the dispersion, in terms of the rate at which colloidal particles in the dispersion agglomerate (see Equation 2, Section 6.3.2.1, DLVO Theory and Surface Complexation). A high value represents a stable dispersion and a value of zero indicates rapid agglomeration. At ionic strengths of about 0.05 m or more, the stability ratio is very low between pH values of about 6 and 11. A relatively low log W_{exp} of approximately 0.2 was selected for abstraction of pH and ionic strength data for use in Figure 7.

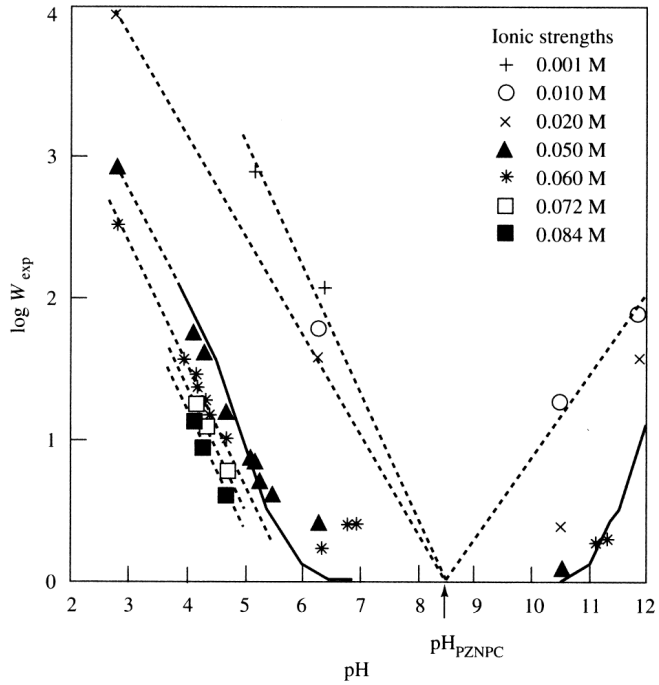

Source: Langmuir 1997 [DIRS 100051].

Figure 6. Experimentally Derived Stability Ratio, W_{exp}, of a Hematite Suspension Plotted as a Function of pH for Differing Ionic Strengths

As described in Section 6.3.1.3, it is stipulated for modeling purposes that iron will corrode and form iron oxyhydroxides. It is further stipulated that the iron oxyhydroxides will occur as immobile scale, large particles that will settle out, and colloid-sized particles. (For modeling purposes two parameters are established, the expected maximum and minimum mass concentrations of iron oxyhydroxide colloids, $M_{coll,FeOx,sampled}$ and $M_{coll,FeOx,min}$, respectively.)

The University of Nevada at Las Vegas research (see Section 6.3.1.3) on miniature waste packages has shown that corrosion proceeds rapidly, and colloid-sized particles have been observed to leave the miniature waste package in concentrations of around 20 mg/L. The release is more or less continuous until it decreases and the aperture clogs with corrosion products. While it was not observed in the University of Nevada at Las Vegas experiments, it is possible that in a repository setting clogging material may become dislodged by an event or changed condition, and release could resume, the overall process possibly occurring more than once.

Accordingly, the mass concentration range was chosen to include the 20 mg/L, and to allow for releases dwindling to a low quantity (0.05 mg/L), as well as for a pulse-like release (up to 50 mg/L). This maximum value is well within the range of colloid concentrations observed experimentally and in natural groundwater (see, for example, Lu et al. 2000 [DIRS 154422], who performed experiments with colloid concentrations of up to 200 mg/L; and Honeyman and Ranville 2002 [DIRS 161657], who acknowledge colloid concentrations in groundwater occasionally in excess of 100 mg/L).

The distribution was chosen to emphasize the upper end of the range, i.e., the 5 to 50 mg/L portion, to reflect the "steady state" conditions and pulses, but also allow for occasional clogging of the aperture in the waste package. The emphasis of the upper end of the range is conservative as it tends toward predicting higher colloid concentrations to which dissolved radionuclides may sorb.

This distribution is valid for ionic strengths less than 0.05 M. The colloid mass concentration at ionic strengths greater than 0.05 M is stipulated to be 1 x 10^{-3} mg/L, representing a very small non-zero number for modeling purposes. This concentration value is between one and two orders of magnitude lower than the lower bound of the distribution used for ionic strengths less than 0.05 M. This value is reasonable based on experimental observations that have shown a very low stability ratio. This very low stability ratio essentially implies complete agglomeration of colloids at ionic strengths exceeding 0.05 M (Liang and Morgan 1990 [DIRS 109524]. Therefore the use of a non-zero value for colloid concentration above ionic strength 0.05 M is conservative.

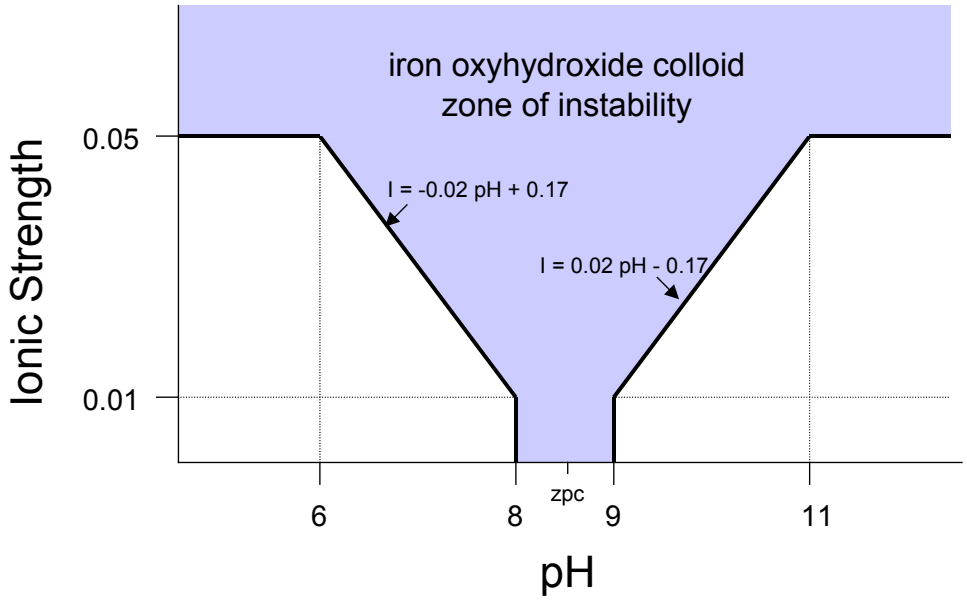

NOTE: Schematic representation (used in abstraction) of iron oxyhydroxide colloid stability as a function of ionic strength and pH. At and near the zero point of charge colloids are unstable, even at low ionic strengths. At higher ionic strengths the pH range at which colloids are unstable is greater. Above ionic strength 0.05 colloids are assumed to be unstable for all pH

Source: Abstracted from Liang and Morgan 1990, [DIRS 109524], Figure 1.

Figure 7. Schematic Representation of Iron Oxyhydroxide Colloid Stability as a Function of pH and Ionic Strength

6.3.2.4 Stability and Concentration of Waste Form Colloids

Colloids were formed in the course of static defense high-level waste glass tests on several of the glasses for different SA/V. It was observed that as the ionic strength increased, colloid concentration generally decreased, and ultimately a threshold value was reached above which the colloids were not observed or were observed in very low quantities (Figure 8). As this threshold

was approached, it was also observed for one glass that the colloid size increased significantly due to aggregation of the colloids. The threshold at which flocculation occurred was approximately I = 0.05m. During the drip tests, ionic strength remained below this value, and colloids were stable throughout the tests.

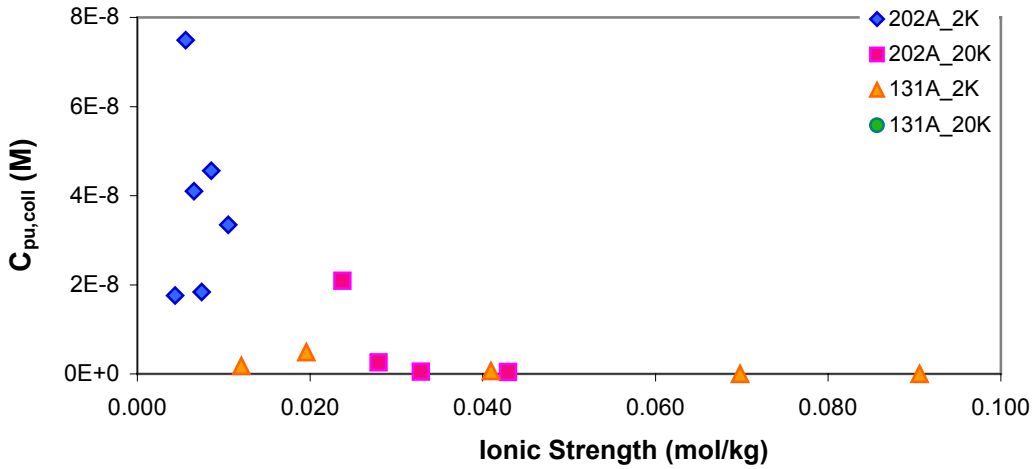

NOTE: Plutonium-bearing colloids as a function of ionic strength for corrosion tests on glass samples SRL 202A and SRL 131A at SA/V or 2,000 and 20,000/m (at 90°C)

Source: Figure 8 in CRWMS M&O 2001 [DIRS 154071]; DTNs: LL000905312241.018 [DIRS 152621], p. 71; LL991109751021.094 (DIRS 142910], p. 30.

Figure 8. Concentrations of Pu and Colloids as a Function of Ionic Strength in Corrosion Tests

The stability of smectite colloids (including smectite colloids formed from defense high-level waste glass degradation) is determined primarily by ionic strength, but also to an extent by pH, as described in Section 6.3.2.2 and shown in Figures 4 and 5. The concentration of total colloid-associated radionuclides in the pH range 2 to 10 is determined by bounding the data shown in Figure 9 as follows:

$$\text{For } 0.01 < I < 0.05,\ [\text{Pu colloid}] = -2.50\text{E-}6 \times I + 1.25\text{E-}7,\ \text{for } .01 < I < .05 \qquad \text{(Eq. 4)}$$

This relationship is valid for ionic strengths greater than 0.01 M and less than 0.05 M. The concentration at ionic strengths greater than 0.05 M is stipulated to be 1×10^{-11} M, representing a very small non-zero number for modeling purposes (Figure 9). This concentration value is approximately three orders of magnitude lower than the lowest value modeled at ionic strengths less than 0.05 and is reasonable based on experimental observations that have shown complete agglomeration of colloids at ionic strengths exceeding 0.05M (CRWMS M&O 2001 [DIRS 154071], Section 6.2.1). At ionic strengths less than 0.01 M, the Pu concentration is modeled as 1×10^{-7} M, also based on experimental observations (Figure 9).

Am concentration is based on Pu concentration. It is determined by multiplying the calculated Pu concentration by the ratio of Am to Pu in the radionuclide inventory of the defense high-level waste glass at each TSPA-LA calculation time step.

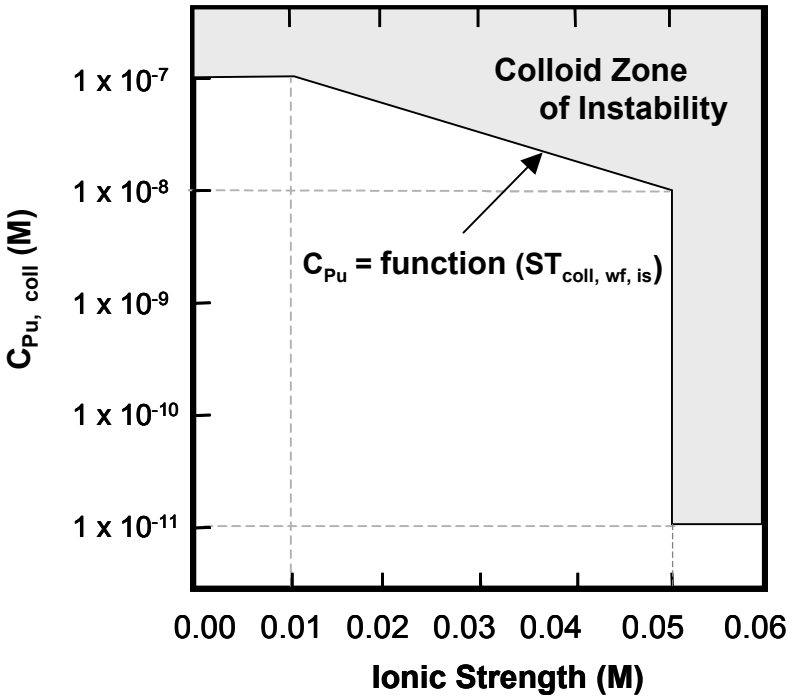

NOTE: Schematic relationship (used in abstraction) between Pu concentration embedded in defense high-level waste glass and ionic strength. The function represents the bound of the defense high-level waste glass corrosion experimental data (see Figure 8); the maximum value represented, 1×10^{-7}, bounds the maximum concentration of colloids observed in the defense high-level waste glass experiments. (The straight line representing the relationship should actually be portrayed with a slight curve, concave downward.) The low value, 1×10^{-11}, represents the steep decline in colloid concentration above ionic strength 0.05 M.

Figure 9. Schematic Relationship Between Pu Concentration in Defense High-Level Waste Glass Colloids and Ionic Strength

6.3.2.5 Stability and Concentration of Seepage Water Colloids

Colloids are thought to exist naturally in groundwater in all subsurface environments with the composition and concentration of colloids being site specific and determined by the geologic nature of the subsurface. Transport of radionuclides by groundwater colloids is a potentially important transport mechanism and is thought to be generally more prevalent than transport by true colloids (McCarthy and Zachara 1989 [DIRS 100778]). It is important to note here that waters and associated colloids potentially coming in contact with repository waste will originate at the ground surface as precipitation. These waters will move downward through the soils, regolith, and tuff materials overlying the repository before coming in contact with the wastes. Groundwater samples extracted from the underlying saturated zone in the vicinity of Yucca Mountain are used as surrogates for these waters.

McCarthy and Degueldre (1993 [DIRS 108215]) and Degueldre et al. (2000 [DIRS 153651]) have characterized the colloids from groundwaters sampled at various locations around the world from crystalline and sedimentary rocks in saturated and unsaturated hydrologic regimes. They showed that the colloid concentration and stability is dependent, among other things, upon pH, redox potential, ionic strength (including relative concentrations of the major cations Na, K, Ca, and Mg), counterion valence, and organic carbon; these factors were studied in the investigation. The results indicate that, in general, colloids tend to be stable if the concentration of alkalis (Na and K) is below approximately 10^{-2} M *and* if alkali-earth elements (Ca and Mg) are below approximately 10^{-4} M (Figure 10). This provides a guideline for assessing colloid stability and allows for very rough estimation of concentration. Whereas the DLVO calculations provide useful inferences on mechanisms of colloid destabilization, these empirical observations are more useful in developing approaches to performance assessment calculations.

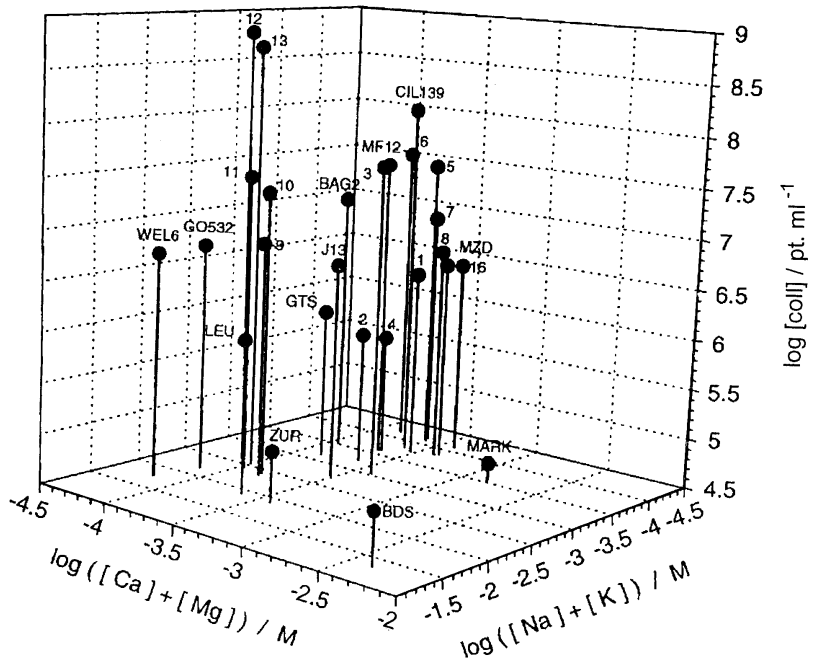

NOTE: Here, concentrations of colloids are compared on the basis of alkali and alkaline-earth element concentration for colloid size greater than 100 nm.

Source: Degueldre et al. 2000 [DIRS 153651].

Figure 10. Colloid Concentrations Versus Alkali and Alkaline-Earth Concentration for Groundwaters from Around the World

Colloid concentration is difficult to correlate precisely with ionic strength because there are other factors that can significantly affect concentration, such as pH. As described above, for example, at a pH of around 8, some iron oxyhydroxide colloids would have a zero net surface charge (since their zero point of charge is approximately 8) resulting in elimination of mutual repulsive forces and the tendency to flocculate, even if the ionic strength were very low. (This is an example—only smectite colloids are modeled as representative of natural seepage water/groundwater colloids.)

Further, site-specific studies of groundwater colloids (e.g., Kingston and Whitbeck 1991 [DIRS 113930]; Degueldre et al. 2000 [DIRS 153651]) suggest that when groundwater conditions favor colloid stability, there may be a very wide range of colloid concentrations observed for a narrow range of groundwater chemistry.

Consideration of the recently acquired data from the Yucca Mountain area and the Nevada Test Site by Los Alamos National Laboratory confirms a highly variable colloid concentration over a relatively narrow range of ionic strength. Figure 11 plots the groundwater colloid concentrations in water samples collected in the vicinity of Yucca Mountain. Data sources included in the figure are:

> Groundwater colloid populations—DTNs: LA0002SK831352.001 [DIRS 149232] LA0002SK831352.002 [DIRS 149194], LA0002SK831352.004 [DIRS 161579], LA9910SK831341.005 [DIRS 144991], LA0211SK831352.001 [DIRS 161580], LA0211SK831352.002 [DIRS 161581], LA0211SK831352.003 [DIRS 161582], LA0211SK831352.004 [DIRS 161458], LA0002SK831352.003 [DIRS 161771]) and colloid concentrations in groundwaters sampled around the world Degueldre et al. (2000 [DIRS 153651]) and DTN: SNT05080598002.001 [DIRS 162744] data.

Ionic Strength data—DTNs: SNT05080598002.001 [DIRS 162744], LA0304PR831232.001 [DIRS 163196], and LA0304PR831232.002 [DIRS 163197].

It is important to note here that the groundwater colloid samples analyzed by Los Alamos National Laboratory represent colloid particle size distributions from 50 nm to 200 nm in diameter while the data from groundwaters around the world (DTN: SNT05080598002.001 [DIRS 162744]) represent colloid particle size distributions from 100 nm to 1000 nm (1.0 μm diameter). Evaluation of the colloid populations in the various size fraction classes for each groundwater sample did not reveal a systematic increase in the number of particles with decreasing particle size class (see Table I-2). Therefore, inclusion of particle size classes smaller than 50 nm should not result in a substantially greater mass concentration in the water sample, especially since the smaller particles would have exponentially lower mass—therefore, omission of the less than 50 nm particle-sized fraction in the mass concentration calculations is reasonable.

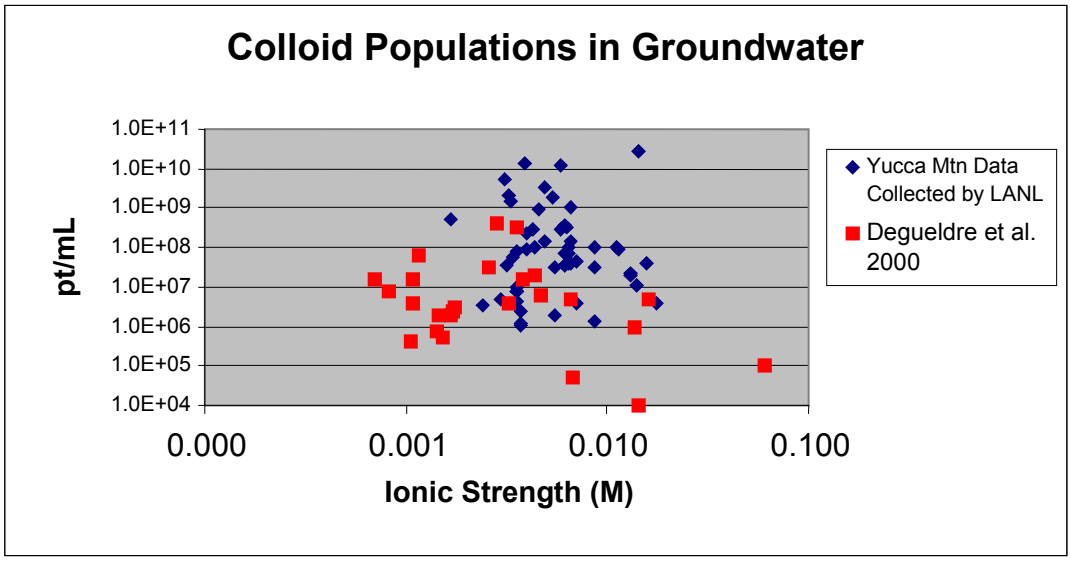

NOTE: Degueldre data (DTN: SNT05080598002.001 [DIRS 162744]) has a greater range in ionic strength than waters in the vicinity of Yucca Mountain.

Figure 11. Groundwater Colloid Concentration Data Collected in the Vicinity of Yucca Mountain Compared with Data Collected from Groundwaters Around the World (the ordinate values are in particles per milliliter)

Colloid particle number data (pt/ml) for groundwater samples from the Yucca Mountain area and Idaho National Engineering and Environmental Laboratory were converted to mass concentrations (mg/L) (Attachment I). It is important to note here that the Degueldre et al. (2000 [DIRS 153651]) and DTN: SNT05080598002.001 [DIRS 162744] data were not used to calculate the mass colloid concentrations (mg/L) and were only used to establish the generally weak relationship between ionic strength and colloid populations in groundwaters around the world and specifically in the Yucca Mountain area (Figure 11).

The groundwater colloid data from the vicinity of Yucca Mountain and Idaho National Engineering and Environmental Laboratory were pooled, and a discrete cumulative distribution function was established to evaluate the uncertainty in colloid concentration distribution. The colloid concentrations data included qualified data (i.e., LA0002SK831352.001 [DIRS 149232], LA0002SK831352.002 [DIRS 149194], LA9910SK831341.005 [DIRS 144991], LA0211SK831352.001 [DIRS 161580], LA0211SK831352.002 [DIRS 161581], LA0211SK831352.003 [DIRS 161582], and LA0211SK831352.004 [DIRS 161458]) used as direct input, and LA0002SK831352.003 [DIRS 161771] and LA0002SK831352.004 [DIRS 161579] used as corroborating/supporting data. Inclusion of the Idaho National Engineering and Environmental Laboratory groundwater colloid data (LA0002SK831352.003) [DIRS 161771] was deemed appropriate for inclusion in the data analysis as corroborative data even though these groundwater colloid data are not from the vicinity of Yucca Mountain (see Attachment I). Water samples that had been filtered were not considered in the development of the uncertainty distribution. Since the colloid particles were measured by dynamic light scattering techniques, any potential error in measurement of colloid populations for the various particle size classes due to filter "ripening" (i.e., clogging of filter pores through time during the filtration process) was avoided by using only non-filtered sample data.

The data shown in Figure 12 reflect observed variability in groundwater colloid concentrations. The goal of the uncertainty distribution for groundwater colloid concentrations is to numerically capture our knowledge about uncertainty on a large scale. Based on the groundwater colloid concentration collected at the two sites (Yucca Mountain and Idaho National Engineering and Environmental Laboratory) and the large uncertainty associated with the collection of groundwater colloids, a reasonable representation of the uncertainty is shown in the discrete cumulative distribution function shown in Figure 12 (see Table 5 for the probabilities associated with the discrete cumulative distribution function). Major factors that contribute to uncertainty in the collection of groundwater colloids include (1) collection techniques, (2) differences in pumping rates at each well, and (3) unknowns factors including the types of additives introduced in the wells during the drilling process itself.

The waste form and engineered barrier system components of the TSPA-LA analyses implement the uncertainty shown in Figure 12 only for ionic strength less than 0.05 M. For ionic strengths greater than or equal to 0.05 M, colloids are assumed to be unstable, based upon experimental work that has shown the flocculation of colloids at high ionic strengths (Liang and Morgan 1990 [DIRS 109524]; Tombacz et al. 1990 [DIRS 112690]; CRWMS M&O 2001 [DIRS 154071]), and a single low value (1 x 10^{-6} mg/L) is used in the waste form and engineered barrier system analysis to represent minimum, non-zero colloid concentration.

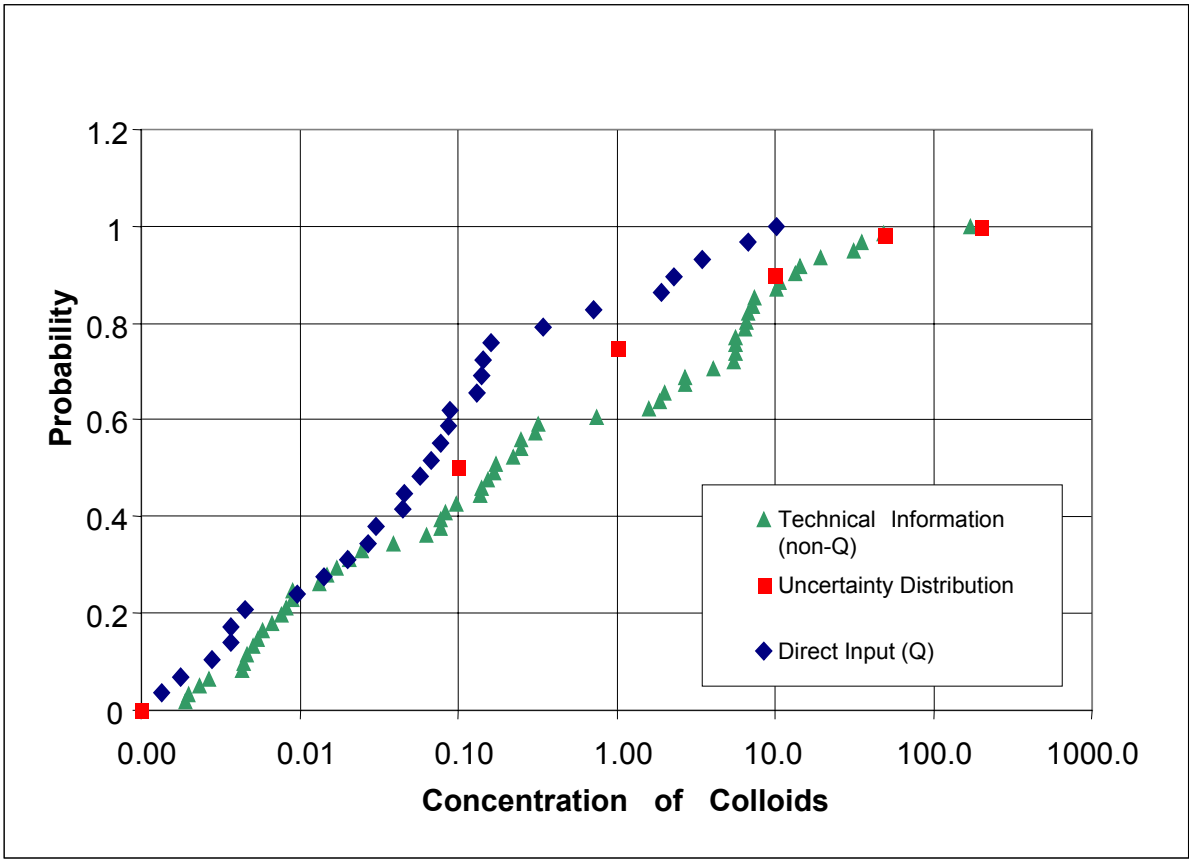

Figure 12. Cumulative Distribution Function Showing the Probability of Occurrence of Colloid Concentration Levels in Groundwater Samples in the Yucca Mountain Area and Idaho National Engineering and Environmental Laboratory

Table 5. Uncertainty Distribution for Groundwater Colloid Concentrations for the Total System Performance Assessment–License Application Analyses Based on Ionic Strength (I) of the Water Sample

Ionic Strength (I)	Groundwater Colloid Concentration (mg/L)	Probability of Occurrence
I < 0.05 M	0.001 to 0.1	50
	0.1 to 1.0	25
	1.0 to 10	15
	10 to 50	8
	50 to 200	2
I ≥0.05 M	1×10^{-6}	100

Review of the colloid data in Attachment I reveals that the largest proportion of groundwater colloid samples had colloid concentration populations between 0.001 and 0.1 mg/L and thus the values between these concentrations are modeled as having a sampling probability of 50 percent if the ionic strength of the solution is less than 0.05 M. Colloid concentration values of 0.1 to 10 mg/L indicate a reasonable probability of occurrence of 40 percent. To account for colloid concentrations between 10 mg/L and 50 mg/L a probability of 8 percent was included. Some of the corroborative (non-Q) data included values as high as 171 to 200 mg/L (see Table I-1, Attachment I), but the uncertainty distribution for the pooled data indicates that these values have a low probability of occurring. Honeyman and Ranville (2002 [DIRS 161657]) point out that although most systems of interest for radioactive waste disposal exhibit relatively low colloid concentrations (less than 10 mg/L), concentrations exceeding 100 mg/L are not uncommonly reported. Therefore, it is recommended that the concentration values between 50 mg/L and 200 mg/L be assigned only a sampling probability of 2 percent when the ionic strength of the solution is less than 0.05 M within the waste form and engineered barrier system components of the TSPA-LA model calculations.

6.3.3 Radionuclide Sorption to Colloids

A description of radionuclide sorption to colloids is presented in this section. Nonradioactive colloids are only important to repository performance insofar as radionuclides sorb to them. "Sorption" as used here is a general term that is governed by: (1) electrostatic forces, (2) ion exchange, (3) surface reaction, and (4) co-precipitation. Sorption may occur by a number of mechanisms and may be considered reversible or irreversible in the time frame of transport. The rate of sorption, desorption, and transport determine the effective reversibility of the sorption. When sorption is fast and reversible, transport on colloids will be controlled by local equilibrium, and simple models, e.g., linear isotherm models, using effective distribution coefficients reasonably describe the radionuclide behavior. When sorption is irreversible or desorption is slow relative to transport times, then local equilibrium models may fail, resulting in over- or under-predictions of transport.

6.3.3.1 Reversible Sorption

Perhaps the most common approach used in assessment of contaminant-rock interactions in the subsurface is the linear isotherm, or K_d value (distribution coefficient) approach, based on results

of batch sorption experiments. The linear isotherm model relationship is defined as follows (Langmuir 1997 [DIRS 100051]):

$$S = K_d C \quad \text{(Eq.5)}$$

where

S = mass of a solute adsorbed on a unit mass of solid
K_d = distribution coefficient (mass-based, e.g., mL/g)
C = concentration of the adsorbing solute in solution

The amount of solute adsorbed on a solid can also be defined on the basis of area as follows:

$$S = K_a C \quad \text{(Eq. 6)}$$

where

S = mass of a solute adsorbed on a unit area of solid
K_a = distribution coefficient (area-based, e.g., m^2/g)
C = concentration of the adsorbing solute in solution

Three critical conditions must be met for this relationship to be applicable. First, the water-contaminant-rock system must be in thermodynamic equilibrium, i.e., sorption must be completely reversible. Second, contaminant uptake must scale linearly with contaminant concentration. Third, the presence of other solutes in the system cannot affect the sorption. Because of the nature of the formation of waste form colloids and the interactions of some radionuclides, particularly some actinides, with mineral surfaces, certain conditions of the linear isotherm model are not met, and other approaches must be taken, as described below.

A large quantity of data exist in published literature for sorption, and, in the past several decades, increasing attention has been given to understanding the mechanisms of sorption. In this section, the development of K_d values for uptake of strontium (Sr), cesium (Cs), thorium (Th), uranium (U), protactinium (Pa), neptunium (Np), plutonium (Pu), and americium (Am) on colloids is described, with caveats. These radionuclide elements were chosen for consideration because they are considered to be important to dose (BSC 2001 [DIRS 154841]), and significant uncertainty surrounds their potential behavior as pseudocolloids.

The radionuclides considered for reversible sorption, and the rationale for their selection, are listed below. Characteristics of the radionuclides considered were a combination of long half-life, relatively strong sorption characteristics, relatively large abundance during the initial 10,000 years in the repository, and observed field and laboratory behavior.

- Plutonium. A large quantity of Pu will exist in the repository. Pu is sparingly soluble but sorbs strongly to oxide mineral surfaces (generally less strongly to silicates). The formation of pseudocolloids through the sorption of Pu particularly to iron oxyhydroxide colloids from corrosion of steel in the repository would increase the effective mobility of

Pu. Pu is observed to sorb strongly to soil minerals, and laboratory investigations have shown that it sorbs readily to colloids as well.

- Americium. Am will be a significant contributor to radioactivity during the first 10,000 years. As is Pu, Am is sparingly soluble but sorbs strongly to mineral surfaces, including colloids. Laboratory investigations have shown that it sorbs strongly to colloids.

- Cesium. ^{135}Cs has a long half-life and can attach strongly to certain sheet silicates (including clays) by means of ion exchange. For this reason Cs has been observed to sorb to soil minerals, and it could potentially form pseudocolloids particularly with groundwater and defense high-level waste glass-derived clay colloids.

- Protactinium. Pa will be a significant contributor to radioactivity during the first 10,000 years. Because of this, and the fact that relatively little is known of the colloid-related behavior of Pa, it was included in this analysis.

- Thorium. Th will be a significant contributor to radioactivity during the first 10,000 years. Because of this, and the fact that there is evidence that Th sorbs strongly to oxides, it was included in this analysis. There is relatively little known of the colloid-related behavior of Th.

- Neptunium. Because Np will be the most significant contributor to radioactivity beyond the first 10,000 years, it was considered for inclusion in this analysis. Np is more soluble under anticipated repository conditions than many of the other important radionuclides, and it sorbs considerably less strongly than, for example, Pu and Am. It would appear then that the mobility of Np is influenced most by its solubility. For these reasons, and to simplify the modeling, Np was not included in the reversible-sorption portion of the colloid-associated radionuclide transport analysis.

- Uranium. U will be by far the most abundant radioactive element in the repository and primarily for this reason was considered for the analysis. U is more soluble under anticipated repository conditions than many of the other important radionuclides, and it sorbs considerably less strongly than, for example, Pu and Am. As with Np, the mobility of U is influenced most by its solubility. Further, field observations at U deposits and mine sites have indicated that little or no colloid-associated U transport occurs (Section 6.3.1.2.4). For these reasons, and to simplify modeling, U was not included in the reversible-sorption portion of the colloid-associated radionuclide transport analysis.

- Strontium. Sr is expected to be a potentially significant contributor to dose but because of its very short half-life was not considered further in this analysis.

To a large extent, the effectiveness of colloids at facilitating contaminant transport is due to their very large surface area (relative to mass and volume) available for sorption. Depending on the size distribution of colloids in the dispersion, the impact of choosing a mass-based K_d value, or a surface-area-based K_a, may be significant. The greatest deviation exists in situations in which an inordinately large number of very small colloids exist, which have a high surface-area-to-mass ratio. Since nearly all available sorption information is mass-based, and conversion to surface-

area-based information is not always straightforward, a mass-based K_d value approach is used here.

By considering the effect of aqueous chemical conditions on sorption, the selection of relevant K_d values is simplified. The behavior of the mineral surface is primarily controlled by pH and ionic strength (particularly concentrations of sodium, calcium, and potassium). The behavior of the sorbate is primarily controlled by its oxidation state, pH, and the partial pressure of carbon dioxide (Pco_2). For minerals in which the sorption mechanism is primarily by ion exchange (e.g., clay minerals), ionic strength impacts sorption of Cs on clay minerals (especially at their edges), because cations compete with radionuclides for exchange sites. Ionic strength is less important for actinides, in that some anions and cations contributing to ionic strength affect sorption by forming complexes with the actinides.

Under the oxidizing conditions at Yucca Mountain, radionuclides will occur in oxidized forms which, in general, results in decreased sorption. Plutonium will disproportionate and be simultaneously present in multiple valence states (IV, V, and VI at YMP). The actinide elements discussed exhibit strong hydrolysis behavior and tend to form strong carbonate complexes. The actinides tend to be completely hydrolyzed at pH values above about 6 where they are present as neutral hydroxo complexes. At slightly alkaline pH values and above, they will exist as negatively charged anionic hydroxyl complexes. Consequently, sorption is greatest in the near neutral pH range. The Pco_2 of the system has minor or negligible effect on sorption of Cs but a strong effect on sorption of the actinides. Carbonate is a strong complexant, and at alkaline pH values, the actinides may form mono-, di-, and tri-carbonato complexes, depending on the actinide (and valence). The presence of these complexes tends to decrease sorption.

To develop colloid K_d values, information provided by project data, a previous project report (CRWMS M&O 2000 [DIRS 152773]), and published literature was considered. Several sources of YMP-specific sorption data exist from Los Alamos National Laboratory research. Lu et al. (1998 [DIRS 100946], 2000 [DIRS 154422]) provide useful information on the sorption of Pu(IV) and Pu(V) on colloidal dispersions of hematite, goethite, montmorillonite, and silica. Information on Am(III) is provided for all but goethite. Sorption was measured as a function of time up to 4 or 10 days. Desorption was measured after 150 days because desorption tends to be much slower in these mineral-sorbate systems. The experimentally determined K_d values are summarized in Table 6.

Table 6. Experimentally Determined K_d Values for Pu and Am Sorption Onto Hematite and Montmorillonite

Phenomena Investigated	K_d Values, mL/g	
	J-13 Water	Synthetic J-13 Water
Plutonium-Hematite (DTN: LA0003NL831352.002 [DIRS 148526])		
Sorption (forward, up to 10 days; colloid concentration not specified in DTN)	5.00×10^3 to 1.10×10^5	1.20×10^5 to 7.00×10^5
Desorption (backward, 200 days; colloid concentration not specified in DTN)	3.40×10^5	3.20×10^5
Colloid Concentration (forward, 10 to 150 mg/L, 10 days)	7.50×10^3 to 3.70×10^4	7.70×10^3 to 2.60×10^4
Temperature (forward, 20^o to 80^o C, 10 days)	1.70×10^5 to 4.90×10^6	[not in DTN]
Plutonium-Montmorillonite (DTN: LA0003NL831352.002 [DIRS 148526])		
Sorption (forward, up to 10 days; colloid concentration not specified in DTN)	2.30×10^2 to 5.80×10^3	2.40×10^2 to 6.50×10^3
Desorption (backward, 200 days; colloid concentration not specified)	6.70×10^3	36.50×10^3
Colloid Concentration (forward, 10 to 150 mg/L, 10 days)	5.20×10^3 to 2.70×10^4	3.20×10^3 to 2.40×10^4
Temperature (forward, 20^o to 80^o C, 10 days)	9.50×10^3 to 2.00×10^5	[not in DTN]
Americium-Hematite (DTN: LA0005NL831352.001 [DIRS 149623])		
Sorption (forward, up to 10 days; colloid concentration not specified in DTN)	7.90×10^4 to 1.00×10^7	1.20×10^5 to 6.20×10^6
Desorption (backward, 200 days; colloid concentration not specified)	1.90×10^5	8.40×10^4
Colloid Concentration (forward, 10 to 150 mg/L, 10 days)	1.90×10^6 to 1.60×10^7	1.80×10^6 to 2.80×10^7
Temperature (forward, 20^o to 80^o C, 10 days)	1.80×10^5 to 6.50×10^5	(not in DTN)
Sorption (forward, up to 10 days; colloid concentration not specified in DTN)	7.10×10^3 to 6.50×10^4	2.30×10^4 to 1.10×10^5
Desorption (backward, 200 days; colloid concentration not specified)	9.10×10^4	1.80×10^4
Colloid Concentration (forward, 10 to 150 mg/L, 10 days)	1.60×10^5 to 1.50×10^6	1.60×10^5 to 8.40×10^5
Temperature (forward, 20^o to 80^o C, 10 days)	6.00×10^4 to 2.70×10^6	(not in DTN)

Source: Lu et al. 1998 [DIRS 100946]; Lu et al. 2000 [DIRS 154422]; DTNs: LA0003NL831352.002 [DIRS 148526], LA0005NL831352.001 [DIRS 149623].

Several significant compendia of sorption data have been assembled in the past decade. One useful example is the compendium developed by the National Cooperative for the Disposal of Radioactive Waste (NAGRA, Switzerland) (Stenhouse 1995 [DIRS 147477]). The objective of that work was to compile a set of K_d values useful for evaluation of waste-disposal in hypothetical sites in Switzerland. The sorbents considered were crystalline rock, marl, and bentonite, all with reducing groundwaters (or pore water, in the case of bentonite). Ionic strengths are similar to J-13 water or greater. Despite differences in those conditions, the information compiled in the National Cooperative for the Disposal of Radioactive Waste document is useful for YMP in that it includes consideration of phenomena affecting sorption.

The mineralogic compositions of crystalline rock, marl, and smectite (bentonite) were compiled and used to weight relevant sorption values from their compendium. The chemical compositions of relevant groundwaters or pore waters, all somewhat reducing, were also compiled. For Yucca Mountain colloid calculations, the sorption values for crystalline rock were selected for two reasons. First, the mineral phase dominating sorption is similar in mineralogy to Yucca Mountain waste form and groundwater colloids. A significant observation made in the National Cooperative for the Disposal of Radioactive Waste report is that sorption by a rock is typically dominated by one mineral constituent, usually a phyllosilicate mineral. Second, the groundwater is closest to Yucca Mountain groundwater in terms of pH, ionic strength, and redox conditions.

National Cooperative for the Disposal of Radioactive Waste proposed "realistic values" and "conservative values." The conservative values for the actinides were developed by National Cooperative for the Disposal of Radioactive Waste to account for uncertainty in oxidation states (composite K_d values were reduced by an order of magnitude). With respect to the oxidation state, the conservative values would be more relevant to Yucca Mountain. However, to compensate for the use of a mass-based K_d approach on colloids, the realistic values are useful. In Table 7, the rock composite K_ds and individual K_d values for smectite and oxides/quartz are compiled. The individual mineral values are probably more suitable to consider for Yucca Mountain colloid K_d values.

Table 7. Summary of Sorption Data Developed by National Cooperative for the Disposal of Radioactive Waste for Bentonite, Crystalline Rock, and Marl

Radionuclide and Oxidation State(s)	NAGRA Database	NAGRA Rock K_d (mL/g) (page)	NAGRA Mineral K_d (mL/g)
Sr(II)	461 entries; 39 references	1,000 (p. Sr-11)	smectite = 20; oxides, quartz = 0
Cs(I)	516 entries; 41 references	1,000 (p. Cs-11)	smectite = 2,000; oxides, quartz = 40
Th(IV)	79 entries; 22 references	5,000 p. Th-7)	smectite = 2,000; oxides, quartz = 1,000
Pa(V)	21 entries; 12 references	1,000 (p. Pa-3)	NAGRA uses Zr(IV) as analog for Pa(IV); use Np(V) for Pa(V) for YMP
U(VI)	382 entries; 32 references	5,000 (p. U-7)	smectite = 100; oxides, quartz = 20
Np(V)	389 entries; 53 references	5,000 (p. Np-8)	smectite = 100; oxides, quartz = 20
Pu(IV, V, VI)	298 entries; 25 references	5,000 (p. Pu-10)	smectite = 1,000; oxides, quartz = 200
Am(III)	198 entries; 34 references	5,000 (p. Am-9)	smectite = 10,000; oxides, quartz = 1,000

NOTE: NAGRA = National Cooperative for the Disposal of Radioactive Waste

Source: Stenhouse 1995 [DIRS 147477].

A second useful compendium was developed for the U.S. Environmental Protection Agency (EPA 1999 [DIRS 147475]). In that work, information on radionuclides including Sr, Cs, Th, U, and Pu is compiled (no information for Pa, Np, or Am). The assembled data are interpreted to predict ranges of K_d values for soils in shallow subsurface environments. Redox conditions for that system are oxidizing, which makes it useful for the redox-sensitive radionuclides at YMP. Unfortunately, the group of radionuclides covered does not provide an analog element for trivalent or pentavalent elements, such as Am(III), Pa(V), or Np(V).

In the EPA (1999 [DIRS 147475]) study, published literature was reviewed to determine the predominant aqueous chemical conditions affecting sorption in soils for each contaminant. For Sr, soil clay content and groundwater pH were used as criteria to recommend K_ds. For Cs, clay content was also used, but pH is less important because Cs exists as an aqueous ion and does not complex, and it sorbs by ion exchange, a process that is not affected by pH-dependent surface charge. For Th, pH and sorbate concentration are important. At concentrations close to its solubility limit, K_ds tend to increase. For U, the pH was important. For Pu, carbonate complexation has a strong influence on sorption, and so carbonate concentration, as well as clay content, were considered as criteria to select a relevant K_d. In Table 8, K_d values are compiled based on aqueous chemical conditions closest to those expected in ambient groundwater at Yucca Mountain. Unfortunately, the K_d values are expressed in a minimum to maximum format, with no indication of distribution. Some ranges, for example U, span almost six orders of magnitude. To narrow the range, the geometric means were calculated below and reported in Table 8, column 4.

Table 8. Summary of Sorption Data Developed by U.S. Environmental Protection Agency

Radionuclide and Oxidation State(s)	Database	Soil and pH Categories: Smectite Colloids ("high clay") Iron Oxyhydroxide Colloids ("low clay")	Smectite K_d (mL/g) Range of Geometric Means Iron Oxyhydroxide K_d (mL/g) Range of Geometric Means
Sr(II)	63 entries (166 in Appendix)	high clay (20-60 wt%); pH 8-10; low clay (<4 wt%); pH 8-10	300 to 1,700 (714); 3 to 120 (19)
Cs(I)	177 K_d values	high clay (20-60 wt%) low clay (<4 wt%)	80 to 26,700 (1,462); 30 to 9,000 (520)
Th(IV)	17 entries	pH 8-10; [Th] $<10^{-9}$ M (pH and Th concentration important)	20 to 2,000 (200)
Pa(V)	not discussed, no good analog	---	---
U(VI)	20 references	pH 8 (pH important)	0.4 to 250,000 (316)
Np(V)	not discussed, no good analog	---	---
Pu(IV, V, VI)		high clay (51-70 wt%); 3-4 meq/L CO_3^{2-}; low clay (<4 wt%); 3-4 meq/L CO_3^{2-}	1,860 to 2,550 (2,178); 80 to 470 (194)
Am(III)	not discussed, no good analog	---	---

Source: EPA 1999 [DIRS 147475].

A second source of sorption data from Los Alamos National Laboratory research is compiled in the project report focusing on transport properties in the unsaturated and saturated zones (CRWMS M&O 2000 [DIRS 152773]), which also considers previous Yucca Mountain reviews by Meijer (1992 [DIRS 100467]) and others. These ranges are generally comparably to values extracted from the National Cooperative for the Disposal of Radioactive Waste report (Table 7). For sorption onto colloids, their large surface areas suggest the use of the larger K_d values in the ranges, which is also conservative with respect to radionuclide transport.

Another source of Yucca Mountain-specific sorption analytical results is presented in Honeyman and Ranville (2002 [DIRS 161657]). This paper investigated several aspects of colloid-facilitated radionuclide transport, including reduction of effective retardation of radionuclides by colloids and the effectiveness of colloids with respect to radionuclide mobility in the presence of stationary phases available for radionuclide sorption. The colloid-stationary phase system is discussed further in Section 6.3.3.2 in the context of irreversible sorption.

Honeyman and Ranville (2002 [DIRS 161657]) summarize an analysis by Contardi et al. (2001 [DIRS 162732]) that incorporated Yucca Mountain-vicinity groundwater chemistry and colloid size and concentration data from Kingston and Whitbeck (1991 [DIRS 113930]). K_d values were calculated with the use of a diffuse layer model and based on three principles: (1) the system is symmetrical, i.e., the colloids and stationary phases are similar with respect to mineralogy; (2) the colloids are stable; and (3) the system is in sorptive equilibrium. The ratio of stationary phase to colloid surface areas ranged up to roughly two orders of magnitude (3.2 to 63). Colloid concentrations of up to about 100 mg/L were included. In the system analyzed, approximate K_d value ranges (mL/g) for five radionuclides were given (Table 9).

Table 9. Modeled K_d Values for Pu, Am, Th, Np, and U Sorption Onto Yucca Mountain-Vicinity Colloids

Radionuclide Sorbate and Oxidation State(s) at YMP	K_d Values, mL/g
U(VI)	1×10^0 to 6×10^2
Np(V)	1×10^1 to 1×10^2
Pu(V)	1×10^3 to 1×10^4
Th(IV)	2×10^3 to 9×10^4
Am(III)	$1 \times 10^4$to 1×10^7

Source: Honeyman and Ranville 2002 [DIRS 161657].

Table 10 lists K_d value ranges used in the TSPA-LA model calculations with their uncertainties developed after examination of the references supporting Tables 6, 7, 8, and 9. Note that values for Am are also used for Th because its properties are not well known and because it has similar sorption tendencies as Am. Values for Am are also used for Pa because its sorption properties are likewise poorly known. Given the non-exact nature of these K_d values, encompassing (bounding) ranges are adopted, with distributions that emphasize the upper parts of the ranges.

Waste form colloids, corrosion-generated colloids, and seepage water/groundwater colloids may become pseudocolloids through reversible sorption of aqueous radionuclides onto them. K_d values for combined adsorption and desorption of Pu, Am, Pa, Th, and Cs on waste form, iron

oxyhydroxides, and groundwater colloids are used to determine effective reversibility of the radionuclides on colloids according to the relationship:

$$RN_{adsorbed/desorbed} = RN_{dissolved} \times K_{d,RN} \times M_{colloid} \quad \text{(Eq. 7)}$$

The K_d values in Table 10 are based on the following:

- Ranges are drawn from the following references: EPA (1999 [DIRS 147475]), Stenhouse (1995 [DIRS 147477]), Lu et al. (1998 [DIRS 100946]), Lu et al. (2000 [DIRS 154422]), CRWMS M&O (2000 [DIRS 152773]), and Honeyman and Ranville (2002 [DIRS 161657]).
- For a given radionuclide (except Cs) the maximum value of each range is the same to allow for the possibility that iron oxyhydroxide will occur both as iron oxyhydroxide colloids and as coatings on, or microcrystalline aggregates in association with, smectite colloids in the iron-rich waste package environment. For Cs, which attaches more strongly to smectite (by ion exchange) than iron oxyhydroxide, the ranges are different for iron oxyhydroxide and smectite.
- The K_d intervals and probabilities are intended to cover the entire ranges and emphasize the higher ends of the ranges but de-emphasize the highest intervals. These distributions are used because (1) the ranges are based on data for both colloids and larger minerals, and it is believed that K_d values for colloids will be higher than for larger minerals due to their higher specific surface area; and (2) because of the mechanisms of surface phenomena that actually prevail, K_d values tend to over-predict desorption over time of actinide metals from iron oxyhydroxide colloids, i.e., they under-predict retention by the colloids.
- K_d values ranges and distributions for Th and Pa are assumed to be those of Am primarily because of limited data on Th and Pa.
- The ranges are believed to incorporate adequately the uncertainties inherent in uncertain data from disparate sources.

Table 10. K_d Values (mL/g) Used for Reversible Radionuclide Sorption on Colloids in Total System Performance Assessment-License Application Calculations

Radionuclide	Colloid	K_d Value Range (mL/g)	K_d Value Intervals (mL/g)	K_d Value Interval Probabilities
Pu	Iron Oxyhydroxide	10^4 to 10^6	$<1 \times 10^4$ 1×10^4 to 5×10^4 5×10^4 to 1×10^5 1×10^5 to 5×10^5 5×10^5 to 1×10^6 $> 1 \times 10^6$	0 0.15 0.2 0.5 0.15 0
	Smectite	10^3 to 10^6	$< 1 \times 10^3$ 1×10^3 to 5×10^3 5×10^3 to 1×10^4 1×10^4 to 5×10^4 5×10^4 to 1×10^5 1×10^5 to 5×10^5 5×10^5 to 1×10^6 $> 1 \times 10^6$	0 0.04 0.08 0.25 0.2 0.35 0.08 0
Am, Th, Pa	Iron Oxyhydroxide	10^5 to 10^7	$< 1 \times 10^5$ 1×10^5 to 5×10^5 5×10^5 to 1×10^6 1×10^6 to 5×10^6 5×10^6 to 1×10^7 $> 1 \times 10^7$	0 0.15 0.2 0.55 0.1 0
	Smectite	10^4 to 10^7	$< 1 \times 10^4$ 1×10^4 to 5×10^4 5×10^4 to 1×10^5 1×10^5 to 5×10^5 5×10^5 to 1×10^6 1×10^6 to 5×10^6 5×10^6 to 1×10^7 $> 1 \times 10^7$	0 0.07 0.1 0.23 0.2 0.32 0.08 0
Cs	Iron Oxyhydroxide	10^1 to 10^3	$< 1 \times 10^1$ 1×10^1 to 5×10^1 5×10^1 to 1×10^2 1×10^2 to 5×10^2 5×10^2 to 1×10^3 $> 1 \times 10^3$	0 0.13 0.22 0.55 0.1 0
	Smectite	10^2 to 10^4	$< 1 \times 10^2$ 1×10^2 to 5×10^2 5×10^2 to 1×10^3 1×10^3 to 5×10^3 5×10^3 to 1×10^4 $> 1 \times 10^4$	0 0.2 0.25 0.5 0.05 0

NOTE: In engineered barrier system calculations, upper bound of Kd ranges for Pu and Am on iron oxyhydroxide reduced by a factor of 100 to be compatible with mechanistic sorption model described in Section 6.3.3.2.

6.3.3.2 Irreversible Sorption of Pu and Am to Colloids and Stationary Phases

The criteria for the linear sorption model described above are not met in defense high-level waste glass degradation experiments, which show that plutonium is (probably) irreversibly attached to smectite colloids generated during the experiments (CRWMS M&O 2001 [DIRS 154071], Section 6.2.2). Further, evidence from sorption experiments with Pu and Am (Lu et al. 2000 [DIRS 154422]) with colloidal hematite and goethite show that the rates of desorption (backward rate) of Pu and Am are significantly slower than the rates of sorption (forward rate). More importantly, over a significant time period (up to 150 days in some experiments), the extent of

desorption is considerably less than the extent of sorption. Special considerations must be made for these situations.

Pu and Am are considered so strongly sorbed to colloids that, in essence, can almost be considered irreversibly sorbed and are modeled in this manner within the engineered barrier system (BSC 2003 [DIRS 163935], Attachment II). Pu transport velocities in soils reflect the fact that Pu binds strongly to soils, leaving very little, if any, soluble Pu available for groundwater transport or plant uptake. Coughtrey et al. (1985 [DIRS 154494]) estimate exchangeable Pu ("soil available," best estimate, Table 2a, p. 119) to be less than one percent. At Rocky Flats, soil Pu is largely bound to soil metal hydroxides. Litaor and Ibrahim (1996 [DIRS 161667]) used 0.01M $CaCl_2$ as an extractant and measured Pu in Rocky Flats soil to be 0.04 to 0.08 percent exchangeable. Bunzl et al. (1995) [DIRS 154468] measured exchangeable 239+240Pu (0.5 to 1 percent) and 241Am (1.5 to 15 percent) from fallout-contaminated soils in Germany using 1M $C_2H_7NO_2$ (ammonium acetate $NH_4C_2H_3O_2$) as the extractant. Transport of colloidal Pu over hundreds of meters was observed at the Nevada Test Site (Kersting et al. 1999 [DIRS 103282]). Laboratory experiments of Pu sorption onto iron oxides have shown that only approximately 1 percent of the initially sorbed Pu can be desorbed into solution, even after months of time have elapsed (Lu et al. 2000 [DIRS 154422]), which is broadly consistent with field observations.

In order to accommodate these observations in the colloid abstraction, the TSPA-LA model calculates irreversible and reversible sorption of Pu and Am as functions of specific surface area (S_A), site density (N_A), mass of corrosion colloids, dissolved concentration of Pu and Am, target-flux out ratio (F_{RN}, Table 16), and other parameters (such as flow and diffusion rate) internal to the TSPA-LA model. This is done in such a way that a majority (90 to 99 percent) of Pu and Am are irreversibly sorbed, due to incorporation of parameter uncertainties (see BSC 2003 [DIRS 163935], Attachment II). The reversibly sorbed portion is determined according to an equilibrium K_d value model (per Section 6.3.3.1; see Table 10 for values, ranges, and distributions).

Note that this approach is mechanistically more advanced than the approach taken for TSPA-SR and in prior efforts. Previous treatments have relied solely on the application of K_ds to describe uptake of dose-critical radionuclides onto colloids. A clearer understanding of the identity and abundance of colloidal material in the waste form and engineered barrier system has prompted the more fundamental modeling effort. At the same time, more recent analyses of actinide transport in the environment have provided evidence for irreversible sorption—the tendency for sorbed material to desorb very slowly and for a strong colloidal component to environmental transport of Pu. To accurately represent each feature, the updated engineered barrier system/waste form colloid model separates sorbed Pu and Am each into two populations—an irreversibly sorbed fraction and a reversibly sorbed fraction. Accordingly, in the waste form and engineered barrier system TSPA-LA model, the upper bound of the K_d range for the reversibly sorbed fraction is reduced by a factor of 100 (which constrains the K_d value to the lower bound, which is a fixed value). The solid fluid partitioning of Pu and Am that the model predicts are consistent with the magnitudes of the respective Am and Pu K_d values used elsewhere in the unsaturated and saturated zone.

It should be kept in mind that K_d values are rough measures of multiple surface reactions that nevertheless must be relied upon to describe sorption in the absence of a more precise understanding of system specifics. In the engineered barrier system and waste form, the nature and abundance of colloidal material is more predictable than elsewhere. There is consequently greater justification for applying a more elaborate model of actinide sorption onto colloids in the waste form and the engineered barrier system. The same level of system understanding cannot be assumed to exist elsewhere or for all other radionuclides. Consequently, the application of the more involved approach described previously cannot presently be justified in other situations.

Sorption to immobile iron oxyhydroxide within the waste package is modeled. Honeyman and Ranville (2002 [DIRS 161657]) incorporated a stationary phase in their analysis of the effects of colloids on radionuclide retardation, as described in Section 6.3.3.1. The stationary phase competes strongly with the colloids for radionuclide sorption. For the symmetrical system described in Section 6.3.3.1, by far most of the Am mass was calculated as attached to the stationary phase; at most, 0.001 percent of the total Am was associated with colloids (Honeyman and Ranville 2002 [DIRS 161657], p. 140). This is a significant finding because due to its strongly sorptive properties Am is one of the radionuclides with the greatest potential (of the radionuclides of interest here: Pu, Pa, Cs, Am) for transport on colloids.

In the colloid abstraction the difference in specific surface areas between the colloids and the stationary corrosion products is taken into account as well as the total surface areas (based on total masses). On the one hand Pu will tend to attach to the colloids with their higher specific surface area; on the other hand the much larger mass of stationary corrosion products relative to total colloid mass results in most of the dissolved Pu attaching to the stationary corrosion products. In order to accommodate the field and laboratory observations as well as the modeling results described, distribution of Pu between colloids and the stationary corrosion products was implemented such that a large fraction of total Pu is sorbed to corrosion products, a small fraction to colloids, and a small fraction remains dissolved in the fluid. These relative fractions are realistic and are simulated in the TSPA-LA model (see BSC 2003 [DIRS 163935]). Allocating a fraction of the total Pu onto the stationary corrosion products in this way reduces the quantity of Pu transported by colloids, but allowing sorption onto stationary corrosion products is more realistic than not including this process.

Specific Surface Area (S_A) and Site Density (N_S)—Values for specific surface area (S_A) and reactive site density (N_S) on three different iron oxyhydroxides, α-FeOOH (goethite), α-Fe_2O_3 (hematite), and $Fe(OH)_3 \cdot nH_2O$ (ferrihydrite or hydrous ferric oxide) as tabulated from the literature are listed in Table 11.

Table 11. Published Values for Specific Surface Area (S_A) and Site Density (N_S) for Iron Phases

Mineral/phase	S_A (m^2/g)		N_S (sites/area or wt.)		Source
	Min	Max	Min	Max	
α-FeOOH (goethite)	45	169	2.6/nm^2	18/nm^2	Langmuir 1997, Table 10.2, p. 345 [DIRS 100051]
			1.35 x 10^{-3} mol/g		
α-Fe_2O_3 (hematite)	1.8 (natural)	3.1 (synthetic)	5/nm^2	22/nm^2	Langmuir 1997, Table 10.2, p. 345 [DIRS 100051]
$Fe(OH)_3 \cdot nH_2O$ (ferrihydrite)	250	600	20/nm^2		Langmuir 1997, Table 10.2, p. 345 [DIRS 100051]
			0.1 mole/ mole Fe	0.91 mol/ mole Fe	
HFO	159	720	0.001 (Type 1) 0.1 (Type 2)	0.01 (Type 1) 0.91 (Type 2)	Dzombak and Morel (1990 [DIRS 105483]), Table 5.1, p.91 for S_A and Tables 5.2 and 5.3, pp. 92 to 93 for N_S

NOTE: Type 1 sites are high-affinity cation binding sites; Type 2 sites are the total reactive sites available for sorption of protons, cations, and anions as determined from observed sorption maxima (Dzombak and Morel 1990 [DIRS 105483], p. 92). HFO = hydrous ferric oxide.

Jenne (1998 [DIRS 162328]) states, "[n]otwithstanding four decades of research on methods of surface area (S_A) and adsorption site concentration measurement, (C_{site}). S_A measurements on similar materials differ by up to an order of magnitude and *a priori* determinations of $C_{site,tot}$ [concentration of all reactive sites] on oxides and clay minerals by titration or tritium exchange are generally higher than $C_{M,ads,max}$ [maximum concentration of adsorbed metal] by up to an order of magnitude..." It has been indicated that the use of a surface area measured on dry samples in a vacuum may not adequately represent the surface area of a mineral in suspension. Further, the variation in site density of $Fe(OH)_3$ may reflect differing microporosities (which could also be true of other oxides and aggregates as well) (Jenne 1998 [DIRS 162328]).

Because of the uncertainties in S_A and C_{site} (or N_S as used here) measurements, it has been recommended (by Davis and Kent 1990 [DIRS 143280]) that specific values be adopted for these parameters. They state (p. 227)…"a parsimonious modeling approach is needed in order to extend surface complexation theory to applications in natural systems. In complex mixtures of minerals it is often difficult to quantify the numbers of surface functional groups that are present from various minerals. *We recommend that binding constants for strong-binding solutes be derived with a site density of 2.31 sites/nm^2* (3.84 μmoles/m^2) *for all minerals*...While the actual Γ_{max} [maximum adsorption density] may vary from 1 to 7 sites/nm^2, it is important that one value be selected to encourage the development of a self-consistent thermodynamic database that can be applied easily to soils and sediments…To encourage unanimity within the field, the particular value of 2.3l sites/nm^2 because has been chosen because it is consistent with the value chosen by Dzombak and Morel (1990 [DIRS 105483]) to describe ferrihydrite (0.205 moles per mole of Fe), assuming a specific surface area of 600 m^2/g of $Fe_2O_3 \cdot H_2O$. The value recommended

approximates the site densities found by adsorption on various minerals, including goethite…and the edge sites of clay minerals…"

Based on these considerations, the following values are used for S_A and N_S of iron oxyhydroxide corrosion phases in the colloid model implemented in TSPA-LA calculations:

S_A 1.8 - 720 m^2/g (log uniform distribution)

N_S 2.31 sites/nm^2 (fixed value)

The S_A value is provided in Table 16.

6.3.3.3 "Embedded" Radionuclides in Defense High-Level Waste Glass Colloids

The colloid model abstraction accounts for waste form smectite colloids observed in the defense high-level waste glass degradation experiments with "embedded" Pu and Am radionuclides by treating them as a separate colloid subtype and assuming that the embedded radionuclides are an intrinsic part of the colloid, not in equilibrium with the aqueous system. These "embedded" radionuclides are effectively attached irreversibly to the colloid. Pu and Am are stipulated to occur as "embedded" in defense high-level waste glass smectite colloids. In this model, waste form colloid parameters are represented entirely by the defense high-level waste glass degradation colloids with embedded radionuclides. See Sections 6.3.1.1 and 6.3.2.4 for further details.

6.3.4 Potential Effects of Microbes and Organic Components

An assumption is made in this abstraction that microbes and organic compounds do not affect the stability of inorganic colloids (Section 5, Assumption 5.9). The assumption is probably conservative, since it appears from information reviewed that such interactions would tend to destabilize colloids, thereby decreasing the mobility of associated radionuclides. However, under certain circumstances organic compounds may tend to stabilize inorganic colloids. Therefore the rationale for this assumption is presented in considerable detail below.

Microbes and microbe fragments may occur in groundwater as colloid-sized particles to which radionuclides can sorb or be actively bioaccumulated across the cell membrane. They may impact local groundwater chemistry in and around the waste package, oxidation of metallic iron, and aggregation of colloidal materials used a food source (resulting in decreased concentration). The effects of microbes in colloid-facilitated transport in the repository can include:

- Microbial oxidation of metallic iron can produce iron-oxide colloids and aggregates.
- Microbially influenced corrosion can accelerate radionuclide release into the surrounding environment (CRWMS M&O 2000 [DIRS 151561]).
- Microorganisms can decrease the concentration of stable colloids by aggregating colloidal material that they use as a food source. This has been shown to result in a decrease in colloid concentrations of up to 91 percent (Hersman 1995 [DIRS 100750]).

Microbes can impact transport of radionuclides a number of ways. First, in some systems, microbes can passively or actively bioaccumulate radionuclides. If the microbes are mobile, they can facilitate transport of the radionuclides. Alternatively, the microbes may be readily filtered by the rock or may form biofilms, in which case they retard transport. Second, microbes may produce exudates, for example organic complexants, which may enhance the solubility of radionuclides and affect their sorption characteristics if complexes are formed. Third, in the course of extracting energy or nutrients, microbes may generate colloids by degrading materials or may actually destroy colloids by consuming them or by facilitating agglomeration. Fourth, in some systems, microbes are able to reduce the oxidation states of some multivalent radioelements (e.g., U, Np, and Pu). Typically, reduced forms of radionuclides are less soluble and more strongly sorptive.

Development of a rigorous model for the impact of microbes would require YMP-relevant data on microbe concentration, size, shape, sorption properties, the effect of microbial activity on mobility, biofilm formation, rock-microbe interaction, plume characteristics, nutrient availability, microbe longevity, etc., as well as the rates of processes. Because of the complexity of collecting these data, a microbe-facilitated transport model was not attempted. For microbes to impact near-field performance, microbes must be present and sufficient energy sources and nutrients be available. Substantial concentrations of nutrients will not be present in the near-field environment. For microbes to have an unfavorable impact on performance, they must bioaccumulate radionuclides and must be transportable. Because of the relatively large size of microbes, they will be readily filtered during transport, along with any bioaccumulated radionuclides, which is beneficial. Inclusion of microbial colloid transport in the waste and engineered barrier system in the TSPA-SR calculation would reduce interpreted doses.

The transport of microbes within the waste package and invert is not currently modeled in TSPA-LA. Microbe-facilitated contaminant transport in shallow saturated systems has been demonstrated in the literature (Fontes et al. 1991 [DIRS 147337]; Harvey et al. 1989 [DIRS 147338]; Kim and Corapcioglu 1996 [DIRS 147342]; Weiss et al. 1995 [DIRS 147345]; Yates and Yates 1988 [DIRS 147348]), but few, if any, studies demonstrate transport through the vadose zone. Interactions among inorganic colloids and various types of organic components in natural systems are ubiquitous and complex. It is generally understood that some forms of natural organic matter, such as fulvic compounds from soils, will stabilize inorganic colloids in natural waters (Buffle et al. 1998 [DIRS 161653]; Hahn and Stumm 1970 [DIRS 161656]). However, certain types of natural organic matter, such as the polysaccharides, have been shown to have a tendency to destabilize colloids (Buffle et al. 1998 [DIRS 161653]; Wilkinson et al. 1997 [DIRS 161734]; Wilkinson et al. 1997 [DIRS 161732]). Further, under certain circumstances they may stabilize colloids (Napper 1983 [DIRS 161735]; Liu et al. 2000 [DIRS 161777]; Walker and Grant 1996a [DIRS 161736]; Walker and Grant 1996b [DIRS 161738]; Yokoyama et al. 1990 [DIRS 161675]). Polysaccharides and other types of organic compounds are produced by microbes and introduced to aqueous systems as byproducts of metabolism and cell fragments. Given the relatively low reported quantities of humic and fulvic compounds in groundwater near Yucca Mountain (Minai et al. 1992) [DIRS 100801], along with the potential for the growth of microbial colonies in the repository, a study of potential effects of microbes on the stability and transport of radionuclide-bearing inorganic colloids was initiated by the project.

6.3.4.1 Potential Microbial Communities Within the Engineered Barrier System

A case for the occurrence of microbes in some abundance in the repository has been modeled and is presented in *In-Drift Microbial Communities* (CRWMS M&O 2000 [DIRS 151561]). That study was performed to develop a model for the possibility and probability of microbial communities occurring in the engineered barrier system of the repository, and in addition to use the model to assist the total system performance assessment calculation group in the modeling of the engineered barrier system geochemical environment. Secondary reasons for the study included the application of portions of the conceptual model to near- and far-field geomicrobiological processes, unsaturated zone and saturated zone transport, portions of the waste package modeling affected by microbe-induced corrosion, and to provide a microbial source term for colloid modeling in the drift.

In assessing the potential effects on microbial populations within the engineered barrier system, *In-Drift Microbial Communities* (CRWMS M&O 2000 [DIRS 151561]) considered the drift mineralogy; drift physical parameters; metals, alloys, and cement used in engineered barrier system components; waste dissolution rates and quantities; groundwater compositions and infiltration rates; and compositions and fluxes of gases (e.g., CO_2, water vapor). Environmental limits on microbial activity considered include redox conditions, temperature, radiation, hydrostatic pressure, water activity, pH, salinity, available nutrients, and others. The abundance of water and phosphorous were found to be the two environmental components which, if in short supply, could limit the development of microbial communities in the Yucca Mountain repository under the probable physicochemical conditions likely to be present in the proposed repository configuration.

Because the water and phosphorous in the repository would potentially be available in sufficient quantities to allow for the growth of microbial communities at certain stages of the postclosure period (CRWMS M&O 2000 [DIRS 151561]), the potential effects of these communities on the transport characteristics of radionuclide-bearing colloids become important. The colloid-type behavior of microbe transport is usually modeled with techniques used to analyze inorganic colloid transport, e.g., DLVO theory, filtration, and advection-dispersion. Microbes also adhere to substrates and colonize in biofilms by producing extracellular polymers, usually exopolysaccharides, resulting in a means of sorption to solid surfaces and to each other.

6.3.4.2 Results of Experiments with Bacteria

Microbes and inorganic colloids in proximity to one another may result in collisions, which allow mutual adhesion or adsorption and result in particle size growth (agglomeration) (Buffle et al. 1998 [DIRS 161653]; Hersman 1995 [DIRS 100750], 1997 [DIRS 100763]). This increase in particle size can have several effects on the potential for colloids to facilitate radionuclide transport within the repository: (1) for a given range of pore sizes in the transport medium, the larger composite particles may become filtered more readily than the individual microbe or colloid; (2) the larger particles will tend to diffuse more slowly and/or may sink through gravitational settling; and (3) the interactions of relatively large populations of colloids and microbes can result in agglomerated particles sufficiently large that the dispersion becomes unstable and the microbe and colloid particles flocculate. Reduced transport from increased particle size is even more significant in the situation where water is present as thin films within

the pore spaces and on the engineered barrier system components. In all of these processes the net result is particle size increase and reduced transport of colloids and associated radionuclides.

The mechanisms which can affect the probability of microbe-colloid interactions are many and include chemotaxis, Brownian motion, electrostatic attraction, van der Waals interaction, electrical double layer effects, and cell surface hydrophobicity (Hersman 1997 [DIRS 100763]). Attraction of a microbe to a stationary surface or other colloids depends on the specific polymers on the microbial surface, which are influenced by microbe species, substrate, and environmental conditions. Hersman (1995 [DIRS 100750]) conducted experiments with Yucca Mountain-native bacteria and bentonite clay. In one test, agglomeration of clay colloids in a sterile microbial growth medium was compared to agglomeration in a medium into which a bacterium was introduced. The test results showed greater agglomeration in the growth medium inoculated with bacteria. In a second test the bacteria were cultured in the medium and the test repeated with those bacteria, and similar results were noted.

The development of biofilms on a substrate has been shown to result in an increased tendency to attract suspended inorganic colloids. Investigators of processes occurring within biofilms have observed water and nutrient movement within and through biofilms and measured diffusion coefficients (Beyenal and Lewandowski 2000 [DIRS 161652]; Lewandowski et al. 1995 [DIRS 161664]; Wanner et al. 1995 [DIRS 161674]). Sprouse and Rittmann (1990 [DIRS 161672]) and Rittmann and Wirtel (1991 [DIRS 161671]) demonstrated that biofilm colonization increased the colloid cohesion efficiency, α, in a system where the collector was granular activated carbon in a methanogenic fluidized bed and the colloids were milk solids approximately 1 micron in diameter. Lo et al. (1996 [DIRS 161669]) concluded from an experiment with Fe(III) oxide colloids in a biofilm reactor that the deposition of Fe(III) oxide colloids increased slightly with biofilms present. Further iron deposition on surfaces increased with increasing particle size, suggesting interception of the colloids and/or sedimentation.

6.3.4.3 Organic Matter and Inorganic Colloid Stability

For purposes of discussion naturally occurring organic matter may be considered to fall into three classes. The most generally abundant class includes the soil-derived humic and fulvic acids, which typically range from 40 to 80 percent of natural organic matter in surface waters (Buffle et al. 1998 [DIRS 161653]). The second class of natural organic matter includes the rigid biopolymers, i.e., structural, fibrillar polysaccharides or peptidoglycans released from plankton as exudates or cell wall components, and range from 10 to 30 percent of natural organic matter in surface waters (Buffle et al. 1998 [DIRS 161653]). The third class includes the flexible biopolymers, the most persistent of which is aquagenic refractory organic matter, which forms from a recombination of amino acids, sugars, etc. released by plankton. aquagenic refractory organic matter concentrations rarely exceed a few milligrams per liter (although in pelagic waters of oceans and large lakes it may comprise 90 percent of the total natural organic matter; Buffle et al. 1998 [DIRS 161653]). Natural organic matter of all three classes may persist in the environment for periods of up to decades to thousands of years (Buffle et al. 1998 [DIRS 161653]).

Under particular circumstances suspended colloids may be mutually attracted, leading to aggregation and flocculation, or repelled, promoting stability of the suspension. In circumstances

favoring aggregation, colloids of a given type (e.g., clays, fulvic acids) may aggregate together (*homoaggregation*) or with colloids of other types (*heteroaggregation*). DLVO theory and Smoluchowski equations have been used to describe phenomena involving homoaggregation. However, there is no general theory to describe heteroaggregation, in particular heteroaggregation involving biopolymers (Buffle et al. 1998 [DIRS 161653]).

Two general types of colloid interactions may be identified: (1) electrostatic and (2) polymeric. Electrostatic interactions are generally evaluated and described in terms of DLVO or related theory and are controlled by electric double-layer repulsion and van der Waals attraction. The stabilizing effect of fulvic acid sorption onto iron oxyhydroxide colloids, for example, results primarily from electrostatic forces.

Polymers may affect inorganic colloid stability whether they are attached to the colloids (*steric* effects) or free in solution (*depletion* effects). (A polymer may be defined as a molecule with relatively high molecular weight consisting of regularly repeating units, or chemically similar units.) Organic polymer chains with molecular weight of about 10,000 have a chain dimension roughly that of, or greater than, the range of van der Waals attraction. Further, the molecular dimensions are relatively insensitive to the electrolyte concentration (Napper 1983 [DIRS 161735]).

Steric effects, where polymers are attached to compact inorganic colloids and may exhibit rod-like or coil-like "appendages," may lead to aggregation through "bridging" between the polymer and colloid if the attractive force between the polymer and colloid is sufficient. On the other hand, a repulsive force between the polymer and colloid may promote stability. Depletion stabilization and aggregation have had little study and are not well understood (Napper 1983 [DIRS 161735]).

There is little information on interactions between flexible polymers and inorganic colloids in natural systems, although it is known that flexible polymers are relatively quickly degraded and so may have limited effect. Flexible polymers act primarily by sorbing to the colloid and modifying its surface charge and promoting flocculation by neutralizing the net surface charge. Neutralization depends, however, on the degree of coverage of the colloid surface—too much or too little coverage would result in a net charge on the colloid surface, which would encourage stability (Buffle et al. 1998 [DIRS 161653]). According to Walker and Grant (1996a [DIRS 161736]) relatively little flexibility is required for adsorption of polymer.

The biopolymers associated with microbial activity are mucopolysaccharides, pectic compounds (microbial cell walls and extracellular products), etc. These are fibrillar structures based on double or triple helix formation and are considered to be rigid polymers (Buffle et al. 1998 [DIRS 161653]). Since it has been postulated that microbial colonies will develop in the repository, and since only very small quantities of humic and fulvic acids have been analyzed in Yucca Mountain groundwater (Minai et al. 1992) [DIRS 100801], then of the several types of organic compounds to be considered in the repository rigid polymers may have the most influence on colloid mobility. However, this would depend on the quantities and nature of materials introduced during construction of the repository and emplacement of waste (this potentially important issue of introduced materials and their effects on inorganic colloids and microbes/microbial products has not been examined).

Interactions between inorganic colloids and rigid biopolymers probably lead to aggregation and sedimentation under most circumstances (Buffle et al. 1998 [DIRS 161653]). Aggregation and sedimentation rates have been positively correlated with increased quantities of fibrillar polysaccharides released by plankton (Buffle et al. 1998 [DIRS 161653]; Wilkinson et al. 1997 [DIRS 161734] and 1997 [DIRS 161732]). Zumstein and Buffle (1989 [DIRS 161740]) showed that in a eutrophic lake environment chain-like organic matter was associated with sedimented clay and calcite colloidal particles and that fulvic acids tended to stabilize the inorganic colloids.

Polymers have, of course, been used in industrial processes to stabilize colloidal dispersions. Liu et al. (2000 [DIRS 161777]) point out that natural polysaccharides have been used in flotation and suppression systems for virtually every type of industrially important mineral. For example, starch is used to suppress hematite, apatite, calcite, and coal while floating quartz and pyrite. (In the TSPA-LA colloid source term model, the inorganic colloids analyzed are stable subject to pH and ionic strength of the fluid and are not affected by organic materials.) Yokoyama et al. (1990) [DIRS 161675] describe the use of water-soluble polysaccharides as colloid stabilizers. These acidic polysaccharides stabilized colloidal dispersions through a steric stabilization mechanism. Their effectiveness was dependent on the steric layer thickness relative to the van der Waals attractive force. Further, increasing temperature increased the thickness of the steric layer, which increased the stability of the dispersion (Yokoyama et al. 1990 [DIRS 161675]). This is in contrast to the generally destabilizing effect of increasing the temperature of a suspension of inorganic colloids.

6.3.4.4 Discussion

The possible effects of the interactions among the large variety of organic compounds and inorganic colloids are dauntingly numerous and complex. Given the overall results of the cited investigators, it appears reasonable to conclude that the presence of organic polymers such as those produced by microbes and their byproducts will generally reduce the stability of inorganic colloids and result in enlargement of particles through heteroaggregation, as has been inferred from the study of the eutrophic lake (Wilkinson 1997 [DIRS 161734] and 1997 [DIRS 161732]; Zumstein and Buffle 1989 [DIRS 161740]). Further, given this conclusion (and neglecting the possible influences of organic materials introduced to the repository during construction and waste emplacement) it is also reasonable that the occurrence of microbial communities in the Yucca Mountain Repository will likewise tend to decrease the stability and mobility of colloids. To the extent that the colloids are associated with radionuclides, this would also decrease the transport of radionuclides.

The large body of literature describing the use of polymers in process technology for both suppression and peptization of colloids for the most part has not yet been reviewed. This is significant as, since much of our understanding of inorganic colloid–organic polymer interactions has been made available from research driven by numerous commercial applications of these principles, a final judgment regarding the effects of microbes and their products on the transport of inorganic colloids and associated radionuclides in the repository should ultimately depend upon a thorough review of the relevant literature.

It is currently anticipated that the repository invert, comprised of crushed volcanic tuff with intergranular void spaces, will remain undersaturated with respect to groundwater. The adhesion

of microbes to unsaturated porous media like the invert can be controlled by the level of fluid saturation and the extent of the air-water interface network within the medium. Since microbes tend to adhere strongly to the air-water interface, lower saturations would result in increased microbe retention and reduced transport. Given the demonstrated capacity of microbes to adsorb uranium (CRWMS M&O 2000 [DIRS 151561]), it follows that retention of microbes within the invert by these processes would result in retention of radionuclides as well. However, it is evident that should the invert become saturated, or nearly so, microbes and fragments with any associated radionuclides may become mobile and be transported, subject to the influences of aqueous chemistry, presence of organics, and pore sizes and fracture apertures of the geologic media.

It is apparent that considerable uncertainty surrounds the rate that microbes would affect the system around the repository. Thus, given the current knowledge, it is difficult to estimate their effects on the colloid source term, in particular the effect of microbes on colloid concentration and stability. However, it is understood that microbial action will tend to increase the sizes of inorganic colloids, which promotes gravitational settling and filtration. Thus, not including the effects of microbes in colloid source term and transport analysis is considered reasonable, and it follows that neglect of the effects of microbes is reasonable with respect to total system performance assessment dose assessments. Thus, given the available evidence, it is proposed that the effects of microbes on colloid-facilitated radionuclide transport in the Yucca Mountain Repository be neglected (see Section 5.9, Microbes and Colloidal Organic Components). Neglecting the effects of microbes would (1) eliminate the effects of colloid-microbe agglomeration, with the concomitant increase in particle size, sedimentation, and pore clogging; and thereby (2) eliminate the effects that result in radionuclide retardation and/or retention.

6.4 CONSIDERATION OF ALTERNATIVE MODELS

The following sections describe three models considered as alternatives to the base-case model. One model considers the potential for colloid development and mobilization from the actinide-rich rind on altered commercial SNF. The second model considers the rate of colloid generation as a function of waste form degradation rate. The third model considers colloid generation as a function primarily of flow rate past the degrading waste. These models are listed in Table 12 along with the principal bases and screening criteria.

Table 12. Alternative Conceptual Models Considered

Alternative Conceptual Model	Basis for Model	Screening Assessment
Production of CSNF Colloids from Spallation of U- and Pu-Rich Alteration Rinds	• Rinds containing fine-grained Pu-bearing particles and U-silicates have been observed on degraded CSNF samples. • Although particles from this layer did not spall during the tests, spallation of colloid-size particles could occur under conditions different from those under which the tests were conducted. • Given the low-water, relatively quiescent conditions of the ANL tests, more extreme conditions and likely "disruptive events" (e.g., fuel rod distortion) would be investigated.	• Given the large quantity of CSNF in the planned repository, the possible mobilization of actinide-rich particles subsequent to alteration of CSNF should be investigated. • Given anticipated "disruptive events" such as the collapse of fuel rod supports within the waste package, investigation should focus on the possible and likely ranges of conditions that could prevail and the postulated events that are likely to occur. • Additional data would be required to support this alternative model. • This ACM could be more conservative than the base-case model if it can be demonstrated that alteration rinds will spall and be transported under repository conditions.
Rate of Colloid Generation (Argonne National Laboratory)	• Rate of colloid spallation depends upon the rate of waste degradation • The rate of waste degradation may be defined by the rate of release to the alteration fluid of B (for DHLWG) and Tc (for CSNF)	• The alternative model is tailored closely to the specific experimental configuration from which the supporting data were acquired. The position of this analysis is that, while promising, the model is currently not sufficiently developed for application to more generalized conditions. • It is uncertain whether this ACM is more conservative than the base-case model.
Mechanisms of Colloid Generation in CSNF (Pacific Northwest National Laboratory)	• Colloid generation at, and mobilization from, the surface of degrading waste is primarily related to flow rate at the waste surface.	• The supporting concepts and data from the peer-reviewed literature were developed in the context of deposition and remobilization of existing colloids under conditions of significant groundwater flow. These conditions likely will not apply to conditions anticipated in the repository. • Mechanisms of colloid generation at the surface of corroding fuel may be different from mechanisms of mobilization of a discrete deposited colloid. • It is not certain whether this ACM is more conservative than the base-case model, although under unsaturated repository conditions radionuclide releases from colloids may be lower in this ACM.

NOTE: ANL = Argonne National Laboratory; CSNF = commercial spent nuclear fuel; DHLWG = defense high-level waste glass; ACM = alternative conceptual model.

6.4.1 Conditions Affecting Integrity of Commercial Spent Nuclear Fuel Alteration Rinds: Colloid Formation and Development Model

Purpose—Corrosion testing of commercial SNF has yielded few colloids, and those detected had no significant associated Pu. However, samples exhibited alteration rinds or crusts

composed of a Pu-bearing fine-grained layer overlain by a mat of U-bearing phases. The purpose of this model is to reduce uncertainties surrounding this alteration rind by simulating the spalling or disintegration of the rind, estimating the potential for colloid formation and associated radionuclides, and estimating the potential effects on releases from the waste package of this additional source of radionuclide mobility.

Experimental Results—As described in Section 6.3.1.2.1 the results of SNF and unirradiated UO_2 degradation testing showed that, although few colloids were formed (or detected), a dense rind of alteration products formed at the surface of the samples. The alteration products in the rind included a concentration of fine particulates containing high levels of Pu in addition to Zr, Ru, and rare earth elements, as well as (and frequently overlain by) U oxyhydroxides and U-silicates, depending on the test conditions. Of the few colloids identified in the commercial SNF tests (CRWMS M&O 2001 [DIRS 154071], Section 6.2.2), one sample contained primarily a hydrous uranium oxide (schoepite) and a partially crystalline uranium silicate (soddyite). The colloids contained the rare earth elements La, Ce, Pr, Nd, Sm, and Eu. Plutonium was not detected in these colloids. In another sample smectite clay colloids were formed that were similar structurally and compositionally to the smectites produced in the glass tests.

Environmental Conditions Not Considered in Experimental Investigations—Several processes that could occur in the waste package have the potential to disrupt the integrity of the alteration rind. Distortion and breakage of a fuel rod due to corrosion and collapse of the fuel rod support system ("basket") inside the package could result in breaking and dislodging of the rind from the fuel surface. High fluid flow rates (see Section 6.4.3) over exposed fuel surfaces could possibly dislodge portions of the rind. High flow rates might occur from high seepage rates into the waste package (continuous or transient), but more likely causes might be local displacements of fluid due to collapse of in-package components (essentially "squeezing" of fluid past the fuel surface), and intermittent or sustained dripping of fluid onto the fuel surface. Vibration or shock during a seismic event could shake loose portions of the rind.

Alternative Model Description and Data Needs—The alternative model would, in addition to calculating colloid and radionuclide concentrations as in the base-case model (Section 6.3), take into account possible repository conditions that were not incorporated into the various commercial SNF degradation tests. The model would require data acquired under the conditions chosen for modeling, including fuel rod distortion, shaking, and breakage; dripping at various rates and impact forces onto the fuel sample surface; various flow rates; combinations of environmental conditions; and isolation of the alteration rind and direct measurement of its properties.

Assessment of Alternative Model—This alternative model is currently at an early conceptual stage. It is intended to supplement and/or integrate with the base-case model as well as perhaps the two alternative models described in Sections 6.4.2 and 6.4.3. To be viable, the model requires data not yet at hand but available from appropriate tests. The data and model are necessary for any real reduction of the uncertainties surrounding the possible effects of breakup of the commercial SNF surface alteration rind on radionuclide releases from the waste package.

6.4.2 Rate of Colloid Generation Model

The following subsections describe an approach to estimating the *rate* of release of Pu from degraded waste, based on the rate of waste degradation. This modeling approach is preliminary and is provided here as an alternative model for prediction of colloid release and transport in the waste package and drift and as a basis for potential subsequent discussion and project planning. It is based on a colloid generation rate model presented in *Colloid-Associated Radionuclide Concentration Limits: ANL* (CRWMS M&O 2001 [DIRS 154071]). The discussions of the formation of colloids from defense high-level waste glass and commercial SNF described in Sections 6.3.1.1 and 6.3.2.2 are based on testing performed at Argonne National Laboratory and are relevant to the rate-of-colloid-generation model.

Background—It was noticed that as the drip tests proceeded, whereas relatively soluble elements such as boron and neptunium increased smoothly with time, after about eight years the concentration in the leachate of the less soluble elements Pu (Figure 13) and Am increased sharply. This was interpreted as evidence that colloid-sized fragments of the clay layer spalled from the clay layer on the surface of the corroding glass and were released into the fluid. This behavior was not observed in the static tests, probably due to increasing ionic strength, which would tend to inhibit colloid release and dispersion.

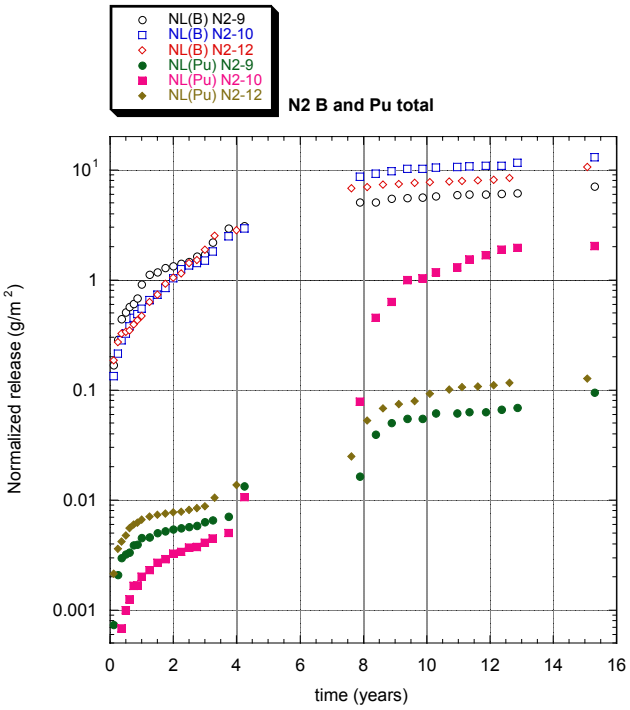

NOTE: The cumulative normalized release of the elements B and Pu from replicate tests in the N2 Series.

Source: B data from MO0301ANLGNN01.527 [DIRS 161914] and Pu DTN: MO0301ANLGNN02.527 [DIRS 161916].

Figure 13. The Cumulative Normalized Release of the Elements B and Pu in Drip Tests Evaluating Defense High-Level Waste Glass Degradation at Argonne National Laboratory

The experimental data on colloid generation resulting from defense high-level waste glass corrosion were used to develop a conceptual model for the "rate" and evolution of radionuclide release, described here, and an expression for use in predicting the rate of radionuclide release, described below. The amount of boron released was used as a marker for the amount of glass corrosion as B was observed to increase smoothly in the leachate with glass corrosion, and it did not become incorporated in alteration phases.

The "normalized release" is the radionuclide release normalized with respect to radionuclide mass fraction, surface area of the corroding glass, and volume of fluid associated with the glass. The relationship presented in *Colloid-Associated Radionuclide Concentration Limits: ANL* (CRWMS M&O 2001 [DIRS 154071]) is: NL_i (g/m^2) = [(i in ng) / (volume in mL)] * ($g/10^9$ng) * (10^6 cm^3/m^3) / (S/V in m-1) / (f_i), where the surface area to volume ratio is the SA/V (surface area to volume ratio) of the experiments and the weight fraction (f_i) of Pu is 0.01 in the glasses.

The normalized (to SA) mass loss of Pu, NL(Pu), from the glass was compared to the normalized mass loss of B, NL(B), as a function of reaction time; the ratio of the two indicates the quantity of Pu released relative to the quantity of glass corroded. In some of the tests, NL(Pu) was consistently lower than NL(B) by at least one order of magnitude. Marked decreases from this ratio can be attributed in specific tests to an increase in the glass corrosion rate due to secondary phase formation as well as destabilization of the colloids (CRWMS M&O 2001 [DIRS 154071], Section 6.2.1). The NL(Pu)/NL(B) can be less than 10^{-3} under solution conditions that inhibit colloid stability (CRWMS M&O 2001 [DIRS 154071, Section 6.4.1).

During the early stages of waste glass corrosion, the glass dissolves and releases components at a rate proportional to the rate of corrosion of the waste form. As this occurs, clay colloids nucleate in the solution and clay alteration layers form on the surface of the glass. These clay phases, which contain embedded radionuclide-bearing phases, also sorb ionic radionuclide species and/or colloidal radionuclide-bearing phases. If the ionic strength of the solution is low, the colloids are generally stable (see Section 6.3.2.2) and the rate of formation of the radionuclide-bearing colloids is proportional to the amount of altered glass (CRWMS M&O 2001 [DIRS 154071], Section 6.2.1).

As the glass alters, the rate of radionuclide-bearing colloids production decreases; this is attributed by the investigators to colloid deposition (by sorption) on the fixed clay alteration layer. Once the cumulative normalized B release is greater than approximately 1 to 3 g m^{-2}, the radionuclide release is controlled by spallation of the clay layer. Figure 14 illustrates the observed increases in colloid production due to the onset of spallation.

Thus, radionuclide release may be viewed as a two-step process: (1) alteration of the glass waste form and precipitation of colloids, and (2) erosion of colloid-sized fragments from the alteration products (CRWMS M&O 2001 [DIRS 154071], Section 6.2.1). The observed concentrations of defense high-level waste glass-derived colloids is discussed in Section 6.3.2, Colloid Stability and Concentration.

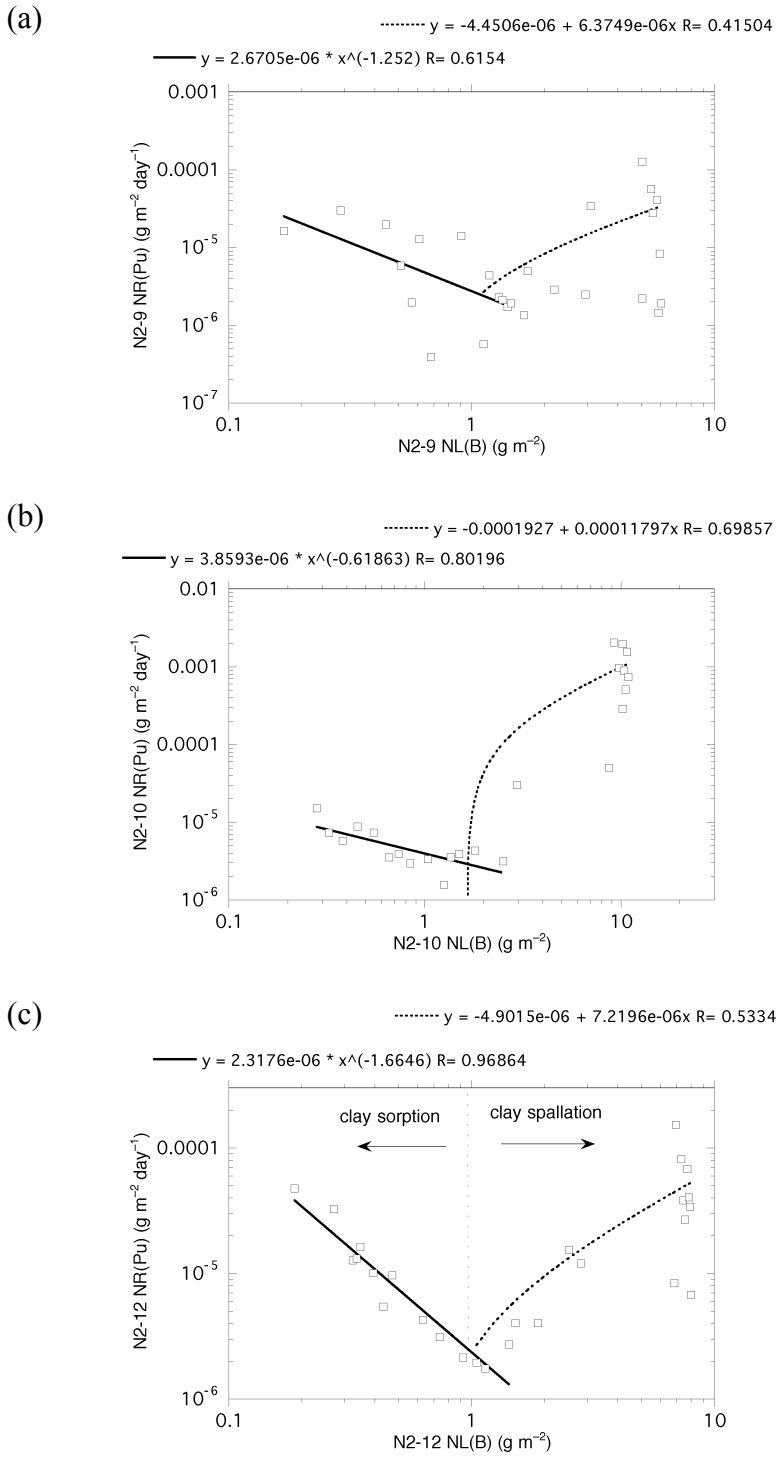

NOTE: Plutonium Release Rate versus Cumulative Boron Release Plutonium Release Rate (calculated for each sampling interval) Versus Cumulative Boron Release: (a) N2-9, (b) N2-10, (c) N2-12. The total plutonium release is used, including vessel acid strip.

Source: Adapted from CRWMS M&O 2001 [DIRS 154071], Figure 29.

Figure 14. Plutonium Release Rate versus Cumulative Boron Release Plutonium Release Rate

(d)

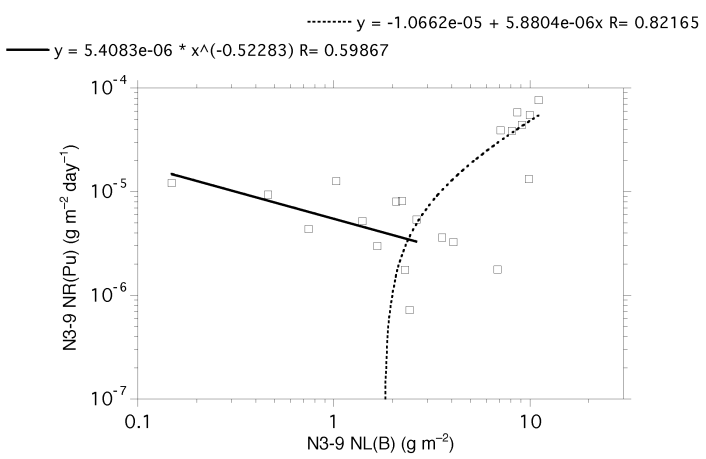

(e)

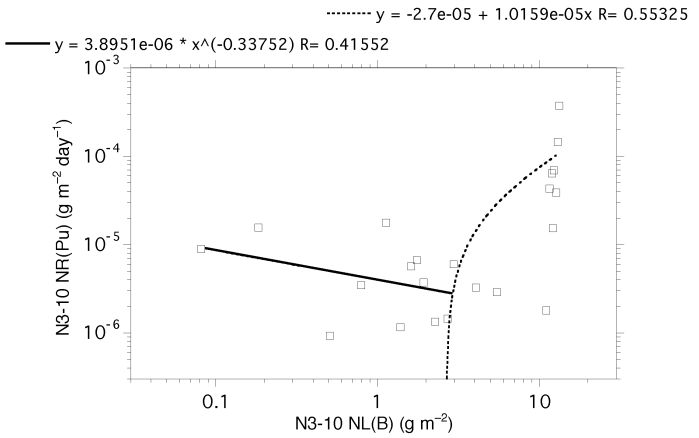

(f)

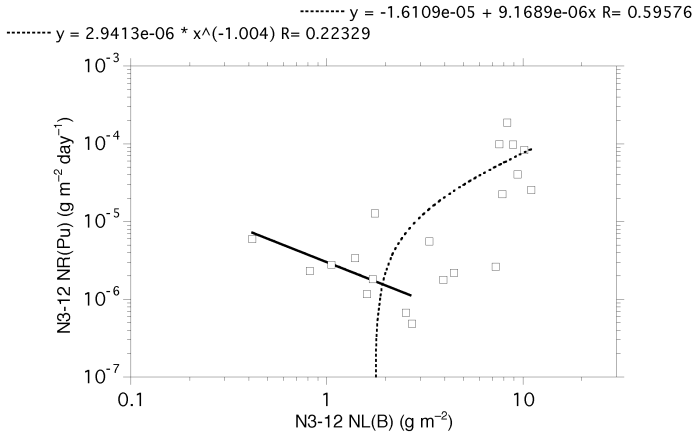

NOTE: Plutonium release rate (calculated for each sampling interval) versus cumulative boron release: (d) N3-9, (e) N3-10, (f) N3-12. The total plutonium release is used, including vessel acid strip.

Source: Adapted from CRWMS M&O 2001 [DIRS 154071], Figure 29.

Figure 14. Plutonium Release Rate versus Cumulative Boron Release Rate (continued)

Rate of Colloid Formation from Defense High-Level Waste Glass—The normalized mass loss of Pu, NL(Pu), was compared to the normalized mass loss of boron, NL(B), to indicate the amount of Pu released relative to the amount of B released, which is stipulated to represent the amount of defense high-level waste glass corroded. As indicated in Figure 15 the NL(Pu) is consistently lower than the NL(B) by at least one order of magnitude. NL(Pu)/NL(B) decreases for the longer duration tests at higher SA/V, up to about 10^{-3} for conditions which inhibit stable colloids.

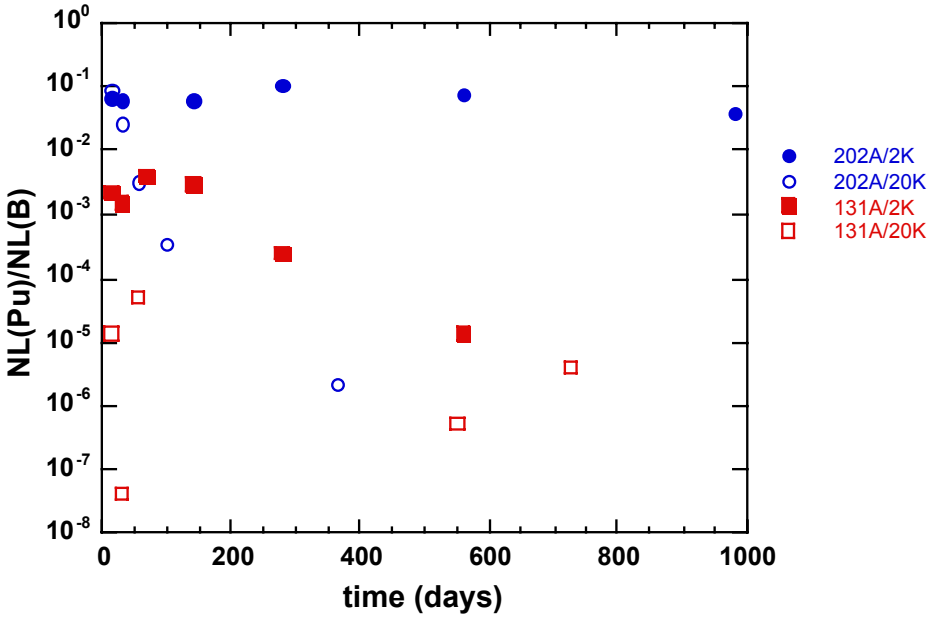

NOTE: Ratio of normalized mass loss of plutonium to normalized mass loss of boron, NL(Pu)/NL(B), as a function of test duration (in days) for static corrosion tests on the SRL 202A and SRL 131A glasses at 2,000 and 20,000/m (T = 90°C)

Source: Ebert 1995 [DIRS 113219], and adapted from Figure 27 of CRWMS M&O 2001 [DIRS 154071].

Figure 15. Ratio of Normalized Mass Loss of Plutonium to Normalized Mass Loss of Boron, NL(Pu)/NL(B)

Under low ionic strength conditions, the colloids are stable in the fluid and the rate of formation of Pu-bearing colloids, $dm_{Pu\text{-}coll}/dt$, is proportional to the amount of altered glass, M_{alt}. As the glass alters, the rate of radionuclide-bearing colloids production decreases, initially following a power-law, attributed to their sorption by the fixed clay alteration layer (CRWMS M&O 2001 [DIRS 154071], Section 6.4.2). The rate of colloid formation can be described by the relationship in Equation 8.

$$\frac{dm_{Pucoll}}{dt} = a\left(M_{alt}\right)^{-b} \qquad \text{(Eq. 8)}$$

The constants, *a* and *b*, derived for the various glasses may be a function of the SA/V, leachate composition (ionic strength, etc.), colloid composition, or other parameters. Table 13 summarizes the ranges and bounding values for *a* and *b*.

Table 13. Ranges and Bounds for the Constants, *a* and *b*, in Equation 8

	Static-Saturated Tests		Drip Tests		Bounding Values
Constant	Low	High	Low	High	
a	8×10^{-12}	4×10^{-6}	2×10^{-6}	5×10^{-6}	10^{-4}
b	3	8	0.3	1.7	1

Source: Data from CRWMS M&O 2001 [DIRS 154071], Section 6.4.2.

At the high ionic strengths encountered in certain static tests, there was no correlation observed between Pu and B production rates since the quantity of colloids was very low. In the drip tests, ionic strength remained low because EJ-13 water was periodically injected.

Once the cumulative B release is greater than approximately 1 to 3 g m^{-2}, the radionuclide release is controlled by spallation of the clay layer. Thus, radionuclide release is a two-step process: (1) alteration of the glass waste form and precipitation of colloids and (2) erosion of colloid-sized fragments from the alteration products.

Release of colloids due to spallation is given by the derived relationship:

$$\frac{dm_{Pu_{coll}}}{dt} = \kappa M_{alt} \qquad \text{(Eq. 9)}$$

where $dm_{Pu_{coll}}$ is the mass release of Pu suspended as colloidal particulates and κ is a parameter that depends on, among other things, the mechanical condition of the altered waste form, the water flow rate over the waste form, and the water chemistry (CRWMS M&O 2001 [DIRS 154071], Section 6.4.2). An empirical bound for κ is 10^{-4} d^{-1}.

Rate of Colloid Formation from Commercial SNF—The normalized mass loss of Pu, NL(Pu), was compared to the normalized mass loss of technetium, NL(Tc), to indicate the amount of Pu released relative to the amount of Tc released, which is stipulated to represent the amount of SNF corroded. It was noted that the reaction of SNF under unsaturated drip test conditions does not exhibit a correlation between the rate of Pu-bearing colloid formation and the corrosion of spent fuel (see Figure 16). The scattered data indicating Pu release rate versus Tc release rate (which are proportional to the NL(Pu) and NL(Tc), respectively) were bounded by assuming conservatively that NL(Pu)/NL(Tc) is equal to 10^{-5} d^{-1}.

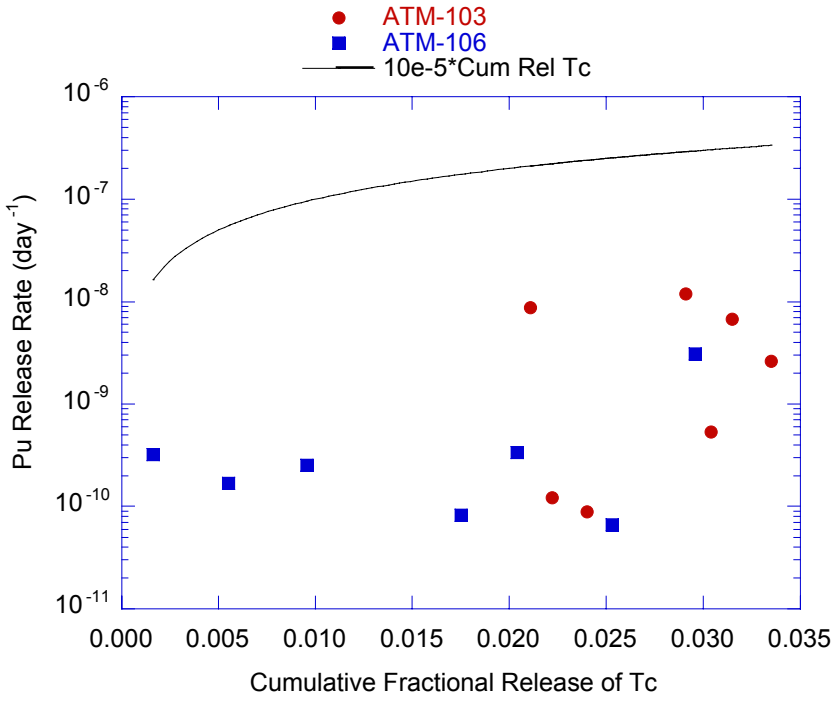

NOTE: The fractional release rate of Pu as a function of cumulative fractional Tc release for the ATM-103 and ATM-106 high-drip-rate tests. The solid line is the conservative bound based upon a constant of 10^{-5} d^{-1} (Figure 30 from CRWMS M&O 2001 [DIRS 154071]).

Figure 16. Fractional Release Rate of Pu as a Function of Cumulative Fractional Tc Release for the ATM-103 and ATM-106 High-drip-rate Tests

Calculation of Quantity and Rate of Production of Irreversibly Attached Radionuclides— Parameters used to calculate mobilized radionuclide quantities and rates of production are listed in Table 14. After the quantities of total mobilized radionuclides are calculated, they are distributed between radionuclides irreversibly attached to colloids, dissolved (aqueous) radionuclides, and radionuclides co-precipitated in immobile secondary phases. Since the experimental evidence indicates that most waste form colloids are radionuclides and/or radionuclide-bearing phases irreversibly associated with smectite colloids, this fraction is given as the difference between the dissolved radionuclides and the total radionuclides mobilized by the waste degradation time step:

$$RN_{coll,irrev} + RN_{layer,irrev} = RN_{mob} - RN_{diss} - RN_{secondaryphase} \quad \text{(Eq. 10)}$$

The irreversibly attached radionuclides are in turn distributed between the clay layers on altered defense high-level waste glass and clay colloids produced from both defense high-level waste glass and SNF; the aqueous radionuclides are available for reversible sorption onto colloids.

If the cumulative release of boron is less than 1 g m^{-2}, then the following relationship is invoked to calculate the quantity of radionuclides irreversibly attached to colloids produced for that time step. The equation for calculating the mass of radionuclides is:

$$\text{Mass of irreversibly attached RN} = a * (B_{cum})^{-b} \quad \text{(Eq. 11)}$$

where B_{cum} represents the mass of defense high-level waste glass degraded and *a* and *b* are empirically-derived constants.

Table 14. Parameters Used in Description of Alternative Model

Parameter	Description	Value /Range/ Distribution	Source
B_{inv}, Tc_{inv}, Pu_{inv}, Am_{inv}	Masses of B, Tc, and RN's in unaltered waste form during time step	--------	Would be calculated by TSPA-LA model
B_{mob}, Tc_{mob}, Pu_{mob}, Am_{mob}	Masses of B and RN's "mobilized" in WF_{deg} during time step	--------	Would be calculated by the TSPA-LA model
B_{cum}	Cumulative mass of B "mobilized" in WF_{deg} for all previous time steps	--------	Would be calculated by the TSPA-LA model
M_{alt}	Amount of a altered glass	--------	CRWMS M&O 2001 [DIRS 154071]
a	Empirically derived constant used in expression for precipitated smectite colloids	10^{-4} (bound)	CRWMS M&O (2001 [DIRS 154071])
b	Empirically derived constant used in expression for precipitated smectite colloids	1 (bound)	CRWMS M&O (2001 [DIRS 154071])
κ	Empirically derived constant used in expression for spalled smectite colloids	10^{-4} (bound)	CRWMS M&O (2001 [DIRS 154071])

NOTE: RN = radionuclide; WF = waste form.

If B_{cum} is greater than 3 g m^{-2}, then the second model is invoked to calculate the quantity of radionuclides irreversibly attached to colloids formed from spallation of the alteration clay layer. The equation for calculating radionuclide mass mobilized due to spallation is:

$$\text{Mass of irreversibly attached spalled RN} = \kappa * B_{cum} \quad \text{(Eq. 12)}$$

where κ is an empirically-derived constant.

If B_{cum} is between 1 and 3, then either the first or second is chosen randomly (0.5 probability).

In the case of SNF, the quantity of radionuclides irreversibly attached to colloids was bounded according to the expression:

$$\text{Mass of irreversibly attached RN} = (Tc_{mob} / Tc_{inv}) * 10^{-5} \quad \text{(Eq. 13)}$$

Assessment of Rate-of-Colloid-Generation Model—This alternative abstraction takes into account many of the results from the Argonne National Laboratory waste form corrosion experimental program as well as models derived from them. It incorporates an analytical approach that would couple the waste form degradation calculations by the TSPA-LA model more closely to the process model derived from the experiments.

While it takes advantage of the most complete information available on waste form corrosion, at the same time it is tailored closely to the experimental conditions and configurations. There are aspects of the experiments that may make them inappropriate to apply to a more general case. A possible example is the rate of spallation of the clay layer from altered defense high-level waste glass, which may be due to the specific dynamics surrounding the impacts of the drips falling on the sample in the defense high-level waste glass drip tests (recall that no spallation was observed in the static tests (CRWMS M&O 2001 [DIRS 154071], Section 6.2.1). If the corroded contents of a failed waste canister assume a geometry that does not allow dripping of water onto the alteration products, spallation may not occur. If dripping does occur, of course, spallation may be a viable process, and an analysis of colloid production and transport would have to consider it.

6.4.3 Mechanisms of Colloid Generation in Commercial Spent Nuclear Fuel

This alternative model, described in Buck 2003 [DIRS 163117], investigates the processes whereby colloid generation at, and mobilization from, the surface of degrading waste is primarily related to flow rate at the waste surface. The supporting concepts and data from the peer-reviewed literature that support this alternative model were developed in the context of deposition and remobilization of existing colloids under conditions of moderate to significant fluid flow. Although it is possible that relatively high flow conditions could prevail or flow transients occur at some point, low flow conditions are expected to prevail over the regulatory period, so that colloid entrainment may not occur.

Under specific experimental environments, a flow rate dependence on colloid release has been observed (Buck 2003 [DIRS 163117]), although a full explanation for these empirical relationships has not yet been developed. In this alternative model flow rate dependence of the entrainment and mobilization of waste form colloids would be determined. In addition, the influences of fluid chemistry and of the actual phases formed and their physical association in a model waste form system would be investigated. This model will allow quantification of changes in particle release under different flow rates, fluid chemistries, and particle-particle interaction scenarios.

Assessment of the Colloid Generation Mechanisms Model—Although transport of colloids within the waste package may be negligible, colloid transport could be initiated and sustained if the system is subjected to sufficient physical or chemical perturbations. Understanding the effects of these perturbations regarding colloid mobilization in the waste package is important to understanding the potential impact of colloids on dose at Yucca Mountain (see also Section 6.4.1). However, this alternative colloid generation model is not considered in detail, and an assessment of the potential effects on the dose calculations that might result from its inclusion in the TSPA-LA model was deemed unnecessary; for example, seepage water flow rates needed to drive the component processes of this model are not anticipated in the repository environment (see Section 1.1).

6.5 MODEL FORMULATION FOR BASE-CASE ASSESSMENT

This section describes in detail the methodology used to incorporate the various model elements formulated in this model analysis into a colloids source term abstraction (i.e., a simplified model intended to retain the important principles and features of the analyses) for implementation in the

TSPA-LA model. The logic and parameters implemented in the TSPA-LA model are provided, although specific programming details are not.

Figure 17 provides an overview of the model methodology with cross-references to the underlying model elements developed in Section 6. Figure 17a illustrates how colloids are modeled in the waste package (Section 6.5.1), and Figure 17b in the drift (Section 6.5.2). Parameters used in the abstraction are described in Table 16. Sections 6.5.1 and 6.5.2 present the details of the abstraction, and Figures 18 through 21 illustrate the logic and flow of the abstraction approach.

At each time step executed in the TSPA-LA calculations, the colloid model uses characteristics of the water in the waste package (ionic strength, pH, and dissolved radionuclide concentrations) to describe the formation and behavior of colloids and the distribution of the radionuclides in the waste package. The elements considered and incorporated into the calculations are Pu, Am, Th, Pa, and Cs. Three types of colloids are considered in the model—waste form, iron oxyhydroxide, and seepage water/groundwater. Waste form colloids generated from defense high-level waste glass are included in the model, but colloids from commercial and DOE SNF are not. Colloids formed from the defense high-level waste glass and the naturally occurring groundwater colloids are stipulated to be smectite colloids. The iron oxyhydroxide colloids are formed during corrosion of steel waste package materials.

The stability of colloids is defined by ionic strength and pH, with separate relationships for smectite colloids (Section 6.3.2.2, Figure 17a and 17b, Table 16) and iron oxyhydroxide colloids (Section 6.3.2.3, Figure 17a and 17b, Table 16). At each time step, the values of I and pH of the waste package solution are used as input to determine whether or not colloids are stable. For both types of colloids, when unstable, a low (non-zero) limit of colloid concentration is used (Figure 17 and Table 16 for smectite; Table 16 for iron oxyhydroxide). Within the stability zone for defense high-level waste glass smectite colloids, a function is used that relates Pu and colloid concentrations to ionic strength (Figures 8, 9, and 17). For iron oxyhydroxide colloids upper and lower limits of ionic strength are used in the definition of stability (Figures 7 and 17; Table 16); for groundwater smectite colloids, an upper limit of colloid concentration is used (Figures 12 and 17; Table 16).

Reversible sorption onto the smectite colloids for each of the five considered radionuclides is modeled (Section 6.3.3.1). For iron oxyhydroxide colloids, irreversible sorption of Pu and Am is also included (Section 6.3.3.2). Within the waste package, the major fractions of total Pu and Am available at each time step are sorbed to stationary corrosion products, a smaller fraction to colloids, and a smaller fraction remains dissolved. Further, a high percentage of the sorbed Pu is irreversibly sorbed onto colloids and stationary corrosion products; a small percentage is reversibly sorbed. Distribution coefficients (K_d values) for each of the radionuclides are used for both smectite and iron oxyhydroxide colloids (Table 16).

The model calculates the concentration of dissolved radionuclides, the concentration of Pu and Am embedded in defense high-level waste glass smectite colloids, the concentration of radionuclides sorbed reversibly onto all colloids, the concentration of radionuclides sorbed irreversibly onto iron-hydroxide colloids, and the mass concentration of each colloid type (Figure 17a).

The colloid and radionuclide concentration values along with the ionic strength and pH of solution serve as source term for the invert. The TSPA-LA model calculates the ionic strength and pH of the resulting solution of the waste package effluent mixed with the invert water (this is not a component of the colloid model). Based on the new values of ionic strength and pH in the invert, the model determines colloid stabilities at the new fluid composition and redistributes the reversibly sorbed radionuclides and dissolved radionuclides based on the distribution coefficients and the total mass of each type of colloid (Figure 17b). All colloids flow unimpeded through the invert to the unsaturated zone. The irreversibly sorbed radionuclides do not get redistributed.

6.5.1 Waste Form Abstraction Implementation in Total System Performance Assessment–License Application

The abstraction uses a set of input parameters for the TSPA-LA model, listed and described in Table 1 in Section 4.1. Input parameters have been taken from the Argonne National Laboratory colloid-related report (CRWMS M&O 2001 [DIRS 154071]) and DTNs: LL000905312241.018 [DIRS 152621] and LL991109751021.094 [DIRS 142910]; others have been extracted from available project documents and the scientific literature.

In addition, the abstraction requires parameters calculated by the TSPA-LA model as output from in-package chemistry, solubility limits, and near-field chemical environment calculations: $C_{RN,diss}$, I_{wp}, and pH_{wp} (see Table 16) (*Dissolved Concentrations of Radioactive Elements*, BSC 2003 [DIRS 163152]; *Engineered Barrier System: Physical and Chemical Environment Model*, BSC 2002 [DIRS 160315], analysis described in Section 1.2.2).

The concentrations of colloids and colloid-associated radionuclides were calculated on the basis of abstractions of the laboratory and field observations and chemical principles described in Section 6.3. A stepwise approach was taken in the abstraction, and each step is set out below with a flow diagram and logic statements that describe the abstraction step. Parameters are defined in Table 16.

6.5.1.1 Waste Form (Smectite) Colloids

Table 1 lists waste form colloid-related input parameters used in the abstraction. Corroborating/supporting data and information used to develop the parameters are listed in Table 2.

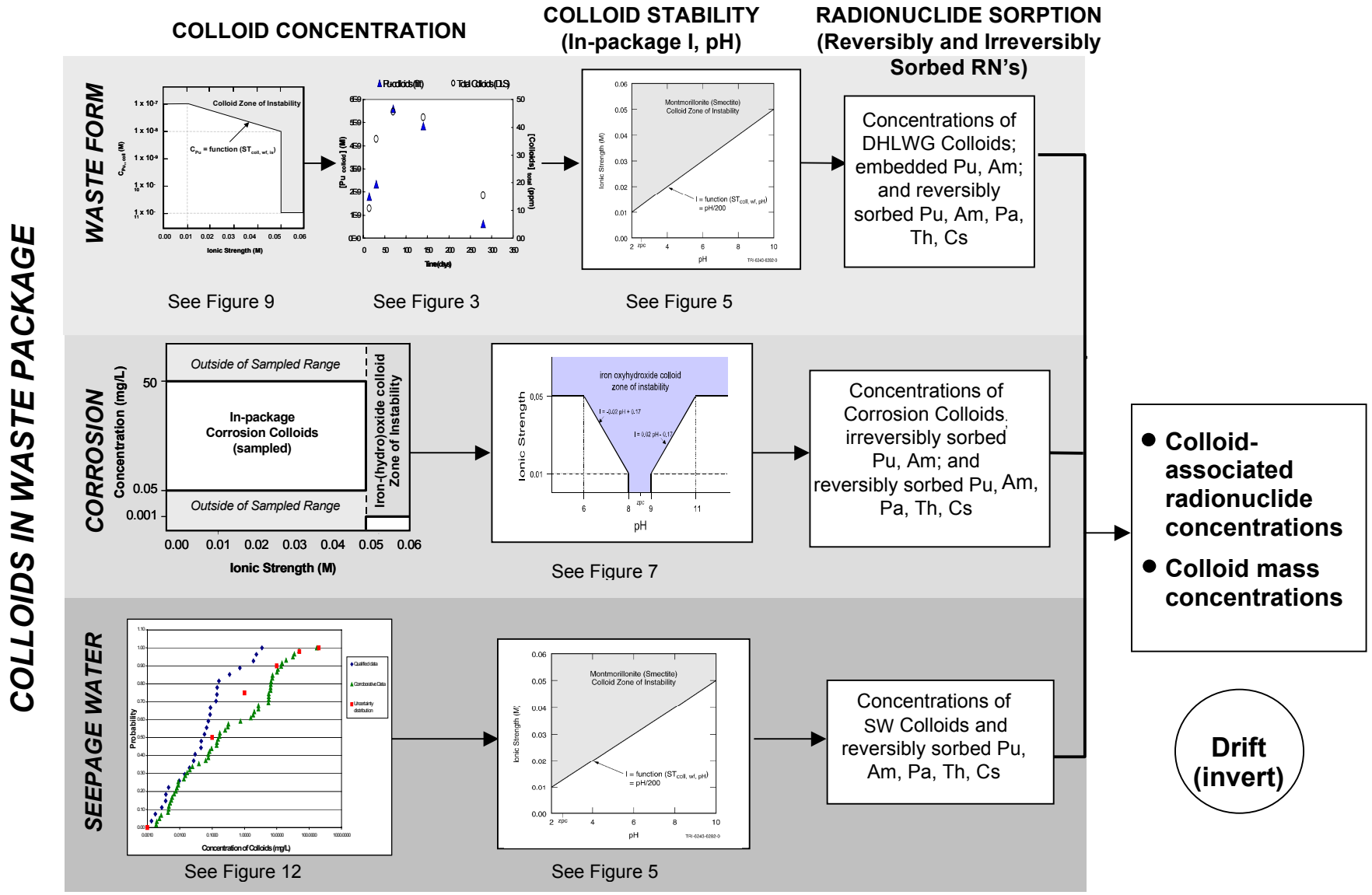

NOTE: RN = radionuclide; SW = seepage water; DHLWG = defense high-level waste glass.

Figure 17a. Processes Within the Waste Package

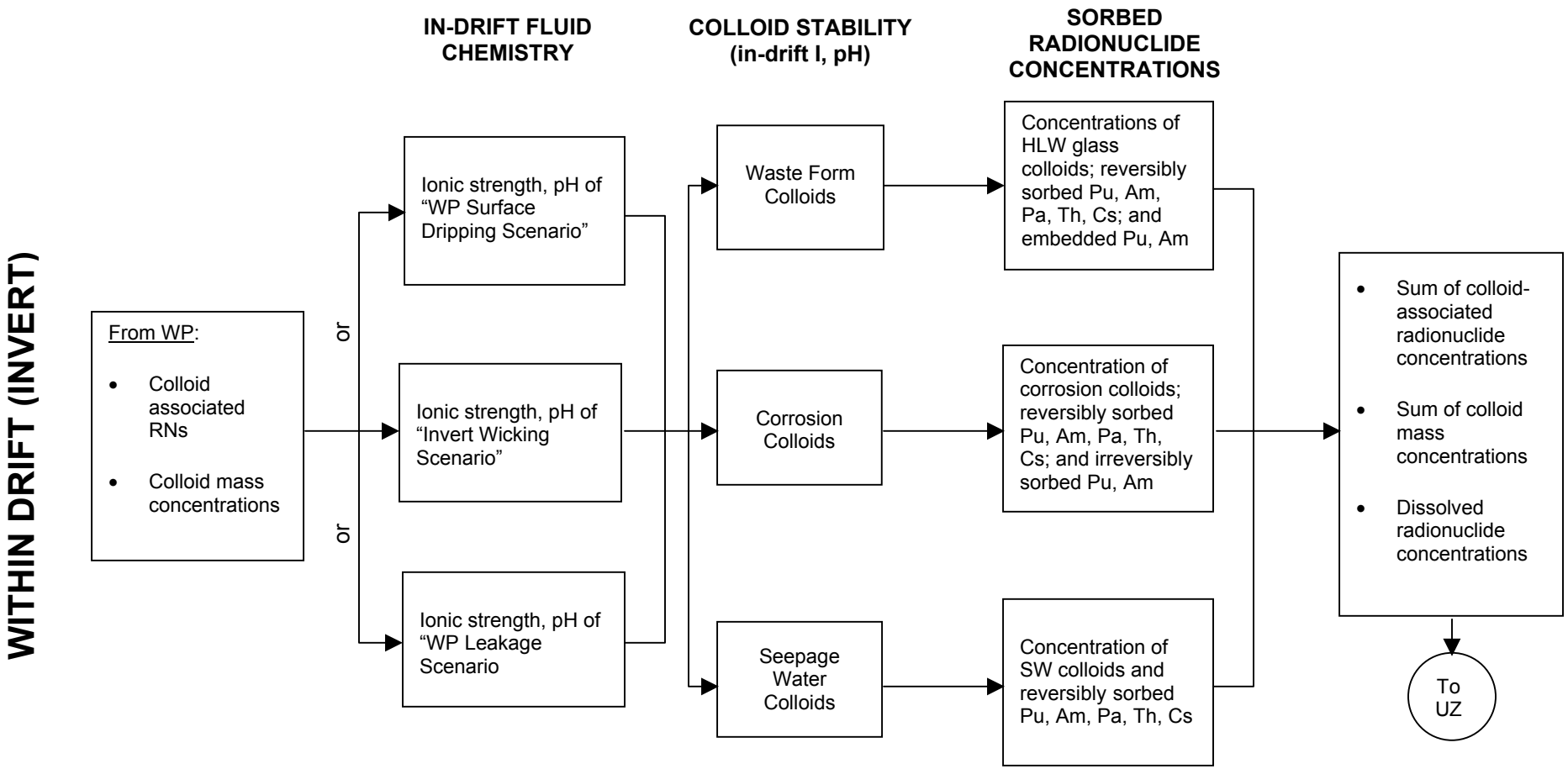

NOTE: WP = waste package; RN = radionuclide; SW = seepage water; HLW = high-level waste; UZ = unsaturated zone.

Figure 17b. Processes within the Drift (Invert)

Step 1a. The radionuclides Pu and Am are modeled in Step 1a (Figure 18a) as embedded within waste form colloids, which are produced from corrosion of defense high-level waste glass. The concentrations are defined by ionic strength, based on experimental observations (Sections 6.3.1.1 and 6.3.2.4).

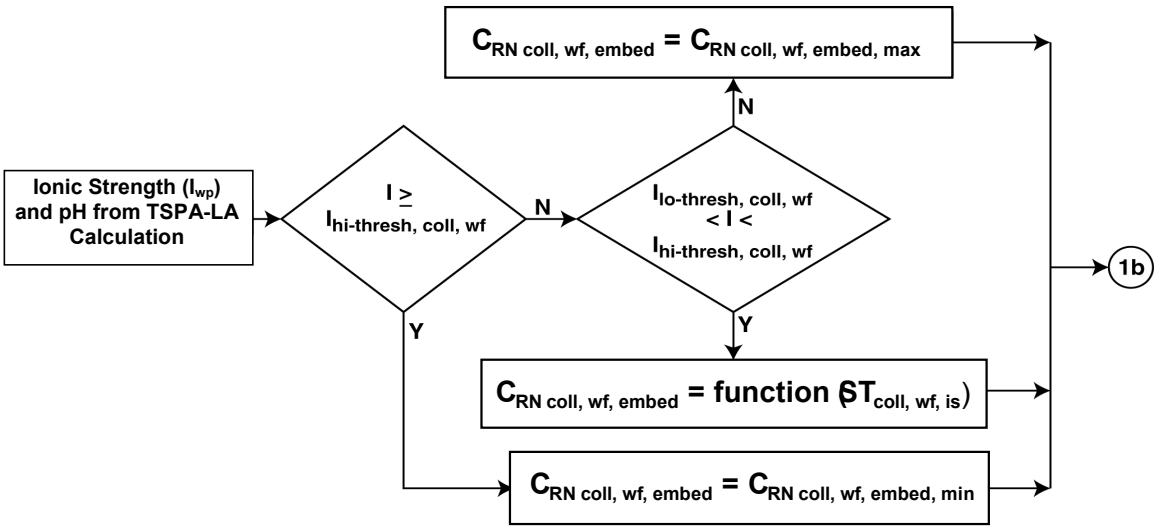

Step 1a Waste-Form Colloids - Generation from Degradation of HLW Glass

Input I_{wp}

IF $I \geq I_{hi\text{-}thresh,coll,wf}$

THEN $C_{RNcoll,wf.embed} = C_{RNcoll,wf,embed,min}$

ELSE

IF $(I > I_{lo\text{-}thresh,coll,wf})$ AND $(I < I_{hi\text{-}thresh,coll,wf})$

THEN $C_{RNcoll,wf,embed} = function(ST_{coll,wf,is})$

ELSE $C_{RNcoll,wf,embed} = C_{RNcoll,wf,embed,.max}$

$function(ST_{coll,wf,is})$: $-2.50E\text{-}6 \times I + 1.25E\text{-}7$ (see Equation 4, Section 6.3.2.4)

Figure 18a. Flow Chart and Logic Statements: Effect of Ionic Strength on the Concentration of Waste Form Colloid-Associated Radionuclides Generated Defense High-Level Waste Glass Degradation Based on Experiments Conducted at Argonne National Laboratory (see Figure 9)

$I_{hi\text{-}thresh,coll,wf}$ and $I_{lo\text{-}thresh,coll,wf}$ are threshold values of the ionic strength of the fluid in the waste package used to calculate the concentration of embedded Pu used in the abstraction. (Am is calculated as the product of the Pu concentration times the Am/Pu ratio in the inventory, which is determined at each time step of the TSPA-LA model calculations. Stability of the defense high-

level waste glass-derived colloids is determined in Step 1b. Colloid mass concentrations are calculated from the amount of Pu embedded in smectite waste form colloids in Step 1c.

Step 1b. The stability of waste form colloids from defense high-level waste glass is determined on the basis of the fluid ionic strength and pH (Figure 18b), based on known properties of smectite colloidal suspensions (Section 6.3.2.2).

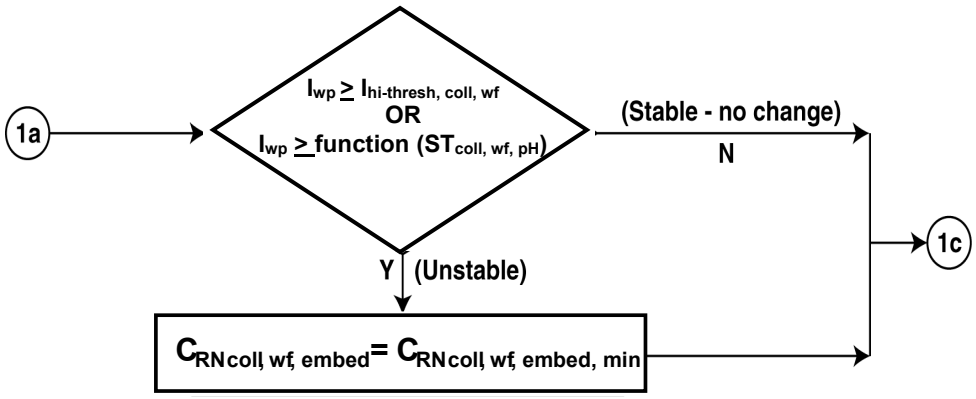

Step 1b Waste-Form Colloids - Effect of pH and Ionic Strength on Stability

Input pH_{wp}

IF ($I_{wp} \geq I_{hi\text{-}thresh,coll,wf}$) OR ($I \geq$ function($ST_{coll,wf,pH}$))

THEN $C_{RNcoll,wf,embed} = C_{RNcoll,wf,embed,min}$

function($ST_{coll,wf,pH}$): pH/200

Figure 18b. Flow Chart and Logic Statements: Effect of pH and Ionic Strength on Waste Form Colloid-Associated Radionuclide Concentration Based on Stability Behavior of Montmorillonite Colloids (see Figure 5)

The $I_{hi\text{-}thresh,coll,wf}$ and $I_{lo\text{-}thresh,coll,wf}$ parameters are the same threshold values of the ionic strength of the fluid in the waste package used to determine Pu concentration (Step 1a). They are used here to determine, along with pH, whether or not the colloids are stable. These threshold values may vary due to specific chemical and environmental conditions and are therefore sampled over a range (Table 16).

Step 1c. Calculation of the mass concentration of waste form colloids from defense high-level waste glass (Figure 18c) is done on the basis of experimental observations (Section 6.3.1.1, Figure 3, Equation 1).

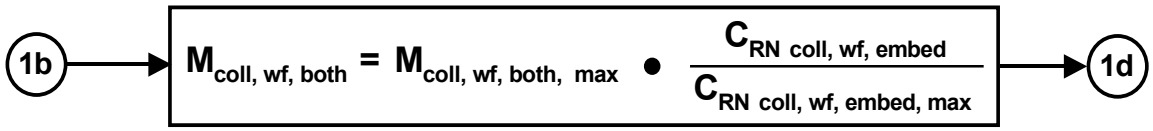

Step 1c Waste-Form Colloids - Mobile Colloid Mass

$$M_{coll,wf,both} = M_{coll,wf,both,max} \times C_{RNcoll,wf,embed} \div C_{RNcoll,wf,embed,max}$$

Figure 18c. Flow Chart and Logic Statements: Determination of Mobile Mass Concentration of Waste Form Colloids $M_{coll,wf,both}$)

The colloid mass concentration is related to the embedded Pu concentration (Equation 1). With reference to Equation 1, $M_{coll,wf,both,max}$ is the maximum colloid mass concentration corresponding to the maximum Pu concentration, $C_{RNcoll,wf,embed,max}$. It is an intermediate result based on the experimental data showing the relationship between embedded Pu concentration and colloid mass concentration (see DTNs, listed in Table 16). $M_{coll,wf,both}$ is a parameter that represents the total mass concentration of defense high-level waste glass colloids with *both* embedded and reversibly sorbed radionuclides (Table 16).

Step 1d. The calculation of the concentration of radionuclides (Pu, Am, Th, Pa, Cs) reversibly sorbed on waste form colloids from defense high-level waste glass (Section 6.3.3.1, Figure 18d) is based on the mass concentration of waste form colloids, K_d values describing the distribution of radionuclides between the fluid and smectite colloids, and the dissolved concentration of radionuclides as calculated by the TSPA-LA model.

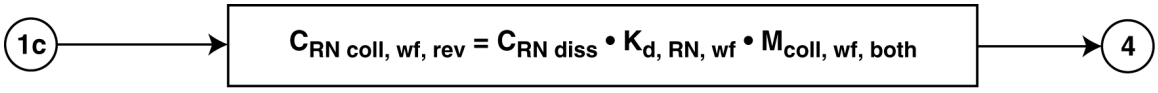

Step 1d Waste-Form Colloids - Sorption of Radionuclides

$$C_{RNcoll,wf,rev} = C_{RNdiss} \times K_{d,RN,coll,wf} \times M_{coll,wf,both} \text{ x } 1E\text{-}6$$

Figure 18d. Flow Chart and Logic Statements: Sorption of Radionuclides on Waste Form Colloids

The C_{RNdiss} is the concentration of radionuclide "RN", determined by the TSPA-LA model as output from the solubility concentration model, that is used as an input to the colloid abstraction. $K_{d,RN,wf}$ is a parameter derived from several sources (see Tables 6-10) and is an equilibrium sorption coefficient used to approximate the partitioning of dissolved radionuclide "RN" between colloids and fluid.

6.5.1.2 Corrosion-Generated (Iron Oxyhydroxide) Colloids

Table 1 lists waste form colloid-related input parameters used in the abstraction. Corroborating/supporting data and information used to develop the parameters are listed in Table 2.

Step 2a. The stability and mass concentration of iron oxyhydroxide colloids formed as a result of the corrosion of waste package components is determined on the basis of the fluid ionic strength and pH (Section 6.3.2.3, Figures 17a and 18e).

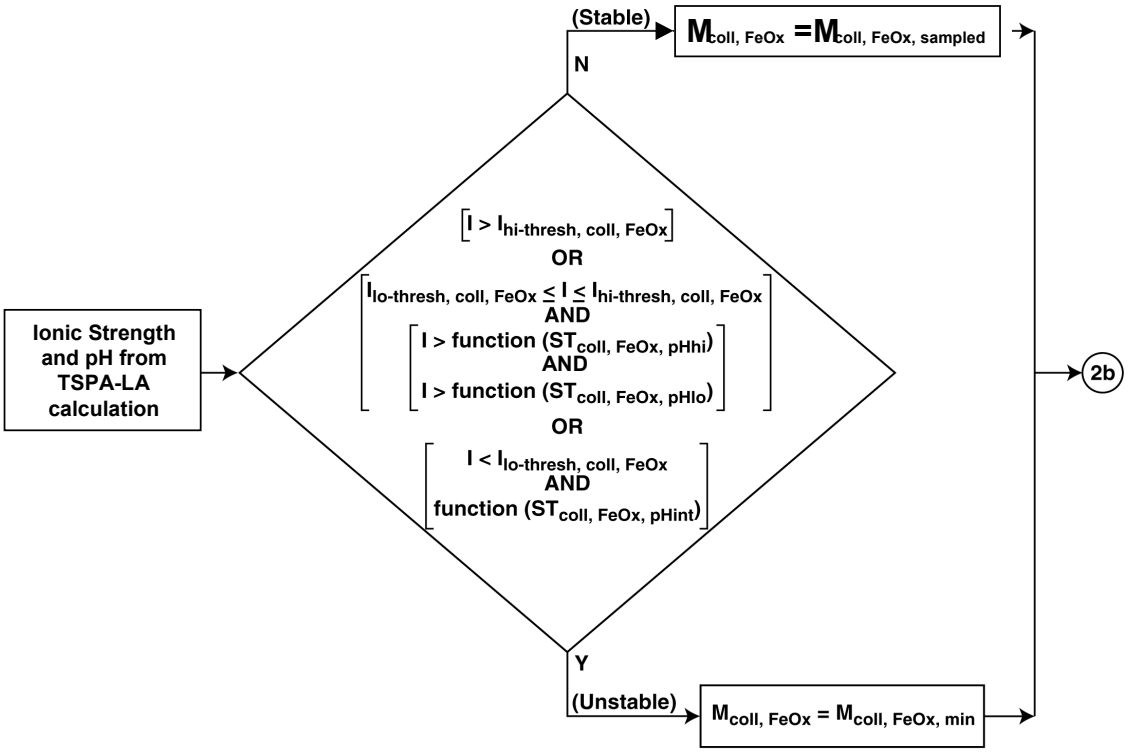

Step 2a Iron Oxyhydroxide Colloids – Effect of pH and Ionic Strength on Stability and Concentration

IF
BEGIN
$(I > I_{hi\text{-}thresh,coll,FeOx})$
OR $((I \ge I_{lo\text{-}thresh,coll,FeOx})$
AND $(I > function(ST_{coll,FeOx,pHhi}))$ OR $(I > function(ST_{coll,FeOx,pHlo})))$
OR $((I < I_{lo\text{-}thresh,coll,FeOx})$ AND $(function(ST_{coll,FeOx,pHint}))$
END
THEN
$M_{coll,FeOx} = M_{coll,FeOx,min}$
ELSE
$M_{coll,FeOx} = M_{coll,FeOx,sampled}$
$function(ST_{coll,FeOx,pHhi})$: $-0.02 \times pH + 0.17$
$function(ST_{coll,FeOx,pHlo})$: $+0.02 \times pH – 0.17$
$function(ST_{coll,FeOx,pHint})$ (boolean): $((pH \ge 8)$ AND $(pH \le 9))$

Figure 18e. Flow Chart and Logic Statements: Effect of Ionic Strength and pH on Stability of Iron Oxyhydroxide Colloids (see Figure 7)

The $I_{hi\text{-}thresh,coll,wf,FeOx}$ and $I_{lo\text{-}thresh,coll,FeOx}$ are threshold values of the ionic strength of the fluid in the waste package used to calculate the stability and concentration of corrosion-generated colloids, similar to the waste form colloid stability determination in Step 1a. $ST_{coll,FeOx,pHhi}$ and $ST_{coll,FeOx,pHlo}$ are functions which incorporate threshold values of pH for determining the stability and concentration of corrosion-generated colloids in conjunction with the ionic strength thresholds.

Step 2b. In this step two types of sorption are modeled, irreversible sorption of Pu and Am onto iron oxyhydroxide corrosion colloids and fixed corrosion products (Section 6.3.3.2, Figure 18f); and reversible sorption of Pu, Am, Pa, Th, and Cs onto iron oxyhydroxide colloids (Section 6.3.3.1). The distribution of irreversibly sorbed Pu and Am onto fixed and colloidal substrates is performed in the TSPA-LA model. It is a kinetic model that is described in *EBS Radionuclide Transport Abstraction* (BSC 2003 [DIRS 163935]). Parameters used include specific surface area (S_A), the sampled corrosion colloid mass concentration ($M_{coll,FeOx,sampled}$), concentration of dissolved radionuclides (C_{RNdiss}), and flux out ratio (F_{RN}).

Reversible sorption is calculated from the sampled mass concentration of corrosion colloids, K_d values describing the distribution of radionuclides between the fluid and iron oxyhydroxide colloids, and the dissolved concentration of radionuclides as calculated by the TSPA-LA model.

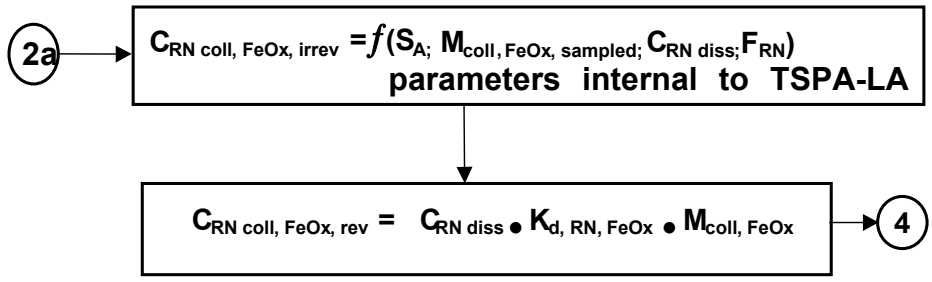

Step 2b Iron Oxyhydroxide Colloids – Sorption of Radionuclides

$$C_{RNcoll,FeOx} = C_{RNdiss} \times K_{d,RN,FeOx} \times M_{coll,FeOx} \text{ x } 1E\text{-}6$$

Figure 18f. Flow Chart and Logic Statements: Sorption of Radionuclide RN on Iron Oxyhydroxide Colloids

In Step 2b the irreversibly sorbed Pu and Am are determined, along with reversibly sorbed Pu, Am, Pa, Th, and Cs. The C_{RNdiss} is the concentration of radionuclide "RN", determined by the TSPA-LA model as output from the solubility concentration model, which is used as an input to the colloid abstraction. $K_{d,RN,FeOx}$ is a parameter derived from several sources (see Tables 6-10) and is an equilibrium sorption coefficient used to approximate the partitioning of dissolved radionuclide between colloids and fluid. The 1E-6 portion of the relationship designates a correction factor to accommodate differences in units among the various parameters.

6.5.1.3 Seepage Water (Smectite) Colloids

Seepage water/groundwater colloid-related input parameters used in the abstraction are listed in Table 16. All information used to develop the parameters is listed in the table, including corroborative information.

Step 3a. The mass concentration of seepage water colloids is calculated on the basis of fluid ionic strength in Step 3a (Sections 6.3.2.2 and 6.3.2.5, Figure 18g).

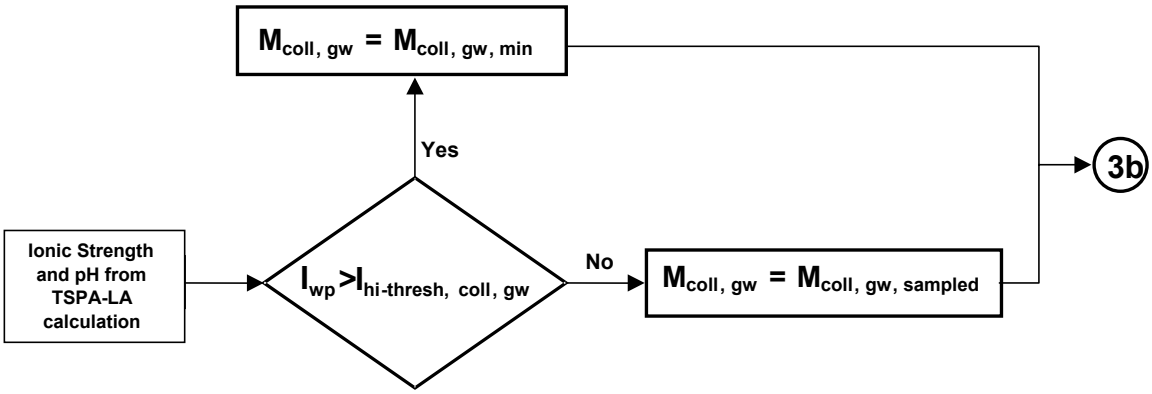

Step 3a Seepage Water Colloids – Effect of Ionic Strength on Mobile Mass

IF $I_{wp} \geq I_{hi\text{-}thresh,coll,gw}$

THEN $M_{coll,gw} = M_{coll,gw,min}$ (1E-6 mg/L)

ELSE IF ($I_{wp} < I_{hi\text{-}thresh,coll,gw}$)

THEN $M_{coll,gw} = M_{coll,gw,sampled}$ (distribution in Table 5)

Figure 18g. Flow Chart and Logic Statements: Effect of Ionic Strength on Mass Concentration of Seepage Water Colloids

$I_{hi\text{-}thresh,coll,gw}$ is a threshold value of the ionic strength of the fluid in the waste package used to calculate the concentration of groundwater colloids (stability is determined in Step 3b). It is identical to the upper threshold used for determining stability and concentration of waste form colloids, since both waste form and groundwater colloids are modeled as smectite. Groundwater colloids are modeled as present in groundwater seeping into the drift and as entering a breached waste package. Colloid concentrations are sampled if the ionic strength is below $I_{hi\text{-}thresh,coll,gw}$ (see Section 6.3.2.5). This ionic strength threshold value may vary due to specific chemical and environmental conditions and therefore is sampled over a range. The groundwater colloid concentration range (and distribution) is an intermediate parameter derived from several sources containing groundwater concentration data vs. ionic strength from the Yucca Mountain vicinity and elsewhere (Sections 6.3.1.4 and 6.3.2.5).

Step 3b. The stability of groundwater colloids is determined in Step 3b on the basis of the fluid ionic strength and pH (Figure 18h), based on known properties of smectite colloidal suspensions (Section 6.3.2.2).

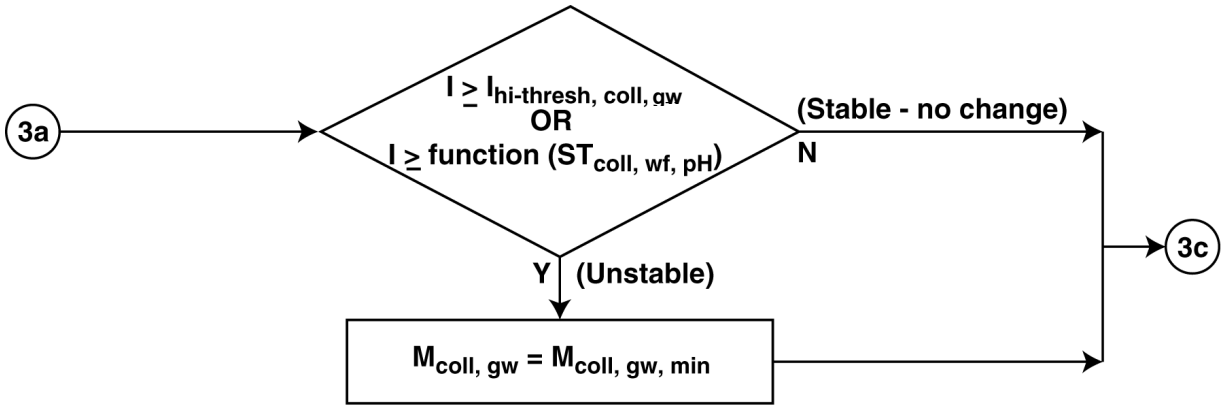

Step 3b Groundwater Colloids - Effect of pH on Stability

IF ($I \geq I_{hi\text{-}thresh,coll,gw}$) OR ($I \geq function(ST_{coll,wf,pH})$)
THEN $M_{coll,gw} = M_{coll,gw,min}$

$function(ST_{coll,wf,pH})$: pH/200

Figure 18h. Flow Chart and Logic Statements: Effect of pH and Ionic Strength on Groundwater Colloids Stability Based on Stability Behavior of Montmorillonite Colloids

$I_{hi\text{-}thresh,coll,gw}$ is the same upper threshold value of the ionic strength of the fluid in the waste package used to determine Pu concentration in Step 1a. It is used here with pH to determine the stability of the smectite groundwater colloids. This threshold value may vary due to specific chemical and environmental conditions and is therefore sampled over a range (Table 16).

Step 3c. The concentrations of radionuclides (Pu, Am, Th, Pa, Cs) reversibly sorbed on groundwater colloids are calculated in Step 3c (Figure 18i), based on the mass of groundwater colloids, K_d values describing the distribution of radionuclides between the fluid and montmorillonite, and the dissolved concentration of radionuclides within the waste package as calculated by the TSPA-LA model.

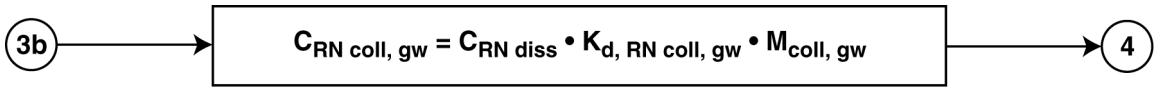

Step 3c Groundwater Colloids - Sorption of Radionuclides

$C_{RNcoll,gw} = C_{RNdiss} \times K_{d,RN,coll,gw} \times M_{coll,gw}$ x 1E-6

Figure 18i. Flow Chart and Logic Statements: Radionuclide Sorption on Groundwater Colloids

The C_{RNdiss} is the concentration of radionuclide "RN", determined by the TSPA-LA model as output from the solubility concentration model, that is used as an input to the colloid abstraction.

$K_{d,RNcoll,gw}$ is a parameter derived from several sources (see Tables 6-10) and is an equilibrium sorption coefficient used to approximate the partitioning of dissolved radionuclide between colloids and fluid. The 1E-6 portion of the relationship designates a correction factor to accommodate differences in units among the various parameters.

6.5.1.4 Outputs from the Waste Package to the Drift

In Steps 1 through 3 the total colloid-associated radionuclide concentrations, total colloid mass concentrations and the remaining radionuclide concentrations in the fluid were calculated for waste form colloids derived from defense high-level waste glass (Step 1), colloids derived from the corrosion of the waste package interior (Step 2), and seepage water/groundwater colloids that entered the waste package. In Step 4 these quantities are passed from the waste package interior to the drift environment.

Step 4. Outputs from the waste package, which are also inputs to the drift, are colloid-associated radionuclide concentrations and colloid mass concentration (Figure 17a).

The colloid-associated radionuclide source term is calculated in Step 4 by passing to the invert the contributions to the source term from Steps 1d, 2b, and 3c (Figure 18j).

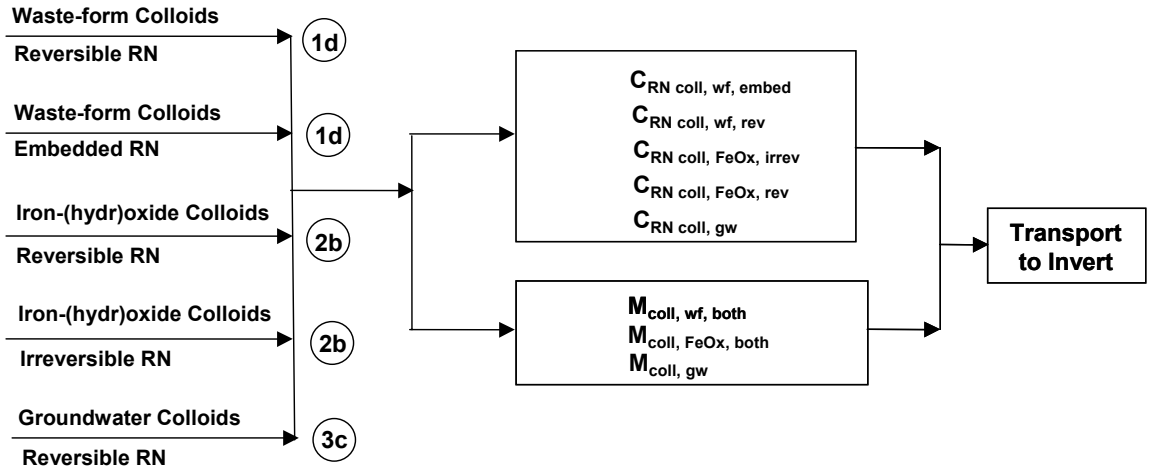

Figure 18j. Flow Chart and Logic Statements: Transfer of Colloid-associated Radionuclide Source Term to Invert

The radionuclide component of the source term is made up of individual radionuclide mass concentrations embedded in and reversibly attached to waste form (smectite) colloids ($C_{RNcoll,wf,embed}$ and $C_{RN,wf,rev}$), irreversibly and reversibly attached to corrosion-generated iron oxyhydroxide colloids ($C_{RNcoll,FeOx,irrev}$ and $C_{RNcoll,FeOx,rev}$), and reversibly attached to groundwater (smectite) colloids ($C_{RNcoll,gw}$).

The colloid component of the source term is the sum of the mass concentrations of the waste form colloids ($M_{coll,wf,both}$; "both" signifies the inclusion of all smectite waste form colloids with embedded radionuclides, or reversibly associated with radionuclides, or both); the iron

oxyhydroxide corrosion-generated colloids ($M_{coll,FeOx,both}$; "both" signifies that all corrosion-generated iron oxyhydroxide colloids irreversibly or reversibly associated with radionuclides, or both, are included); and the smectite groundwater colloids.

6.5.2 In-Drift Abstraction Implementation in Total System Performance Assessment–License Application

6.5.2.1 In-Drift Colloid Stability and Mass Concentrations

Step 5 incorporates the outputs from the waste package in Step 4 with the invert fluid properties, ionic strength (I_{inv}) and pH (pH_{inv}), from TSPA-LA calculations.

Table 1 lists in-drift seepage water/groundwater colloid-related input parameters (qualified data) used in the abstraction. Corroborating/supporting data and information used to develop the parameters are listed in Table 2..

Step 5. The primary function of Step 5 is incorporation of the invert fluid chemical properties and the calculation of resulting stabilities and mass concentrations of colloids entering the invert fluid from the waste package as shown in Figure 19.

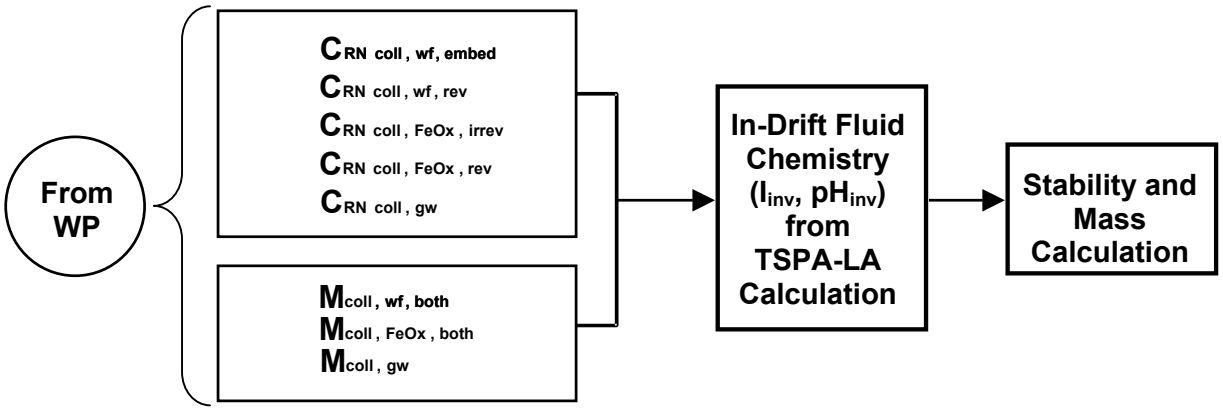

Figure 19. Inputs to Drift from Waste Package

The I_{inv} and pH_{inv} are inputs calculated by the TSPA-LA model (in-drift environment calculations) (BSC 2002 [DIRS 160315], analysis described in Section 1.2.2). The concentrations of colloids and colloid-associated radionuclides within the drift are calculated on the basis of abstractions of the laboratory and field observations and chemical principles described in Section 6.3, with methods similar to those used to determine radionuclide and colloid concentrations within the waste package (these calculations are described in Section 6.5.1 and illustrated in Figures 18a through 18e and 18g through 18i). A stepwise approach was taken in the abstraction, and each step is set out below with a flow diagram and logic statements that describe the abstraction step. Parameters are defined in Table 16.

In the TSPA-LA model calculations, the colloids with embedded and sorbed radionuclides leave the failed waste package and enter the drift geochemical environment. The drift geochemical environment is modeled as one of three possible scenarios (Aguilar 2003 [DIRS 163770]): (1) the waste package surface dripping scenario, (2) the invert wicking scenario, and (3) the effluent from the failed waste package. The colloids leave in-package chemical conditions and enter invert chemical conditions which are potentially different from in-package conditions. Once the colloids are subject to the invert chemical conditions, the stability and concentration of the colloids are recalculated, based on I_{inv} and pH_{inv}. Therefore, if the colloid mass concentrations change (due to loss of colloid stability), the concentrations of sorbed radionuclides are recalculated as shown in Figure 20.

6.5.2.2 Recalculation of Colloid-Associated Radionuclides Concentrations in Drift

Step 6. In Step 6, the concentrations of radionuclides sorbed to colloids exiting the waste package are recalculated because of different chemical conditions in the invert. The new concentrations of dissolved radionuclides sorbed onto the colloids are determined. This step is illustrated by the flow chart in Figure 20 and by the logic statements below.

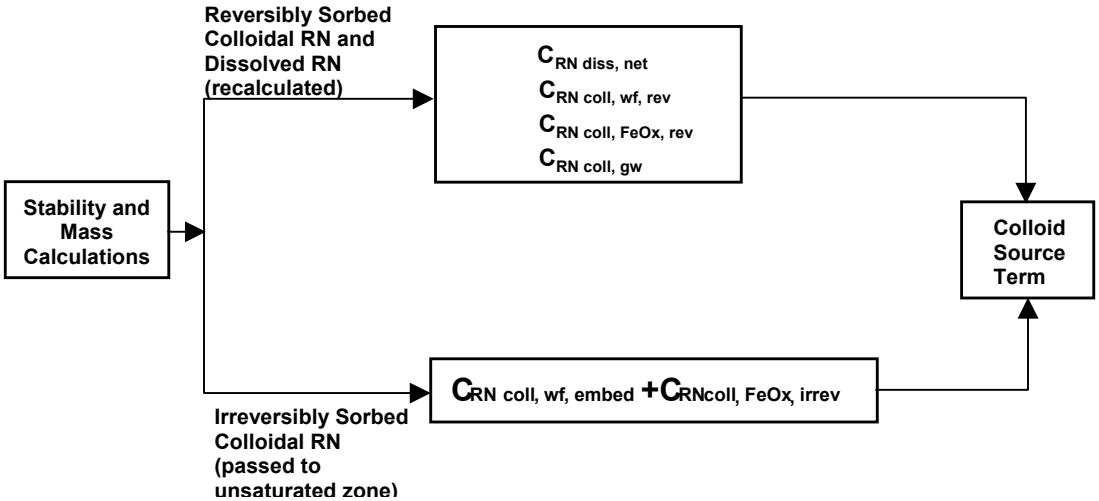

Figure 20. Recalculation of Colloid-Associated Radionuclides in Drift

$C_{RNdiss,net}$ is the net concentration of dissolved radionuclides after removal of radionuclides from fluid by sorption onto waste form, corrosion, and seepage water colloids. $C_{RNtotal}$ is therefore equivalent to C_{RNdiss} in Steps 1d, 2b, and 3c.

Calculation of radionuclide sorption on colloids:

$$C_{RNcoll,wf,rev} = C_{RNdiss} \times K_{d,RN,wf} \times M_{coll,wf,both}$$

$$C_{RNcoll,FeOx,rev} = C_{RNdiss} \times K_{d,RN,FeOx} \times M_{coll,FeOx,both}$$

$$C_{RNcoll,gw} = C_{RNdiss} \times K_{d,RN,gw} \times M_{coll,gw}$$

6.5.2.3 Calculation of Colloid Source Term for Radionuclide Element (RN)

Step 7. The colloid source term is calculated by summing the determined concentrations of waste form, iron oxyhydroxide, and seepage water/groundwater colloids and the concentrations of the radionuclides associated with the colloids, as shown in Figure 21.

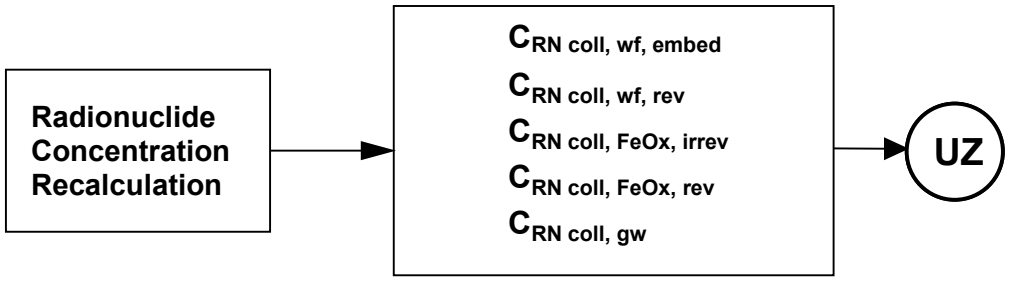

Figure 21. Source Term Summation for Colloid-Associated Radionuclide Concentrations in Drift

The sum of all of the radionuclides sorbed to colloids (embedded, reversibly sorbed, and irreversibly sorbed) and net dissolved radionuclides (those remaining after sorption) are passed to the unsaturated zone for disposition in TSPA-LA calculations.

6.5.3 Implementation of Colloid-Facilitated Transport in the Natural Barrier System

The maximum groundwater colloid concentration used in the unsaturated zone and saturated zone models is a sampled value based on the data presented in Sections 6.3.2.5 and in Figures 11 and 12. The groundwater colloid mineralogy is stipulated as smectite; smectite colloids are available to form pseudocolloids through sorption of dissolved radionuclides. The radionuclides Pu, Am, Th, Pa, and Cs are considered in the unsaturated zone and saturated zone models for colloid-facilitated transport. The colloids considered in the models include, in addition to groundwater colloids, primary waste form colloids (smectite) and corrosion-product colloids (iron oxyhydroxides). The smectite waste form colloids, which originate from alteration of high-level waste glass, contain both embedded radionuclides (Pu and Am that are stipulated to be irreversibly sorbed) and reversibly-sorbed radionuclides. Corrosion-product colloids also contain both reversibly- and irreversibly-sorbed radionuclides, although the latter are not thought to be embedded; they simply have extremely high sorption affinities for the iron oxyhydroxides. All of these colloids and associated radionuclides are passed to the unsaturated zone from the engineered barrier system.

Colloid parameters used in the waste form/engineered barrier system models and recommended for the unsaturated zone/saturated zone models are listed in Table 15.

Table 15. Colloid Parameters Used in the Waste Form and Engineered Barrier System and Recommended for the Unsaturated Zone, and Saturated Zone Models

Parameter	WF/EBS	UZ	SZ
Groundwater colloid concentration	CDF[a]	CDF[a]	CDF[a]
K_d—Pu on colloids (mL/g)	10^4 to 10^6 (Iron Oxyhydroxide) 10^3 to 10^6 (Smectite)	10^3 to 10^6 (Smectite)	10^3 to 10^6 (Smectite)
K_d—Am on colloids (mL/g)	10^5 to 10^7 (Iron Oxyhydroxide) 10^4 to 10^7 (Smectite)	10^4 to 10^7 (Smectite)	10^4 to 10^7 (Smectite)
K_d—Th on colloids (mL/g)	10^5 to 10^7 (Iron Oxyhydroxide) 10^4 to 10^7 (Smectite)	10^4 to 10^7 (Smectite)	10^4 to 10^7 (Smectite)
K_d—Pa on colloids (mL/g)	10^5 to 10^7 (Iron Oxyhydroxide) 10^4 to 10^7 (Smectite)	10^4 to 10^7 (Smectite)	10^4 to 10^7 (Smectite)
K_d—Cs on colloids (mL/g)	10^1 to 10^3 (Iron Oxyhydroxide) 10^2 to 10^4 (Smectite)	10^2 to 10^4 (Smectite)	10^2 to 10^4 (Smectite)

NOTES: [a]Cumulative Distribution Function (CDF)–Figure 12, Section 6.3.2.5, Groundwater Concentration in mg/L.
UZ = unsaturated zone; SZ = saturated zone; CDF = cumulative distribution function; WF = waste form; EBS = engineered barrier system.

All colloid transport in the unsaturated zone (BSC 2003 [DIRS 163933]) and saturated zone (BSC 2003 [DIRS 163932]) occurs by advective transport; colloid diffusion is considered negligible because colloids have free diffusion coefficients that are 2 to 4 orders of magnitude smaller than solutes. Colloids will transport wherever water flows, which in the unsaturated zone is a combination of fractures and the matrix, and in the saturated zone it is almost exclusively in fractures or through advective flow pathways in alluvium. The project has no site-specific data on colloid transport under unsaturated conditions, so colloid transport parameters developed from tests conducted in saturated fractured volcanic tuffs are applied to the unsaturated zone (BSC 2003 [DIRS 163933]). This approach is considered conservative, as it is widely recognized that colloids tend to be more retarded under unsaturated conditions than under saturated conditions in media that is otherwise similar. This greater retardation in the unsaturated zone occurs because (1) immobile air-water interfaces serve as additional surfaces to trap colloids and (2) unsaturated zone porewaters tend to have higher ionic strengths than saturated zone porewaters, resulting in a greater tendency for colloids to attach to rock surfaces.

Some of the Pu and Am leaving the engineered barrier system is stipulated to be irreversibly sorbed/embedded to colloids. The irreversibly sorbed/embedded fractions of these radionuclides travel through the unsaturated zone and saturated zone at the same rate as the colloids they are associated with. Irreversibly sorbed radionuclides on colloids leaving the engineered barrier system are split into two fractions: one retarded by colloid filtration and detachment processes and the other assumed to be completely unretarded. The fraction that travels unretarded depends on the groundwater travel time through the natural barrier system (unsaturated zone and

saturated zone combined), with greater travel times resulting in smaller fractions. However, the unretarded fraction is always less than 0.01, so the vast majority of the colloids experience filtration processes in the natural barriers that result in colloid retardation. The fraction of unretarded colloids is determined by a procedure described in the Saturated Zone Colloid Transport report (BSC 2003 [DIRS 163932]). The rationale for assuming that a small colloid mass fraction travels unretarded through the natural barriers is that (1) some finite fraction of colloids almost always travels unretarded in laboratory and field transport tests, and (2) there have been several observations of very small mass fractions of contaminants migrating with colloids over large distances in relatively short times in field settings (e.g., Kersting et al. 1999 [DIRS 103282]; Penrose et al. 1990 [DIRS 100811]; Buddemeier and Hunt 1988 [DIRS 100712]).

For colloids that experience filtration in the natural barrier system, colloid retardation factors, R_c, are randomly sampled from cumulative distribution functions developed separately for both the fractured volcanics and the alluvium. These cumulative distribution functions are constructed using retardation factors derived from laboratory and field colloid transport tests conducted under varying geochemical conditions with different colloid types and sizes. The value of R_c is dependent on several factors such as colloid size, colloid type and geochemical conditions (e.g., pH, Eh, and ionic strength). For any total system performance assessment simulation, the cumulative distribution functions are sampled independently for the volcanics and alluvium. However, the value sampled for the volcanics is used for both the unsaturated zone and the volcanic portion of the saturated zone flow system, implying perfect correlation between the colloid retardation factors in the unsaturated zone and saturated zone. No correlation is assumed between retardation factors in the volcanics and alluvium. The cumulative distribution functions in both the volcanics and the alluvium are truncated at the lower end so that the minimum retardation factor in the volcanics is 6 and the minimum in the alluvium is 8. These truncations result in the vast majority of colloids (with the exception of the small unretarded fraction) experiencing significant retardation in the natural barrier system.

The transport of radionuclides that are reversibly sorbed to colloids is governed by equilibrium partitioning of the radionuclides between the solution phase, the immobile rock matrix, and mobile colloids. Radioisotopes of Pu are transported as one group, radioisotopes of Am, Th, and Pa are transported as a second group, and Cs is transported as a third species. Groundwater travel times through the natural barriers are slow enough that equilibrium sorption can be assumed even for very slow radionuclide sorption and desorption rates. Any radionuclide mass that desorbs from colloids at rates slow enough to be comparable to travel times through the system is inherently considered part of the irreversibly sorbed/embedded radionuclide mass fraction. Colloid-facilitated transport of reversibly sorbed radionuclides depends on colloid transport parameters, the mobile colloid mass concentrations, and radionuclide partition coefficients onto both colloids and the immobile rock matrix. High colloid concentrations and large radionuclide partition coefficients onto colloids (relative to the rock matrix) favor colloid-facilitated radionuclide transport at rates that can significantly exceed transport rates in the absence of colloids. Because reversibly-sorbed radionuclides will readily desorb from retarded colloids to resume partitioning between the solution phase, mobile colloids, and the immobile rock matrix, the retardation of colloids works to counterbalance the otherwise enhanced mobility

of the radionuclide. However, because the sorption of this fraction is assumed to be reversible, colloids still serve to facilitate transport, even if they are retarded due to filtration processes.

6.6 BASE-CASE MODEL RESULTS

This section provides an overview of the model abstraction results, with a general discussion of the range of results, important couplings among processes and their impact on performance measures, and data uncertainty and propagation of the uncertainties through the model.

6.6.1 Overview

As discussed in Section 6.1, colloids may affect repository performance if they are generated in significant quantities, are stable within the waste package, engineered barrier system, and unsaturated and saturated zones (respectively). Colloids could potentially carry a significant radionuclide load and readily transport these contaminants from the engineered barrier system to the unsaturated zone and saturated zone and beyond. Output quantities from the waste form and engineered barrier system colloids models to downstream natural barrier system models and/or analyses include waste form colloid source terms, including defense high-level waste glass colloid concentrations with embedded radionuclides and dissolved waste form radionuclides derived from commercial and DOE SNF waste form colloids. Also, the waste form and engineered barrier system colloids models determine the concentration of natural seepage water/groundwater colloids and corrosion product (iron oxyhydroxide) colloids that are propagated from the engineered barrier system onto the underlying natural barrier system.

6.6.2 Uncertainty Associated with the Model Analysis

As discussed previously in Section 4.1, Data and Parameters, the parameters developed in this model analysis are in some cases based on data that are not site- or Yucca Mountain Project (YMP)-specific. Additionally, supporting technical and corroborative information may not have been developed specifically from physical and chemical conditions approximating those of the repository. Therefore, departure from anticipated repository conditions must be accounted for by acknowledging uncertainties in the parameters developed and providing a means to incorporate these uncertainties into the total system performance assessment calculations. In this model analysis, value ranges and probability distributions, and bounding assumptions deemed appropriate for each given parameter or process modeled have been established as a means to incorporate these uncertainties into the TSPA-LA model calculations. Another potential uncertainty issue is related to the circumstances and conditions of data acquisition and the departure from those circumstances and conditions assumed during the application of the data to the total system performance assessment models. The three types of parameter range-related issues relate to (1) “temporal scaling,”(2) “spatial scaling,” and (3) extrapolation from the physical and chemical conditions of data acquisition.

Temporal Scaling—In the implementation of a total system performance assessment, it is often necessary to use experimental data gathered over days to a few years and field observations recorded over days to a few decades to arrive at conclusions on what is anticipated to occur over the repository’s regulatory compliance period and beyond (i.e., periods extending from thousands to hundreds of thousands of years). Parameters based on fundamental physical and/or

chemical principles, such as radionuclide half-life, should be robust over these extended time parameters. Other types of parameters such as association of dissolved radionuclide ions with attachment sites on the surface of colloids, which is influenced by kinetics, must be used cautiously when speculating about future conditions. This aspect of uncertainty is best addressed with the formulation and use of scientifically sound assumptions.

Spatial Scaling—This refers to the extrapolation or application of a documented process occurring at laboratory scale (centimeters), for example, to the scale of the repository setting (kilometers). Theory and observations of colloid behavior at the molecular and microscopic level used in this model report have been corroborated and/or validated to the extent possible with empirical field observations. An example of data that could be used to validate model predictions with actual field observations is the data reported by Kersting et al. (1999 [DIRS 103282]). In this study observations of colloidal Pu transport over kilometer-scale distances at a nuclear detonation site (Kersting et al. 1999 [DIRS 103282]) were used to demonstrate the potential for long-distance transport of colloid-associated Pu within and from the repository to the accessible biosphere – these results can be used to assess the validity of Pu transport models at a more localized scale (i.e., perhaps at the localized scale of meters or even smaller distances of transport). This aspect of uncertainty is best addressed with the application of established physical and chemical principles with the formulation of scientifically sound assumptions applicable at the scale in question, coupled with the consideration of limitations inherent to the application of these assumptions at other scales.

Extrapolation From Physical and Chemical Conditions of Data Acquisition—Experiments, both in the laboratory and field, may yield potentially useful data for total system performance assessment models, but these may have employed several parameters (e.g., pH or redox conditions) whose ranges may not have been directly relevant to repository conditions. In such cases the experimental conditions must be examined in detail so that a valid comparison between the experimental conditions and the conditions incorporated into the model can be made–only then can a valid judgment be made regarding the applicability of the data to the model in question. An example is the measurement of colloid particle concentrations in solutions of high pH and the validity of using those measurements to describe modeled processes at moderate (neutral) pH. Again, this aspect of uncertainty is best addressed with the application of established physical and chemical principles and the formulation and use of scientifically sound assumptions.

Uncertainty Associated with Waste Form Colloid Formation—There is uncertainty in the model for colloid generation and the quantity of colloids generated from the three waste forms (defense high-level waste glass, commercial SNF, and DOE SNF) considered in this analysis. Uncertainties associated with these data and the Argonne National Laboratory experiments used to obtain them include measurement uncertainties and uncontrolled experimental factors and the subsequent extrapolation of these results to potential repository conditions. For example, a potentially significant contribution to this uncertainty for commercial SNF is the potential for the "sequestration" of colloids formed during the degradation process within rinds of waste degradation products. The formation of alteration product rinds on the surface of the waste forms could impede the release of colloids from the waste and result in an underestimation of the total quantity of colloids produced (see Section 6.3.1.2.1). Additionally, uncertainties during the measurement of colloids formed from the various waste forms can potentially arise in the course

of determination of mass, calculation of volume, determination of particle sizes by filtration, and measurement of concentrations by the various detection methods employed. Specific uncertainty associated with the measurement of all three types of waste form colloids is discussed in Sections 6.3.1.1, Colloids from the Corrosion of Defense High-Level Waste Glass, and Section 6.3.1.2, Potential for Colloids from the Corrosion of Commercial and DOE SNF.

Uncertainty Associated with Corrosion Product Colloid Formation—There is limited information in the literature on the quantity of corrosion product colloids that could potentially form during the degradation of waste package materials and the corrosion of other steel components in the engineered barrier system (see Section 6.3.1.3, Colloids from the Corrosion of Waste Package and Metallic Invert Materials). Therefore, the values and ranges developed for the corrosion colloid source term parameters have a large degree of uncertainty. To reduce some of this uncertainty and increase the defensibility of the developed parameters, consideration was given to the observed quantities of iron oxyhydroxide colloids observed in scaled-down miniature waste package degradation experiments by an ongoing DOE-funded research project at University of Nevada at Las Vegas (see Section 6.3.1.3). The use of appropriately scaled-down waste package configurations (i.e., surface area to total package volume scaled-down proportionally to approximately 1/70 the size of actual proposed repository waste packages) and the use of water of similar chemical composition to the groundwater found at Yucca Mountain render the experiments directly relevant to conditions anticipated in the proposed Yucca Mountain repository. Additionally, conservative, but realistic bounding values have been established for the corrosion product colloid parameters recommended for use in the model in order to propagate the uncertainty associated with these parameters throughout the TSPA-LA analysis.

Uncertainty Associated with the Measurement of Seepage Water/Groundwater Colloids—The determination of colloid concentrations in groundwater samples presents many challenges that add to the uncertainty of developed parameters. Major factors that contribute to uncertainty in the concentrations of colloids in the groundwater samples used to establish parameters for use in the total system performance assessment analysis include (1) field sampling techniques, including differences in pumping rates at each well during extraction of the water samples, (2) other unknown factors affecting the quantities of particles suspended in the water samples, including the types of additives introduced in the wells during the drilling process itself, (3) errors inherent to the laboratory methods used to measure the quantities of colloids suspended in the water samples (e.g., filter ripening, interference and detection limitations for dynamic light scattering measurement techniques). At the spatial scale, there is the issue of the appropriateness of extrapolation of specific water sample measurements to represent the colloid concentrations in waters over a wider region or area. Temporal scaling issues could include potential seasonal variations in the quantities of colloids suspended in water samples extracted, or even shorter time-scale changes in colloid concentrations in water samples during the sampling of wells. To reduce some of this uncertainty, mass concentrations considered to establish the groundwater colloid concentration parameters were pooled using primarily groundwater samples extracted in the vicinity of Yucca Mountain (a few samples collected from Idaho National Engineering and Environmental Laboratory were also used in the analysis) and a discrete cumulative distribution function was established to evaluate the uncertainty in colloid concentration distribution (see Section 6.3.2.5, Figure 12). The goal of the uncertainty distribution for groundwater colloid concentrations is to numerically estimate uncertainty on a large scale. Based on the groundwater

colloid concentration collected at the two sites (Yucca Mountain and Idaho National Engineering and Environmental Laboratory) and the high uncertainty associated with the collection of groundwater colloids, a reasonable representation of the uncertainty is shown in the cumulative distribution function. The establishment of groundwater colloid concentrations from the cumulative distribution function allowed for the stochastic sampling over a wide range of colloid mass concentrations, including the sampling of high concentrations (i.e., exceeding 100 mg/L) in the TSPA-LA model calculations some of the time (2 percent of the model iterations), while probabilistically allowing for the selection of lower mass concentrations (0.001–1.0 mg/L) 75 percent of the time, as observed in the majority of samples used in the analysis. Exclusive consideration of samples collected by the same research team from Los Alamos National Laboratory reduces the uncertainty that could potentially result from differences in field sampling techniques.

Uncertainty Associated with the Determination of Colloid Stability—The ionic strength and pH of the water are the major considerations influencing the stability of all colloids considered in the model analysis (Section 6.3.2, Colloid Stability and Concentration). As with other parameters and data used or established in this analysis, uncertainty in the stability of colloids (smectite and iron oxyhydroxide) as a function of pH and ionic strength is associated mostly with the extrapolation of laboratory data reported in the literature or project-supported experimental work to actual conditions (i.e., solution chemistry) that would be present in the repository environment over the regulatory compliance period. Again, much of this uncertainty is accommodated by establishing conservative, but reasonable, bounding values and ranges of parameter values whose stability is affected by pH and ionic strength. This uncertainty is propagated through the TSPA-LA model by stochastic sampling of these distributions during Monte Carlo simulations employed in the model calculations.

Uncertainty Associated with Radionuclide Sorption Onto Colloids—A large degree of uncertainty associated with the development of sorption partition coefficients (K_d values) to describe the degree of sorption of specific radionuclides to colloids results from the scarcity of pertinent published data. Values reported in the literature are primarily the result of experimental work designed to establish K_d values for contaminants sorbed onto rocks, soils and other minerals, but literature specific to colloid-size minerals is not readily available. For this reason, the K_d value parameters established for smectite and iron oxyhydroxide colloids in this analysis relay heavily on limited experimental work conducted at Los Alamos National Laboratory (see Section 6.3.3.1, Reversible Sorption). Corroborative data reported in the literature were evaluated to augment the limited Los Alamos National Laboratory data. Therefore, the use of data from multiple sources contribute to uncertainties due to differences in laboratory techniques employed. Within specific experimental data sets, results were subject to experimental measurement uncertainties (e.g., detection limitations, quantification methods, interferences, etc.). The establishment of reasonable, bounding values and ranges of K_d values for each radionuclide considered in the model analysis reduces the potential effects of these uncertainties in the overall TSPA-LA model.

Model Implementation of Uncertainty—Implementation of the uncertainties associated with the parameters established during this model analysis is accomplished through the use of parameter ranges and distributions, rather than single, deterministic parameter values in the model analysis – reasonable bounding values were established for most of the parameters.

Within the TSPA-LA model, implementation of the colloids model abstraction incorporates the parameter uncertainties through the use of Monte Carlo simulation techniques, thereby ensuring that parameter uncertainties are propagated throughout the abstraction during computation and therefore reflected in the calculated results. Implementation of the various sub-model components of the model abstraction during their implementation in the TSPA-LA model is detailed in Section 6.5, Model Formulation for Base-Case Assessment. In general, the uncertainty associated with each of these submodel components is related to the incomplete knowledge of the system and its properties (epistemic).

Table 16. Summary of Intermediate Parameters and Results Produced in Abstraction

Data Tracking Number (DTN)	Parameter Name	Data/Parameter Description	Units[a]	Locations in Model Report	Value/ Range	Distribution/ Uncertainty
Waste Form Colloids						
SN0304T0504103.004	$C_{RNcoll,wf,embed,max}$	Highest observed or expected concentration of irreversibly attached (embedded as a solid inclusion) Pu associated with waste form colloids	mol/L	Section 6.3.2.4 Figure 18a	1E-7 mol/L[b]	Fixed value Epistemic
SN0304T0504103.004	$C_{RNcoll,wf,embed,min}$	Lowest observed or expected concentration of irreversibly attached (embedded as a solid inclusion) Pu associated with waste form colloids	mol/L	Section 6.3.2.4 Figure 18a	1E-11 mol/L[b] (small non-zero number)	Fixed value Epistemic
N/A	$C_{RNcoll,wf,embed}$	Concentration of irreversibly attached (embedded as a solid inclusion) radionuclide element RN (Pu, Am) associated with waste form colloids	mol/L	Section 6.5.1 and Figure 18a	N/A; calculated at each time step	N/A; calculated at each time step Epistemic
SN0304T0504103.004	$M_{coll,wf,both,max}$	Highest observed or expected mass of waste form colloids per unit volume or mass of water	mg/L	Sections 6.3.1.1 and 6.3.2.4 Figure 18c	5.0 mg/L[c]	Fixed value Epistemic
LL000905312241.018 [DIRS 152621] LL991109751021.094 [DIRS 142910]	$M_{coll,wf,both,min}$	Lowest observed or expected mass of waste form colloids per unit volume or mass of water	mg/L	Sections 6.3.1.1 and 6.3.2.4 Figure 18c	5.0×10^{-4} mg/L[c]	Fixed value Epistemic
LL000905312241.018 [DIRS 152621] LL991109751021.094 [DIRS 142910]	$M_{coll,wf,both}$	Mass of waste form colloids with reversibly sorbed or irreversibly attached (embedded) radionuclide element RN per unit volume or mass of water	mg/L	Section 6.5.1 and Figures 18c and 18d	N/A; calculated at each time step	N/A; calculated at each time step Epistemic
N/A; References: Tombacz et al. 1990 [DIRS 112690]; Figure 4	$I_{lo\text{-}thresh,coll,wf}$	Ionic strength below which waste form colloids are stable	mol/L	Sections 6.3.2.2 and 6.3.2.3 and Figures 4, 5, 8, and 9	0.01 mol/L	Fixed value Epistemic
N/A; References: Tombacz et al. 1990 [DIRS 112690]; Figure 4	$I_{hi\text{-}thresh,coll,wf}$	Ionic strength above which waste form colloids are unstable	mol/L	Sections 6.3.2.2 and 6.3.2.3 and Figures 4, 5, 8, and 9	0.05 mol/L	Fixed value Epistemic

Table 16. Summary of Intermediate Parameters and Results Produced in Abstraction (Continued)

Data Tracking Number (DTN)	Parameter Name	Data/Parameter Description	Units[a]	Locations in Model Report	Value/ Range	Distribution/ Uncertainty
N/A	$ST_{coll,wf,is}$	Function relating stability of waste form colloids to ionic strength, based on results of DHLWG degradation experiments (based on Pu concentration)	mol/L	Section 6.5.1 and Figure 18b	[Pu colloid] = -2.50E-6 × I +1.25E-7	N/A; calculated at each time step Epistemic
N/A	$ST_{coll,wf,pH}$	Function relating stability of waste form colloids to ionic strength and pH, over limited pH range (pH 2 to 10), based on results of montmorillonite stability experiments	mol/L	Section 6.3.2.2 and 6.3.2.3 and Figures 4, 5, 8, and 9 Section 6.5.1 and Figure 18b	I = pH/200	N/A; calculated at each time step Epistemic
SN0304T0504103.002	$K_{d,Pucoll,wf}$	Distribution coefficient for reversible sorption of Pu onto waste form (smectite) colloids	mL/g colloid	Section 6.3.3.1 Figure 18d	10^3 to 10^6 mL/g colloid	See Table 10 Epistemic
SN0304T0504103.002	$K_{d,Amcoll,wf}$	Distribution coefficient for reversible sorption of Am onto waste form (smectite) colloids	mL/g colloid	Section 6.3.3.1 Figure 18d	10^4 to 10^7 mL/g colloid	See Table 10 Epistemic
SN0304T0504103.002	$K_{d,Thcoll,wf}$	Distribution coefficient for reversible sorption of Th onto waste form (smectite) colloids	mL/g colloid	Section 6.3.3.1 Figure 18d	10^4 to 10^7 mL/g colloid	See Table 10 Epistemic
SN0304T0504103.002	$K_{d,Pacoll,wf}$	Distribution coefficient for reversible sorption of Pa onto waste form (smectite) colloids	mL/g colloid	Section 6.3.3.1 Figure 18d	10^4 to 10^7 mL/g colloid	See Table 10 Epistemic
SN0304T0504103.002	$K_{d,Cscoll,wf}$	Distribution coefficient for reversible sorption of Cs onto waste form (smectite) colloids	mL/g colloid	Section 6.3.3.1 Figure 18d	10^2 to 10^4 mL/g colloid	See Table 10 Epistemic
N/A	$C_{RNcoll,wf,rev}$	Concentration of reversibly attached radionuclide element RN (Pu, Am, Th, Pa, Cs) associated with waste form colloids	mol/L	Section 6.5.1 Figure 18d	N/A; calculated at each time step	N/A; calculated at each time step Epistemic
N/A; calculated by the TSPA-LA model (in-package chemistry)	I_{wp}	Ionic strength of fluid within and exiting breached waste package	mol/L	Section 6.5.1 and Figure 18a	N/A	N/A

Table 16. Summary of Intermediate Parameters and Results Produced in Abstraction (Continued)

Data Tracking Number (DTN)	Parameter Name	Data/Parameter Description	Units[a]	Locations in Model Report	Value/ Range	Distribution/ Uncertainty
N/A; calculated by the TSPA-LA model (in-package chemistry)	pH_{wp}	pH of fluid within and exiting breached waste package	pH units	Section 6.5.1 and Figure 18b	N/A	N/A
N/A; calculated by the TSPA-LA model (solubility limits)	C_{RNdiss}	Concentration of dissolved radionuclide element RN per unit volume or mass of water (Pu, Am, Th, Pa, Cs)	mol/L	Sections 6.5.1 and 6.5.2	N/A	N/A
N/A; calculated by the TSPA-LA model	I_{inv}	I of fluid within drift resulting from mixing of WP fluid and groundwater	mol/L	Section 6.5.2 Figure 19	N/A	N/A
N/A; calculated by the TSPA-LA model	pH_{inv}	pH of fluid within drift resulting from mixing of WP fluid and groundwater	pH units	Section 6.5.2 Figure 19	N/A	N/A
Corrosion-Generated Colloids						
SN0304T0504103.003	$M_{coll,FeOx,sampled}$	Highest observed or expected mass of iron oxyhydroxide colloids per unit volume or mass of water	mg/L	Section 6.3.2.3 Figure 18e	0.05 to 50 mg/L	Uniform Epistemic
SN0304T0504103.003	$M_{coll,FeOx,min}$	Lowest observed or expected mass of iron oxyhydroxide colloids per unit volume or mass of water	mg/L	Section 6.3.2.3 Figure 18e	1E-3 mg/L	Fixed value Epistemic
N/A	$M_{coll,FeOx}$	Mass of iron oxyhydroxide colloids per unit volume or mass of water	mg/L	Section 6.5.1 and Figure 18e	N/A; calculated at each time step	N/A; calculated at each time step Epistemic
N/A	$M_{coll,FeOx,\ both}$	Mass of iron oxyhydroxide colloids per unit volume or mass of water with both reversibly and irreversibly sorbed Pu and Am.	mg/L	Section 6.5.1 and Figure 18j	N/A; calculated at each time step	N/A; calculated at each time step Epistemic
SN0304T0504103.002	$K_{d,Pucoll,FeOx}$	Distribution coefficient for reversible sorption of Pu onto corrosion-generated (iron oxyhydroxide) colloids	mL/g colloid	Sections 6.3.3.1 and 6.3.3.2 Figure 18f	10^4 mL/g colloid (EBS) 10^4 to 10^6 mL/g colloid (UZ/SZ)	See Table 10 Epistemic

Table 16. Summary of Intermediate Parameters and Results Produced in Abstraction (Continued)

Data Tracking Number (DTN)	Parameter Name	Data/Parameter Description	Units[a]	Locations in Model Report	Value/ Range	Distribution/ Uncertainty
SN0304T0504103.002	$K_{d,Amcoll,FeOx}$	Distribution coefficient for reversible sorption of Am onto corrosion-generated (iron oxyhydroxide) colloids	mL/g colloid	Sections 6.3.3.1 and 6.3.3.2 Figure 18f	10^5 mL/g colloid (EBS) 10^5 to 10^7 mL/g colloid (UZ/SZ)	See Table 10 Epistemic
SN0304T0504103.002	$K_{d,Thcoll,FeOx}$	Distribution coefficient for reversible sorption of Th onto corrosion-generated (iron oxyhydroxide) colloids	mL/g colloid	Section 6.3.3.1 Figure 18f	10^5 to 10^7 mL/g colloid	See Table 10 Epistemic
SN0304T0504103.002	$K_{d,Pacoll,FeOx}$	Distribution coefficient for reversible sorption of Pa onto corrosion-generated (iron oxyhydroxide) colloids	mL/g colloid	Section 6.3.3.1 Figure 18f	10^5 to 10^7 mL/g colloid	See Table 10 Epistemic
SN0304T0504103.002	$K_{d,Cscoll,FeOx}$	Distribution coefficient for reversible sorption of Cs onto corrosion-generated (iron oxyhydroxide) colloids	mL/g colloid	Section 6.3.3.1 Figure 18f	10^1 to 10^3 mL/g colloid	See Table 10 Epistemic
SN0304T0504103.003	$S_{A,FeOx,coll}$	Specific (effective) surface area of corrosion-generated (iron oxyhydroxide) colloids	m^2/g colloid	Section 6.3.3.2 Figure 18f	1.8 to 720 m^2/g	Log Uniform Epistemic
SN0304T0504103.003	F_{RN}	Target-flux out ratio: ratio of radionuclide mass associated with colloids (reversible and irreversible) to radionuclide mass associated with colloids and dissolved radionuclide mass	------	Section 6.3.3.2 Figure 18f	0.9 to 0.99	Uniform Epistemic
N/A	$C_{Rncol\ l,FeOx,rev}$	Concentration of radionuclide element RN sorbed reversibly onto corrosion-generated (iron oxyhydroxide) colloids (Am, Th, Pa, Cs)	mol/L	Section 6.5.1.2 and Figure 18f	N/A; calculated at each time step	N/A; calculated at each time step Epistemic
N/A	$C_{PuAm,coll,FeOx,irrev}$	Concentration of Pu and Am irreversibly sorbed onto corrosion-generated (iron oxyhydroxide) colloids	mol/L	Section 6.5.1.2 and Figure 18f, and Section 6.3.3.2	N/A; calculated at each time step	N/A; calculated at each time step Epistemic

Table 16. Summary of Intermediate Parameters and Results Produced in Abstraction (Continued)

Data Tracking Number (DTN)	Parameter Name	Data/Parameter Description	Units[a]	Locations in Model Report	Value/ Range	Distribution/ Uncertainty
N/A	$ST_{coll,FeOx,pHlo}$	Function relating stability of iron oxyhydroxide colloids to pH and ionic strength at relatively low pH values	mol/L	Section 6.5.1 and Figure 18e	$I = -0.02 \times pH + 0.17$	N/A; calculated at each time step Epistemic
N/A	$ST_{coll,FeOx,pHhi}$	Function relating stability of iron oxyhydroxide colloids to pH and ionic strength at relatively high pH values	mol/L	Section 6.5.1 and Figure 18e	$I = +0.02 \times pH – 0.17$	N/A; calculated at each time step Epistemic
N/A	$ST_{coll,FeOx,pHint}$	Function relating stability of iron oxyhydroxide colloids to pH and ionic strength at intermediate pH values	Boolean	Section 6.5.1 and Figure 18e	Boolean ($pH \geq 8$ AND $pH \leq 9$)	N/A; calculated at each time step Epistemic
N/A; Reference: Liang and Morgan 1990 [DIRS 109524]	$I_{lo\text{-}thresh,coll,FeOx}$	Ionic strength below which iron oxyhydroxide colloids are stable	mol/L	Section 6.3.2.3 Figures 6 and 7	0.01 mol/L	Fixed value Epistemic
N/A; Reference: Liang and Morgan 1990 [DIRS 109524]	$I_{hi\text{-}thresh,coll,FeOx}$	Ionic strength above which iron oxyhydroxide colloids are unstable	mol/L	Section 6.3.2.3 Figures 6 and 7	0.05 mol/L	Fixed value Epistemic
N/A; calculated by the TSPA-LA model (in-package chemistry)	I_{wp}	Ionic strength of fluid within and exiting breached waste package	mol/L	Section 6.5.1 and Figure 18e	N/A	N/A
N/A; calculated by the TSPA-LA model (in-package chemistry)	pH_{wp}	pH of fluid within and exiting breached waste package	pH units	Section 6.5.1 and Figure 18e	N/A	N/A
N/A; calculated by the TSPA-LA model (solubility limits)	C_{RNdiss}	Concentration of dissolved radionuclide element RN per unit volume or mass of water (Pu, Am, Th, Pa, Cs)	mol/L	Sections 6.5.1 and 6.5.2; Figure 18f	N/A	N/A
N/A; calculated by the TSPA-LA model	I_{inv}	I of fluid within drift	mol/L	Section 6.5.2 Figure 19	N/A	N/A
N/A; calculated by the TSPA-LA model	pH_{inv}	pH of fluid within	pH units	Section 6.5.2 Figure 19	N/A	N/A

Table 16. Summary of Intermediate Parameters and Results Produced in Abstraction (Continued)

Data Tracking Number (DTN)	Parameter Name	Data/Parameter Description	Units[a]	Locations in Model Report	Value/ Range	Distribution/ Uncertainty
Groundwater Colloids						
N/A	$M_{coll,gw}$	Mass of groundwater colloids per unit volume or mass of water	mg/L	Section 6.5.1 Figure 18g	N/A; calculated at each time step	N/A; calculated at each time step Epistemic
SN0304T0504103.001	$M_{coll,gw,\ sampled}$	Mass of groundwater colloids per unit volume or mass of water sampled at each time step	mg/L	Section 6.3.2.5 Figure 18g	See Table 5	See Table 5
SN0304T0504103.001	$M_{coll,gw,\ min}$	Minimum mass of groundwater colloids per unit volume or mass of water sampled at each time step	mg/L	Section 6.3.2.5 Figure 18g	1×10^{-6}	N/A
SN0304T0504103.002	$K_{d,Pucoll,gw}$	Distribution coefficient for reversible sorption of Pu onto groundwater (smectite) colloids	mL/g colloid	Section 6.3.3.1 Figure 18i	10^3 to 10^6mL/g colloid	See Table 10 Epistemic
SN0304T0504103.002	$K_{d,Amcoll,gw}$	Distribution coefficient for reversible sorption of Am onto groundwater (smectite) colloids	mL/g colloid	Section 6.3.3.1 Figure 18i	10^4 to 10^7mL/g colloid	See Table 10 Epistemic
SN0304T0504103.002	$K_{d,Thcoll,gw}$	Distribution coefficient for reversible sorption of Th onto groundwater (smectite) colloids	mL/g colloid	Section 6.3.3.1 Figure 18i	10^4 to 10^7mL/g colloid	See Table 10 Epistemic
SN0304T0504103.002	$K_{d,Pacoll,gw}$	Distribution coefficient for reversible sorption of Pa onto groundwater (smectite) colloids	mL/g colloid	Section 6.3.3.1 Figure 18i	10^4 to 10^7mL/g colloid	See Table 10 Epistemic
SN0304T0504103.002	$K_{d,Cscoll,gw}$	Distribution coefficient for reversible sorption of Cs onto groundwater (smectite) colloids	mL/g colloid	Section 6.3.3.1 Figure 18i	10^2 to 10^4 mL/g colloid	See Table 10 Epistemic
N/A	$C_{RNcoll,gw}$	Concentration of reversibly attached radionuclide element RN associated with groundwater colloids (Pu, Am, Th, Pa, Cs)	mol/L	Section 6.5.1 and Figure 18i	N/A; calculated at each time step	N/A; calculated at each time step Epistemic
N/A; calculated by the TSPA-LA model (in-package chemistry)	I_{wp}	Ionic strength of fluid within and exiting breached waste package	mol/L	Section 6.5.1 and Figure 18g	N/A	N/A

Table 16. Summary of Intermediate Parameters and Results Produced in Abstraction (Continued)

Data Tracking Number (DTN)	Parameter Name	Data/Parameter Description	Units[a]	Locations in Model Report	Value/ Range	Distribution/ Uncertainty
N/A; calculated by the TSPA-LA model (in-package chemistry)	pH_{wp}	pH of fluid within and exiting breached waste package	pH units	Section 6.5.1 and Figure 18h	N/A	N/A
N/A; calculated by TSPA-LA model (solubility limits)	C_{RNdiss}	Concentration of dissolved radionuclide element RN per unit volume or mass of water (Pu, Am, Th, Pa, Cs)	mol/L	Sections 6.5.1 and 6.5.2; Figure 18i	N/A	N/A
N/A; References: Tombacz et al. 1990 [DIRS 112690]; Figure 4	$I_{hi\text{-}thresh,coll,gw}$	Ionic strength above which groundwater colloids are unstable	mol/L	Sections 6.3.2.2 and 6.3.2.5 Figures 4 and 5	0.05 mol/L	Fixed value Epistemic
N/A; calculated by the TSPA-LA model (solubility limits and near-field chemical environment)	C_{RNdiss}	Concentration of dissolved radionuclide element RN per unit volume or mass of water (Pu, Am, Th, Pa, Cs)	mol/L	Sections 6.5.1 and 6.5.2; Figure 18i	N/A	N/A
Invert Parameters						
N/A; calculated by the TSPA-LA model	$C_{Rndiss,net}$	Net concentration of dissolved radionuclides after removal of radionuclides by sorption to colloids	mol/L	Section 6.5.2.2 and Figure 20	N/A	N/A Epistemic
N/A; calculated by the TSPA-LA model	$C_{RNtotal}$	Sum of net dissolved and sorbed-to-colloids radionuclide concentrations	mol/L	Section 6.5.2.2 and Figure 20	N/A	N/A Epistemic
N/A; calculated by the TSPA-LA model	I_{inv}	I of fluid within drift	mol/L	Section 6.5.2 Figure 19	N/A	N/A Epistemic
N/A; calculated by the TSPA-LA model	pH_{inv}	pH of fluid within drift	pH units	Section 6.5.2 Figure 19	N/A	N/A Epistemic

NOTES: [a]Concentration, mol/L, is treated here as moles/liter of dispersion and therefore is not molarity in the strict sense
[b]Uncertainty is linked to uncertainty for ionic strength, an input parameter in the TSPA-LA model (no additional uncertainty is added)
[c]Mass is correlated with irreversible radionuclide concentration
WP = waste package; DHLWG = defense high-level waste glass; N/A = not applicable; RN = radionuclide; UZ = unsaturated zone; SZ = saturated zone; EBS = engineered barrier system.

6.7 DESCRIPTION AND ANALYSES OF THE BARRIER CAPABILITY

As discussed in Section 1, Purpose**,** the abstraction of the process models reported in this document is intended to capture the most important characteristics of radionuclide-colloid behavior for use in predicting the potential impact of colloid-facilitated radionuclide transport on repository performance. Colloid information from this report will be considered in evaluation of the unsaturated zone as a barrier to radionuclide transport. As modeled in total system performance assessment, colloids may act to facilitate transport of radionuclides from the waste package to the surrounding engineered barrier system and beyond to the underlying unsaturated zone component of the natural barrier system of the repository. Therefore, a description and analyses of barrier capability associated with colloids is not applicable and is not included in this document.

6.8 EVALUATION OF ALTERNATIVE MODELS

The alternative models described in Section 6.4 were evaluated and considered not to be desirable as alternative approaches to generating a colloid source term. Justification for not considering these alternative models was that either (1) the additional data required to support the alternative model is not available, and therefore the model cannot be developed for application to the repository environment, or (2) the conditions necessary to drive the alternative model processes are not anticipated in the repository (see Table 12, Section 6.4). Accordingly, the models were not quantitatively evaluated.

7. VALIDATION

The waste form and in-drift colloids abstraction model is used to describe the possible consequences of colloid-facilitated radionuclide transport during postclosure. Sensitivity studies (BSC 2002 [DIRS 160780]) showed that the colloid model had a small effect on the TSPA-LA results and therefore was given an "importance to expected risk" of "Not Significant." Therefore a relatively low level of confidence is required in validating this model (BSC 2002 [DIRS 160780], Section 4.6, p. 4-4).

The types and characteristics (including stability and concentration) of colloids formed from the degradation of the waste forms as used in the abstraction is based on extensive observations of colloids from testing programs and natural groundwaters. Because of the minute dimensions and unique properties of colloids, their study presents formidable difficulties; the body of work used for the abstraction developed in this analysis represents a significant fraction of the state-of-the-art colloid research performed to date.

The validation activities for this model analysis and abstraction took into account the criteria established in the Yucca Mountain Review Plan (NRC 2002 [DIRS 158449]) (see Section 4.2). Post-model development validation is accomplished through corroboration of model predictions and data used with data published in refereed journals or literature and through corroboration by comparison to data from natural analog sites. Validation is described in the following subsections. Corroborating/supporting data and information used to develop and validate the parameters are listed in Table 17.

Table 17. Supporting (Corroborating) Information Used to Validate the Colloid Model

Criterion	**Supporting (Corroborating) Information Source**	**Data/Information**
-----	BSC 2002 [DIRS 160780]	Measure of "importance to expected risk" of colloid model
2	Tombacz et al. 1990 [DIRS 112690]	Stability of smectite (which is used as a surrogate mineralogy for defense high-level waste glass colloids) at full range of conditions anticipated in TSPA-LA calculations
3,4	Mertz et al. 2003 [DIRS 162032]	Corroborative data supporting conclusion of no significant colloids generated from CSNF degradation.
3,4	Short et al. 1988 [DIRS 113937]	Corroborative information and data regarding low colloid-associated U concentrations in the vicinity of mines
3,4	Payne et al. 1992 [DIRS 124812]	Corroborative information and data regarding low colloid-associated U concentrations in the vicinity of mines
3,4	Zanker et al. 2000 [DIRS 162746]	Corroborative information and data regarding low colloid-associated U concentrations in the vicinity of mines
3,4	Vilks et al. 1993 [DIRS 108261]	Corroborative information and data regarding low colloid-associated U concentrations in the vicinity of mines
3,4	Brady et al. 2002 [DIRS 161649]	Corroborative information and data regarding limited extent of dissolved U plumes
6	DTN LA0002SK831352.003 [DIRS 161771] DTN LA0002SK831352.004 [DIRS 161579]	Corroborative (non-Q) data for qualified groundwater data
8	Coughtrey et al. 1985 [DIRS 154494]	Corroborative information regarding irreversibility of Pu on mineral particles
8	Litaor and Ibrahim 1996 [DIRS 161667]	Corroborative information regarding irreversibility of Pu on mineral particles
8	Bunzl et al. 1995 [DIRS 154468]	Corroborative information regarding irreversibility of Pu on mineral particles

7.1 VALIDATION OF WASTE FORM COLLOID PARAMETERS

Consistant with *Technical Work Plan for Waste Form Degradation Modeling, Testing, and Analyses in Support of SR and LA* (BSC 2002 [DIRS 160779], Section 2.1.4.3), model validation will require meeting the following criteria:

Criterion 1 (Relevant to Technical Work Plan Validation Criterion 2)

Are the concentrations of colloids and associated Pu produced in defense high-level waste glass degradation experiments and incorporated into the colloid abstraction reasonable with respect to scientific principles and observed colloid concentrations in the Project and peer-reviewed literature?

Of the laboratory data generated from the defense high-level waste glass testing at Argonne National Laboratory, colloid mass (smectite) and colloid-associated Pu concentration were used in the model and therefore need to be validated. Other radionuclides were detected in the colloids (see Section 6.3.1.1) but not quantified and so these were not incorporated into the model. The experimentally determined colloid masses and Pu concentrations were loosely bounded in order to account for the potential effects of the other detected embedded radionuclides, as well as to address potential uncertainty described in Criterion 2.

The specific defense high-level waste glass test data set used in the model were validated by assessing their reasonableness and by comparing the data to other defense high-level waste glass data generated during the testing program. Smectite colloids from any particular source must behave similarly under a given set of physicochemical conditions in terms of stability and maximum concentration. As can be seen in Figure 3, the smectite colloid concentrations encountered in the defense high-level waste glass testing (up to ~5 mg/L) are within the range of observed smectite concentrations in natural groundwaters, which can range up to a few hundred mg/L. Therefore the concentrations determined are reasonable.

Since the Argonne National Laboratory defense high-level waste glass tests are one-of-a-kind, the mechanism of Pu attachment has not been specifically determined, and no natural analogs allow comparison, the stipulation that Pu is irreversibly associated with the colloids cannot be directly validated. However, the stipulation is definitely conservative, in that irreversible attachment of Pu to the colloids maximizes Pu's potential mobility.

Criterion 2 (Relevant to Technical Work Plan Validation Criterion 1)

Were the test conditions for the defense high-level waste glass colloid generation experiments representative of physicochemical conditions anticipated in the proposed repository and incorporated into the abstraction?

The range of chemical conditions in the laboratory testing represent a subset of the conditions expected in the repository. Specifically, the pH encountered in the experiments ranged from approximately 9 and 11.5 (Buck and Bates 1999 [DIRS 109494]). The pH range anticipated in the waste form and drift environments for the majority of the time is expected to be 4 to 11. According to the in-package chemistry modeling study (BSC 2003 [DIRS 163919]), the pH range for fluids reacting with commercial SNF is 3.9 to 8.1, while the range for fluids reacting with co-disposal materials is from 4.8 to 10. This suggests that this portion of the model upon which these high-pH data are based does not adequately represent the full range of conditions expected and that extrapolation of the model to substantially lower pHs is tenuous.

In defense of the data, it is well known that smectite colloids have a zero point of charge of approximately 2 (see Section 6.3.2.2) and thus are stable at pH greater than 2. The stability does decrease as the zero point of charge is approached and maximum colloid concentration increases. This relationship is accommodated by the pH vs. ionic strength stability relationship described in Section 6.3.2.2 and Figure 5. This does not account for the decreased maximum possible concentration of smectite colloids at lower pH, but this turns out to be conservative, as it overestimates the smectite concentration at pH's lower than those of the experimental conditions.

Further, high pH would be reasonable in proximity to the surface of degrading defense high-level waste glass, consistent with the high-pH experimental conditions (Section 6.3.2.2) (Buck and Bates 1999 [DIRS 109494]). Smectite colloids would remain stable if and when the fluids in which they occur became diluted (lower ionic strength) and became lower in pH.

The above argument in defense of the high-pH data does not account for the possibility that the colloid-associated Pu concentration may be different at lower pH. This is difficult to evaluate, since the Argonne National Laboratory defense high-level waste glass tests are one-of-a-kind,

the mechanism of Pu attachment has not been specifically determined, and there are no natural analogs for comparison. If the attached Pu *decreases* with lower pH, the model is conservative, since the Pu concentration on colloids would be *over*estimated at lower pH. If, however, the attached Pu *increases* with lower pH, the model would *under*estimate the Pu concentration. The relationship for the colloid-associated Pu concentrations described in Criterion 1 was chosen to bound loosely the experimental data.

Criterion 3 (Relevant to Technical Work Plan Validation Criteria 1 and 2)

Is the model approach used, which stipulates that commercial SNF will not produce colloids in significant quantities, consistent with commercial SNF-specific test results and peer-reviewed literature on field observations near uranium mines and deposits?

Data on experimental degradation of commercial SNF (drip tests) have been collected for several years, and to date very few colloids have been observed (Section 6.3.1.2.1). It was tentatively concluded in *Waste Form Colloid-Associated Concentrations Limits: Abstraction and Summary* (CRWMS M&O 2001 [DIRS 153933]), pending additional confirmation data, that commercial SNF was not an important source of colloids, and therefore potential colloid-associated radionuclides from commercial SNF could be omitted from the colloid model. The original conclusion, based on the first five years of data, has not changed. It is corroborated with the subsequent three years of data (Section 6.3.1.2.1); with preliminary data from a recent set of experiments that characterized the mineralogy, size characteristics, and stability of particles in a U-bearing-colloid dispersion (Section 6.3.1.2.3); and with field observations (see Section 6.3.1.2.4).

The three additional years of testing have not yielded anything to alter that conclusion. A possible criticism of the test design, namely that the apertures in the sample-holding zircaloy screen were small and became clogged with alteration products, was addressed with the introduction of a redesigned screen. This change had no apparent effect on the results, i.e., an increased number of particles was not observed after the change in screen configuration, although on two occasions somewhat elevated colloid concentrations were encountered at the first sampling after a configuration change (Section 6.3.1.2.1).

A recent set of experiments involved the generation under ideal chemical conditions of a stable colloidal suspension composed of meta-schoepite and UO_2. It was observed that the colloid concentrations were stable over the short term but appear to dissolve under repository-relevant conditions (Section 6.3.1.2.3). This observation may be consistent with the small numbers of colloids developed in the Argonne National Laboratory drip tests. It is emphasized that the data are preliminary.

However, the creation of a stable U-substrate colloid suspension is significant and merits further investigation. Determination and confirmation that meta-schoepite and UO_2 colloid suspensions are inherently unstable under potential repository conditions would increase confidence in that conclusion.

Field evidence from investigations in the vicinity of uranium deposits and uranium mines appear to corroborate the conclusions from testing that persistent U-substrate colloid suspensions are

unlikely to form (Section 6.3.1.2.4). Studies in the literature (Short et al. 1988 [DIRS 113937]; Payne et al. 1992 [DIRS 124812]; Vilks et al. 1993 [DIRS 108261]; Zänker et al. 2000 [DIRS 162746]) suggest that no significant primary U-bearing colloids have been observed in the vicinities of uranium and other types of mines under repository-relevant conditions.

Criterion 4 (Relevant to Technical Work Plan Validation Criteria 1 and 2)

Is the model approach used, which stipulates that DOE SNF will not produce colloids in significant quantities, consistent with DOE SNF-specific test results and peer-reviewed literature on field observations near uranium mines and deposits?

Degradation tests on metallic uranium fuel, one type of DOE SNF, have resulted in the rapid breakdown of the fuel to abundant particles, some as small as colloids (Section 6.3.1.2.2). The particle compositions were primarily meta-schoepite and UO_2 as well as smectite (see below). The conclusion that these types of colloids from DOE SNF degradation will not persist in the repository setting is based on arguments similar to those presented under Criterion 3. It is corroborated with data from a recent set of experiments that characterized the mineralogy, size characteristics, and stability of particles in a U-bearing-colloid dispersion, and with field observations. The reader is referred to the discussion in Criterion 3.

The majority (approximately 90%) of the total waste slated for the repository is commercial spent nuclear fuel, with approximately 8% of the total being co-disposed defense high-level waste glass and DOE SNF and less than two percent being Naval Fuel (DOE 2002 [DIRS 155943], Table 3-3). It is currently planned that of the DOE waste approximately two-thirds will be defense high-level waste glass and DOE SNF will constitute about one-third (Lytle 1995 [DIRS 104398]). Therefore, DOE SNF would constitute less than three percent of the total repository waste inventory. N Reactor fuel comprises approximately 85% of the DOE SNF inventory (DOE 2002 [DIRS 158405]) and is the surrogate for DOE SNF in the TSPA-LA model. As stated previously, during degradation testing uranium metal has undergone rapid oxidation, breaking down to abundant particulate corrosion products including colloids. The colloids range from UO_2 to higher oxides of U to U- and Pu-bearing smectite. Preliminary findings from testing on the degradation of DOE SNF (Section 6.3.1.2.2) suggest that the U concentrations associated with colloids (either U oxides or smectite or both) can be high. In summary, these lines of evidence support the conclusion that although some primary uranium colloids may form from degradation of DOE SNF, colloid-related U transport will not be a major contributor to radionuclide transport. Further investigation may be necessary to ascertain the growth and potential contribution to release of Pu-bearing smectite.

Conclusion—Based on the discussions presented under Criteria 1 through 4, it is concluded that the waste form colloid concentration values appear to conform with accepted scientific principles with respect to colloid suspensions, and they are reasonable with respect to observations of colloids of similar mineralogy in the Project and peer-reviewed literature (Criterion 1). The stipulation that commercial and DOE SNF (Criteria 3 and 4) do not produce colloids in significant quantities is corroborated by the few observations of colloids in the vicinity of uranium mines and deposits. The applicability of the conditions of the defense high-level waste glass tests to repository conditions (Criterion 2) has been evaluated by considering the physicochemical properties of smectite colloids, similarities between test conditions and the

probable microenvironment at the degrading glass surface, and uncertainty in Pu concentration by using a bounding value believed to be conservative. It is therefore concluded that the validation activities performed for building confidence in the model elements and data discussed have sufficiently strong scientific bases, and that Criteria 1 through 4 used to determine that the required level of confidence in the model have been achieved.

7.2 CORROSION PRODUCT COLLOID PARAMETERS

Criterion 5 (Relevant to Technical Work Plan Validation Criterion 2)

Is the range of 0.05 to 50 mg/L adopted for maximum iron oxyhydroxide colloid concentrations from corrosion of ferrous repository materials reasonable, considering the lack of relevant peer-reviewed literature?

Iron oxyhydroxide colloids are expected to form as a result of internal and external corrosion of the waste package and associated engineered barrier system components (Section 6.3.1.3). There are few, if any, peer-reviewed publications that present information on colloid concentrations as a function of aqueous chemistry. For the colloid model, a reasonable estimate was made based on expert judgment, corroborated by laboratory experiments investigating the corrosion of small-scale waste package replicas, and by maximum colloid concentrations observed in groundwater.

The range of values for maximum iron oxyhydroxide colloids concentration, 0.05 to 50 mg/L, was chosen so that it was substantially greater than iron oxyhydroxide colloid levels found in groundwater, but high enough to reflect the masses of corroded ferrous metal anticipated in the repository. Additionally, the value acknowledges the high end of the range of colloids in general reported in groundwaters.

Research at the University of Nevada at Las Vegas have been studying the corrosion characteristics of miniature stainless steel waste packages and has characterized the quantities of corrosion particles produced with a variety of aqueous chemical conditions (Sections 6.3.1.3 and 6.3.2.3). While the measured colloid quantities may not be directly transferable to colloid model quantities, the experiments suggest that abundant colloids will be produced (as much as 20 mg/L in the first four weeks of the experiment (DTN: MO0212UCC034JC.002) [DIRS 161457]). Further, it has been demonstrated in every case in which a hole has been placed in a canister to simulate a breach that the hole, after passing quantities of corrosion particles, relatively quickly plugs with corrosion product and effectively seals against further outflows. The stipulation that continuous production and outflow of colloids in the waste package would continue unimpeded is therefore considered conservative.

Conclusion—Based on this line of reasoning, the value chosen for continuous production of corrosion-generated iron oxyhydroxide colloids over the regulatory period is reasonable and realistic. This value is perhaps on the high side (conservative with respect to mobility of attached radionuclides). The production of iron oxyhydroxides has been corroborated by laboratory-scale waste package corrosion tests. The stipulation that colloid production will continue unimpeded from the waste packages as corrosion proceeds is probably conservative, based on the observations that small apertures in the waste package become plugged and prevent

subsequent corrosion products from passing through the aperture. It is concluded that the criteria established to achieve the required level of confidence in the model have been satisfied.

7.3 SEEPAGE WATER/GROUNDWATER COLLOID PARAMETERS

Criterion 6 (Relevant to Technical Work Plan Validation Criteria 1 and 2)

Is the determined range and distribution for concentrations of groundwater colloids, based on a limited set of Yucca Mountain-vicinity data, reasonable?

Several hydrologic investigations in the Yucca Mountain vicinity have yielded a quantity of data on groundwater chemistry and colloid content (*cf.* Kingston and Whitbeck 1991 [DIRS 113930]; DTNs listed in Section 6.3.2.5). Most of the colloid data include information on total colloid concentrations and concentrations of several size ranges. Aqueous parameters such as major ion concentration, ionic strength, and pH were obtained for many of the samples. These data have been used in the colloid model to provide a colloid concentration range as a function of ionic strength. Validation of the groundwater colloid data used in the colloid model was accomplished by corroborating the mean, range, and distribution by comparison of independently generated subsets within the overall data set (see Section 6.3.2.5 and Figures 11 and 12), and with similar data from several different sites and geologic settings around the world (see CRWMS M&O 2001 [DIRS 153933], Figure 9).

Conclusion—The groundwater colloid data are site-specific, have been bounded conservatively and realistically, are internally consistent, and are determined to be similar to colloid concentration data from disparate geologic terrains around the world. Therefore the criteria established to achieve the required level of confidence in the established distribution in groundwater colloid concentrations have been satisfied.

7.4 RADIONUCLIDE SORPTION CHARACTERISTICS

Criterion 7 (Relevant to Technical Work Plan Validation Criterion 1)

Is the stipulation that Pu is "embedded" or otherwise irreversibly sorbed to defense high-level waste glass colloids reasonable and conservative with respect to radionuclide mobility?

The assumption of embedded Pu in smectite waste form colloids is based on the results of defense high-level waste glass degradation testing at Argonne National Laboratory (see Section 5, Assumption 5.5 and Section 6.3.1.1). Data derived from the testing indicated that Pu was associated with the colloids. The colloid-associated Pu concentrations were quantified, although the mechanisms of attachment or incorporation were not determined. Validation of these one-of-a-kind data can only be accomplished by noting the similar results from repeated sample analyses and the professional judgment of the investigators regarding the Pu-colloid association. The stipulation that the Pu is permanently attached, whatever the mechanism of attachment, is conservative, as it effectively increases the potential mobility of the Pu.

Criterion 8 (Relevant to Technical Work Plan Validation Criteria 1 and 2)

Is the use of a modeling approach in which a large fraction of Pu sorbed onto iron oxyhydroxide pseudocolloids is irreversibly sorbed reasonable?

A modeling approach is taken to characterize sorption onto iron oxyhydroxide colloids in which a large fraction of sorbed Pu effectively becomes permanently sorbed (see Section 6.3.3.2). This approach is validated by laboratory experiments, which show almost complete retention of Pu onto iron oxyhydroxide colloids over the duration of the experiments (up to approximately 6 months), and field observations (over periods up to about 50 years), which indicate that soils strongly bind Pu, leaving little dissolved Pu in the pore fluids (see Section 6.3.3.2). Based on these observations it is concluded that providing for this type of irreversible attachment in the abstraction is reasonable and justified.

Criterion 9 (Relevant to Technical Work Plan Validation Criteria 1 and 2)

Are the distribution coefficients for radionuclides onto colloids (K_d values) reasonable and supported by peer-reviewed literature and analytical modeling results?

The K_d value ranges chosen for reversibly attached radionuclides are based on Project laboratory results and peer-reviewed literature, which are described in detail in Section 6.3.3. Validation of K_d values for several radionuclides adopted in the abstraction, and particularly validation of the use of published literature, was accomplished by considering alternative calculations for determining effective K_d values. Table 10 lists the radionuclides to which K_d values have been assigned in this model report. Tables 6, 7, and 8 list colloid types and K_d values based on the Los Alamos National Laboratory results and literature review (see Section 6.3.3.1). Table 9 lists K_d values which are the results of modeling described by Honeyman and Ranville (2002 [DIRS 161657], from Figure 7-5). As described in Section 6.3.3.1, Yucca Mountain vicinity-specific colloid concentrations and groundwater chemistry from Kingston and Whitbeck (1991 [DIRS 113930]) were used as input to a mechanistic sorption model and surface complexation calculations. The K_d ranges vary in part as a function of colloid concentration, which ranged from 0.1 to 100 mg/L.

Comparison among the K_d values listed in Tables 6, 7, and 8; and the modeled K_d values in Table 9 indicates that there is rather good agreement between the literature- and observation-based K_d values and those derived from mechanistic model calculations for Pu, Am, U, and Np; these data may be considered mutually corroborative, assuming a fairly high degree of uncertainty.

Conclusion—The modeling approach regarding the three types of radionuclide attachment to colloids (Criteria 7 through 9) either have strong scientific bases (Criteria 8 and 9) or are conservative with respect to radionuclide mobility (Criterion 7). It is concluded that these criteria, used to determine that the required level of confidence in the model, have been satisfied.

7.5 PROPAGATION OF MODEL UNCERTAINTY THROUGH ABSTRACTION

Criterion 10 (Not Specifically Relevant to any Criteria Specified in the Technical Work Plan)

Has model uncertainty been propagated throughout the abstraction satisfactorily?

Ranges and distributions are provided to TSPA-LA to represent uncertainties of input parameters. The abstraction logic is provided along with the parameters to total system performance assessment. Within the TSPA-LA model, the abstraction implementation incorporates the parameter uncertainties with Monte Carlo simulation techniques. In this way parameter uncertainties are propagated throughout the abstraction during computation and are reflected in the calculated results.

Conclusion—Uncertainty propagation throughout the abstraction has been addressed by means of the methodology of incorporating the abstraction into the TSPA-LA calculations. It is concluded that the level of confidence required of the model has been achieved through the use of this methodology.

7.6 PROCESSES NOT INCORPORATED INTO THE ABSTRACTION

Certain processes were not incorporated into the abstraction, including filtration of colloids in the waste package, sorption to the air-water interfaces in unsaturated environments, and gravitational settling. It was considered realistic and conservative to do so. It may be argued that gravitational settling would facilitate the exit of colloids from a breach at the bottom of the waste package; the net effect, however, is the same.

Conclusion—Omission of these processes is conservative, in that it maximizes the mobility of colloids and associated radionuclides.

7.7 VALIDATION ACTIVITIES EXTENDING BEYOND CURRENT DOCUMENTATION OF THE MODEL

The disposition of the various validation criteria described in Sections 7.1 through 7.5 is that the level of confidence required for validation of the various components considered in this model analysis has been achieved. No further validation activities are needed to complete the model's validation for its intended use.

8. CONCLUSIONS

8.1 SUMMARY OF MODEL AND ITS IMPLEMENTATION

The colloids process models for the waste form and engineered barrier system components of the TSPA-LA model describe the types and concentrations of colloids that could potentially be generated in the waste package from degradation of the waste forms and the corrosion of the waste package materials and the concentrations of colloids present in natural waters in the vicinity of Yucca Mountain that could potentially come in contact with the repository waste. In addition, stability and sorption/desorption mechanisms and transport characteristics of colloids

anticipated in the repository are addressed, based on the range in geochemical conditions anticipated in the repository environment within the regulatory compliance period.

The types and quantities of colloid formed from the degradation of defense high-level waste glass, commercial and DOE SNF are based largely on ongoing experimental work at Argonne National Laboratory and appropriate studies, albeit limited, documented in the open literature. The quantities and characteristics of defense high-level waste glass are well documented based on several years of research at Argonne National Laboratory (see Section 6.3.1.1). The colloids formed from the degradation products of high-level waste glass have been shown to be primarily smectite clay containing discrete radionuclide-bearing phases, which are incorporated in the clay. These "embedded" radionuclides are stipulated to be permanently fixed in the clay particles and therefore are modeled as irreversible sorbed colloids that will be transported with the colloids and will not be detached from the colloid particles.

There are no direct colloid source term contributions from commercial and DOE SNF wastes in the TSPA-LA model. Argonne National Laboratory investigations (described in Section 6.3.1.2) indicate the formation of some quantities of stable colloids. However, these research findings are too preliminary at this time to incorporate into the TSPA-LA model. Specifically, U colloids that have been observed to form are meta-schoepite or other oxyhydroxides that are soluble at (more dilute) anticipated repository chemical conditions. Consequently, these colloids will eventually dissolve, in part because of their very small size and large reactive surface area, and in part because of increasingly dilute groundwater conditions away from the waste package and drift. The model is set up such that the U will be present within the engineered barrier system as U aqueous complexes and not associated with colloids. Therefore, commercial and DOE SNF degradation is accommodated in the colloid model with the stipulation that degradation-product U will occur entirely as aqueous complexes and will be transported with the fluid within the breached WP and released into the drift. U sorption onto stationary corrosion materials is modeled within the waste package, but this process is ignored in the engineered barrier system outside the waste package. This approach was taken because of the uncertainty in the quantity and physical/chemical characteristics of the drift stationary corrosion materials and also because ignoring sorption onto these materials would lead to a more pessimistic contribution to the dose calculations by U.

The TSPA-LA colloid model has been constructed in such a way that a large fraction of dissolved Pu and Am sorbed onto colloids is irreversibly sorbed (i.e., is embedded within or becomes permanently attached) and the remainder is reversibly sorbed according to an equilibrium K_d value model with a small fraction occurring as dissolved species. Further, a parameter (the target-flux out ratio, F_{RN}) defines the ratio of Pu and Am mass sorbed to colloids (irreversibly and reversibly) to the total Pu and Am mass leaving the waste package (sorbed to colloids plus dissolved). This ratio ranges between 0.9 and 0.99. Additionally, sorption to immobile iron oxyhydroxide corrosion products is modeled. The difference in specific surface areas between the colloids and the stationary corrosion products is taken into account. Allocating a fraction of the total Pu and Am onto the stationary corrosion products would reduce the quantity of Pu and Am transported by colloids, but some degree of sorption onto stationary corrosion products is realistic.

Stability of all colloids (smectite, both natural seepage water/groundwater colloids and those formed from defense high-level waste glass degradation products, and iron oxyhydroxide colloids formed from steel corrosion) is evaluated based on solution chemistry, specifically ionic strength and pH (Section 6.3.2).

In the TSPA-LA model, natural seepage water/groundwater colloids are stipulated to come in contact with and enter breached waste packages and will subsequently sorb radionuclides. The resulting pseudocolloid (radionuclide complexes) will subsequently be subjected to transport from the engineered barrier system to the downstream unsaturated and saturated zones. Furthermore, in contrast to the modeling effort for the TSPA-SR, wherein colloid concentration parameters were based upon data from groundwaters around the world (Degueldre et al. 2000 [DIRS 153651], DTN: SNT05080598002.001 [DIRS 162744], more recent data from groundwater samples collected from wells within the Yucca Mountain area and Idaho National Engineering and Environmental Laboratory are used to develop the parameters used for the TSPA-LA. These data suggested higher seepage water/groundwater colloids concentrations (perhaps as high as one to two orders of magnitude greater than those used previously in the TSPA-SR) and are appropriate for the TSPA-LA model calculations.

Recent experimental work on the corrosion of miniature steel waste packages have provided needed data on the probable concentrations of iron oxyhydroxide colloids that might be expected within the engineered barrier system upon contact of seepage water and subsequent corrosion of the waste packages. These data indicate that values as high as 50 mg/L should be sampled in the TSPA-LA model calculations. These high values represent a reasonable maximum for iron oxyhydroxide colloid releases from a waste package following a potential breach (Section 6.3.2.3).

In summary:

- A model has been developed for TSPA-LA to calculate radionuclide and colloid mass concentrations as a function of fluid chemistry (ionic strength and pH), dissolved radionuclide concentrations, and sorption characteristics of the radionuclides. Colloids from waste form degradation, corrosion of steel repository components, and seepage water/groundwater are included in the model.

- The abstraction incorporates bounding data and relationships that are based on the results colloid-related research programs (both laboratory and field) conducted at Argonne National Laboratory and Los Alamos National Laboratory.

- The abstraction is intended to be conservative *and* realistic.

There are several significant sources of uncertainty attached to this abstraction. The potential formation of colloids from degradation of N-Reactor fuel, and the potential contribution of these colloids to repository performance, bears further investigation. For now, the position is taken that, due to the small quantity of N-Reactor fuel in a codisposal canister, radionuclide-bearing colloids generated from degradation of N-Reactor fuel will add little to the releases provided by defense high-level waste glass.

In degradation testing of commercial SNF, rinds were observed containing fine-grained Pu-bearing particles and U silicates. Spallation of the rinds did not occur during the tests but could possibly spall under different test conditions. Given the large quantity of commercial SNF planned for the repository, the possible fate of Pu-rich rinds also bears further investigation.

The abstraction is considered valid and usable in TSPA-LA calculations for any time after the temperature in the repository has decreased to below boiling after the thermal pulse. Many of the waste degradation tests were performed at 90°C, but colloids produced were mostly sampled at near room temperature. Therefore the test results may be applied to this post-thermal period. The range of ionic strength and pH for which colloid masses and stability are calculated in the abstraction are within the ranges anticipated from in-package chemistry calculations and abstraction.

In general, the bounding relationships employed in the abstraction incorporate uncertainty present in the data to formulate the abstraction. Additional uncertainty may result from the TSPA-LA model and the ways in which the dose calculations are performed. For example, the choices of distributions and the method of sampling specific distributions may result in uncertainties in determination of colloid concentrations, ionic strength, pH, and radionuclide concentrations.

8.2 MODEL OUTPUTS

Developed data for use directly by the TSPA-LA calculations or other submodel components in the TSPA-LA model calculations include both intermediate parameters (see Table 16 for parameter listing and associated DTNs) and model output parameters (see Table 17).

In the colloid model abstraction, several parameters are calculated with TSPA-LA model as outputs from the model and are passed to the unsaturated zone component of TSPA-LA to be used as inputs. These colloid model outputs are listed and described in Table 18.

The parameters calculated as intermediate results within the TSPA-LA model calculations are listed in Table 16.

Table 18. Summary of Model Output Parameters

Parameter Name	Parameter Description	Units	Basis for Value/ Source	Value/Range/ Distribution
$C_{Rncoll,wf,embed}$ $C_{Rncoll,wf,rev}$ $C_{Rncoll,FeOx,irrev}$ $C_{Rncoll,FeOx,rev}$ $C_{Rncoll,gw}$	Concentration of mobile colloidal radionuclide element RN per unit volume or mass of water	mol/L	Determined in PA calculation; Figure 21	Calculated at each time step; uncertainty propagated through the TSPA-LA model calculations

NOTE: PA = performance assessment; RN = radionuclide.

Additionally, parameters developed in this analysis for use elsewhere in the TSPA-LA model include waste form colloid mass concentrations (derived from defense high-level waste glass), corrosion product colloid mass concentrations, K_d values for selected radionuclides onto smectite and iron oxyhydroxide colloids, and specific surface area on iron oxyhydroxide colloids.

Developed DTNs include: SN0304T0504103.001, SN0304T0504103.002, SN0304T0504103.003 and SN0304T0504103.004 (see Table 16).

The uncertainties associated with the output parameters result from propagation of the individual aleatoric uncertainties (explicitly represented by ranges and distributions, and implicitly represented by bounding values) of the inputs and epistemic uncertainty (implicit uncertainty in the model elements) through the TSPA-LA model calculations. The TSPA-LA model represents a parameter uncertainty with a probability distribution. The aggregate uncertainties associated with the individual inputs are translated into output uncertainties, using Monte Carlo simulation, by sampling all of the parameters' probability distributions for each of a large number of realizations. The overall effects of the input uncertainties on the outputs are estimated (approximated) from observation of the output parameter ranges resulting from the realizations.

9. INPUTS AND REFERENCES

9.1 DOCUMENTS CITED

Aguilar, R. 2003. "P&CE Model Report Citation in MDL-EBS-PA-000004 Rev 00D." E-Mail from R. Aguilar to T. Reeder, June 13, 2003. ACC: MOL.20030615.0217. [DIRS 163770]

Aguilar, R.; Papenguth, H.W.; and Rigby, F. 1999. "Retardation of Colloidal Actinides through Filtration in Intrusion Borehole Backfill at the Waste Isolation Pilot Plant (WIPP)." *Actinide Speciation in High Ionic Strength Media, Experimental and Modeling Approaches to Predicting Actinide Speciation and Migration in the Subsurface, Proceedings of an American Chemical Society Symposium on Experimental and Modeling Studies of Actinide Speciation in Non-ideal Systems, held August 26-28, 1996, in Orlando, Florida.* Reed, D.T.; Clark, S.B.; and Rao, L.; eds. Pages 215-225. New York, New York: Kluwer Academic/Plenum Publishers. TIC: 253961. [DIRS 161648]

Beyenal, H. and Lewandowski, Z. 2000. "Combined Effect of Substrate Concentration and Flow Velocity on Effective Diffusivity in Biofilms." *Water Research, 34,* (2), 528-538. [New York, New York]: Elsevier. TIC: 253702. [DIRS 161652]

Brady, P.V.; Jové-Colon, C.F.; Carr, G.; and Huang, F. 2002. "Soil Radionuclide Plumes." Chapter 8 of *Geochemistry of Soil Radionuclides.* Zhang, P-C., and Brady, P.V., eds. SSSA Special Publication Number 59. Madison, Wisconsin: Soil Science Society of America. TIC: 253952. [DIRS 161649]

BSC (Bechtel SAIC Company) 2001. *Inventory Abstraction.* ANL-WIS-MD-000006 REV 00 ICN 02. Las Vegas, Nevada: Bechtel SAIC Company. ACC: MOL.20010416.0088. [DIRS 154841]

BSC 2001. *Technical Work Plan for Saturated Zone Flow and Transport Modeling and Testing.* TWP-NBS-MD-000001 REV 02. Las Vegas, Nevada: Bechtel SAIC Company. ACC: MOL.20010924.0269. [DIRS 156308]

BSC 2002. *Risk Information to Support Prioritization of Performance Assessment Models.* TDR-WIS-PA-000009 REV 01 ICN 01. Las Vegas, Nevada: Bechtel SAIC Company. ACC: MOL.20021017.0045. [DIRS 160780]

BSC 2002. *Technical Work Plan for Waste Form Degradation Modeling, Testing, and Analyses in Support of SR and LA.* TWP-WIS-MD-000008 REV 02. Las Vegas, Nevada: Bechtel SAIC Company. ACC: MOL.20020819.0359. [DIRS 160779]

BSC 2002. *Technical Work Plan for: Engineered Barrier System Department Modeling and Testing, FY 02 Work Activities.* TWP-MGR-MD-000015 REV 02. Las Vegas, Nevada: Bechtel SAIC Company. ACC: MOL.20021014.0209. [DIRS 160315]

BSC 2002. *Technical Work Plan for: Performance Assessment Unsaturated Zone.* TWP-NBS-HS-000003 REV 02. Las Vegas, Nevada: Bechtel SAIC Company. ACC: MOL.20030102.0108. [DIRS 160819]

BSC 2002. *Test Plan for: Laboratory Sorption Measurements – UZ and SZ.* SITP-02-UZ-011 REV 00. Las Vegas, Nevada: Bechtel SAIC Company. ACC: MOL.20020225.0261. [DIRS 158197]

BSC 2002. *Test Plan for: Laboratory Sorption Measurements-SZ.* SITP-02-SZ-004 REV 01. Las Vegas, Nevada: Bechtel SAIC Company. ACC: MOL.20020906.0298. [DIRS 161535]

BSC 2002. *Test Plan Waste form Colloids Characterization and Concentration Studies.* SITP-02-WF-003 REV 00. Las Vegas, Nevada: Bechtel SAIC Company. ACC: MOL.20020402.0443. [DIRS 161534]

BSC 2002. *The Enhanced Plan for Features, Events, and Processes (FEPs) at Yucca Mountain.* TDR-WIS-PA-000005 REV 00. Las Vegas, Nevada: Bechtel SAIC Company. ACC: MOL.20020417.0385. [DIRS 158966]

BSC 2003. *Dissolved Concentrations of Radioactive Elements.* ANL-WIS-MD-000010 REV 02. Las Vegas, Nevada: Bechtel SAIC Company. URN-1089 [DIRS 163152]

BSC 2003. *EBS Radionuclide Transport Abstraction.* ANL-WIS-PA-000001 REV 01A. Las Vegas, Nevada: Bechtel SAIC Company. ACC: MOL.20030617.0222. TBV-5179 [DIRS 163935]

BSC 2003. *In-Package Chemistry Abstraction.* ANL-EBS-MD-000037 REV 02B. Las Vegas, NV: Bechtel SAIC Company. ACC: MOL.20030617.0224. TBV-5175. [DIRS 163919]

BSC 2003. *Particle Tracking Model and Abstraction of Transport Processes.* MDL-NBS-HS-000020 REV 00A. Las Vegas, Nevada: Bechtel SAIC Company. ACC: MOL.20030611.0040. TBV-5181 [DIRS 163933]

BSC 2003. *Saturated Zone Colloid Transport.* ANL-NBS-HS-000031 REV 01A. Las Vegas, Nevada: Bechtel SAIC Company. ACC: MOL.20030602.0288. TBV-5180 [DIRS 163932]

BSC 2003. *Software Code: GoldSim.* 7.50.100. PC. 10344-7.50.100-00. [DIRS 161572]

Buck, E.C. 2003. "Transmittal of Draft Alternative Conceptual Model for Colloid Generation from Commerical Spent Nuclear Fuel, Pacific Northwest National Laboratory." Interoffice memorandum from E. C. Buck (BSC) to Y. Chen, June 17, 2003, 0613037655, with attachment. ACC: MOL.20030617.0258. TBV-5182 [DIRS 163117]

Buck, E.C. and Bates, J.K. 1999. "Microanalysis of Colloids and Suspended Particles from Nuclear Waste Glass Alteration." *Applied Geochemistry, 14,* 635-653. [New York, New York]: Elsevier. TIC: 245946. [DIRS 109494]

Buddemeier, R.W. and Hunt, J.R. 1988. "Transport of Colloidal Contaminants in Groundwater: Radionuclide Migration at the Nevada Test Site." *Applied Geochemistry, 3,* 535-548. Oxford, England: Pergamon Press. TIC: 224116. [DIRS 100712]

Buffle, J.; Wilkinson, K.J.; Stoll, S.; Filella, M.; and Zhang, J. 1998. "A Generalized Description of Aquatic Colloidal Interactions: The Three-Colloidal Component Approach." *Environmental Science & Technology, 32,* (19), 2887-2899. [Washington, D.C.]: American Chemical Society. TIC: 253710. [DIRS 161653]

Bunzl, K.; Flessa, H.; Kracke, W.; and Schimmack, W. 1995. "Association of Fallout $^{239+240}$Pu and ^{241}Am with Various Soil Components in Successive Layers of a Grassland Soil." *Environmental Science & Technology, 29,* (10), 2513-2518. Washington, D.C.: American Chemical Society. TIC: 234160. [DIRS 154468]

Contardi, J.S.; Turner, D.R.; and Ahn, T.M. 2001. "Modeling Colloid Transport for Performance Assessment." *Journal of Contaminant Hydrology, 47,* ([2-4]), 323-333. [New York, New York]: Elsevier. TIC: 253918. [DIRS 162732]

Coughtrey, P.J.; Jackson, D.; Jones, C.H.; Kane, P.; and Thorne, M.C. 1985. *Radionuclide Distribution and Transport in Terrestrial and Aquatic Ecosystems, A Compendium of Data.* Volume 6. Rotterdam, The Netherlands: A.A. Balkema. TIC: 240299. [DIRS 154494]

CRWMS M&O 2000. *In-Drift Colloids and Concentration.* ANL-EBS-MD-000042 REV 00. Las Vegas, Nevada: CRWMS M&O. ACC: MOL.20000509.0242. [DIRS 129280]

CRWMS M&O 2000. *In-Drift Microbial Communities.* ANL-EBS-MD-000038 REV 00 ICN 01. Las Vegas, Nevada: CRWMS M&O. ACC: MOL.20001213.0066. [DIRS 151561]

CRWMS M&O 2000. *Summary of In-Package Chemistry for Waste Forms.* ANL-EBS-MD-000050 REV 00. Las Vegas, Nevada: CRWMS M&O. ACC: MOL.20000217.0217. [DIRS 111880]

CRWMS M&O 2000. *Total System Performance Assessment for the Site Recommendation.* TDR-WIS-PA-000001 REV 00 ICN 01. Las Vegas, Nevada: CRWMS M&O. ACC: MOL.20001220.0045. [DIRS 153246]

CRWMS M&O 2000. *Unsaturated Zone and Saturated Zone Transport Properties (U0100).* ANL-NBS-HS-000019 REV 00. Las Vegas, Nevada: CRWMS M&O. ACC: MOL.20000829.0006. [DIRS 152773]

CRWMS M&O 2001. *Colloid-Associated Radionuclide Concentration Limits: ANL.* ANL-EBS-MD-000020 REV 00 ICN 01. Las Vegas, Nevada: CRWMS M&O. ACC: MOL.20010216.0003. [DIRS 154071]

CRWMS M&O 2001. *Waste Form Colloid-Associated Concentrations Limits: Abstraction and Summary.* ANL-WIS-MD-000012 REV 00 ICN 01. Las Vegas, Nevada: CRWMS M&O. ACC: MOL.20010130.0002. [DIRS 153933]

Davis, J.A. and Kent, D.B. 1990. "Surface Complexation Modeling in Aqueous Geochemistry." *Mineral-Water Interface Geochemistry.* Hochella, M.F., Jr. and White, A.F., eds. Reviews in Mineralogy Volume 23. Pages 177-260. Washington, D.C.: Mineralogical Society of America. TIC: 224085. [DIRS 143280]

Degueldre, C.; Triay, I.; Kim, J-I; Vilks, P.; Laaksoharju, M.; and Miekeley, N. 2000. "Groundwater Colloid Properties: A Global Approach." *Applied Geochemistry, 15,* ([7]), 1043-1051. [New York, New York]: Pergamon Press. TIC: 249340. [DIRS 153651]

DOE (U.S. Department of Energy) 2002. *DOE Spent Nuclear Fuel Information in Support of TSPA-SR.* DOE/SNF/REP-047, Rev. 2. Idaho Falls, Idaho: U.S. Department of Energy, Idaho Operations Office. TIC: 252089. [DIRS 158405]

DOE (U.S. Department of Energy) 2002. *Yucca Mountain Science and Engineering Report.* DOE/RW-0539, Rev. 1. Washington, D.C.: U.S. Department of Energy, Office of Civilian Radioactive Waste Management. ACC: MOL.20020404.0042. [DIRS 155943]

DOE (U.S. Department of Energy) 2003. *Quality Assurance Requirements and Description.* DOE/RW-0333P, Rev. 13. Washington, D.C.: U.S. Department of Energy, Office of Civilian Radioactive Waste Management. ACC: DOC.20030422.0003. [DIRS 162903]

Dzombak, D.A. and Morel, F.M.M. 1987. "Adsorption of Inorganic Pollutants in Aquatic Systems." Journal of Hydraulic Engineering, 113, (4), 430-474. New York, New York: American Society of Civil Engineers. TIC: 245735. [DIRS 109505]

Dzombak, D.A. and Morel, F.M.M. 1990. *Surface Complexation Modeling, Hydrous Ferric Oxide.* New York, New York: John Wiley & Sons. TIC: 224089. [DIRS 105483]

Ebert, W.L. 1995. *The Effects of the Glass Surface Area/Solution Volume Ratio on Glass Corrosion: A Critical Review.* ANL-94/34. Argonne, Illinois: Argonne National Laboratory. TIC: 215400. [DIRS 113219]

EPA (U.S. Environmental Protection Agency) 1999. *Understanding Variation in Partition Coefficient, Kd, Values.* EPA 402-R-99-004A&B Two volumes. Washington, D.C.: U.S. Environmental Protection Agency. TIC: 249201. TBV-5183 [DIRS 147475]

Fontes, D.E.; Mills, A.L.; Hornberger, G.M.; and Herman, J.S. 1991. "Physical and Chemical Factors Influencing Transport of Microorganisms Through Porous Media." *Applied and Environmental Microbiology, 57,* (9), 2473-2481. [Washington, D.C.]: American Society for Microbiology. TIC: 247563. [DIRS 147337]

Freeze, G.A.; Brodsky, N.S.; and Swift, P.N. 2001. *The Development of Information Catalogued in REV00 of the YMP FEP Database.* TDR-WIS-MD-000003 REV 00 ICN 01. Las Vegas, Nevada: Bechtel SAIC Company. ACC: MOL.20010301.0237. [DIRS 154365]

Hahn, H.H. and Stumm, W. 1970. "The Role of Coagulation in Natural Waters."*American Journal of Science, 268,* (4), 354-368. [New Haven, Connecticut: Yale University, Kline Geology Laboratory]. TIC: 253963. [DIRS 161656]

Harvey, R.W.; George, L.H.; Smith, R.L.; and LeBlanc, D.R. 1989. "Transport of Microspheres and Indigenous Bacteria Through a Sandy Aquifer: Results of Natural- and Forced-Gradient Tracer Experiments." *Environmental Science & Technology, 23,* (1), 51-56. [Washington, D.C.]: American Chemical Society. TIC: 224869. [DIRS 147338]

Hersman, L. 1995. *Microbial Effects on Colloidal Agglomeration.* LA-12972-MS. Los Alamos, New Mexico: Los Alamos National Laboratory. ACC: MOL.19971210.0253. [DIRS 100750]

Hersman, L.E. 1997. "Subsurface Microbiology: Effects on the Transport of Radioactive Wastes in the Vadose Zone." Chapter 16 of *The Microbiology of the Terrestrial Deep Subsurface.* Amy, P.S. and Haldeman, D.L., eds. Boca Raton, Florida: CRC Lewis Publishers. TIC: 232570. [DIRS 100763]

Honeyman, B.D. and Ranville, J.F. 2002. "Colloid Properties and their Effects on Radionuclide Transport through Soils and Groundwaters." Chapter 7 of *Geochemistry of Soil Radionculides.* Zhang, P-C. and Brady, P.V., eds. SSSA Special Publication Number 59. Madison, Wisconsin: Soil Science Society of America. TIC: 253952. TBV-5184 [DIRS 161657]

Jenne, E.A. 1998. "Adsorption of Metals by Geomedia: Data Analysis, Modeling, Controlling Factors, and Related Issues." *Adsorption of Metals by Geomedia.* Jenne, E.A, ed. Pages 1-73. San Diego, California: Academic Press. TIC: 254037. [DIRS 162328]

Kersting, A.B.; Efurd, D.W.; Finnegan, D.L.; Rokop, D.J.; Smith, D.K.; and Thompson, J.L. 1999. "Migration of Plutonium in Ground Water at the Nevada Test Site." *Nature, 397,* ([6714]), 56-59. [London, England: Macmillan Journals]. TIC: 243597. [DIRS 103282]

Kim, J.I. 1994. "Actinide Colloids in Natural Aquifer Systems." *MRS Bulletin, 19,* (12), 47-53. Pittsburgh, Pennsylvania: Materials Research Society. TIC: 246128. [DIRS 109521]

Kim, S. and Corapcioglu, M.Y. 1996. "A Kinetic Approach to Modeling Mobile Bacteria-Facilitated Groundwater Contaminant Transport." *Water Resources Research, 32,* (2), 321-331. Washington, D.C.: American Geophysical Union. TIC: 247566. [DIRS 147342]

Kingston, W.L. and Whitbeck, M. 1991. *Characterization of Colloids Found in Various Groundwater Environments in Central and Southern Nevada.* DOE/NV/10384-36. [Las Vegas, Nevada]: Desert Research Institute, Water Resources Center. ACC: NNA.19930607.0073. [DIRS 113930]

Laaksoharju, M.; Degueldre, C.; and Skarman, C. 1995. *Studies of Colloids and Their Importance for Repository Performance Assessment.* SKB TR-95-24. Stockholm, Sweden: Svensk Kärnbränsleförsörjning A.B. TIC: 223428. [DIRS 106449]

Langmuir, D. 1997. *Aqueous Environmental Geochemistry.* Upper Saddle River, New Jersey: Prentice Hall. TIC: 237107. [DIRS 100051]

Langmuir, D. 1997. "The Use of Laboratory Adsorption Data and Models to Predict Radionuclide Releases from a Geological Repository: A Brief History." *Scientific Basis for Nuclear Waste Management XX, Symposium held December 2-6, 1996, Boston, Massachusetts.* Gray, W.J. and Triay, I.R., eds. *465,* 769-780. Pittsburgh, Pennsylvania: Materials Research Society. TIC: 238884. [DIRS 125369]

Lewandowski, Z.; Stoodley, P.; and Altobelli, S. 1995. "Experimental and Conceptual Studies on Mass Transport in Biofilms." *Water Science and Technology, 31,* (1), 153-162. [London, England]: International Association on Water Quality. TIC: 242312. [DIRS 161664]

Liang, L. and Morgan, J.J. 1990. "Chemical Aspects of Iron Oxide Coagulation in Water: Laboratory Studies and Implications for Natural Systems." *Aquatic Sciences, 52,* (1), 32-55. Basel, Switzerland: Birkhauser Verlag. TIC: 246125. [DIRS 109524]

Lide, D.R., ed. 1995. *CRC Handbook of Chemistry and Physics.* 76th Edition. Boca Raton, Florida: CRC Press. TIC: 216194. TBV-5185 [DIRS 101876]

Litaor, M.I. and Ibrahim, S.A. 1996. "Plutonium Association with Selected Solid Phases in Soils of Rocky Flats, Colorado, Using Sequential Extraction Technique." *Journal of Environmental Quality, 25,* (5), 1144-1151. Madison, Wisconsin: American Society of Agronomy. TIC: 252783. [DIRS: 161667]

Liu, Q.; Zhang, Y.; and Laskowski, J.S. 2000. "The Adsorption of Polysaccharides Onto Mineral Surfaces: An Acid/Base Interaction." *International Journal of Mineral Processing, 60,* ([3-4]), 229-245. [New York, New York]: Elsevier. TIC: 253706. [DIRS 161777]

Lo, W.; Nelson, Y.M.; Lion, L.W.; Shuler, M.L.; and Ghiorse, W.C. 1996. "Determination of Iron Colloid Size Distribution in the Presence of Suspended Cells: Application to Iron Deposition Onto a Biofilm Surface." *Water Research, 30,* (10), 2413-2423. [New York, New York]: Elsevier. TIC: 253698. [DIRS 161669]

Lu, N.; Conca, J.; Parker, G.R.; Leonard, P.A.; Moore, B.; Strietelmeier, B.; and Triay, I.R. 2000. Adsorption of Actinides Onto Colloids as a Function of Time, Temperature, Ionic Strength, and Colloid Concentration, Waste Form Colloids Report for Yucca Mountain Program

(Colloid Data Summary from 1999 to 2000 Research). LA-UR-00-5121. Los Alamos, New Mexico: Los Alamos National Laboratory. TIC: 249708. TBV-5186 [DIRS 154422]

Lu, N.; Triay, I.R.; Cotter, C.R.; Kitten, H.D.; and Bentley, J. 1998. *Reversibility of Sorption of Plutonium-239 onto Colloids of Hematite, Goethite, Smectite, and Silica.* LA-UR-98-3057. Los Alamos, New Mexico: Los Alamos National Laboratory. ACC: MOL.19981030.0202. TBV-5187 [DIRS 100946]

Lytle, J.E. 1995. "Disposal of DOE-owned High Level Waste and Spent Nuclear Fuel." Memorandum from J.E. Lytle (DOE) to D.A. Dreyfus (DOE/OCRWM), October 26, 1995. ACC: HQO.19951116.0015. [DIRS 104398]

Marty, R.C.; Bennett, D.; and Thullen, P. 1997. "Mechanism of Plutonium Transport in a Shallow Aquifer in Mortandad Canyon, Los Alamos National Laboratory, New Mexico." *Environmental Science & Technology, 31,* (7), 2020-2027. Washington, D.C.: American Chemical Society. TIC: 253960. [DIRS 161670]

McCarthy, J.F. and Degueldre, C. 1993. "Sampling and Characterization of Colloids and Particles in Groundwater for Studying Their Role in Contaminant Transport." *Environmental Particles.* Buffle, J. and van Leeuwen, H.P., eds. Environmental Analytical and Physical Chemistry Series Volume 2. Pages 247-315. Boca Raton, Florida: Lewis Publishers. TIC: 245905. [DIRS 108215]

McCarthy, J.F. and Zachara, J.M. 1989. "Subsurface Transport of Contaminants." *Environmental Science & Technology, 23,* (5), 496-502. Easton, Pennsylvania: American Chemical Society. TIC: 224876. [DIRS 100778]

McGraw, M.A. 1996. The Effect of Colloid Size, Colloid Hydrophobicity, and Volumetric Water Content on the Transport of Colloids Through Porous Media. Ph.D. dissertation. Berkeley, California: University of California. TIC: 245722. [DIRS 108218]

Meijer, A. 1992. "A Strategy for the Derivation and Use of Sorption Coefficients in Performance Assessment Calculations for the Yucca Mountain Site." *Proceedings of the DOE/Yucca Mountain Site Characterization Project Radionuclide Adsorption Workshop at Los Alamos National Laboratory, September 11-12, 1990.* Canepa, J.A., ed. LA-12325-C. Pages 9-40. Los Alamos, New Mexico: Los Alamos National Laboratory. ACC: NNA.19920421.0117. [DIRS 100467]

Mertz, C.J.; Finch, R.J.; Fortner, J.A.; Jerden, J.L., Jr.; Yifen, T.; Cunnane, J.C.; and Finn, P.A. 2003. *Characterization of Colloids Generated from Commercial Spent Nuclear Fuel Corrosion.* Activity Number: PAWTP30A. Argonne, Illinois: Argonne National Laboratory. ACC: MOL.20030422.0337. [DIRS 162032]

Minai, Y.; Choppin, G.R.; and Sisson, D.H. 1992. "Humic Material in Well Water from the Nevada Test Site." *Radiochimica Acta, 56,* 195-199. Munchen, Germany: R. Oldenbourg Verlag. TIC: 238763. [DIRS 100801]

Napper, D.H. 1983. "Basic Concepts of Colloid Stability." *Polymeric Stabilization of Colloidal Dispersions.* Pages 1-17. New York, New York: Academic Press. TIC: 253897. [DIRS 161735]

NRC (U.S. Nuclear Regulatory Commission) 2002. *Yucca Mountain Review Plan, Draft Report for Comment.* NUREG-1804, Rev. 2. Washington, D.C.: U.S. Nuclear Regulatory Commission, Office of Nuclear Material Safety and Safeguards. TIC: 252488. [DIRS 158449]

Payne, T.E.; Edis, R.; and Seo, T. 1992. "Radionuclide Transport by Groundwater Colloids at the Koongarra Uranium Deposit." *Scientific Basis for Nuclear Waste Management XV, Symposium held November 4-7, 1991, Strasbourg, France.* Sombret, C.G., ed. *257,* 481-488. Pittsburgh, Pennsylvania: Materials Research Society. TIC: 204618. [DIRS 124812]

Penrose, W.R.; Polzer, W.L.; Essington, E.H.; Nelson, D.M.; and Orlandini, K.A. 1990. "Mobility of Plutonium and Americium Through a Shallow Aquifer in a Semiarid Region." *Environmental Science & Technology, 24,* 228-234. Washington, D.C.: American Chemical Society. TIC: 224113. [DIRS 100811]

Rittmann, B.E. and Wirtel, S.A. 1991. "Effect of Biofilm Accumulation on Colloid Cohesion." *Journal of Environmental Engineering, 117,* (5), 692-695. New York, New York: American Society of Civil Engineers. TIC: 253699. [DIRS 161671]

Short, S.A.; Lowson, R.T.; and Ellis, J. 1988. "234U/238U and 230Th/234U Activity Ratios in the Colloidal Phases of Aquifers in Lateritic Weathered Zones." *Geochimica et Cosmochimica Acta, 52,* (11), 2555-2563. New York, New York: Pergamon Press. TIC: 239054. [DIRS 113937]

Sprouse, G. and Rittmann, B.E. 1990. "Colloid Removal in Fluidized-Bed Biofilm Reactor." *Journal of Environmental Engineering, 116,* (2), 314-329. New York, New York: American Society of Civil Engineers. TIC: 254391. [DIRS 161672]

Stenhouse, M.J. 1995. *Sorption Databases for Crystalline, Marl and Bentonite for Performance Assessment.* NAGRA Technical Report 93-06. Wettingen, Switzerland: National Cooperative for the Disposal of Radioactive Waste. TIC: 247885. TBV-5188 [DIRS 147477]

Tombacz, E.; Abraham, I.; Gilde, M.; and Szanto, F. 1990. "The pH-Dependent Colloidal Stability of Aqueous Montmorillonite Suspensions." *Colloids and Surfaces, 49,* 71-80. Amsterdam, The Netherlands: Elsevier. TIC: 246046. [DIRS 112690]

van Olphen, H. 1977. *An Introduction to Clay Colloid Chemistry for Clay Technologists, Geologists, and Soil Scientists.* 2nd Edition. New York, New York: John Wiley & Sons. TIC: 208918. [DIRS 114428]

Vilks, P.; Cramer, J.J.; Bachinski, D.B.; Doern, D.C.; and Miller, H.G. 1993. "Studies of Colloids and Suspended Particles, Cigar Lake Uranium Deposit, Saskatchewan, Canada." *Applied Geochemistry, 8,* (6), 605-616. London, England: Pergamon Press. TIC: 237449. [DIRS 108261]

Walker, H.W. and Grant, S.B. 1996a. "Role of Polymer Flexibility in the Stabilization of Colloidal Particles by Model Anionic Polyelectrolytes." *Journal of Colloid and Interface Science, 179,* ([2]), 552-560. [New York, New York]: Academic Press. TIC: 253705. [DIRS 161736]

Walker, H.W. and Grant, S.B. 1996b. "Coagulation and Stabilization of Colloidal Particles by Adsorbed DNA Block Copolymers: The Role of Polymer Confirmation." *Langmuir, 12,* (13), 3151-3156. [Washington, D.C.]: American Chemical Society. TIC: 253704. [DIRS: 161738]

Wan, J. and Tokunaga, T.K. 1997. "Film Straining on Colloids in Unsaturated Porous Media: Conceptual Model and Experimental Testing." *Environmental Science & Technology, 31,* (8), 2413-2420. [Washington, D.C.: American Chemical Society]. TIC: 234804. [DIRS 108285]

Wan, J. and Wilson, J.L. 1994. "Colloid Transport in Unsaturated Porous Media." *Water Resources Research, 30,* (4), 857-864. Washington, D.C.: American Geophysical Union. TIC: 222359. [DIRS 114430]

Wanner, O.; Cunningham, A.B.; and Lundman, R. 1995. "Modeling Biofilm Accumulation and Mass Transport in a Porous Medium Under High Substrate Loading." *Biotechnology and Bioengineering, 47,* (6), 703-712. [New York, New York]: John Wiley & Sons. TIC: 253701. [DIRS 161674]

Weiss, T.H.; Mills, A.L.; Hornberger, G.M.; and Herman, J.S. 1995. "Effect of Bacterial Cell Shape on Transport of Bacteria in Porous Media." *Environmental Science & Technology, 29,* (7), 1737-1740. [Washington, D.C.]: American Chemical Society. TIC: 247490. [DIRS 147345]

Wilkinson, K.J.; Joz-Roland, A.; and Buffle, J. 1997. "Different Roles of Pedogenic Fulvic Acids and Aquagenic Biopolymers on Colloid Aggregation and Stability in Freshwaters." *Limnilogy and Oceanography, 42,* (8), 1714-1724. Waco, Texas: American Society of Limnology and Oceanography. TIC: 253707. [DIRS 161734]

Wilkinson, K.J.; Nègre, J.-C.; and Buffle, J. 1997. "Coagulation of Colloidal Material in Surface Waters: The Role of Natural Organic Matter." *Journal of Contaminant Hydrology, 26,* ([1-4]), 229-243. [New York, New York]: Elsevier. TIC: 253708. [DIRS 161732]

Williams, N.H. 2003. "Thermal Inputs for Evaluations Supporting TSPA-LA, Supplement." Interoffice memorandum from N.H. Williams (BSC) to Distribution, April 4, 2003, 0205035938, with enclosures. ACC: MOL.20030501.0081. [DIRS 162731]

Wronkiewicz, D.J.; Buck, E.C.; and Bates, J.K. 1997. "Grain Boundary Corrosion and Alteration Phase Formation During the Oxidative Dissolution of UO2 Pellets." *Scientific Basis for Nuclear Waste Management XX, Symposium held December 2-6, 1996, Boston, Massachusetts.* Gray, W.J. and Triay, I.R., eds. *465,* 519-526. Pittsburgh, Pennsylvania: Materials Research Society. TIC: 238884. [DIRS 102048]

Yates, M.V. and Yates, S.R. 1988. "Modeling Microbial Fate in the Subsurface Environment." *Critical Reviews in Environmental Control, 17,* (4), 307-344. Boca Raton, Florida: CRC Press. TIC: 247762. [DIRS 147348]

Yokoyama, A.; Srinivasan, K.R.; and Fogler, H.S. 1990. "Stabilization of Colloidal Particles by Acidic Polysaccharides. Effect of Temperature on Stability." *Langmuir, 6,* (3), 702-706. Washington, D.C.: American Chemical Society. TIC: 253703. [DIRS 161675]

Zänker, H.; Richter, W.; Brendler, V.; and Nitsche, H. 2000. "Colloid-Borne Uranium and Other Heavy Metals in the Water of a Mine Drainage Gallery." *Radiochimica Acta, 88,* ([9/11]), 619-624. München, Germany: R. Oldenbourg Verlag. TIC: 253959. [DIRS 162746]

Zumstein, J. and Buffle, J. 1989. "Circulation of Pedogenic and Aquagenic Organic Matter in an Eutrophic Lake." *Water Research, 23,* (2), 229-239. New York, New York: Pergamon Press. TIC: 253878. [DIRS 161740]

9.2 CODES, STANDARDS, REGULATIONS, AND PROCEDURES

10 CFR 63. 2002. Energy: Disposal of High-Level Radioactive Wastes in a Geologic Repository at Yucca Mountain, Nevada. Readily available. [DIRS 158535]

40 CFR 197. 2001. Protection of Environment: Public Health and Environmental Radiation Protection Standards for Yucca Mountain, Nevada. Readily available. [DIRS 155238]

AP-2.22Q, Rev 0, ICN 1. *Classification Criteria and Maintenance of the Monitored Geologic Repository Q-List.* Washington, D.C.: U.S. Department of Energy, Office of Civilian Radioactive Waste Management. ACC: DOC.20030422.0009

AP-SI.1Q, Rev 5. *Software Management.* Washington, D.C.: U.S. Department of Energy, Office of Civilian Radioactive Waste Management. ACC: DOC.20030422.0012

AP-SIII.10Q, Rev. 1. *Models.* Washington D.C., Washington D.C.: Office of Civilian Radioactive Waste Management. ACC: DOC.20030312.0039.

ASTM C 1174-97. 1998. Standard Practice for Prediction of the Long-Term Behavior of Materials, Including Waste Forms, Used in Engineered Barrier Systems (EBS) for Geological Disposal of High-Level Radioactive Waste. West Conshohocken, Pennsylvania: American Society for Testing and Materials. TIC: 246015. [DIRS 105725]

9.3 SOURCE DATA

LA0002SK831352.001. Total Colloidal Particles Concentration and Size Distribution in Groundwaters from the Nye County Early Warning Drilling Program. Submittal date: 02/24/2000. [DIRS 149232]

LA0002SK831352.002. Total Colloidal Particles Concentration and Size Distribution in Groundwaters Around Yucca Mountain. Submittal date: 02/25/2000. [DIRS 149194]

LA0002SK831352.003. Colloid Size Distribution and Total Colloid Concentration in Ineel Groundwater Samples. Submittal date: 02/25/2000. [DIRS 161771]

LA0002SK831352.004. Colloid Size Distribution and Total Colloid Concentration in Groundwater's from the Nuclear Test Site. Submittal date: 02/25/2000. [DIRS 161579]

LA0003NL831352.002. The KD Values of ^{239}Pu on Colloids of Hematite, Ca-Montmorillonite and Silica in Natural and Synthetic Groundwater. Submittal date: 03/29/2000. [DIRS 148526]

LA0005NL831352.001. The Kd Values of 243Am on Colloids of Hematite, Montmorillonite and Silica in Natural and Synthetic Groundwater. Submittal date: 05/03/2000. [DIRS 149623]

LA0211SK831352.001. Colloid Concentration and Size Distribution from Crater Flats Wells. Submittal date: 12/04/2002. [DIRS 161580]

LA0211SK831352.002. Colloid Concentration and Size Distribution from Nye County Early Warning Drilling Program, Alluvial Testing Complex (ATC) Wells. Submittal date: 12/04/2002. [DIRS 161581]

LA0211SK831352.003. Colloid Concentration and Size Distribution from Nellis/Desert Rsearch Institute (DRI) Wells. Submittal date: 12/04/2002. [DIRS 161582]

LA0211SK831352.004. Colloid Concentration and Size Distribution from Nye County Early Warning Drilling Program, Fall 2000 Field Sampling. Submittal date: 12/04/2002. [DIRS 161458]

LA0304PR831232.001. Calculation of Ionic Strengths Based on Cation Concentrations in Various Groundwater Samples in which Colloid Concentrations were Measured. Submittal date: 05/13/2003. [DIRS 163196]

LA0304PR831232.002. Calculation of Ionic Strengths Based on Non-Q Cation Concentrations in Various Groundwater Samples in Which Colloid Concentrations were Measured. Submittal date: 05/13/2003. [DIRS 163197]

LA9910SK831341.005. Total Colloidal Particles Concentration and Size Distribution in NTS-ER-20-5-1, NTS-ER-20-5-3, and J-13 Groundwater. Submittal date: 12/07/1999. [DIRS 144991]

LL000905312241.018. Data Associated with the Detection and Measurement of Colloids Recorded in Scientific Notebook 1644. Submittal date: 09/29/2000. [DIRS 152621]

LL991109751021.094. Data Associated with the Detection and Measurement of Colloids in Scientific Notebook SN 1644. Submittal date: 01/10/2000. [DIRS 142910]

MO0212UCC034JC.002. Mass Transport of Solids in Effluent Solution During Miniature Waste Package Corrosion. Submittal date: 12/09/2002. [DIRS 161457]

MO0301ANLGNN01.527. Glass Unsaturated (Drip) Test Results (BSC Test Plan: SITP-02-WF-002): Boron Release. Submittal date: 01/15/2003. [DIRS 161914]

MO0301ANLGNN02.527. Glass Unsaturated (Drip) Test Results (BSC Test Plan: SITP-02-WF-002): TC, NP, PU, and AM Releases. Submittal date: 01/15/2003. [DIRS 161916]

MO0302UCC034JC.003. Graphical X-Ray Diffractometer Data and Mineral Analysis of Filtered Solids from Effluent Solution During Miniature Waste Package Corrosion. Submittal date: 2/10/2003. [DIRS 162871]

MO0306ANLSf001.459. Colloids Generated from Irradiated N Reactor Fuel, Data Report. Submittal date: 06/04/2003. [DIRS 163910]

SNT05080598002.001. Engineered Barrier System (EBS) Transport Sorption and Colloid Parameters for the TSPA-VA (Total System Performance Assessment-Viability Assessment) Rip Calculations. Submittal date: 11/06/1998. [DIRS 162744]

9.4 OUTPUT DTNs

SN0304T0504103.001. Groundwater Colloid Concentration Parameters for TSPA. Submittal date: 04/01/2003.

SN0304T0504103.002. Partition Coefficients (Kd Values) for Selected Radionuclides Modeled in TSPA. Submittal date: 04/01/03.

SN0304T0504103.003. Iron Oxyhydroxide Colloid Concentration Parameters and Specific Surface Area (SA) for Iron Oxyhydroxide Colloids. Submittal date: 04/01/03.

SN0304T0504103.004. Concentration of Embedded Radionuclides (Pu and Am) in Waste Form Colloids, Mass Concentrations of Waste Form Colloids. Submittal date: 04/01/03.

ATTACHMENT I—CALCULATION OF GROUNDWATER COLLOID PARAMETERS

CALCULATION OF GROUNDWATER COLLOID PARAMETERS

The groundwater colloid parameters for use in the TSPA-LA model were based on a dataset that included 79 groundwater samples collected in the vicinity of Yucca Mountain and 11 samples collected from the Idaho National Engineering and Environmental Laboratory (Table I-1). Inclusion of the Idaho National Engineering and Environmental Laboratory groundwater colloid data (DTN: LA0002SK831352.003) was deemed appropriate for inclusion in the data analysis among the groundwater data from the Yucca Mountain area because the climate in Idaho Falls is also arid and the bedrock geology is also volcanic in nature (fractured basalts).

Conversion of colloid populations (pt/mL) in the groundwater samples to mass concentrations (mg/L) involved only simple mathematical manipulations (addition, multiplication, and division) and could readily have been executed with the use of a hand-held calculator. However, the calculations were handled with the aid of Microsoft Excel 2000®. Excel was also used for tabular presentation of the groundwater data in Table I-1 and to graph the cumulative distribution function of the data (see Figure 12, Section 6.3.2.5).

Conversion of the Colloid Populations to Mass Concentrations:

The conversion of the colloid population to mass concentration required the establishment of two basic assumptions (see Section 5, Assumption 5.10):

1. All colloid particles were assumed to be spherical colloids. The assumption that all colloid particles are spherical enables the calculation of volume for each colloid. This assumption is ultimately conservative in that it results in larger masses than the use of other configurations such as sheet-shaped or rod-shaped, etc., particles of a given diameter size.

2. A colloid mineral density of 2.5 g/cm^3 (2.5E-18 mg/nm^3) was assumed to be appropriate for all colloid particles. This assumption was founded on the copious scientific measurements of particle density on a large range of minerals, including silicate layer-lattice clays. Silicate minerals have shown to have a particle density of ranging from 2.27 to 2.33 g/cm^3 at the low range, cristobalite and tridymite respectively, and 2.67 g/cm^3 at the high range (pure quartz) (Lide 1995 [DIRS 101876], pp. 4-132 through 4-138).

The volume of a sphere (V) can be calculated from the radius (R) by the following relationship:

$$V = 4/3\ \pi\ R^3 \qquad \text{(Eq. I-1)}$$

The colloid population data for each groundwater sample consisted of population data recorded at 10 nm increments from the particle-size diameter range 50 nm to 200 nm as reported in the DTNs. The midpoint of the particle diameter size class ranges that are reported in the groundwater datasheets was used to establish the radius for the particle volume calculations using Equation I-1. For example, those particles with diameter ranging from 50 to 60 nm were assigned a size 55 nm. Thus, the radius (R), for this particle diameter size population was 27.5 nm.

After calculating an estimate of volume for each particle diameter size class interval, the mass concentration (mg/L) for each particle size interval was calculated by multiplying particle volume (nm^3) by particle density (mg nm^{-3})—this product was then multiplied by the total number of particles in the size class interval to derive an estimate of the total colloid mass in each particle-size class interval. The total colloid mass in the water sample (Column 4 in Table I-1) was then estimated by summing the mass concentrations in each particle-size class interval. For example, the total colloid concentration for the groundwater sample extracted from Well NC-EWDP-01s was calculated as outlined in Table I-2.

Table I-1. Groundwater Samples Used to Develop Cumulative Distribution Function Developed to Establish Colloid Concentration Sampling Frequency in GoldSim Calculations for TSPA-LA for Solutions with Ionic Strength Less Than 0.05

Groundwater Sample	Well ID	Colloid Population (pt/mL)	Colloid Concentration (mg/L)
Data Source DTN LA0002SK831352.001 [DIRS 149232] Alluvium (Direct Input)			
1	NC-EWDP-01s, Depth 170	1.07E+07	3.02E-02
2	NC-EWDP-01s, Depth 250	2.08E+07	4.62E-02
3	NC-EWDP-03s, Depth 449	3.56E+08	3.48E-01
4	NC-EWDP-03s, Depth 390	1.78E+09	1.90E+00
5	NC-EWDP-09SX, Depth 310	3.85E+07	4.49E-02
6	NC-EWDP-09SX, Depth 270	7.24E+07	8.74E-02
7	NC-EWDP-09SX, Depth 150	9.73E+07	1.62E-01
8	NC-EWDP-09SX, Depth 112	7.14E+07	8.89E-02
9	Nc airport	7.95E+07	1.41E-01
Data Source DTN LA0002SK831352.002 [DIRS 149194] Volcanics (Direct Input)			
10	UE-25 J-13	1.19E+06*	1.35E-03
11	UE-25 J-13	1.046E+06*	1.75E-03
12	USW SD-6	5.07E+08*	7.24E-01
13	USW SD-6	1.05E+08*	1.43E-01
14	UE-25 WT #17	2.11E+09*	3.49E+00
15	UE-25 WT #17	1.475E+09*	2.32E+00
16	UE-25 WT #17	2.633E+07*	2.69E-02
17	UE-25 WT #17	8.236E+07*	1.32E-01
18	UE-25 WT #3	7.78E+06*	2.02E-02
19	UE-18 WW #8	2.93E+06*	2.79E-03
20	UE-18 WW #8	3.31E+06*	3.70E-03
21	U-20 WW #20	5.16E+07*	5.83E-02
22	U-20 WW #20	5.72E+07*	7.71E-02
23	UE-29 a #1	7.45E+06*	1.44E-02
24	UE-29 a #2	3.66E+07*	6.73E-02
25	UE-25 c #1	4.63E+06*	9.68E-03
26	UE-25 c #1	2.82E+06*	4.49E-03
Data Source DTN LA9910SK831341.005 [DIRS 144991] Volcanics (Direct Input)			
27	NTS-ER-20-5-3	1.43E+10	1.02E+01
28	NTS-ER-20-5-1	1.25E+10	6.74E+00
29	UE-25 J-13	1.54E+06	3.72E-03

Table I-1. Groundwater Samples Used to Develop Cumulative Distribution Function Developed to Establish Colloid Concentration Sampling Frequency in GoldSim Calculations for TSPA-LA for Solutions with Ionic Strength Less Than 0.05 (Continued)

Groundwater Sample	Well ID	Colloid Population (pt/mL)	Colloid Concentration (mg/L)
Data Source DTN LA0211SK831352.004 [DIRS 161458] Nye Co. Phase 2 – Alluvium (Direct Input)			
30	NC=EWDP-15P	1.34E+08	1.73E-01
31	NC-EWDP-7S	3.02E+06	9.01E-03
32	NC-EWDP-4PB	1.41E+09	2.03E+00
33	NC-EWDP-4PA	2.34E+08	3.05E-01
34	NC-EWDP-5SB	9.38E+08	2.69E+00
35	NC-EWDP-12PA	7.52E+07	1.42E-01
36	NC-EWDP-12PB	8.54E+07	1.53E-01
37	NC-EWDP-12PC	2.11E+07	6.29E-02
38	NC-EWDP-19D	8.27E+07	7.73E-02
Data Source DTN LA0211SK831352.002 [DIRS 161581] ATC Wells (Direct Input)			
39	ATC-IM1-A	1.01E+10	7.39E+00
40	ATC-IM1-B	9.51E+09	7.20E+00
41	NC-EWDP-19IM-2-A	1.71E+10	1.35E+01
42	NC-EWDP-19IM-2-B	1.76E+10	1.46E+01
43	NC-EWDP-19IM1-Z1	6.40E+09	5.61E+00
44	NC-EWDP-19IM1-Z2	3.23E+09	2.70E+00
45	NC-EWDP-19IM1-Z3	7.73E+09	5.67E+00
46	NC-EWDP-19IM1-Z4	8.52E+09	6.40E+00
47	NC-EWDP-19IM1-Z5	2.33E+10	1.93E+01
48	NC-EWDP-19D-Z5	1.27E+10	1.08E+01
49	ATC-19D1-011602-1350C	1.01E+10	6.57E+00
50	ATC-19D1-011702-1215C	9.28E+09	5.64E+00
51	ATC-19D1-011602-011702	7.33E+10	4.84E+01
52	ATC-19D1-012802-1500	5.19E+10	3.15E+01
53	NC-EWDP-19D, Z1	5.13E+09	4.12E+00
54	NC-EWDP-19D-Z1	8.27E+07	7.74E-02
55	NC-EWDP-19D, Z2	8.73E+07	9.75E-02
56	NC-EWDP-19D, Z2	2.29E+08	2.47E-01
57	NC-EWDP-19D, Z2	2.24E+08	2.24E-01
58	NC-EWDP-19D	9.34E+08	7.47E-01
59	NC-EWDP-19D	2.77E+08	2.52E-01
60	NC-EWDP-19D	3.51E+09	1.87E+00
Data Source DTN LA0211SK831352.001 USGS wells at Crater Flat (Direct Input)			
61	USGS-VH-1	1.33E+07	2.45E-02
62	USGS-VH-2	1.18E+06	5.03E-03
63	USGS-VH-1-A	2.17E+07	2.07E-02
64	USGS-VH-1-B	1.09E+07	1.34E-02
Data Source DTN LA0211SK831352.003 (Direct Input)			
65	DRI-EH-2-091200-0800	2.17E+06	4.36E-03
66	DRI-BLM-091200-0915	3.24E+07	3.93E-02
67	DRI-TTR3B-091200-1430	4.25E+06	6.77E-03

Table I-1. Groundwater Samples Used to Develop Cumulative Distribution Function Developed to Establish Colloid Concentration Sampling Frequency in GoldSim Calculations for TSPA-LA for Solutions with Ionic Strength Less Than 0.05 (Continued)

Groundwater Sample	Well ID	Colloid Population (pt/mL)	Colloid Concentration (mg/L)
68	DRI-Cedar Pass-091200-1325	1.01E+06	2.67E-03
69	DRI-EH-7-091200-1040	8.58E+05	1.89E-03
70	DRI-Sandia 7-091300-1030	1.05E+07	1.70E-02
71	DRI-Sandia 6-091300-0930	6.29E+07	8.29E-02
72	DRI-Tolicha Peak-091400-0745	6.98E+06	7.62E-03
73	DRI-Airforce 3A-091300-1500	1.34E+09	1.58E+00
74	DRI-Roller Coaster-091300-0930	1.12E+06	4.48E-03
Data Source DTN: LA0002SK831352.003 [DIRS 161771] INEEL Wells (Corroborating Data)			
75	USGS 117-1	4.23E+06	8.97E-03
76	M7S-1	1.30E+06	2.35E-03
77	USGS 120-1	3.76E+06	5.80E-03
78	USGS 119-1	8.13E+06	1.48E-02
79	M3S-1	1.24E+06	1.97E-03
80	M1S-1	3.28E+06	5.42E-03
81	USGS-87-1	2.63E+06	4.63E-03
82	M10S-1	9.37E+07	1.71E-01
83	BLR-99-1	7.73E+07	1.38E-01
84	M14S-1	4.28E+06	8.21E-03
85	USGS 92-1	8.00E+10	1.72E+02
Data Source DTN: LA0002SK831352.004 [DIRS 161579] NTS Wells (Corroborating Data)			
86	NTS-ER-20-5-1	1.25E+10	6.74E+00
87	NTS-ER-20-5-3	1.43E+10	1.02E+01
88	NTS-U20n, ~2511 ft	2.57E+08	3.20E-01
89	NTS-U20n, lower zone	5.19E+09	5.47E+00
90	NTS-U19q	2.72E+10	3.51E+01

Table I-2. Example Calculation for Total Colloid Mass in Well NC-EWDP-01s, Depth 170

Particle Diameter Size Range (nm)	**Particle Diameter (nm)**	**Colloid Number (pt/mL)**	**Calculated Colloid Mass (mg/L)**
50-60	55	9.27E+05	2.0189E-04
60-70	65	1.01E+06	3.6308E-04
70-80	75	8.64E+05	4.7713E-04
80-90	85	8.01E+05	6.4392E-04
90-100	95	8.51E+05	9.5508E-04
100-110	105	1.14E+06	1.7275E-03
110-120	115	8.01E+05	1.5947E-03
120-130	125	7.26E+05	1.8561E-03
130-140	135	5.26E+05	1.6941E-03
140-150	145	6.26E+05	2.4981E-03
150-160	155	5.76E+05	2.8077E-03
160-170	165	4.51E+05	2.6520E-03
170-180	175	4.13E+05	2.8974E-03
180-190	185	3.13E+05	2.5942E-03
190-200	195	3.63E+05	3.5233E-03
200	200	3.51E+05	3.6757E-03
	Totals	**1.07E+07**	**3.02E-02**

Source: DTN: LA0002SK831352.001 [DIRS 149232].

Establishment of Groundwater Colloid Parameters for Use in the TSPA-LA Model:

Mass concentrations (mg/L) of the groundwater in Table I-1 were pooled and a discrete cumulative distribution function was established to evaluate the uncertainty in colloid concentration distribution (see Figure 12, Section 6.3.2.5). Water samples that had been filtered were not considered in the development of the cumulative distribution function. Since the colloid particles were measured by dynamic light scattering techniques, any potential error in measurement of colloid populations for the various particle size classes due to filter "ripening" (i.e., clogging of filter pores through time during the filtration process) was avoided by using only non-filtered sample data.

The data shown in Figure 12, Section 6.3.2.5 reflect observed variability in groundwater colloid concentrations. The goal of the uncertainty distribution for groundwater colloid concentrations is to numerically capture our knowledge about uncertainty on a large scale. Based on the groundwater colloid concentration collected at the two sites (Yucca Mountain and Idaho National Engineering and Environmental Laboratory) and the tremendous uncertainty associated with the collection of groundwater colloids, a reasonable representation of the uncertainty is shown in the cumulative distribution function. Major factors that contribute to uncertainty in the concentrations of colloids in the groundwater samples include (1) collection techniques, (2) differences in pumping rates at each well, and (3) unknowns factors including the types of additives introduced in the wells during the drilling process itself.